Univerzita Karlova v Praze
Přírodovědecká fakulta
Vývojová a buněčná biologie

Mgr. Jiřina Tylečková (Martinková)

Proteom nádorové buňky a studium změn po působení protinádorových léčiv

The cancer cell proteome and its changes after anti-cancer drug treatment

Dizertační práce

Školitel: RNDr. Hana Kovářová CSc.

Praha 2012

Prohlášení:

Prohlašuji, že jsem tuto práci vypracovala samostatně a že jsem uvedla všechny použité informační zdroje a literaturu. Tato práce ani její podstatná část nebyla předložena k získání jiného nebo stejného akademického titulu.

V Praze,

Jiřina Tylečková

Dizertační práce byla vypracována na Ústavu živočišné fyziologie a genetiky AV ČR, v.v.i. v Liběchově a v Praze.

Poděkování:

Na tomto místě bych chtěla v prvé řadě poděkovat své školitelce RNDr. Haně Kovářové, CSc. za její stálou podporu a motivující vedení během celého doktorského studia. Dále bych chtěla poděkovat všem členům Laboratoře biochemie a molekulární biologie zárodečných buněk Ústavu živočišné fyziologie a genetiky AV ČR, v.v.i. za podporu a vytvoření příjemného pracovního prostředí během studia, jmenovitě Ritě Hrabákové. V neposlední řadě děkuji členům Laboratoře charakterizace molekulární struktury Mikrobiologického ústavu AV ČR, v.v.i., jmenovitě Ing. Petru Haladovi, PhD., docentu Miroslavu Šulcovi, PhD. a Mgr. Petru Novákovi, PhD., za jejich péči, vedení a poskytnutí přístrojového vybavení pro identifikace proteinů hmotnostní spektrometrií.

Ráda bych také poděkovala své rodině za jejich pochopení, podporu a vytvoření podmínek pro vypracování dizertační práce.

Práce vznikla za finanční podpory výzkumného záměru RVO 67985904 a Centra nádorové proteomiky MŠMT LC07017.

OBSAH

1 ABSTRAKT 2
2 ABSTRACT 3
3 ÚVOD 4
3.1 Biologie nádorů 4
3.1.1 Protein p53 a jeho úloha v nádorové buňce 4
3.2 Protinádorová chemoterapie 5
3.2.1 Antracyklinová antibiotika 6
3.3 Cílená biologická léčba 6
3.3.1 Inhibitory cyklin-dependentních kináz 7
3.3.2 Aurora kinázové inhibitory 7
3.4 Nádorová chemorezistence 7
3.5 Biomarkery ve výzkumu rakoviny 8
3.6 Proteomika ve výzkumu rakoviny 8
4 METODY 10
4.1 Příprava vzorků 10
4.2 Separace proteinů pomocí dvourozměrné gelové elektroforézy (2-DE) a pomocí dvourozměrné kapalinové chromatografie (2D-HPLC) 10
4.3 Identifikace a kvantifikace proteinů pomocí MS 11
4.4 Protilátkové verifikace proteinových změn 11
5 CÍLE PRÁCE 13
6 PŘEHLED PUBLIKACÍ 14
7 KOMENTÁŘ K PUBLIKACÍM 16
7.1 Odpověď nádorové buňky na antracykliny: proteiny skryté za účinkem těchto léčiv 16
7.2 Rezistence nádorové buňky na léčivo se zaměřením na konkrétní proteiny: Rho GDP disociační inhibitor 2, Y-box binding protein 1 a HSP70/90 organizující protein v aplikacích klinické proteomiky 20
7.3 Rezistence nádorové buňky k inhibitorům aurora kináz: identifikace nových cílů nádorové terapie 22
7.4 Problematika výzkumu rakoviny a možnosti studia nádorových biomarkerů .. 26
7.5 Relativní kvantifikace proteinů frakcionovaných pomocí ProteomeLab™ PF 2D systému za použití isobarického značení pro relativní a absolutní kvantifikaci (iTRAQ) 28
8 ZÁVĚR 30
9 SEZNAM ZKRATEK 31
10 SEZNAM CITOVANÉ LITERATURY 32

1 ABSTRAKT

Rakovina představuje velmi heterogenní skupinu onemocnění a výsledky v současnosti dostupné protinádorové léčby jsou vysoce variabilní s nedostatečnými počty vyléčených pacientů. Pro hledání a vývoj nových, selektivních a specifických, nádorových biomarkerů, které mohou být použity ke sledování stavu nemoci a terapie, se používá celá řada proteomických technik.

S ohledem na výše zmíněné skutečnosti jsme se v této práci zaměřili na studium proteomu nádorových buněk a jeho změn po působení protinádorových léčiv se specifickým zaměřením na (a) odpověď ke konvenčním léčivům ze skupiny antracyklinů s přihlédnutím k jejich rozdílnému klinickému využití a (b) identifikaci nových terapeutických cílů v nádorových buňkách rezistentních k biologickým preparátům jako jsou inhibitory (b1) cyklin-dependentních kináz a (b2) Aurora kináz.

V této studii jsme identifikovali několik klíčových aspektů, které se vztahovaly k účinkům daunorubicinu, doxorubicinu a mitoxantronu. Zaměřili jsme se na časné intervaly po působení léčiv, kdy je minimalizován vliv apoptózy, a nalezli jsme změny proteinů metabolických a celulárních procesů společné pro všechna tři léčiva. Podstatnější bylo pozorování signifikantních změn proteinů účastnících se tvorby metabolických a energetických prekurzorů, které byly specifické pro působení daunorubicinu, transportních proteinů v odpovědi na působení doxorubicinu a skupiny proteinů imunitního systému, které byly charakteristické pro působení mitoxantronu. Jak párové porovnání tak multivariační analýza odhalili daunorubicin jako nejrozdílnější ze sledované skupiny léčiv.

Práce zabývající se rezistencí nádorové buňky odhalila klíčovou úlohu Rho GDP-disociačního inhibitoru, Y-box binding proteinu a HSP70/90 organizujícího proteinu v rozvoji rezistence k inhibitoru cyklin-dependentních kináz. Výsledky dále ukazují, že pro rozvoj chemorezistence jsou důležité i další parametry jako jsou zkracování proteinů nebo jejich posttranslační modifikace. Na dalším příkladu zaměřeném na rezistenci k Aurora kinázovým inhibitorům se projevil vliv stavu proteinu p53 v nádorové buňce, ale také přímé spojení na proteinu p53 nezávislého mechanismu rezistence k CYC116 s procesem autofagie. Serin hydroxymethyltransferáza, serpin B5 a kalretinin představují proteiny, které mohou pomoci k překonání rezistence u kombinovaných terapií.

Změny proteinů typických pro konkrétní léčiva, které mohou pomoci k objasnění protinádorového účinku těchto léčiv, spolu s využitím blokace aktivovaných adaptivních nádorových signálních drah mohou významně přispět ke zlepšení výsledků protinádorové terapie. Stále ale zůstává potřeba provést relevantní biologickou a funkční interpretaci proteomických výsledků a poté je pečlivě validovat před jejich úspěšným zavedením do klinické onkologie.

2 ABSTRACT

Cancers represent a group of unprecedented heterogeneous diseases and currently available anti-cancer therapies provide highly variable efficacy with unsatisfactory cure rates. A wide range of proteomic technologies are being used in quest for newer approaches which could significantly contribute to the discovery and development of selective and specific cancer biomarkers for monitoring the disease state and anti-cancer therapy success.

Taking into consideration the above aspects, this research was undertaken to study cancer cell proteomes and their changes after anti-cancer treatment with specific focus on: (a) response to conventional anthracycline/anthracenedione drugs with respect to their different clinical efficacy and (b) identification of novel targets for therapy in cancer cells resistant to biological drugs such as inhibitors of (b1) cyclin-dependent kinases and (b2) Aurora kinases.

This study identified several interesting key aspects related to the effects of daunorubicin, doxorubicin and mitoxantrone. With the main focus on early time intervals when the influence of apoptosis is minimised, changes common for all three drugs belonging mainly to metabolic and cellular processes were observed. More importantly, significant changes in proteins involved in the generation of precursor metabolites and energy specific for daunorubicin, transport proteins participating in response to doxorubicin and a group of proteins of immune system characterising response to mitoxantrone were observed. Both a paired comparison and the multivariate evaluation of quantitative data revealed daunorubicin as a distinct member of monitored anthracycline/anthracenedione drugs.

Studies on the development of cancer cell resistance revealed that Rho GDP-dissociation inhibitor 2, Y-box binding protein 1, and the HSP70/90 organizing protein have a critical role to play in resistance to cyclin-dependent kinases inhibitor. The results indicated that various other parameters such as protein truncation and post-translational modification(s) are involved in drug-resistance. Another example focused on resistance to Aurora kinases inhibition underlined the important influence of p53 background functionality of cancer cell resistance and highlighted a direct link of p53-independent mechanism of resistance to CYC116 with autophagy. Importantly, serine hydroxymethyltransferase, serpin B5 and calretinin represent the proteins which may help overcome resistance with a combination therapy approach.

A combination of identified drug specific protein changes, which may help to explain anti-cancer activity, together with the benefit of blocking activation of adaptive cancer pathways, presents important approaches to improving treatment outcomes in cancer. In order to combat cancers, proteomic research derived findings may play a critical role, however, careful interpretation of the results and their relevance to biological and functional parameters need to be carefully considered prior to successful translation into clinic.

3 ÚVOD

3.1 Biologie nádorů

Jako rakovinu označujeme heterogenní skupinu nádorových onemocnění, která jsou v současnosti druhou nejčastější příčinou úmrtí v České republice. Vznik nádoru je komplexní vícestupňový proces spojený s mutacemi nebo epigenetickými změnami v genomu buňky, hlavně v genech kontrolujících proliferaci a přežívání buňky. Tyto mutace mění jak primární strukturu genu, tak jeho kvantitativní zastoupení, například amplifikace genu nebo změny v počtu chromozomů. Rizikové faktory pro vývoj nádorového onemocnění jsou životní prostředí a styl včetně nepříznivých a toxických činitelů jako kouření tabáku nebo ionizujícího a UV záření, ale i infekčních onemocnění nebo chronických zánětů [1]. Základní biologické znaky charakteristické pro nádorové buňky shrnuté v roce 2000 jsou samostatná produkce proliferačních signálů, necitlivost k růstovým supresorům, poškození mechanismů apoptózy, neomezený replikační potenciál, indukce angiogeneze a schopnost metastázovat [2]. V nedávné době byly jako další znaky přispívající ke vzniku nádorů navrženy také změny v energetickém metabolismu buňky vedoucí k neustálé podpoře buněčného růstu a proliferace a únik nádorových buněk imunitnímu systému. K posílení výše navržených charakteristik, které se snaží nádorová buňka získat, přispívá genetická nestabilita a s tumorem spojený zánět, kterého se účastní hlavně složky přirozené imunity (Obr. 1) [3].

3.1.1 Protein p53 a jeho úloha v nádorové buňce

Protein p53 je multifunkční protein označovaný za „strážce genomu“. Jedná se o transkripční faktor, který reguluje přes 100 různých genů. Jeho dvě hlavní funkce jsou cytostatická, kdy dojde k dočasnému zastavení buněčného cyklu v případě poškození DNA buňky s následnou podporou enzymů účastnících se oprav DNA, nebo aktivace apoptózy jako odpověď na masivní poškození DNA nebo hypoxii v buňce. Gen pro protein p53 je pravděpodobně nejčastěji mutovaný gen v lidských nádorech. Díky svým různým funkcím hraje významnou úlohu v mnohastupňovém procesu vzniku nádoru. Nádorová buňka profituje již z bodových mutací v jedné alele genu p53, které mohou posléze vést až k eliminaci proteinu p53 z buňky. Narušením funkce proteinu p53 pak buňka uniká jeho cytostatickým a pro-apoptotickým účinkům a i s poškozeným genomem může dále proliferovat. Navíc snáze toleruje hypoxii, ke které při růstu nádoru dochází. Protein p53 podporuje mimo jiné i expresi anti-angiogenního faktoru trombospondinu 1 a jeho eliminace nádorovou buňkou tak přináší i výhodu při regulaci angiogeneze v nádoru [4].

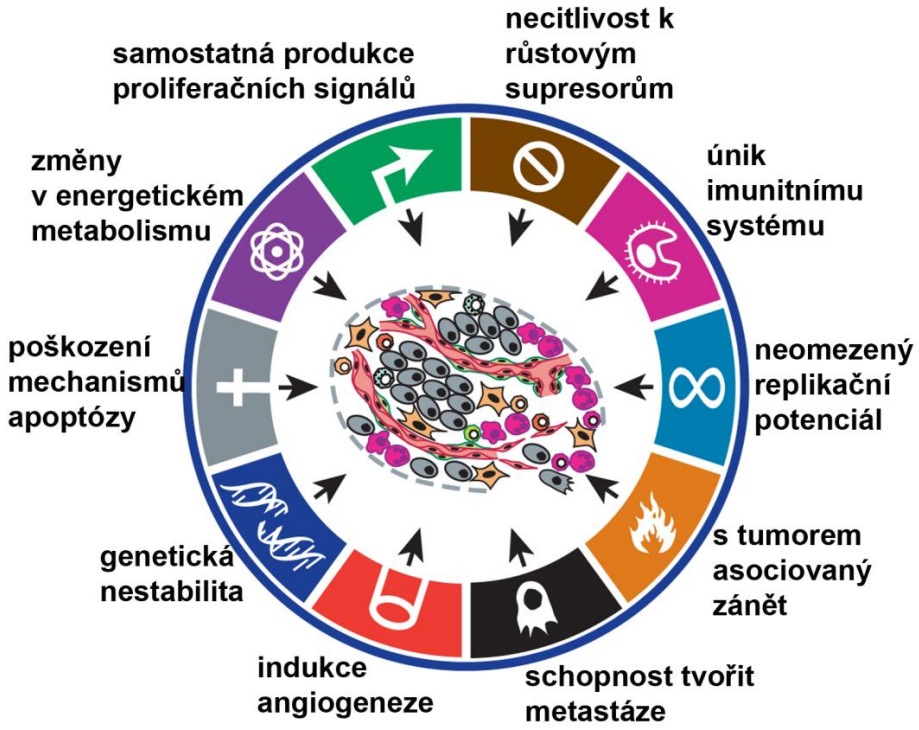

Obr. 1 Základní biologické znaky rakoviny. Převzato z Hanahan a Weinberg 2011 [3]

3.2 Protinádorová chemoterapie

V současnosti se pro léčbu nádorových onemocnění nejčastěji používá kombinace tradiční chirurgie s radioterapií anebo chemoterapií. Zatímco první dvě jmenované jsou lokální, jediná chemoterapie má systémové účinky a tím i schopnost eliminace diseminovaných nádorových buněk, které bývají hlavní příčinou selhání léčby a opakovaného výskytu nádoru. Chemoterapie zahrnuje podávání cytostatických nebo cytotoxických léků s potenciálem zabít nádorovou buňku. Léčiva jsou syntetického původu nebo se může jednat o deriváty získané z rostlin nebo plísní. Mezi další farmakologickou protinádorovou léčbu patří hormonální léčba, léčba diferenciačními látkami nebo cílená biologická léčba. Mechanismy účinku protinádorové chemoterapie jsou různé, většina léčiv indukuje poškození DNA a/nebo narušení buněčného cyklu. Podle mechanismu účinku se v současnosti používaná konvenční protinádorová chemoterapeutika dělí na několik skupin: alkylační cytostatika (melfalan, cyklofosfamid), antimetabolity (metotrexát, 5-fluorouracil), protinádorová antibiotika (doxorubicin, daunorubicin), rostlinné alkaloidy (taxol, vinka alkaloidy) a další (platinová cytostatika). Nevýhodou těchto konvenčních léčiv je, že poškozují nejenom nádorové buňky, ale i jiné hlavně rychle proliferující buňky. Léčba se pak stává kompromisem mezi dostatečnou účinností podávané látky a ještě přijatelnými vedlejšími účinky. Obecné terapeutické standardy jsou odvozené z průměrné účinnosti léku stanovené na základě klinických zkoušek na velkém počtu pacientů. Bohužel individuální odpověď konkrétního pacienta na léčbu může být od zlatého standardu značně odlišná a je-li nízká, se zjistí až po několika týdnech až měsících terapie. Jeden z důležitých cílů ve

výzkumu protinádorových léčiv je proto i personalizace protinádorové terapie. Nalezení spolehlivých markerů citlivosti nádorů na léčivo za použití molekulárních, genetických nebo proteomických testů je jedním z klíčových úkolů klinického vývoje nových léčiv, ať již se jedná o cytotoxická léčiva nebo o cílená léčiva, jinak hrozí pokračování současného stavu, kdy z drahé terapie s řadou závažných vedlejších účinků profituje pouze část pacientů [5].

3.2.1 Antracyklinová antibiotika

Antracyklinová antibiotika doxorubicin a daunorubicin patří mezi nejúčinnější protinádorová léčiva již od 60. let minulého století, kdy byla izolována z plísně *Streptomyces peucetius.* Spektrum jejich použití je široké od léčby solidních tumorů po léčbu hematologických nádorových onemocnění, a to buď jako monoterapie nebo v kombinovaných režimech [6]. Mezi jejich hlavní mechanismy účinku patří inhibice topoizomerázy II, kdy dochází ke kovalentní vazbě mezi DNA a enzymem a tím ke zlomům v DNA řetězci [7], dále interkalace do DNA a tvorba reaktivních kyslíkových radikálů. Právě reaktivní kyslíkové radikály se zároveň zdají být hlavní příčinou závažných vedlejších účinků, z nichž nejzávažnější je kardiotoxicita [8]. Mitoxantron, syntetický derivát s antracendionovou strukturou je především strukturálně velmi příbuzný antracyklinům [9]. Zajímavou biologickou otázkou zůstává, proč má skupina léčiv s tak podobnou chemickou strukturou poměrně dost odlišné klinické využití. Stejně tak chybí porozumět detailnímu mechanismu účinku těchto léčiv z molekulárního pohledu.

3.3 Cílená biologická léčba

Nejnovější poznatky buněčné biologie pomohly porozumět s rakovinou souvisejícím změnám genů, proteinů a signálních drah, které se tak staly zajímavým cílem pro vývoj nových protinádorových léčiv. Tato cílená léčiva jsou namířena proti klíčovým mechanismům vzniku nádorů na úrovni buňky jako jsou zvýšená exprese nebo mutace v buněčných receptorech nebo jejich efektorech. Příklady takových moderních cílů jsou receptory růstových faktorů nebo tyrosin-kinázové receptory (EGFR, VEGFR, PDGFR, stem-cell factor, c-Kit nebo Bcr-Abl protein) [10, 11]. Typickým příkladem je právě vývoj léčiva Glivec (Imatinib mesylát), což je inhibitor fúzního proteinu Bcr-Abl vznikajícího díky chromozomální translokaci typické pro chronickou myeloidní leukémii (CML) [12]. Při léčbě pacientů v chronické fázi CML dochází ke kompletnímu ústupu nemoci asi u 90% pacientů [13], zatímco u pacientů v akutní leukemické fázi dochází po krátkodobé remisi k návratu onemocnění s klony buněk rezistentních k léčivu [14]. Dalšími typickými cíli biologické léčby jsou látky inhibující intracelulární onkogenní signální dráhy jako jsou Ras-Raf-Mek-Erk MAPK a následné efektory mTOR kinázy, látky zacílené na integriny [15], účastnící se angiogeneze (Avastin), selektivní inhibitory histon deacetyláz, ubiquitin-

proteazomového (Velcade-bortezomid) systému nebo matrix-metaloproteináz [16]. I pro cílená léčiva platí totéž co pro konvenční terapie. Tato léčba je účinná pro určité skupiny pacientů s daným molekulárním profilem, lépe se osvědčuje kombinovaná terapie s klasickým léčivem [17] a i zde dochází k rozvoji chemorezistence.

3.3.1 Inhibitory cyklin-dependentních kináz

Cyklin-dependentní kinázy (CDKs) v komplexu s cykliny patří mezi klíčové molekuly regulující buněčný cyklus [18]. Hyperaktivace CDKs nebo disregulace endogenních inhibitorů CDKs (CDKI) je velmi častou vlastností nádorových buněk [19]. Tyto změny vedou hlavně k deregulaci progrese S-fáze buněčného cyklu. Předpokládá se tedy, že ovlivnění těchto aberantních CDKs může být užitečné v protinádorové terapii. Do pilotních klinických testů se v nedávné době dostalo několik inhibitorů CDKs jako například flavopiridol. Z cytokininů, rostlinných hormonů, byly odvozeny syntetické inhibitory CDKs roscovitin (CYC202), olomoucin nebo bohemin. Tyto látky inhibují CDK1/CDK2, CDK4 a CDK7 [20]. Roscovitin prochází v současné době první a druhou fází klinického testování například u nemalobuněčného plicního karcinomu. Monitorování proteinové odpovědi nádoru na léčivo a s ní souvisejících mechanismů vzniku chemorezistence může přispět k implementaci těchto preparátů do jejich klinického využití.

3.3.2 Aurora kinázové inhibitory

Jako Aurora kinázy (AURKs) je označována rodina serine/treoninových protein kináz Aurora A, B a C. Tyto kinázy regulují buněčné dělení, účastní se mnoha procesů v mitóze jako například segregace chromozomů nebo cytokineze. V mnoha různých lidských nádorech byla detekována jejich zvýšená exprese, která může podle předpokladů vést ke genomické nestabilitě a aneuploidii. Z tohoto důvodu se AURKs staly zajímavým cílem protinádorové terapie a inhibitory AURKs vykazují antiproliferační účinky [21]. Do současnosti prošlo či prochází preklinickým nebo klinickým testováním již více než 30 AURK inhibitorů. Jedním ze slibných inhibitorů AURKs procházející první fází klinického testování u solidních tumorů je i CYC116, který kromě celé rodiny AURKs inhibuje i VEGFR2 a má tak i antiangiogenní účinky. Prvním detailně charakterizovaným AURK inhibitorem, který se používal hlavně pro studium biologických vlastností AURKs, je ZM447439 od společnosti AstraZeneca [22].

3.4 Nádorová chemorezistence

Rozvoj chemorezistence k nádorovým léčivům je jedním z hlavních důvodů selhání terapie. Rezistence na léčivo může být primární nebo získaná sekundární. Existuje několik mechanismů nádorové chemorezistence. Mezi farmakologické a fyziologické faktory patří

zvýšené množství P450 enzymů účastnících se metabolismu léčiv nebo zvýšené odstranění léčiva z buněk pomocí transportérů. Dále u léčiv, která poškozují DNA, může dojít k nadměrné aktivaci DNA opravného systému. Další skupinou mechanismů účastnících se rozvoje rezistence jsou faktory přispívající ke zvýšenému přežívání buněk jako je například blokace apoptózy nebo senescence [23]. Nemalou roli hrají i nádorové kmenové buňky, které jsou díky své kmenovosti schopné sebeobnovy a neomezeného počtu dělení, s čímž jsou spojeny právě zvýšená kapacita DNA oprav a odolnost vůči apoptóze [24].

3.5 Biomarkery ve výzkumu rakoviny

V současnosti se pro diagnostiku, výběr léčebného postupu, prognózu a predikci vývoje nádorového onemocnění používá nejčastěji patomorfologické vyšetření. Bohužel se ukazuje, že pro přesnou identifikaci a klasifikaci mnoha různých subtypů onemocnění je tento systém mnohdy nedostačující. V některých případech je možno použít cytogenetické metody schopné detekovat genetické změny v nádorech na úrovni chromozomů nebo mutací jednotlivých genů. Ještě lépe charakterizovat a klasifikovat nádory do skupin se specifickými vlastnostmi se povedlo v transkriptomických studiích, které se zaměřovaly na změny v množství mRNA nebo změny alternativního splicingu [25]. Většina těchto studií se zaměřuje hlavně na objevení nových biomarkerů, které budou více specifické a selektivní v porovnání se současnými a pomohou lépe popsat tak komplexní biologický systém jako je rozvoj nádorového onemocnění a jeho terapie. Stejně tak se očekává, že i proteomické techniky pomohou nalézt nové nádorové proteinové markery pro diagnostiku, prognózu, predikci a monitorování terapie. Takovéto markery by měly být pokud možno specifickou odpovědí organismu na daný typ nádoru a ideálně sekretovány přímo nádorovou buňkou do tělesných tekutin. Tělesné tekutiny se tak stávají slibným materiálem pro studium biomarkerů. Nejvyšší koncentrace těchto markerů bude podle předpokladů v tkáňových intersticiálních tekutinách a bude postupně klesat se vzdáleností od nádoru až do krevní plazmy [26]. Krevní plazma/sérum je jednou z nejdostupnějších a nejstudovanějších tekutin, ale za cenu očekávaných nízkých koncentrací potenciálních nových nádorových markerů za přítomnosti obrovského koncentračního rozsahu ostatních složek krevní plazmy /séra [27]. Zdá se být nezbytné redukovat komplexnost tělesných tekutin, ať již se jedná o krev, moč nebo jiné, za použití různých strategií jako je například deplece nejvíce abundantních proteinů pomocí protilátek [28], zaměření se na určitý subtyp proteinů jako jsou glykoproteiny [29] nebo kombinace protilátkových technik s vysoce citlivou hmotnostní spektrometrií [30].

3.6 Proteomika ve výzkumu rakoviny

Proteomika se obecně zabývá výzkumem proteinů kódovaných genomem daného organismu s následným sledováním exprese těchto proteinů v různých buňkách tohoto

organismu, jejich subcelulární lokalizací, posttranslačních modifikací, vzájemných interakcí mezi nimi a vztahem mezi strukturou a funkcí. Tyto cíle proteomiky byly formované organizací HUPO na konferenci v americké Virginii již v roce 2001. Proteomika ve výzkumu rakoviny si zaslouží pozornost hned z několika důvodů. I přes naše lepší porozumění genomickým aberacím nádorových buněk a charakterizaci nádorových fenotypů pomocí transkriptomiky je obecně korelace mezi množstvím mRNA a skutečným množstvím proteinu v buňce malá, geny mohou díky odlišnému splicingu a translaci kódovat několik různých proteinových variant nebo klíčové proteiny pro maligní chování nádoru mohou být posttranslačně modifikovány. Je zřejmé, že proteom nádorové buňky lépe odráží funkci a dynamické změny v čase a tím umožňuje sledovat průběh onemocnění a odpověď na terapii. Předpokládá se, že pro zhruba 20 000 protein-kódujících genů může počet proteinových variant dosahovat i přes milion [31]. Naproti tomu výzvami proteomického výzkumu jsou extrémní heterogenita a v případě nádorů i proměnlivost buněčných populací v tkáních, široké dynamické rozpětí koncentrací proteinů v tělních tekutinách, dosahujícího asi 10 řádů i potřeba validace molekulárních změn na velké skupině pacientů nejlépe za použití jiné nezávislé techniky.

Proteomika využívá celé řady metod, které lze cíleně použít již při přípravě vzorku jeho obohacením ať již z hlediska subcelulární frakcionace nebo zaměřením se na konkrétní subproteom (glykoproteom, fosfoproteom). Ve standardním proteomickém schématu následuje globální profilování nebo srovnávací funkční analýza vzorku tkání, buněk nebo tělních tekutin [32]. Nejčastější separační metodiky využívají buď gelových technik jako je jedno- nebo dvourozměrná gelová elektroforéza nebo ne-gelových separačních technik jako je jedno- i dvourozměrná kapalinová chromatografie. Následuje identifikace proteinů, respektive jejich posttranslačních modifikací a jejich kvantifikace pomocí hmotnostní spektrometrie (MS). K relativní kvantifikaci využíváme různých druhů značení jako je „stable isotope labeling by amino acids in cell culture (SILAC)“, „isobaric tags for relative and absolute quantification (iTRAQ)“, „isotope coded protein labeling (ICPL)“ nebo tzv. label-free kvantifikace, bez značení, kdy se využívá počítání píků spekter nebo porovnání LC-MS profilů. Absolutní kvantifikace je také možná, a to přidáním izotopicky značeného vnitřního standardu proteotypického peptidu. Specifickou modifikací užití absolutní kvantifikace je metoda Selected Reaction Monitoringu (SRM), která umožňuje pomocí měření kombinace retenčního času peptidu, peptidové hmoty a specifických fragmentací konkrétního předem zvoleného peptidu přesně určit množství tohoto peptidu i v komplexním vzorku. Takto se dá v jednom vzorku během krátké doby monitorovat současně až několik desítek peptidů [33].

Ve výzkumu rakoviny se proteomika využívá mimo jiné pro sledování nádorových profilů, účinku protinádorových léčiv, ať již konvenční chemoterapie nebo experimentálních preparátů, rozvoje a mechanismů chemorezistence a hledání nových biomarkerů, včetně studia tělních tekutin.

4 METODY

4.1 Příprava vzorků

CEM T-lymfoblastická linie buněk, resp. další buněčné linie byly kultivovány v Laboratoři experimentální medicíny ve Fakultní nemocnici Olomouc [34]. Pro kultivace bylo použito RPMI-1640 médium, resp. DMEM médium doplněné o glutamin, antibiotika a 10% fetální bovinní sérum. Buňky ošetřené léčivem byly kultivovány po příslušnou dobu v médiu s rozpuštěným léčivem daunorubicinem, doxorubicinem, mitoxantronem, cisplatinou a taxolem. Pro určení cytotoxicity bylo použito MTT testu [35] a pro každé léčivo byla vypočtena hodnota poloviční inhibiční koncentrace $IC_{50.}$ Čas do nástupu apoptózy (TA) pro každé léčivo pro hodnotu 10x IC_{50} byl vypočten podle aktivace kaspáz 3 a 7 [36]. Rezistentní linie buněk byly ustanoveny z mateřské linie dlouhodobou kultivací buněk v subletálních dávkách léčiva (CDKI bohemin) pro CEM buňky nebo jednorázovým ošetřením vysokou dávkou léčiva (AURKIs CYC116 a ZM447439) pro HCT116 buňky. Kontrolní neošetřené buňky, buňky ošetřené léčivem, rezistentní buňky i rezistentní ošetřené buňky byly sklizeny v příslušných časových intervalech, promyty a lyzovány v pufru obsahujícím 7 M močovinu, 2 M thiomočovinu, 3% w/v CHAPS, 2% v/v Nonidet P40, 5 mM TCEP a inhibitory proteáz a fosfatáz (Roche) pro 2-DE nebo 7,5 M močovinu, 2,5 M thiomočovinu, 62,5 mM Tris, 2,5% oktyl glukosid, 6,25 mM TCEP, 12,5% glycerol a inhibitory proteáz (Roche) pro 2D-HPLC. Byla stanovena koncentrace proteinů a lyzáty buněk byly zamraženy na -80 ^{0}C pro jejich další použití.

4.2 Separace proteinů pomocí dvourozměrné gelové elektroforézy (2-DE) a pomocí dvourozměrné kapalinové chromatografie (2D-HPLC)

Lyzáty buněk byly pomocí 2-DE separovány v první dimenzi podle izoelektrického bodu proteinů na imobilizovaném pH gradientu 4-7 a 6-11 a ve druhé dimenzi podle molekulové hmotnosti proteinů na vertikální 12% polyakrylamidové SDS elektroforéze. Po separaci byly proteiny v gelech vizualizovány pomocí fluorescenčního Sypro nebo stříbrného barvení podle Shevchenka [37], digitalizovány na skeneru Pharos FX a vzniklé proteinové mapy byly počítačově vyhodnoceny v software Redfin Solo (Ludesi). Signifikantně diferenční spoty mezi kontrolními a ošetřenými/rezistentními vzorky buněk byly vybrány pro identifikaci pomocí MS.

Analogicky byly lyzáty buněk separovány pomocí 2D-HPLC systému ProteomeLab^{TM} PF 2D, kdy separace v první dimenzi proběhla opět pomocí izoelektrického bodu proteinů na chromatofokusační koloně a ve druhé dimenzi pomocí hydrofobicity proteinů na reverzní fázi. Detekce proteinů probíhala pomocí monitorování UV při 280 nm

po chromatofokusaci, respektive 220 nm po reverzní fázi. Získaný záznam byl počítačově převeden na proteinové mapy, ty byly vyhodnoceny pro signifikantně regulované proteiny mezi vzorky a tyto proteinové frakce byly vybrány pro MS identifikace.

4.3 Identifikace a kvantifikace proteinů pomocí MS

Pro identifikace proteinů z 2-DE byly nejprve připraveny preparativní gely s dvounásobnou nanáškou pro pH 6-11 gely a pětinásobnou nanáškou pro pH 4-7 gely oproti původním analytickým gelům. Proteinové spoty vybrané pro verifikace byly z gelů manuálně vyříznuty, tyto gelové kostky odbarveny a následně byly proteiny v gelu přes noc naštípány pomocí trypsinu na peptidy, které byly odsoleny, zakoncentrovány, naneseny v matrici na terčík a analyzovány na přístroji Ultraflex III MALDI-TOF/TOF (Bruker Daltonics). Získaná peptidová spektra byla metodou peptide mass fingerprinting (PMF) prohledána proti lidské Swiss-Prot 2011-09 databázi. Proteiny identifikované na hranici spolehlivosti byly potvrzeny měřením MS/MS spekter.

Pro identifikace proteinů z 2D-HPLC byl použit stejný postup s tím rozdílem, že příslušné proteinové frakce po druhé dimenzi separace byly nejprve vysušeny a přímo rozpuštěny v pufru obsahujícím trypsin.

Přestože lze použité metodiky 2-DE i 2D-HPLC použít k relativní kvantifikaci proteinů získaných proteinových skvrn či píků, v určitých případech, například je-li ve vzorku analyzovaném na MS směs více proteinů, je výhodné provést další relativní MS kvantifikaci proteinů pomocí značení peptidů. V našem případě bylo provedeno značení iTRAQ. Po štěpení proteinů trypsinem byl do protokolu implementován krok značení peptidů pomocí iTRAQ reagentu, kdy pro různé vzorky byla použita jiná izobarická značka a postup byl optimalizován pro koncentrace proteinů nižší než v původně použitých celobuněčných lyzátech [38]. Příslušné vzorky byly smíchány, naneseny na MALDI terčík a analyzovány společně. Identifikace proteinů probíhala pomocí PMF, kvantifikace následně pomocí relativního porovnání poměru reportérových iontů z MS/MS spekter.

Veškeré MS analýzy byly provedeny ve spolupráci s Mikrobiologickým ústavem AV ČR.

4.4 Protilátkové verifikace proteinových změn

Pro ověření kvantitativních změn vyhodnocených z předchozích analýz bylo pro vybrané proteiny použito protilátkové metody imunoblotu. Pro imunoblot byly proteinové lyzáty smíchány s SDS pufrem a rozděleny na jednorozměrné gelové chromatografii. Separované proteiny byly přeneseny na PVDF membránu za pomocí *semi-dry* blotovacího

systému, konjugovány se specifickou primární a následně sekundární protilátkou. Detekce probíhala za pomocí chemiluminiscence na fotografický film nebo pomocí fluorescence skenováním gelu. Získaný signál byl digitalizován a počítačově vyhodnocen pomocí QuantityOne software (Bio-Rad).

5 CÍLE PRÁCE

Cílem dizertační práce byla proteomická analýza nádorové buňky a studium jejích změn po působení protinádorových léčiv.

Specifické cíle práce jsou:

- Studium specifických i společných účinků klasických protinádorových léčiv ze skupiny antracyklinů na úrovni proteomu u modelového systému hematologické nádorové buněčné linie.
- Identifikace potenciálních cílů chemorezistence proti inhibitoru cyklin-dependentních kináz v nádorové buňce reprezentující hematologickou malignitu.
- Identifikace potenciálních cílů nádorové rezistence k inhibitorům aurora kináz na modelové linii kolorektálního karcinomu reprezentující solidní tumor s přihlédnutím k fenotypu proteinu p53.
- Optimalizace relativní kvantifikace proteinů pomocí iTRAQ předcházejícího tandemové hmotnostně-spektrometrické analýze proteinových frakcí s nízkým obsahem a počtem přítomných proteinů.

6 PŘEHLED PUBLIKACÍ

P1 (Příloha 1): Cancer cells response to anthracycline effects: Mysteries of the hidden proteins associated with these drugs

Tyleckova J., Hrabakova R., Mairychova K., Halada P., Radova L., Dzubak P., Hajduch M., Kovarova H.

Int J Mol Sci (2012) *13*(12): 15536-15564; IF 2,598; citovanost 0

P2 (Příloha 2): Cancer drug-resistance and a look at specific proteins: Rho GDP-dissociation inhibitor 2, Y-box binding protein 1, and HSP70/90 organizing protein in proteomics clinical application

Skalnikova H.[#], **Martinkova J.**[#], Hrabakova R., Halada P., Dziechciarkova M., Hajduch M., Gadher S.J., Hammar A., Enetoft D., Ekefjard A., Forsstrom-Olsson O., Kovarova H.

J Proteome Res (2011) Feb 4; 10(2): 404-15; IF 5,113; citovanost 3

P3 (Příloha 3): Cancer cell resistance to Aurora kinase inhibitors: identification of novel targets for cancer therapy

Hrabakova R., Kollareddy M., **Tyleckova J**., Halada P., Hajduch M., Gadher S.J., Kovarova H.

J Proteome Res (přijaté k uveřejnění; DOI: **10.1021/pr300819m); IF: 5,113; citovanost 0**

P4 (Příloha 4): Challenges in cancer research and multifaceted approaches for cancer biomarker quest

Martinkova J., Gadher S.J., Hajduch M., Kovarova H.

FEBS Letters (2009) June 5, 583(11): 1772-84, Epub 2009 March 25; IF: 3,601; citovanost 12

P5 (Příloha 5): Relative quantification of proteins fractionated by the ProteomeLab^{TM} PF 2D system using isobaric tags for relative and absolute quantification (iTRAQ)

Skalnikova H., Rehulka P., Chmelik J., **Martinkova J.**, Zilvarova M., Gadher S.J., Kovarova H.

Anal Bioanal Chem (2007) 389: 1639-1645; IF: 2,867, citovanost 4

Publikace nesouvisející s tématem dizertační práce, ale zapadající do tématu po stránce metodické a zpracovávaného materiálu:

P6 (Příloha 6): Proteome mining of human follicular fluid reveals a crutial role of complement cascade and key biological pathways in women undergoing in vitro fertilization

Jarkovska K., **Martinkova J.**, Liskova L., Halada P., Moos J., Rezabek K., Gadher S.J., Kovarova H.

J Proteome Res (2010) Mar 5; 9(3): 1289-301; IF: 5,113; citovanost 6

7 KOMENTÁŘ K PUBLIKACÍM

7.1 Odpověď nádorové buňky na antracykliny: proteiny skryté za účinkem těchto léčiv

Cancer cells response to anthracycline effects: Mysteries of the hidden proteins associated with these drugs

Tyleckova J., Hrabakova R., Mairychova K., Halada P., Radova L., Dzubak P., Hajduch M., Gadher S.J., Kovarova H., Int J Mol Sci (2012) *13*(12): 15536-15564; IF: 2,598

V této práci jsme pomocí proteomického profilování porovnávali velmi časný účinek antracyklinových léčiv daunorubicinu (DNR) a doxorubicinu (DOXO) a antracendionu mitoxantronu (MTX) na buněčnou linii T-lymfoblastické leukemie jako modelu hematologické malignity. Hlavními cíli byla nejenom charakterizace typických markerů protinádorové odpovědi ke konkrétnímu léčivu, ale také definice biologických procesů zodpovědných za tyto reakce na léčivo a porovnání těchto tří léčiv mezi sebou, které by mohlo přispět k vysvětlení jejich rozdílného klinického použití. Abychom rozlišili typickou odpověď proti antracyklinům od obecné odpovědi nádorové buňky na léčivo, zahrnuli jsme do analýzy porovnání s dalšími dvěma protinádorovými preparáty s odlišným mechanismem účinku – cisplatinou (CisPt) a taxolem (TAX).

V naší analýze jsme se zaměřili na velmi časné účinky léčiv, které předchází nástupu apoptózy. Nejprve byla pro všechna léčiva stanovena poloviční inhibiční koncentrace léčiv IC_{50} pomocí MTT testu [35]. Protože k nástupu apoptózy dochází pro různé preparáty v různém čase, bylo nutno čas nástupu apoptózy (TA) pro používanou koncentraci léčiv 10x IC_{50} změřit pomocí aktivace kaspáz [36] a ošetření buněk tomuto času přizpůsobit, aby byla analýza mezi více léčivy objektivněji porovnatelná. Následně byla CEM T-lymfoblastická linie buněk ošetřena v polovičním čase nástupu do apoptózy (TA_{50}) koncentrací daného léčiva odpovídající 10x IC_{50} (Tabulka 1; Příloha 1, Table 1, str. 40). TA_{50} se pohyboval mezi 120 – 150 minutami s výjimkou doxorubicinu, jehož TA_{50} byl 250 minut.

Tabulka 1: Přehled analyzovaných protinádorových léčiv spolu s jejich zkratkami, mechanismem účinku a hodnotami 10x poloviční inhibiční koncentrace IC_{50} a odpovídajícího polovičního času nástupu apoptózy TA_{50}. Převzato z Tylečková et al. IJMS 2012

Anti-cancer drug	Abbreviation	Mechanism of action	10× IC_{50} (μg/mL)	TA_{50} (min)
Daunorubicin	DNR	intercalation, topo II inhibitor	0.03	120
Doxorubicin	DOXO	intercalation, topo II inhibitor	0.05	250
Mitoxantrone	MTX	intercalation, topo II inhibitor	1.88×10^{-3}	150
Cisplatin	CisPt	alkylating-like	7.57	150
Paclitaxel	TAX	mitotic inhibitor	9.00×10^{-5}	120

Buňky byly po ošetření léčivem sklizeny, promyty a lyzovány do pufru pro dvourozměrnou elektroforézu. Koncentrace proteinů ve vzorcích byla stanovena pomocí Pierce 660 nm protein assay kitu. Následně byly buněčné lyzáty separovány pomocí 2-DE ve dvou pH gradientech pH 4-7 a pH 6-11, aby došlo k pokrytí co největšího množství proteinů ve vzorcích. 2D gely byly obarveny fluorescenční barvou Sypro a digitalizovány. Vzniklé 2D mapy byly počítačově vyhodnoceny pomocí software Redfin Solo (Ludesi) pro nalezení diferenčních proteinových spot mezi léčivem neošetřenými kontrolami a vzorky ošetřenými jednotlivými léčivy. V průměru bylo detekováno 2180 proteinových spot na pH 4-7 gelech a 570 proteinových spot na pH 6-11 gelech. Celkově bylo pro všech 5 léčiv nalezeno 133 signifikantních diferenčně regulovaných proteinových spot s nárůstem abundance oproti kontrolám a 86 signifikantně regulovaných proteinových spot s poklesem abundance oproti kontrolám (fold-change >1.2 pro *p*-value <0.01 nebo fold-change >1.5 pro *p*-value <0.05). Mezi nimi bylo 40 spot regulovaných po ošetření DNR, 47 spot regulovaných po ošetření DOXO a 54 spot po ošetření MTX (Tabulka 2; Příloha 1, Table 2, str. 42). Regulované proteinové spoty byly vyřezány z preparativních gelů a proteiny v nich identifikovány pomocí MALDI-TOF/TOF MS.

Tabulka 2: Analyzovaná léčiva s počtem signifikantně regulovaných proteinových spot v porovnání s neošetřenou kontrolou spolu s trendem jejich regulace a počtem identifikovaných proteinů. Převzato z Tylečková et al. IJMS 2012

Anti-cancer drug	No. Different Spot	4–7		No. ID proteins	No. Different Spot	6–11		No. ID proteins	No. Different Spot	Total		No. ID proteins
		Up	Down			Up	Down			Up	Down	
DNR	32	8	24	24	8	1	7	5	40	9	31	29
DOXO	29	15	14	21	18	13	5	10	47	28	19	31
MTX	40	24	16	30	14	9	5	10	54	33	21	40
CisPt	24	21	3	18	23	16	7	13	47	37	10	31
TAX	29	25	4	21	2	1	1	1	31	26	5	22
Total	154	93	61	114	65	40	25	39	219	133	86	153

Proteiny, které byly identifikovány jako jeden protein v jedné proteinové spotě pro DNR, DOXO a MTX jsou znázorněny v obrázku 2 (Příloha 1, Figure 3, str.48).

Obrázek 2: Grafické znázornění identifikovaných proteinů se signifikantními změnami po ošetření nádorových CEM buněk léčivy daunorubicinem (DNR), doxorubicinem (DOXO) a mitoxantronem (MTX). Světle modré obdélníky představují buňku ošetřenou konkrétním léčivem a jednotlivé uzly představují protein označený podle genového symbolu. Barva uzlů znázorňuje biologický proces Gene Ontology podle klasifikace pomocí Panther SW (www.pantherdb.org), kdy žlutá je buněčný proces, červená produkce prekurzorů metabolitů a energie, zelená imunitní proces/odpověď na stimul, modrá metabolický proces, fialová reprodukce, šedá transport a bílou barvou jsou znázorněné proteiny, pro které nebyl biologický proces, kterého se účastní, definován. Tvar uzlů znázorňuje trend regulace, proteiny zvýšené po ošetření léčivem v porovnání s kontrolou představují trojúhelníky obrácené směrem nahoru, proteiny snížené po ošetření léčivem v porovnání s kontrolou představují trojúhelníky obrácené směrem dolů a proteiny s rozdílným trendem regulace představují kosočtverce. Převzato z Tylečková et al. IJMS 2012

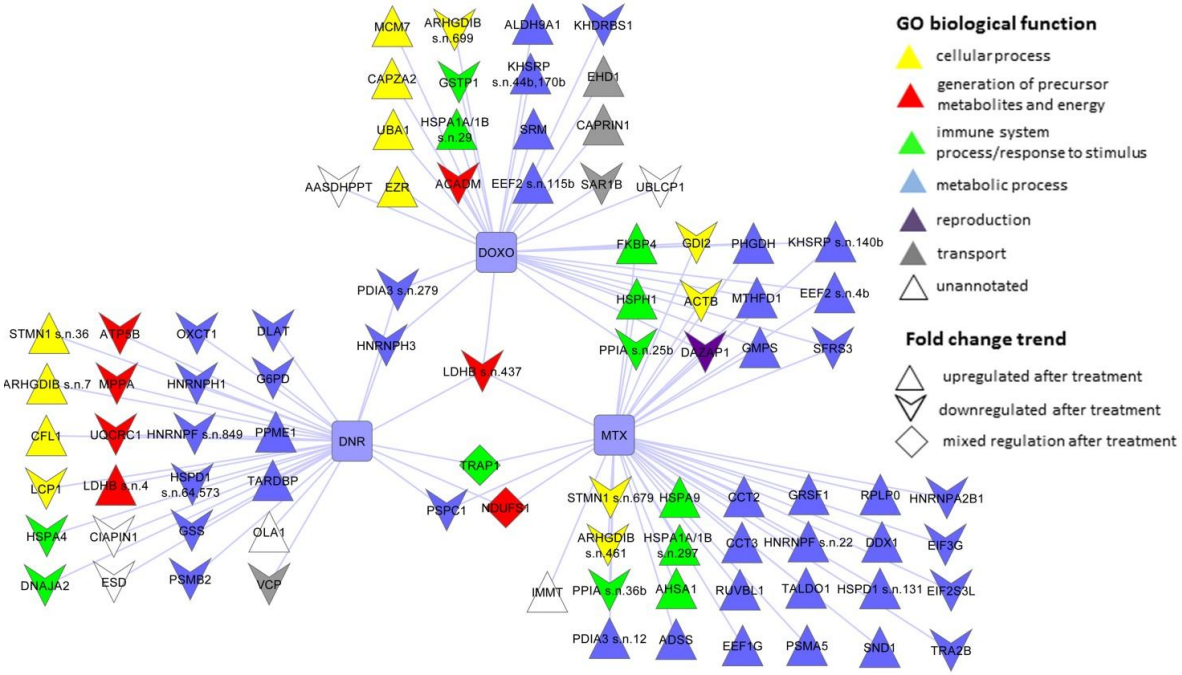

Pro daunorubicin bylo nalezeno 24 typických proteinů, oproti dalším léčivům bylo množství většiny z nich po ošetření léčivem sníženo. Typickou skupinou proteinů ovlivněných daunorubicinem je skupina proteinů účastnících se energetického metabolismu. Doxorubicin v naší analýze typicky ovlivnil 18 proteinů, za specifickou skupinu proteinů můžeme označit transportní proteiny. Největší počet léčivem ovlivněných proteinů jsme nalezli pro mitoxantron, a to 25, s naprostou převahou proteinů účastnících se metabolických procesů (Příloha 1, Figure 5, str. 50). 12 proteinových spot bylo shodně ovlivněno po působení doxorubicinu a mitoxantronu, zatímco byla nalezena pouze jedna proteinová spota shodně ovlivněná všemi třemi léčivy. Obecně nejvíce regulovaných proteinů je podle Gene Ontology klasifikováno jako proteiny metabolických procesů nukleových kyselin nebo proteinů.

Zároveň byla provedena multivariační klasifikace všech pěti studovaných léčiv spolu s neošetřenými kontrolními buňkami pomocí analýzy hlavních komponent (PCA), kde bylo zjištěno, že v první dimenzi, která má největší varianci, se oddělí antracyklinová léčiva od kontrol a ostatních léčiv. Ve druhé dimenzi se potom oddělí daunorubicin od doxorubicinu s mitoxantronem a třetí dimenze separuje hlavně daunorubicin od neošetřených kontrol (Příloha 1, Figure 6, str. 53).

Tato práce ukazuje, že i přesto, že si jsou námi studovaná tři léčiva ze skupiny antracyklinů/antracendionů strukturálně velmi blízká, odpověď nádorové buňky na ošetření těmito léčivy je pro každé z nich na proteinové úrovni specifická. Jedním z proteinů specifických pro protinádorovou odpověď na daunorubicin je zvýšení hladiny TAR DNA-binding proteinu 43 (TARDBP), což bylo povrzeno i pomocí western blotu. Tento protein je spojován s neurotoxicitou in vivo [39], microRNA biosyntézou, apoptózou i s buněčným dělením [40] a jeho zvýšení by tak mohlo přispívat k toxicitě léčiva k nádorové buňce. Mezi proteiny, které jsou specifické pro protinádorovou odpověď buněk na ošetření doxorubicinem, patří mimo jiné zvýšení hladiny spermidine syntázy, zvýšení hladiny dvou proteinových spot elongačního faktoru 2 katalyzujícího ribozomální translokaci při translaci nebo snížení hladiny proteinu KH domain-containing RNA-binding, signal transduction-associated proteinu 1. U posledních dvou jmenovaných dochází k regulaci jejich funkce pomocí fosforylace a bylo by proto vhodné zabývat se jejich posttranslačními modifikacemi a lokalizací v buňce, aby bylo možné plně objasnit jejich funkci v protinádorové odpovědi na doxorubicin. Důležitou skupinou proteinů po odpovědi buněk na doxorubicin se zdají být transportní proteiny, konkrétně snížený protein GTP-binding protein SAR1b a zvýšený Caprin-1. Toto zjištění může ukazovat na možnou úlohu proteotoxického stresu vycházejícího ze stresu v endoplasmatickém retikulu, který může vést až k apoptóze nebo k autofagii [41]. Většina změn na proteinové úrovni, které provázely ošetření mitoxantronem, byly menší či střední změny proteinů metabolických procesů. Jedním z nich je zvýšení ATPázy RuvB-like 1, které bylo potvrzeno také western blotem. Zvýšení množství tohoto proteinu bylo zjištěno u různých druhů rakoviny, v případě lidského hepatocelulárního karcinomu bylo popsáno jeho spojení s vyšší tumorigenicitou [42].

V závěru práce jsou okrajově diskutovány i proteiny, jejichž změny nejsou typické pouze pro antracyklinová léčiva. Tyto proteiny se účastní různých biologických procesů, hlavně základního buněčného metabolismu, a několik z nich jsou proteiny notoricky známé svou rolí v různých nádorových onemocněních.

Ze studie tedy vyplývá, že každé z námi studovaných léčiv je schopné indukovat specifické změny na proteinové úrovni, z nichž některé mohou objasnit molekulární mechanismy, které přispívají k protinádorové odpovědi těchto léčiv. Na druhou stranu jsme nalezli i změny proteinů, které spíše představují adaptační mechanismy, pomocí nichž se snaží nádorová buňka zajistit svůj další růst. Blokace těchto adaptačních mechanismů by se dala využít pro zlepšení odpovědi nádorové buňky na tento typ léčiv.

Podíl autora J.T. na publikaci je 70 %. J.T. je první autor práce, podílela se na plánování experimentů spolu s H.K. a M.H., prováděla 2D elektroforézu spolu s R.H., vyhodnocení výsledků 2DE, výběr spot na MS, MS identifikace pod vedením P.H., western blot verifikace spolu s R.H. a K.M., klasifikaci proteinů Gene Ontology, přípravu publikace. Podílela se spolu s H.K. a se S.G. na psaní publikace.

7.2 Rezistence nádorové buňky na léčivo se zaměřením na konkrétní proteiny: Rho GDP disociační inhibitor 2, Y-box binding protein 1 a HSP70/90 organizující protein v aplikacích klinické proteomiky

Cancer drug-resistance and a look at specific proteins: Rho GDP-dissociation inhibitor 2, Y-box binding protein 1, and HSP70/90 organizing protein in proteomics clinical application

Skalnikova H.[#], Martinkova J.[#], Hrabakova R., Halada P., Dziechciarkova M., Hajduch M., Gadher S.J., Hammar A., Enetoft D., Ekefjard A., Forsstrom-Olsson O., Kovarova H., J Proteome Res (2011) 10(2): 404-15; IF 5,46

V této práci byly pomocí proteomických technik analyzovány změny spojené s rozvojem získané rezistence k inhibitoru cyklin-dependentních kináz (CDKs), boheminu. Primárním cílem byla identifikace potenciálních cílů rezistence v buňce. Studie odhalila klíčovou úlohu proteinů Rho GDP disociačního inhibitoru 2, Y-box binding proteinu 1 a HSP70/90 organizujícího proteinu. Dále byly tyto proteiny validovány v dalších buněčných liniích rezistentních k jiným léčivům jako je vinkristin nebo daunorubicin.

Práce je založena na porovnání rozdílů v proteinovém složení mezi buněčnou linií CEM rezistentní k CKD inhibitoru boheminu (CEM-BOH) a její mateřskou linií CEM, která je na léčivo citlivá. Proteiny buněčných lyzátů byly frakcionovány pomocí dvourozměrné kapalinové chromatografie PF 2D. Celkem byly lyzáty rozděleny na 15 pI frakcí s více než 1200 proteinovými píky. Výsledné proteomové mapy, konstruované z chromatografických profilů, byly vyhodnoceny novým SW Viper (Ludesi, Švédsko). Bylo nalezeno celkem 6 frakcí obsahujících diferenční proteinové píky s hodnotou pravděpodobnosti $p < 0,05$ a dalších 12 frakcí obsahujících píky s fold change větší než 1,6. Proteiny v těchto frakcích byly identifikovány pomocí MS. Celkem bylo identifikováno 26 různých proteinů, mezi nimi bylo několik ribozomálních proteinů velké 60S ribozomální podjednotky (proteiny L4, L6, L7a, L15 a L26), stejně jako malé ribozomální 40S podjednotky (S4_X izoforma, S8, S13, S24 a S25). Dále bylo detekováno několik variant histonů (histon H2A typ 1-H, histon H2B typ 1-B, typ 1-D a typ 1-J a histon H4). Změny v množství těchto ribozomálních proteinů a histonů můžou ukazovat na deregulaci translace

a transkripce, případně i epigenetické regulace. Toto bylo pozorováno i u modelování možných interakčních sítí, které spojují interakční partnery identifikovaných proteinů (Příloha 2, Figure 7, str. 76).

Následně jsme se zaměřili na detailní verifikaci proteinů se signifikantním nárůstem v rezistentní CEM-BOH linii, a to proteiny Rho GDP disociačního inhibitoru 2 (Rho GDI2), Y-box binding proteinu 1 (YB-1) a HSP70/90 organizujícího proteinu (Hop) pomocí imunoblotu a imunohistochemie. Tyto proteiny mohou mezi nalezenými představovat nejvhodnější potenciální cíle léčiv. Nejprve byla provedena analýza celkových buněčných lyzátů pomocí western blotu. Pro Rho GDI2 se podařil potvrdit jeho nárůst v rezistentních buňkách. Pro další dva proteiny se ale změna mezi senzitivní a rezistentní linií na celobuněčném lyzátu nepotvrdila. Dále byly proteiny verifikovány přímo v PF 2D pH frakcích. Na těchto frakcích byla pozorována přítomnost kyselých pH izoforem YB-1 proteinu v senzitivních buňkách, které nebyly přítomné u rezistentních buněk. Oproti tomu pro Hop byl pozorován posun ke kyselým izoformám proteinu v rezistentních buňkách. Dále jsme pro Hop protein sledovali jeho lokalizaci v buňce pomocí imunohistochemie vzhledem k dosud publikovaným pracím [43, 44], podle kterých by měla fosforylace proteinu mít vliv nejenom na jeho lokalizaci ale i na buněčnou funkci. V senzitivních buňkách byl protein lokalizován hlavně v jádře asociovaný s chromozomy, zatímco v rezistentních buňkách byla jeho lokalizace kromě jádra i v cytoplazmě.

Detailní verifikace pomocí imunoblotu pro YB-1 a Hop proteiny tak odhalila, že pozorované změny se týkají spíše než celkového množství proteinů změn různých proteinových variant nebo modifikací mezi citlivou a rezistentní linií buněk.

Proteiny byly dále studovány na buněčných liniích CEM rezistentních k vinkristinu a daunorubicinu (CEM-VCR, CEM-DNR) a na buněčné linii A549 jako modelu solidního tumoru rezistentního k boheminu a vinkristinu (A549-BOH, A549-VCR). Pomocí imunoblotu byl zjištěn nárůst proteinu Rho GDI2 ve všech rezistentních liniích v porovnání se senzitivními buňkami. Pro YB-1 byl pozorován jeho pokles v CEM-VCR a CEM-DNR liniích pro celý 50 kDa protein, dále byla pozorována přítomnost zkrácené 20 kDa formy a nárůst zkrácené 32 kDa izoformy proteinu u A549-BOH. Celkové množství proteinu Hop nevykazovalo na úrovni celobuněčných lyzátů žádné změny.

Rho GDI2 patří do rodiny GDP disociačních inhibitorů, které regulují GTPázy, včetně proteinů Ras1, Cdc42 nebo RhoA. Zvýšená exprese Rho GDI2 v některých typech nádorových buněk rezistentních k protinádorovým léčivům již byla popsána v předchozích studiích [45]. V naší práci byl potvrzen nárůst v množství tohoto proteinu u všech námi sledovaných linií. Mechanismus, kterým může Rho GDI2 přispívat k rezistenci k léčivu, je pravděpodobně spojen s jeho antiapoptotickým účinkem. Rho GDI2 proto podle nás představuje slibný potenciální marker rezistence pro různá léčiva u různých druhů rakoviny.

YB-1 je proteinem z cold shock domain proteinové rodiny s různými funkcemi v regulaci transkripce, translace, oprav DNA a buněčné odpovědi na prostředí [46]. Jeho aktivita a lokalizace může být regulována fosforylací i jeho proteolýzou v proteazomu [47]. Zkrácená izoforma YB-1 byla detekována v CEM i A549 rezistentních buňkách k boheminu, vinkristinu i daunorubicinu. Toto pozorování souhlasí s rolí proteazomem zkrácené formy YB-1 ve vzniku rezistence [46, 47]. Zároveň jsme prokázali přítomnost více bazických forem YB-1 typických pro bohemin-rezistentní buňky. Tento posun může být způsoben právě rozdílnou fosforylací proteinu [48].

Protein Hop je ko-chaperonem molekulárních chaperonů Hsp70 a Hsp90 [49]. Nejlépe popsanou známou funkcí tohoto proteinu je jeho role v přenosu signálu steroidních receptorů včetně odpovědi na glukokortikoidy [50]. V naší studii byl Hop v rezistentních buňkách posunut k více kyselému pH, což může znamenat jeho zvýšenou fosforylaci v těchto buňkách. Tento posun se zdá být spojen i se změnou jeho lokalizace, kdy u rezistentních buněk je lokalizován kromě jádra také v cytoplazmě. Na základě těchto výsledků můžeme usuzovat, že změny v posttranslačních modifikacích Hop proteinu jsou spojeny s rozvojem rezistence k boheminu díky ovlivnění přenosu signálu přes steroidní receptory.

Výsledky této práce naznačují, že pro rozvoj rezistence k protinádorovým léčivům nejsou důležité pouze proteinové změny na kvalitativní/kvantitativní úrovni, ale že důležitou úlohu hrají také další parametry jako jsou zkrácené formy proteinů s jinou biologickou rolí, posttranslační modifikace vedoucí ke změnám pI proteinů stejně tak jako jejich lokalizace uvnitř buněk, které tak mohou kontrolovat odpověď nádorové buňky na léčivo.

Podíl autora J.M. na publikaci je 40 %. J.M. je spolu s H.S. prvním autorem práce. J.M. prováděla separace proteinů pomocí PF 2D, analýzu 2D map, podílela se na veškerých verifikacích proteinů pomocí imunoblotu i analýze jejich výsledků a na plánování a psaní publikace.

7.3 Rezistence nádorové buňky k inhibitorům aurora kináz: identifikace nových cílů nádorové terapie

Cancer cell resistance to Aurora kinase inhibitors: identification of novel targets for cancer therapy

Hrabakova R., Kollareddy M., Tyleckova J., Halada P., Hajduch M., Gadher S.J., Kovarova H., J Proteome Res (přijaté k uveřejnění; DOI: 10.1021/pr300819m); IF: 5,113

V této práci jsme se zaměřili na rozdíly v proteinovém složení buněčných lyzátů buněk kolorektálního karcinomu HCT116 citlivých a rezistentních k inhibitorům aurora kináz (AURKs) CYC116 a ZM447439 za použití dvourozměrné gelové elektroforézy a MALDI-TOF/TOF MS. Protože byla v nedávno publikovaných studiích popsána spojitost mezi inhibicí AURKs a stavem proteinu p53 [51, 52], zahrnuli jsme do analýzy jak wild type $p53^{+/+}$ tak i mutované $p53^{-/-}$ HCT116 buňky a sledovali jsme tak i rozvoj rezistence k inhibitorům AURKs v závislosti na fenotypu p53 v nádorových buňkách.

Rezistentní klony buněk byly odvozeny z citlivých linií $p53^{+/+}$ a $p53^{-/-}$ HCT116 buněk krátkodobým ošetřením 1μm AURK inhibitorem CYC116 i ZM447439. Po pěti týdnech bylo získáno několik rezistentních klonů, které měly řádově vyšší hodnotu poloviční inhibiční koncentrace IC_{50} v porovnání s mateřskými liniemi. Pro analýzu byly vybrány 4 klony rezistentní k CYC116, z nichž klony R1.2 a R1.3 nesly wild-type alelu $p53^{+/+}$ a klony R2.1 a R2.2 mutovanou $p53^{-/-}$, a 4 klony rezistentní k ZM447439, z nichž klony R3.1 a R3.2 nesly wild-type alelu $p53^{+/+}$ a klony R4.2 a R4.3 mutovanou $p53^{-/-}$ (Obrázek 3).

Obrázek 3: Analyzované klony HCT116 buněk rezistentních k AURKs inhibitorům ZM447439 a CYC116. Rezistentní klony nesoucí wild type (WT) alely $p53^{+/+}$ byly porovnány s kontrolní (CT) sensitivní linií HCT116 buněk nesoucí wild type alely $p53^{+/+}$, rezistentní klony s mutovaným proteinem $p53^{-/-}$ byly porovnány s kontrolní sensitivní linií s mutovaným proteinem $p53^{-/-}$. Převzato z Hrabakova et al. JPR 2012

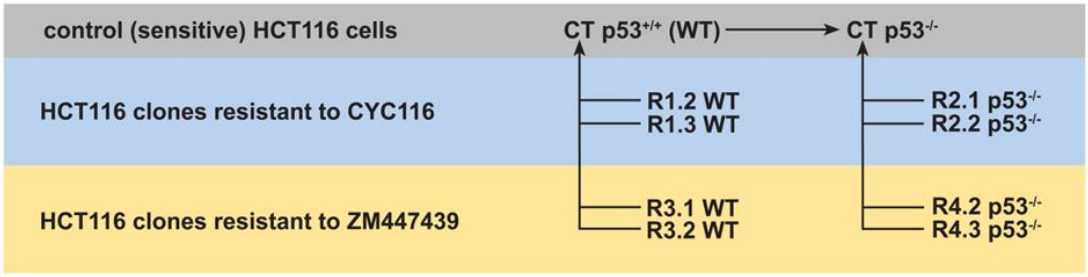

Buňky byly kultivovány do 80% konfluence, promyty PBS a přímo na miskách lyzovány do pufru pro 2-DE. Proteinové lyzáty byly rozděleny pomocí 2-DE, v první dimenzi na dvou pH gradientech, pH 4-7 a pH 6-11, ve druhé dimenzi na 12% polyakrylamidovém gelu. Po obarvení byly proteinové spoty v gelech vizualizovány fluorescenčním barvením a vzniklé proteinové mapy rezistentních klonů byly porovnány s příslušnými citlivými mateřskými liniemi (Obrázek 3). Diferenční proteinové spoty s hodnotou *p*-value < 0.05 a minimální změnou fold change > 1.2 byly následně vyříznuty a identifikovány pomocí MALDI-TOF/TOF hmotnostní spektrometrie. Celkem bylo ve 144 proteinových spotách identifikováno 127 proteinů. 6 vybraných proteinů jsme verifikovali pomocí western blotu u všech 8 HCT116 rezistentních klonů a jejich kontrolních senzitivních linií (Obrázek 4A). 4 z těchto 6 proteinů byly dále vybrány pro western blotové

verifikace na liniích lymfoblastické leukémie a plicního adenokarcinomu rezistentních k několika protinádorovým léčivům s různým mechanismem účinku (Obrázek 4B).

Většina proteinových změn byla pozorována pouze u individuálních klonů nádorových buněk. Pro buňky rezistentní k inhibitoru CYC116 jsme nalezli pět specifických proteinů se signifikantními změnami ve všech 4 rezistentních klonech oproti citlivým kontrolám, které tak nesouvisely se stavem proteinu p53 v těchto klonech, a to translationally-controlled tumor protein, 60 kDa heat shock protein, heterogeneous nuclear ribonucleoprotein G, leukocyte elastase inhibitor a serin hydroxymethyltransferáza (Příloha 3, Figure 3). Modelování protein-proteinových interakcí těchto pěti proteinů odhalilo jejich přímou interakci přes autophagy protein 5 a WD repeat domain phosphoinositide-interacting protein 2 (Příloha 3, Figure 5), která ukazuje na možnou roli procesů autofagie v mechanismu rezistence k inhibitoru AURK CYC116. Navíc serin hydroxymethyltransferáza již byla popsána jako potenciální cíl nádorové terapie [53]. Hladina tohoto proteinu byla v naší práci zvýšena nejenom u HCT116 buněk rezistentních k CYC116, ale také v dalších dvou buněčných liniích CEM a A549 rezistentních k jiným léčivům (Obrázek 4B). Tento protein tak představuje potenciální cílovou molekulu pro překonání rezistence k nádorové terapii.

Jako specificky regulovaný protein v rezistentních buňkách s wild-type alelami p53 oběma inhibitory CYC116 i ZM447439 byl nalezen elongační faktor 2. Na druhou stranu mezi proteiny specificky regulované v $p53^{-/-}$ buňkách rezistentních k oběma inhibitorům patří známý protein s ochranou funkcí proti oxidačnímu stresu lyzozym C a anti-apoptotický protein 78 kDa glucose-regulated protein.

Co se týká proteinů specificky regulovaných pouze v buňkách rezistentních k inhibitoru ZM447439, hladina proteinu PAF acetylhydrolázy byla snížena v $p53^{-/-}$ klonech a hladina proteinu GTP-binding nuclear protein Ran byla zvýšena pouze v $p53^{+/+}$ klonech (Obrázek 4A). Oba tyto proteiny také představují nové slibné molekulární cíle v nádorové terapii [54, 55].

Mezi proteiny extrémně zajímavými z hlediska rozvoje rezistence patří proteiny související s regulací apoptózy. Jedním z takovýchto proteinů, který byl v naší práci nalezen ve zvýšeném množství nejen u buněk kolorektálního karcinomu, ale i u buněk lymfoblastické leukémie a plicního adenokarcinomu, je serpin B5. Dalšími proteiny související s apoptózou nalezenými v naší práci jsou kalretinin a voltage-dependent anion-selective channel protein 2. U těchto dvou proteinů bylo prokázáno jejich zvýšení v AURK rezistentních buňkách i v buňkách A549 (Obrázek 4).

Obrázek 4: Verifikace vybraných proteinových změn pomocí western blotu. 4A) Analýza hladin šesti proteinů, β-tubulin sloužil jako kontrola nanášky. Vzorky HCT116 buněk citlivých k inhibitorům Aurora kináz jsou označeny jako CT, buňky nesoucí wild-type alely proteinu p53 jako WT, buňky nesoucí mutované alely proteinu p53 jako -/-.

Vzorky buněk rezistentních k inhibitorům Aurora kináz jsou označeny příslušným inhibitorem ZM447439 a CYC116 a označením klonu. 4B) Analýza hladin proteinů serpin B5, kalretinin, voltage-dependent anion-selective channel protein 2 a serine hydroxymethyltransferázy v lyzátech buněk CEM lymfoblastické leukémie a A549 plicního adenokarcinomu. Kontrolní citlivé buňky jsou označeny jako CT, buňky rezistentní k daunorubicinu DNR, vinkristinu VCR, cytarabinu ARA a taxolu TAX. Převzato z Hrabáková et al. JPR 2012

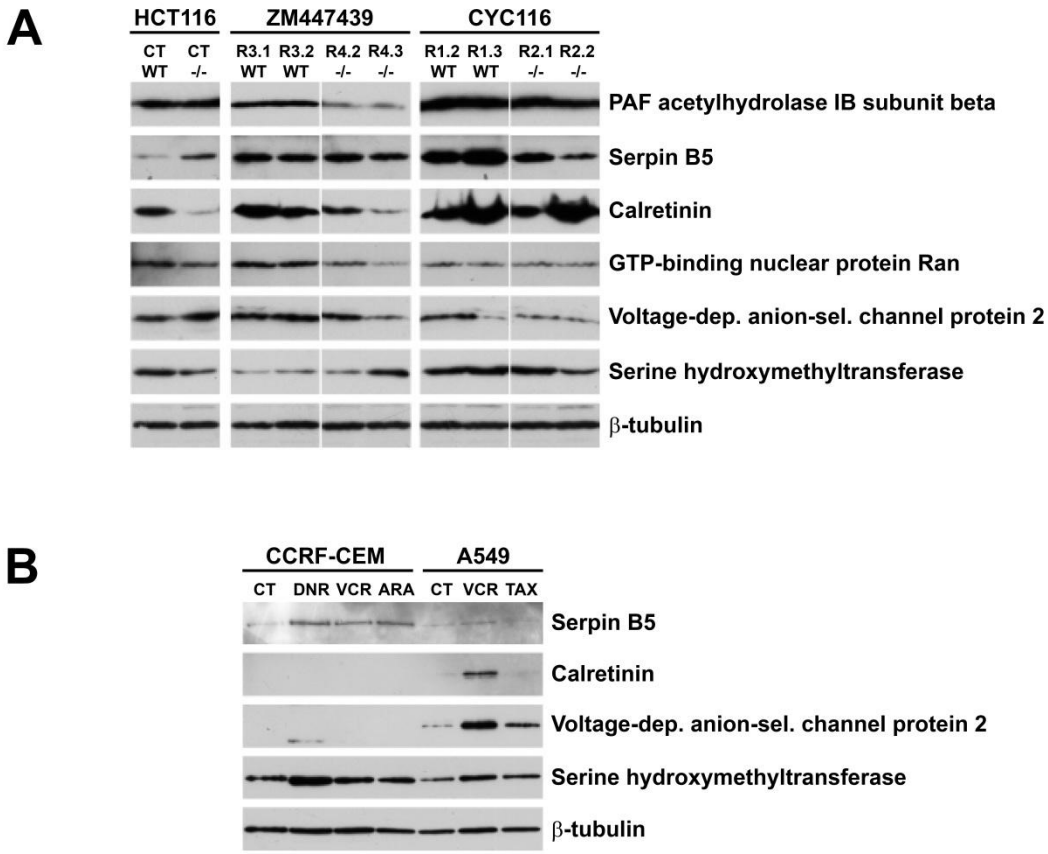

Výše jmenované proteiny tedy mohou přispívat k rozvoji rezistence k Aurora kinázovým inhibitorům. Navíc byly prokázány změny v hladinách proteinů serin hydroxymethyltransferáza, serpin B5, kalretinin a voltage-dependent anion-selective channel protein 2 u leukemických buněk CEM a buněk plicního karcinomu A549 rezistentních k jiným typům protinádorových léčiv. Tyto proteiny tak mohou představovat nové molekulární cíle pro překonání rezistence na léčiva. Hladiny některých proteinů vybraných z této práce jsou v současné době analyzovány v pacientských vzorcích a jsou předmětem patentové ochrany.

Podíl autora J.T. na publikaci je 30 %. J.T. se podílela na 2D elektroforézách včetně optimalizací protokolu, MS identifikacích a verifikacích proteinů pomocí western blotu.

7.4 Problematika výzkumu rakoviny a možnosti studia nádorových biomarkerů

Challenges in cancer research and multifaceted approaches for cancer biomarker quest

Martinkova J., Gadher S.J., Hajduch M., Kovarova H., FEBS Letters (2009) 583: 1772-1784; IF: 3,601

V tomto přehledném článku shrnujeme z pohledu hlavně proteomického přístupu poslední výsledky ve výzkumu nádorových biomarkerů.

Pojmem rakovina označujeme heterogenní skupinu onemocnění, která jsou zodpovědná za velké procento celkové úmrtnosti v populaci. Poznatky z biologie nádorů ukázaly, že se normální buňka transformuje v nádorovou díky několikanásobným změnám v jejím genomu. Tyto změny významně zasahují do signálních sítí v buňce [56], narušují buněčnou komunikaci a tím přispívají ke vzniku a progresi rakoviny. Proto identifikace takto postižených genů a na ně navazujících signálních drah a jejich cílů může ve velké míře přispět ke zlepšení prevence, diagnostiky, prognostiky a cílené terapie nádorových onemocnění. Hlavním cílem na míry šité protinádorové terapie je použití aktivní dávky léčiva přímo zacílené na konkrétní tumor s definovaným molekulárním profilem. Několik takových nových molekulárně cílených léčiv již bylo schváleno k použití nebo jsou v klinických testech [57, 58, 59, 60], i když se ukazuje, že jako monoterapie často selhávají a proto je potřeba jejich použití v kombinovaných terapiích, kdy je zacíleno na stejnou signální dráhu, případně na dvě různé dráhy nebo kombinace cíleného léčiva s konvenční chemoterapií [61].

Diagnostika pacienta s rakovinou a rozhodnutí o léčbě je v současnosti založeno hlavně na histologickém hodnocení nádoru patologem (tzv. gradingu). Tato morfologická klasifikace ale nemusí být dostatečná pro identifikaci a klasifikaci mnoha rozdílných subtypů choroby. Zahrnutí genomických a transkriptomických dat mohou tuto charakterizaci spojenou se specifickým nádorovým fenotypem významně zlepšit [25]. Transkriptomické studie se zaměřují na změny v hladinách mRNA stejně jako změny v alternativním splicingu [62]. Tyto vysoce výkonné analýzy za použití cDNA mikroarayí umožňují screening s rakovinou spojených genů a charakterizaci molekulárních znaků diferenčně exprimovaných genů mezi normální a nádorovou tkání. Tento molekulární přístup následně umožní objektivní klasifikaci nádorů. Dále byly studie pomocí mikroarayí použity při monitorování protinádorové terapie klasickými [63, 64] i cílenými léčivy [65]. Limitace, které v současnosti zabraňují plnému využití této techniky v klinické analýze, se kromě technických problémů týkají hlavně nutnosti použít čerstvě zamražené vzorky tkání a omezená znalost specifické funkce mnoha genů [66]. Metodiky, které jsou použitelné i na formalínem fixované parafínové preparáty, zahrnují qRT-PCR anebo DASL (cDNA

mediated annealing, selection, extension and ligation) a mohou tak být použity pro větší retrospektivní studie [67].

V recentních pracích bylo dále dokázáno, že na rozvoji nádorových onemocnění se mohou podílet i miRNA [68, 69], které regulují celou řadu biologických procesů včetně růstu, diferenciace a apoptózy. Analýza exprese 217 miRNA ve 334 vzorcích různých nádorů umožnila seskupení těchto nádorů podle tkání původu a jejich porovnání s normální tkání odráželo stadium diferenciace [70]. Pro tuto analýzu bylo využito modifikace multiplexové Luminex xMAP technologie, což je metoda, která se dá úspěšně využít i pro multiplexovou analýzu proteinů z komplexních vzorků.

Proteomické metody pro studium nových nádorových markerů oproti genomickým nebo transkriptomickým metodám lépe odráží aktuální stav s rakovinou spojených změn molekul a signálních drah. Tyto nádorové markery jsou buď přímo sekretované nádorovou buňkou nebo jsou reakcí okolí na nádor. Vyskytují se proto v největší koncentraci v tkáňové intersticiální tekutině a čím dále jsou od místa jejich sekrece tím více jejich koncentrace klesá. Výhodným materiálem pro studim nádorových markerů je krevní plazma/sérum a to díky své snadné dostupnosti. Zároveň ale plazma představuje velmi komplexní materiál s obrovským koncentračním rozdílem mezi různými proteiny a nádorové markery jsou v krevní plazmě podstatně naředěné. Analýze nádorových markerů v různých tělesných tekutinách se věnuje celá řada prací [71, 72].

K identifikaci nových diagnostických nebo prognostických biomarkerů charakterizujících rozvoj nebo progresi nádorů nebo cílů léčiv se často používá proteomických technik zaměřených na přímou analýzu nádorových buněk nebo tkání. Pomocí DIGE bylo analyzováno 64 benigních, hraničních i maligních vzorků tkání z ovariálních tumorů. Multivariační klasifikační analýza umožnila rozdělit tyto vzorky do skupin podle progrese rakoviny a zároveň signifikantní změny v proteinových spotách, které byly za toto rozdělení zodpovědné, představují potenciální diagnostické nádorové markery [73]. Další rozsáhlá studie využívající DIGE byla publikována skupinou Kondo a kol. [74]. Studie věnující se invazivitě nádorových buněčných linií využila metodiky MudPIT (Mutlidimensional Protein Identification Technology) [75].

Rostoucí zájem je věnován hledání nových markerů pro monitorování protinádorové terapie. Takovéto markery by přispěly k rozhodnutí o nejúčinnější možné terapii s minimem negativních účinků. Proteinové mikroaraye byly použity pro predikci protinádorové odpovědi u skupiny 60 lidských nádorových buněčných linií, tzv. NCI-60 panelu [76]. Celkem byla sledována aktivita 118 agens měřením růstové inhibice po 48 hodin a sledováním celkem 52 protilátek. Z výsledků lze předpovědět chemosenzitivitu k těmto 118 preparátům bez jakéhokoliv sledování mechanismu jejich účinku. Pomocí detailních proteomických studií používajících komparativní analýzu změn v množství proteinů po ošetření léčivem lze určit možné molekulární mechanismy účinku léčiv, respektive mechanismů vzniku rezistence k terapii. Studie jsou shrnuty v článku v tabulce 2. (Příloha

4, Table 2, str. 102-104) Většina těchto studií se ale zaměřuje na pozdní časové intervaly po působení léčiva, kdy již dochází k významnému rozvoji procesů směřujících k apoptóze. Proto monitorování molekulárních mechanismů, které nástupu apoptózy předcházejí v časných intervalech po expozici léčivem, může lépe přispět k pochopení primárních změn v signálních drahách, které později vedou k buněčné smrti.

Podíl autora J.M na publikaci je 40 %. J.M. prováděla rešerši literatury, podílela se významným způsobem na přípravě struktury publikace i a na jejím sepsání.

7.5 Relativní kvantifikace proteinů frakcionovaných pomocí ProteomeLab™ PF 2D systému za použití izobarického značení pro relativní a absolutní kvantifikaci (iTRAQ)

Relative quantification of proteins fractionated by the ProteomeLab™ PF 2D system using isobaric tags for relative and absolute quantification (iTRAQ)

Skalnikova H., Rehulka P., Chmelik J., Martinkova J., Zilvarova M., Gadher S.J., Kovarova H., Anal Bioanal Chem (2007) 389: 1639-1645; IF: 2,867

Práce popisuje optimalizovaný protokol izobarického značení pro relativní a absolutní kvantifikaci iTRAQ a tandemové hmotnostní spektrometrie, kterého lze využít pro relativní kvantifikaci proteinů rozdělených pomocí dvourozměrné kapalinové chromatografie na systému ProteomeLab™ PF 2D.

Dvourozměrná separace komplexních proteinových vzorků jako jsou například sérum nebo buněčné lyzáty pomocí 2D-HPLC systému PF 2D probíhá v první dimenzi na chromatofokusační koloně a ve druhé na reverzní fázi. Kvantifikace proteinů probíhá pomocí UV detekce a jednotlivé separované kapalné frakce jsou sbírány pro případné další analýzy například identifikace proteinů hmotnostní spektrometrií. Kvantifikace pomocí UV má ovšem své limity v případě, kdy ve stejné frakci koeluuje najednou více proteinů. I pro tento případ jsme upravili protokol, který využívá značení peptidů iTRAQ. Tato technika je založena na chemickém označení N-konců peptidů po tryptickém digestu proteinů. Pro různé vzorky buněčných proteinových lyzátů kultivovaných v různých podmínkách se používají různě těžké značky, naznačené vzorky jsou následně spojeny a analyzovány tandemovou MS. Fragmentované peptidy jsou nejprve prohledány proti databázi za účelem identifikace peptidů, resp. příslušných proteinů. Zároveň dochází k fragmentaci značky na nízkomolekulární tzv. reportérový iont, který je unikátní pro každý vzorek. Porovnání intenzit reportérových iontů umožňuje relativní kvantifikaci na peptidové úrovni. V době provedení studie byly komerčně k dispozici čtyři různé značky poskytující reportérové ionty

s *m/z* 114, 115, 116 a 117 Da a tím bylo možno relativně kvantifikovat až 4 různé vzorky v jednom experimentu.

Původní iTRAQ analýza je určena pro značení a kvantifikaci asi 5-100 µg komplexních proteinových směsí. Pro množství proteinů pod 0,5 µg tryptického digestu bovinního albuminu nebyl detekován signál specifických peptidů, a to pravděpodobně díky přítomnosti interferujících látek jako je SDS, TCEP a autolytické produkty trypsinu. Množství proteinů v jedné frakci po frakcionaci na PF 2D se ale obvykle pohybuje mezi 0,01 a 0,5 µg. Proto jsme standardní výrobcem doporučovaný protokol pro značení pomocí iTRAQ optimalizovali. Hlavní změny spočívají v nahrazení 0,1 % SDS v rozpouštěním pufru 1 M močovinou, použití řádově menšího množství modifikovaného Promega trypsinu, který nepodléhá autolýze v takové míře jako nemodifikovaný trypsin, celkové redukci reakčním objemů minimálně desetkrát a purifikaci a zakoncentrování vzorků na mikrokolonách naplněných materiálem Poros R2.

Proveditelnost modifikovaného protokolu jsme demonstrovali na vzorcích buněčného lyzátu T-lymfoblastické linie CEM buněk bez a po ošetření CDK inhibitorem boheminem, které byly frakcionovány pomocí PF 2D. Konkrétní proteinová frakce s pI 4,9-5,2 a retenčním časem 17,2-17,3 minuty vykazovala na UV 1,94 násobný nárůst v ošetřených buňkách v porovnání s neošetřenou kontrolou. Celkem se nám podařilo v této frakci po označení iTRAQ značnami s *m/z* 117 (CDKI ošetřené buňky) a 114 (kontrola) identifikovat a kvantifikovat na MALDI-TOF/TOF spektrometru 6 peptidů vimentinu s průměrným nárůstem 2,26 ± 0,2, což je v dobré shodě s kvantifikací pomocí UV.

Námi optimalizovaný protokol umožňuje s vysokou citlivostí relativně kvantifikovat malá množství proteinů/peptidů pomocí značení iTRAQ na MALDI-TOF/TOF bez nutnosti další separace značených peptidů, čímž zároveň dojde k významnému zjednodušení komplexity dat.

Podíl autora J.M. na publikaci je 15 %. J.M. se podílela na frakcionaci proteinů pomocí PF 2D a na zpracování a značení PF 2D frakcí pro MS analýzu.

8 ZÁVĚR

Rakovina je i přes současné pokroky v porozumění nádorové biologii a nových léčebných strategiích stále druhou nejčastější příčinou úmrtí v rozvinutých zemích. Studie zabývající se molekulárními mechanismy, kterými působí konvenční, cílená i experimentální léčiva na nádorové buňky a které mohou odhalit markery protinádorové odpovědi a/nebo rezistence i nové cíle léčiv jsou jednou z priorit celosvětového základního i klinického výzkumu. Přitom právě validace experimentálních dat a jejich zavedení do klinického využití představuje nejnáročnější část tohoto úkolu.

V této dizertační práci jsem sledovala účinek konvenčních protinádorových léčiv ze skupiny antracyklinů/antracendionů na nádorovou buňku na proteinové úrovni. Práce odhalila, že každé z námi studovaných léčiv vyvolává specifickou protinádorovou odpověď bez ohledu na vysokou strukturní podobnost těchto léčiv. Zároveň byly nalezeny změny v proteinech, které jsou společné pro tato léčiva. Nejrozdílnější ze studované skupiny antracyklinových léčiv byl shledán daunorubicin. Výsledky mohou napomoci k vysvětlení rozdílného klinického využití těchto léčiv.

Dále jsme charakterizovali změny v proteomu buněk po získání chemorezistence ke slibnému experimentálnímu preparátu ze skupiny inhibitorů cyklin-dependentních kináz boheminu. Výsledky odhalily obecnou deregulaci v transkripci a translaci u chemorezistentních buněk a regulační roli proteinů Y-box binding protein 1 a HSP70/90 organizující protein v rozvoji rezistence k tomuto preparátu. Důležité jsou nejenom kvantitativní změny v celkovém množství proteinů, ale také změny na úrovni posttranslačních modifikací nebo rozdílné role jednotlivých proteinových forem. Dále se podařilo odhalit potenciální víceúčelový marker rezistence k různým cytostatickým léčivům, a to Rho GDP-disociační inhibitor 2.

Identifikovali jsme nové potenciální molekulární cíle nádorové terapie na buněčných liniích rezistentních k aurora kinázovým inhibitorům. Mezi klíčové molekuly patří serin hydroxymethyltransferáza, PAF acetylhydroláza, GTP-binding nuclear protein Ran, serpin B5, voltage-dependent anion-selective channel protein 2 nebo kalretinin.

Zavedli jsme optimalizovaný protokol pro relativní kvantifikaci proteinů separovaných pomocí dvourozměrné kapalinové chromatografie na systému ProteomeLab PF 2D isobarickým značením iTRAQ. Tento protokol je oproti původnímu protokolu citlivější a umožňuje tak kvantifikovat i proteiny o velmi nízké koncentraci z frakcí obsahujících směs proteinů.

Stále zůstává potřeba dalších následných validačních studií námi identifikovaných proteinů/potenciálních markerů, aby bylo možno uvažovat o jejich případném klinickém využití.

9 SEZNAM ZKRATEK

2-DE	dvourozměrná gelová elektroforéza
2D-HPLC	dvourozměrná kapalinová chromatografie
A549-BOH	A549 buněčná linie rezistentní k boheminu
A549-VCR	A549 buněčná linie rezistentní k vinkristinu
ARA	cytarabin
AURKs	Aurora kinázy
CDKs	cyklin-dependentní kinázy
CDKI	inhibitor cyklin-dependentních kináz
CEM-BOH	CEM buněčná linie rezistentní k boheminu
CEM-DNR	CEM buněčná linie rezistentní k daunorubicinu
CEM-VCR	CEM buněčná linie rezistentní k vinkristinu
CisPt	cisplatina
DASL	cDNA mediated annealing, selection, extension and ligation
DNR	daunorubicin
DOXO	doxorubicin
Hop	HSP70/90 organizing protein
IC_{50}	poloviční inhibiční koncentrace
ICPL	isotope coded protein labeling
iTRAQ	isobaric tags for relative and absolute quantification
MS	hmotnostní spektrometrie
MTX	mitoxantron
PCA	analýza hlavních komponent (principal component analysis)
PMF	peptide mass fingerprinting
Rho GDI2	Rho GDP-dissociation inhibitor 2
SILAC	stable isotope labeling by amino acidc in cell culture
SRM	selected reaction monitoring
TA	čas nástupu do apoptózy
TAX	taxol
VCR	vinkristin
YB-1	Y-box binding protein 1

10 SEZNAM CITOVANÉ LITERATURY

1. Adam, Z.; Vorlíček, J.; Koptíková, J.; al., e., *Obecná onkologie a podpůrná léčba*; Grada: **2003**; p. 788; ISBN 80-247-0677-6.
2. Hanahan, D.; Weinberg, R.A. The hallmarks of cancer. *Cell* **2000**, *100*, 57-70.
3. Hanahan, D.; Weinberg, R.A. Hallmarks of cancer: the next generation. *Cell* **2011**, *144*, 646-674.
4. Weinberg, R.A. *The biology of cancer* Garland Science: **2006**; p. 796; ISBN 0-8153-4076-1
5. Chabner, B.A.; Roberts, T.G., Jr. Timeline: Chemotherapy and the war on cancer. *Nat Rev Cancer* **2005**, *5*, 65-72.
6. Carvalho, C.; Santos, R.X.; Cardoso, S.; Correia, S.; Oliveira, P.J.; Santos, M.S.; Moreira, P.I. Doxorubicin: the good, the bad and the ugly effect. *Curr Med Chem* **2009**, *16*, 3267-3285.
7. Nitiss, J.L. Targeting DNA topoisomerase II in cancer chemotherapy. *Nat Rev Cancer* **2009**, *9*, 338-350.
8. Simunek, T.; Sterba, M.; Popelova, O.; Adamcova, M.; Hrdina, R.; Gersl, V. Anthracycline-induced cardiotoxicity: overview of studies examining the roles of oxidative stress and free cellular iron. *Pharmacol Rep* **2009**, *61*, 154-171.
9. Minotti, G.; Menna, P.; Salvatorelli, E.; Cairo, G.; Gianni, L. Anthracyclines: molecular advances and pharmacologic developments in antitumor activity and cardiotoxicity. *Pharmacol Rev* **2004**, *56*, 185-229.
10. Scott, A.M.; Wolchok, J.D.; Old, L.J. Antibody therapy of cancer. *Nat Rev Cancer* **2012**, *12*, 278-287.
11. Zhang, J.; Yang, P.L.; Gray, N.S. Targeting cancer with small molecule kinase inhibitors. *Nat Rev Cancer* **2009**, *9*, 28-39.
12. Druker, B.J.; Talpaz, M.; Resta, D.J.; Peng, B.; Buchdunger, E.; Ford, J.M.; Lydon, N.B.; Kantarjian, H.; Capdeville, R.; Ohno-Jones, S.; Sawyers, C.L. Efficacy and safety of a specific inhibitor of the BCR-ABL tyrosine kinase in chronic myeloid leukemia. *N Engl J Med* **2001**, *344*, 1031-1037.
13. Kantarjian, H.; Sawyers, C.; Hochhaus, A.; Guilhot, F.; Schiffer, C.; Gambacorti-Passerini, C.; Niederwieser, D.; Resta, D.; Capdeville, R.; Zoellner, U.; Talpaz, M.; Druker, B.; Goldman, J.; O'Brien, S.G.; Russell, N.; Fischer, T.; Ottmann, O.; Cony-Makhoul, P.; Facon, T.; Stone, R.; Miller, C.; Tallman, M.; Brown, R.; Schuster, M.; Loughran, T.; Gratwohl, A.; Mandelli, F.; Saglio, G.; Lazzarino, M.; Russo, D.; Baccarani, M.; Morra, E. Hematologic and cytogenetic responses to imatinib mesylate in chronic myelogenous leukemia. *N Engl J Med* **2002**, *346*, 645-652.
14. Shah, N.P.; Nicoll, J.M.; Nagar, B.; Gorre, M.E.; Paquette, R.L.; Kuriyan, J.; Sawyers, C.L. Multiple BCR-ABL kinase domain mutations confer polyclonal resistance to the tyrosine kinase inhibitor imatinib (STI571) in chronic phase and blast crisis chronic myeloid leukemia. *Cancer Cell* **2002**, *2*, 117-125.
15. Desgrosellier, J.S.; Cheresh, D.A. Integrins in cancer: biological implications and therapeutic opportunities. *Nat Rev Cancer* **2010**, *10*, 9-22.
16. Engelman, J.A. Targeting PI3K signalling in cancer: opportunities, challenges and limitations. *Nat Rev Cancer* **2009**, *9*, 550-562.

17. Slamon, D.J.; Leyland-Jones, B.; Shak, S.; Fuchs, H.; Paton, V.; Bajamonde, A.; Fleming, T.; Eiermann, W.; Wolter, J.; Pegram, M.; Baselga, J.; Norton, L. Use of chemotherapy plus a monoclonal antibody against HER2 for metastatic breast cancer that overexpresses HER2. *N Engl J Med* **2001**, *344*, 783-792.
18. Morgan, D.O. Principles of CDK regulation. *Nature* **1995**, *374*, 131-134.
19. Sherr, C.J. Cancer cell cycles. *Science* **1996**, *274*, 1672-1677.
20. Vesely, J.; Havlicek, L.; Strnad, M.; Blow, J.J.; Donella-Deana, A.; Pinna, L.; Letham, D.S.; Kato, J.; Detivaud, L.; Leclerc, S.; et al. Inhibition of cyclin-dependent kinases by purine analogues. *Eur J Biochem* **1994**, *224*, 771-786.
21. Kollareddy, M.; Dzubak, P.; Zheleva, D.; Hajduch, M. Aurora kinases: structure, functions and their association with cancer. *Biomed Pap Med Fac Univ Palacky Olomouc Czech Repub* **2008**, *152*, 27-33.
22. Kollareddy, M.; Zheleva, D.; Dzubak, P.; Brahmkshatriya, P.S.; Lepsik, M.; Hajduch, M. Aurora kinase inhibitors: Progress towards the clinic. *Invest New Drugs* **2012**, *30*, 2411-2432.
23. Raguz, S.; Yague, E. Resistance to chemotherapy: new treatments and novel insights into an old problem. *Br J Cancer* **2008**, *99*, 387-391.
24. Dean, M.; Fojo, T.; Bates, S. Tumour stem cells and drug resistance. *Nat Rev Cancer* **2005**, *5*, 275-284.
25. Hanash, S. Integrated global profiling of cancer. *Nat Rev Cancer* **2004**, *4*, 638-644.
26. Surinova, S.; Schiess, R.; Huttenhain, R.; Cerciello, F.; Wollscheid, B.; Aebersold, R. On the development of plasma protein biomarkers. *J Proteome Res* **2011**, *10*, 5-16.
27. Anderson, N.L.; Anderson, N.G. The human plasma proteome: history, character, and diagnostic prospects. *Mol Cell Proteomics* **2002**, *1*, 845-867.
28. Brand, J.; Haslberger, T.; Zolg, W.; Pestlin, G.; Palme, S. Depletion efficiency and recovery of trace markers from a multiparameter immunodepletion column. *Proteomics* **2006**, *6*, 3236-3242.
29. Zhang, H.; Li, X.J.; Martin, D.B.; Aebersold, R. Identification and quantification of N-linked glycoproteins using hydrazide chemistry, stable isotope labeling and mass spectrometry. *Nat Biotechnol* **2003**, *21*, 660-666.
30. Nicol, G.R.; Han, M.; Kim, J.; Birse, C.E.; Brand, E.; Nguyen, A.; Mesri, M.; FitzHugh, W.; Kaminker, P.; Moore, P.A.; Ruben, S.M.; He, T. Use of an immunoaffinity-mass spectrometry-based approach for the quantification of protein biomarkers from serum samples of lung cancer patients. *Mol Cell Proteomics* **2008**, *7*, 1974-1982.
31. Legrain, P.; Aebersold, R.; Archakov, A.; Bairoch, A.; Bala, K.; Beretta, L.; Bergeron, J.; Borchers, C.H.; Corthals, G.L.; Costello, C.E.; Deutsch, E.W.; Domon, B.; Hancock, W.; He, F.; Hochstrasser, D.; Marko-Varga, G.; Salekdeh, G.H.; Sechi, S.; Snyder, M.; Srivastava, S.; Uhlen, M.; Wu, C.H.; Yamamoto, T.; Paik, Y.K.; Omenn, G.S. The human proteome project: current state and future direction. *Mol Cell Proteomics* **2011**, *10*, M111 009993.
32. Hanash, S.; Taguchi, A. The grand challenge to decipher the cancer proteome. *Nat Rev Cancer* **2010**, *10*, 652-660.
33. Stahl-Zeng, J.; Lange, V.; Ossola, R.; Eckhardt, K.; Krek, W.; Aebersold, R.; Domon, B. High sensitivity detection of plasma proteins by multiple reaction monitoring of N-glycosites. *Mol Cell Proteomics* **2007**, *6*, 1809-1817.
34. Kovarova, H.; Hajduch, M.; Korinkova, G.; Halada, P.; Krupickova, S.; Gouldsworthy, A.; Zhelev, N.; Strnad, M. Proteomics approach in classifying the biochemical basis of the anticancer activity of the new olomoucine-derived synthetic cyclin-dependent kinase inhibitor, bohemine. *Electrophoresis* **2000**, *21*, 3757-3764.

35. Mihal, V.; Hajduch, M.; Noskova, V.; Janostakova, A.; Safarova, M.; Orel, M.; Kouzmina, G.; Stary, J.; Blazek, B.; Pospisilova, D. The analysis of correlations between drug resistance and clinical/laboratory measures found in a group of children with all treated by ALL-BFM 90 protocol. *Bull Cancer* **2004**, *91*, E80-89.
36. Lee, B.W.; Johnson, G.L.; Hed, S.A.; Darzynkiewicz, Z.; Talhouk, J.W.; Mehrotra, S. DEVDase detection in intact apoptotic cells using the cell permeant fluorogenic substrate, (z-DEVD)2-cresyl violet. *Biotechniques* **2003**, *35*, 1080-1085.
37. Shevchenko, A.; Wilm, M.; Vorm, O.; Mann, M. Mass spectrometric sequencing of proteins silver-stained polyacrylamide gels. *Anal Chem* **1996**, *68*, 850-858.
38. Ross, P.L.; Huang, Y.N.; Marchese, J.N.; Williamson, B.; Parker, K.; Hattan, S.; Khainovski, N.; Pillai, S.; Dey, S.; Daniels, S.; Purkayastha, S.; Juhasz, P.; Martin, S.; Bartlet-Jones, M.; He, F.; Jacobson, A.; Pappin, D.J. Multiplexed protein quantitation in Saccharomyces cerevisiae using amine-reactive isobaric tagging reagents. *Mol Cell Proteomics* **2004**, *3*, 1154-1169.
39. Li, Y.; Ray, P.; Rao, E.J.; Shi, C.; Guo, W.; Chen, X.; Woodruff, E.A., 3rd; Fushimi, K.; Wu, J.Y. A Drosophila model for TDP-43 proteinopathy. *Proc Natl Acad Sci U S A* **2010**, *107*, 3169-3174.
40. Kawahara, Y.; Mieda-Sato, A. TDP-43 promotes microRNA biogenesis as a component of the Drosha and Dicer complexes. *Proc Natl Acad Sci U S A* **2012**, *109*, 3347-3352.
41. Kumano, M.; Furukawa, J.; Shiota, M.; Zardan, A.; Zhang, F.; Beraldi, E.; Wiedmann, R.M.; Fazli, L.; Zoubeidi, A.; Gleave, M.E. Cotargeting Stress-Activated Hsp27 and Autophagy as a Combinatorial Strategy to Amplify Endoplasmic Reticular Stress in Prostate Cancer. *Mol Cancer Ther* **2012**.
42. Rousseau, B.; Menard, L.; Haurie, V.; Taras, D.; Blanc, J.F.; Moreau-Gaudry, F.; Metzler, P.; Hugues, M.; Boyault, S.; Lemiere, S.; Canron, X.; Costet, P.; Cole, M.; Balabaud, C.; Bioulac-Sage, P.; Zucman-Rossi, J.; Rosenbaum, J. Overexpression and role of the ATPase and putative DNA helicase RuvB-like 2 in human hepatocellular carcinoma. *Hepatology* **2007**, *46*, 1108-1118.
43. Longshaw, V.M.; Chapple, J.P.; Balda, M.S.; Cheetham, M.E.; Blatch, G.L. Nuclear translocation of the Hsp70/Hsp90 organizing protein mSTI1 is regulated by cell cycle kinases. *J Cell Sci* **2004**, *117*, 701-710.
44. Odunuga, O.O.; Longshaw, V.M.; Blatch, G.L. Hop: more than an Hsp70/Hsp90 adaptor protein. *Bioessays* **2004**, *26*, 1058-1068.
45. Goto, T.; Takano, M.; Sakamoto, M.; Kondo, A.; Hirata, J.; Kita, T.; Tsuda, H.; Tenjin, Y.; Kikuchi, Y. Gene expression profiles with cDNA microarray reveal RhoGDI as a predictive marker for paclitaxel resistance in ovarian cancers. *Oncol Rep* **2006**, *15*, 1265-1271.
46. Kuwano, M.; Oda, Y.; Izumi, H.; Yang, S.J.; Uchiumi, T.; Iwamoto, Y.; Toi, M.; Fujii, T.; Yamana, H.; Kinoshita, H.; Kamura, T.; Tsuneyoshi, M.; Yasumoto, K.; Kohno, K. The role of nuclear Y-box binding protein 1 as a global marker in drug resistance. *Mol Cancer Ther* **2004**, *3*, 1485-1492.
47. Sorokin, A.V.; Selyutina, A.A.; Skabkin, M.A.; Guryanov, S.G.; Nazimov, I.V.; Richard, C.; Th'ng, J.; Yau, J.; Sorensen, P.H.; Ovchinnikov, L.P.; Evdokimova, V. Proteasome-mediated cleavage of the Y-box-binding protein 1 is linked to DNA-damage stress response. *EMBO J* **2005**, *24*, 3602-3612.
48. Zhu, K.; Zhao, J.; Lubman, D.M.; Miller, F.R.; Barder, T.J. Protein pI shifts due to posttranslational modifications in the separation and characterization of proteins. *Anal Chem* **2005**, *77*, 2745-2755.
49. Lassle, M.; Blatch, G.L.; Kundra, V.; Takatori, T.; Zetter, B.R. Stress-inducible, murine protein mSTI1. Characterization of binding domains for heat shock proteins

and in vitro phosphorylation by different kinases. *J Biol Chem* **1997**, *272*, 1876-1884.
50. Daniel, S.; Bradley, G.; Longshaw, V.M.; Soti, C.; Csermely, P.; Blatch, G.L. Nuclear translocation of the phosphoprotein Hop (Hsp70/Hsp90 organizing protein) occurs under heat shock, and its proposed nuclear localization signal is involved in Hsp90 binding. *Biochim Biophys Acta* **2008**, *1783*, 1003-1014.
51. Dreier, M.R.; Grabovich, A.Z.; Katusin, J.D.; Taylor, W.R. Short and long-term tumor cell responses to Aurora kinase inhibitors. *Exp Cell Res* **2009**, *315*, 1085-1099.
52. Mao, J.H.; Wu, D.; Perez-Losada, J.; Jiang, T.; Li, Q.; Neve, R.M.; Gray, J.W.; Cai, W.W.; Balmain, A. Crosstalk between Aurora-A and p53: frequent deletion or downregulation of Aurora-A in tumors from p53 null mice. *Cancer Cell* **2007**, *11*, 161-173.
53. Agrawal, S.; Kumar, A.; Srivastava, V.; Mishra, B.N. Cloning, expression, activity and folding studies of serine hydroxymethyltransferase: a target enzyme for cancer chemotherapy. *J Mol Microbiol Biotechnol* **2003**, *6*, 67-75.
54. Biancone, L.; Cantaluppi, V.; Del Sorbo, L.; Russo, S.; Tjoelker, L.W.; Camussi, G. Platelet-activating factor inactivation by local expression of platelet-activating factor acetyl-hydrolase modifies tumor vascularization and growth. *Clin Cancer Res* **2003**, *9*, 4214-4220.
55. Honma, K.; Takemasa, I.; Matoba, R.; Yamamoto, Y.; Takeshita, F.; Mori, M.; Monden, M.; Matsubara, K.; Ochiya, T. Screening of potential molecular targets for colorectal cancer therapy. *Int J Gen Med* **2009**, *2*, 243-257.
56. Skvortsova, I.; Skvortsov, S.; Stasyk, T.; Raju, U.; Popper, B.A.; Schiestl, B.; von Guggenberg, E.; Neher, A.; Bonn, G.K.; Huber, L.A.; Lukas, P. Intracellular signaling pathways regulating radioresistance of human prostate carcinoma cells. *Proteomics* **2008**, *8*, 4521-4533.
57. Gasparini, G.; Longo, R.; Torino, F.; Gattuso, D.; Morabito, A.; Toffoli, G. Is tailored therapy feasible in oncology? *Crit Rev Oncol Hematol* **2006**, *57*, 79-101.
58. Longo, R.; Gasparini, G. Anti-VEGF therapy: the search for clinical biomarkers. *Expert Rev Mol Diagn* **2008**, *8*, 301-314.
59. Sathornsumetee, S.; Reardon, D.A.; Desjardins, A.; Quinn, J.A.; Vredenburgh, J.J.; Rich, J.N. Molecularly targeted therapy for malignant glioma. *Cancer* **2007**, *110*, 13-24.
60. Tortora, G.; Ciardiello, F.; Gasparini, G. Combined targeting of EGFR-dependent and VEGF-dependent pathways: rationale, preclinical studies and clinical applications. *Nat Clin Pract Oncol* **2008**, *5*, 521-530.
61. Gasparini, G.; Gion, M.; Mariani, L.; Papaldo, P.; Crivellari, D.; Filippelli, G.; Morabito, A.; Silingardi, V.; Torino, F.; Spada, A.; Zancan, M.; De Sio, L.; Caputo, A.; Cognetti, F.; Lambiase, A.; Amadori, D. Randomized Phase II Trial of weekly paclitaxel alone versus trastuzumab plus weekly paclitaxel as first-line therapy of patients with Her-2 positive advanced breast cancer. *Breast Cancer Res Treat* **2007**, *101*, 355-365.
62. Grosso, A.R.; Martins, S.; Carmo-Fonseca, M. The emerging role of splicing factors in cancer. *EMBO Rep* **2008**, *9*, 1087-1093.
63. Iwao-Koizumi, K.; Matoba, R.; Ueno, N.; Kim, S.J.; Ando, A.; Miyoshi, Y.; Maeda, E.; Noguchi, S.; Kato, K. Prediction of docetaxel response in human breast cancer by gene expression profiling. *J Clin Oncol* **2005**, *23*, 422-431.
64. Maxwell, P.J.; Longley, D.B.; Latif, T.; Boyer, J.; Allen, W.; Lynch, M.; McDermott, U.; Harkin, D.P.; Allegra, C.J.; Johnston, P.G. Identification of 5-

fluorouracil-inducible target genes using cDNA microarray profiling. *Cancer Res* **2003**, *63*, 4602-4606.
65. Kunz, M. Genomic signatures for individualized treatment of malignant tumors. *Curr Drug Discov Technol* **2008**, *5*, 9-14.
66. Collins, F.S.; Green, E.D.; Guttmacher, A.E.; Guyer, M.S. A vision for the future of genomics research. *Nature* **2003**, *422*, 835-847.
67. Bibikova, M.; Yeakley, J.M.; Wang-Rodriguez, J.; Fan, J.B. Quantitative expression profiling of RNA from formalin-fixed, paraffin-embedded tissues using randomly assembled bead arrays. *Methods Mol Biol* **2008**, *439*, 159-177.
68. Esquela-Kerscher, A.; Slack, F.J. Oncomirs - microRNAs with a role in cancer. *Nat Rev Cancer* **2006**, *6*, 259-269.
69. Negrini, M.; Ferracin, M.; Sabbioni, S.; Croce, C.M. MicroRNAs in human cancer: from research to therapy. *J Cell Sci* **2007**, *120*, 1833-1840.
70. Lu, J.; Getz, G.; Miska, E.A.; Alvarez-Saavedra, E.; Lamb, J.; Peck, D.; Sweet-Cordero, A.; Ebert, B.L.; Mak, R.H.; Ferrando, A.A.; Downing, J.R.; Jacks, T.; Horvitz, H.R.; Golub, T.R. MicroRNA expression profiles classify human cancers. *Nature* **2005**, *435*, 834-838.
71. Hanash, S.M.; Pitteri, S.J.; Faca, V.M. Mining the plasma proteome for cancer biomarkers. *Nature* **2008**, *452*, 571-579.
72. Maurya, P.; Meleady, P.; Dowling, P.; Clynes, M. Proteomic approaches for serum biomarker discovery in cancer. *Anticancer Res* **2007**, *27*, 1247-1255.
73. Bengtsson, S.; Krogh, M.; Szigyarto, C.A.; Uhlen, M.; Schedvins, K.; Silfversward, C.; Linder, S.; Auer, G.; Alaiya, A.; James, P. Large-scale proteomics analysis of human ovarian cancer for biomarkers. *J Proteome Res* **2007**, *6*, 1440-1450.
74. Kondo, T. Tissue proteomics for cancer biomarker development: laser microdissection and 2D-DIGE. *BMB Rep* **2008**, *41*, 626-634.
75. Sodek, K.L.; Evangelou, A.I.; Ignatchenko, A.; Agochiya, M.; Brown, T.J.; Ringuette, M.J.; Jurisica, I.; Kislinger, T. Identification of pathways associated with invasive behavior by ovarian cancer cells using multidimensional protein identification technology (MudPIT). *Mol Biosyst* **2008**, *4*, 762-773.
76. Nishizuka, S.; Charboneau, L.; Young, L.; Major, S.; Reinhold, W.C.; Waltham, M.; Kouros-Mehr, H.; Bussey, K.J.; Lee, J.K.; Espina, V.; Munson, P.J.; Petricoin, E., 3rd; Liotta, L.A.; Weinstein, J.N. Proteomic profiling of the NCI-60 cancer cell lines using new high-density reverse-phase lysate microarrays. *Proc Natl Acad Sci U S A* **2003**, *100*, 14229-14234.

PŘÍLOHA 1

Int. J. Mol. Sci. **2012**, *13*, 15536-15564; doi:10.3390/ijms131215536

OPEN ACCESS
International Journal of
Molecular Sciences
ISSN 1422-0067
www.mdpi.com/journal/ijms

Article

Cancer Cell Response to Anthracyclines Effects: Mysteries of the Hidden Proteins Associated with These Drugs

Jirina Tyleckova [1], Rita Hrabakova [1], Katerina Mairychova [1], Petr Halada [2], Lenka Radova [3], Petr Dzubak [3], Marian Hajduch [3], Suresh J. Gadher [4] and Hana Kovarova [1,*]

[1] Institute of Animal Physiology and Genetics AS CR, v.v.i., 277 21 Libechov, Czech Republic; E-Mails: tyleckova@iapg.cas.cz (J.T.); hrabakova@iapg.cas.cz (R.H.); mairychova@iapg.cas.cz (K.M.)

[2] Institute of Microbiology AS CR, v.v.i., 142 20 Prague, Czech Republic; E-Mail: halada@biomed.cas.cz

[3] Laboratory of Experimental Medicine, Institute of Translational and Molecular Medicine, Faculty of Medicine and Dentistry, Palacky University and University Hospital, 775 15 Olomouc, Czech Republic; E-Mails: avodar@gmail.com (L.R.); dzubakp@gmail.com (P.D.); marian.hajduch@upol.cz (M.H.)

[4] Life Technologies, Frederick, MD 21704, USA; E-Mail:gadhersuresh@hotmail.com

* Author to whom correspondence should be addressed; E-Mail: kovarova@iapg.cas.cz; Tel.: +420-315-639-582; Fax: +420-315-639-510.

Received: 31 August 2012; in revised form: 26 October 2012 / Accepted: 7 November 2012 / Published: 22 November 2012

Abstract: A comprehensive proteome map of T-lymphoblastic leukemia cells and its alterations after daunorubicin, doxorubicin and mitoxantrone treatments was monitored and evaluated either by paired comparison with relevant untreated control and using multivariate classification of treated and untreated samples. With the main focus on early time intervals when the influence of apoptosis is minimized, we found significantly different levels of proteins, which corresponded to 1%–2% of the total amount of protein spots detected. According to Gene Ontology classification of biological processes, the highest representation of identified proteins for all three drugs belong to metabolic processes of proteins and nucleic acids and cellular processes, mainly cytoskeleton organisation and ubiquitin-proteasome pathway. Importantly, we observed significant proportion of changes in proteins involved in the generation of precursor metabolites and energy typical for daunorubicin, transport proteins participating in response to doxorubicin and a group of proteins of immune system characterising response to mitoxantrone. Both a paired comparison and the multivariate evaluation of quantitative data revealed

daunorubicin as a distinct member of the group of anthracycline/anthracenedione drugs. A combination of identified drug specific protein changes, which may help to explain anti-cancer activity, together with the benefit of blocking activation of adaptive cancer pathways, presents important approaches to improving treatment outcomes in cancer.

Keywords: anthracycline/anthracenedione; T-lymphoblastic leukemia; proteomics; early anti-cancer response; adaptive cancer mechanisms; protein biosynthesis; ubiquitin-proteasome system; energy metabolism; transport proteins; tumor immunity

1. Introduction

The anthracycline antibiotics doxorubicin (DOXO) and daunorubicin (DNR) belong to the most effective anti-cancer drugs. They have been widely used in clinics for the treatment of both solid tumors and hematological malignancies since the early 1960s, when these products of *Streptomyces peucetius* were first isolated [1]. Structurally, there is only a subtle difference between DNR and DOXO in the side chain of the molecules [2] and mitoxantrone (MTX), an anthracenedione, has also very similar structure to that of anthracyclines [3] (Figure 1).

Figure 1. Chemical structures of daunorubicin, doxorubicin and mitoxantrone.

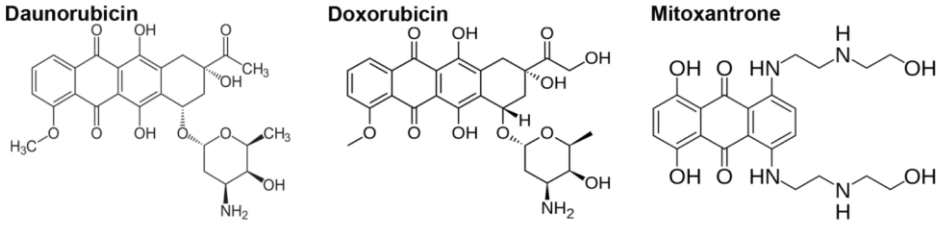

The mechanism of action of these drugs is attributed mainly to the inhibition of topoisomerase II activity. Topoisomerase II binds to DNA and allows its cleavage but this covalent complex is trapped in the presence of anthracycline drug and DNA cannot re-ligate, thus subsequently blocking transcription and replication [4,5]. Other proposed mechanisms of action are DNA intercalation and the production of reactive oxygen species [6], which appears to be responsible for the serious toxic side effects of these chemotherapeutic drugs, namely cardiotoxicity [7,8]. Despite the similarity in the structure of anthracyclines and anthracenediones, they differ widely in clinical use. DOXO has the widest spectrum of activity amongst anthracyclines and is used for the treatment of both solid tumors and hematological malignancies. It is administered as a single agent or in combination chemotherapy regimens. On the contrary, DNR shows activity mainly in acute leukemia's [9]. MTX is active both in solid tumors and leukemia with slightly lower activity than DOXO but also with lower toxicity [3]. Even though these drugs are frequently used in clinics, the exact molecular mechanisms of their effects on tumor cells, as well as toxicity, are not completely understood. Importantly, such deeper knowledge might contribute to the clarification of different therapeutic efficiency of structurally very close groups of anthracyclines and anthracenediones.

Proteomic approaches involving gel-based techniques, gel-free chromatography and advanced mass spectrometry for protein fractionation, identification and quantification, allow us to study the effects of drug treatments on cells at protein level in a comprehensive way. The main advantage of 2-D gel based fractionation is the high resolution including assessment of multiple forms of individual protein (s) on the basis of differences in isoelectric point and molecular mass. Using a suitable protein stain, this popular and reliable technique may facilitate comprehensive quantification [10]. Several proteomic studies have been recently performed for monitoring the effect of DOXO on hepatocellular carcinoma [11], breast cancer [12], non-Hodgkin lymphoma [13], acute lymphoblastic leukemia cells [14] or the effect of DNR on pancreatic carcinoma [15] *in vitro.* In addition, proteomic techniques have been used for studying drug resistance mechanisms to DOXO or MTX in lung cancer cells [16,17].

In this study, we performed proteomic comparison of very early effects of DNR, DOXO and MTX treatments on T-lymphoblastic leukemia cells as representative of hematological malignancies. The main goals have been to characterise and identify typical markers of cell response to individual drugs, to define biological processes responsible for their anti-tumor activity and to compare the effects of these structurally linked drugs in order to explain their different therapeutic effectiveness in clinics.

2. Results

2.1. Determination of IC_{50}, TA_{50}

Our intention was to investigate the early effects of the anthracycline/anthracenedione anti-cancer drugs that precede the onset of apoptosis in CEM cells and loss of cell viability. The IC_{50} of drugs were determined using the MTT test as mentioned above. The induction of apoptosis in cells began at different time intervals for different drugs. It was therefore necessary to measure time to onset of apoptosis (TA) at first and then to adjust the time of the treatments for each individual drug to the half time of TA (TA_{50}). Hence, for all proteomic experiments the cells were treated with 10× IC_{50} doses of the drugs for time interval corresponding to TA_{50} (Table 1). This combination of dose and time of the treatment led to measurable changes in protein composition before onset of apoptosis in treated cells.

Table 1. The list of studied anti-cancer drugs with their abbreviations, 10 times of inhibitory concentrations corresponding to 50% of cell growth (10× IC_{50}) and half times to apoptosis induction (TA_{50}) for 10× IC_{50} doses of individual drugs.

Anti-cancer drug	Abbreviation	Mechanism of action	10× IC_{50} (μg/mL)	TA_{50} (min)
Daunorubicin	DNR	intercalation, topo II inhibitor	0.03	120
Doxorubicin	DOXO	intercalation, topo II inhibitor	0.05	250
Mitoxantrone	MTX	intercalation, topo II inhibitor	1.88×10^{-3}	150
Cisplatin	CisPt	alkylating-like	7.57	150
Paclitaxel	TAX	mitotic inhibitor	9.00×10^{-5}	120

2.2. Proteome 2-D Maps—Number of Spots per Gel and Number of Differentially Abundant Spots per Anti-Cancer Drug

In order to cover the most significant part of the cancer cell proteome, two different pH ranges, pH 4–7 and pH 6–11, were used. The 2D gel images were analyzed using Redfin Solo SW protocol. In

this approach, spot detection and image segmentation takes place in a composite image and the same spot positions and borders are then assigned to all images, after compensation for geometric distortions. On average, 2180 and 570 protein spots were detected in pH 4–7 and pH 6–11, respectively (Figure 2). In total for all five anticancer drugs in this study, 133 protein spots showed significantly increased intensity pattern after drug treatment, while 86 protein spots were decreased according to criteria of fold-change >1.2 for p-value <0.01 and fold-change >1.5 for p-value <0.05. Amongst these, 47 protein spots occurred at different levels in DOXO treatment, 40 protein spots in DNR treatment and 54 protein spots in MTX treatment. Differentially expressed protein spots were selected for mass spectrometry identification and 153 proteins were identified in 174 protein spots which were excised out of all 219 significantly different spots (Table 2). Amongst the identified proteins, there were seven proteins present in two spots and six proteins present in three spots. Contrary to this, two proteins in one spot were identified for seven spots (Table S1). More detailed data regarding mass spectrometry protein identifications including spot number, protein name, UniProt database number, number of peptides matched to the identified protein, number of unassigned peaks, sequence coverage, Mascot score of the identified protein, Mascot score for the highest ranked hit to a non-homologous protein, peptide sequences confirmed by MS/MS (Mascot score given in parenthesis), MW and pI are reported in Table S1.

Figure 2. Representative 2-D protein map of treated CEM T-lymphoblastic leukemia cells.

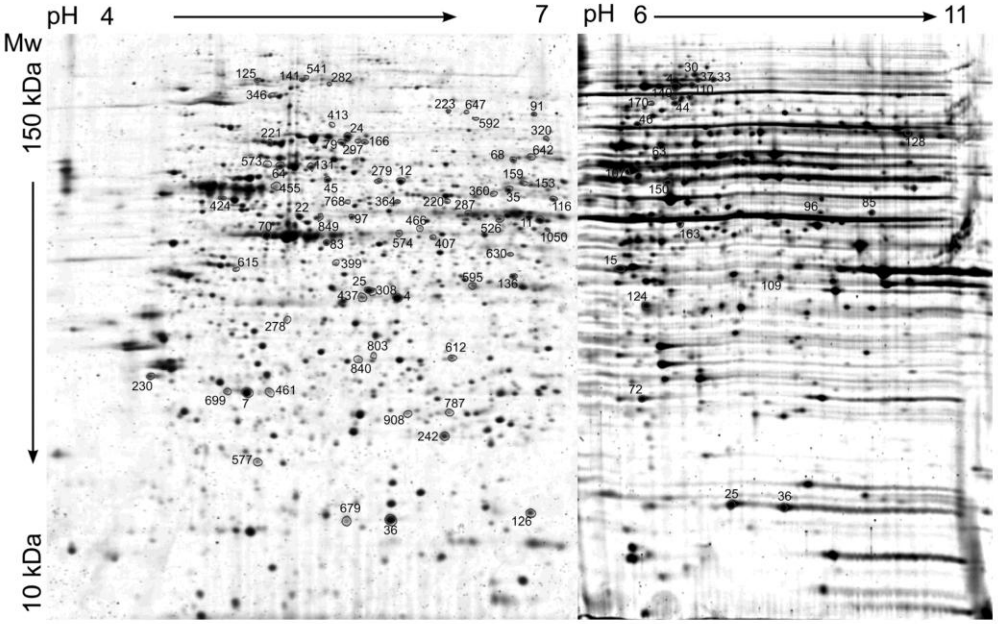

Table 2. The list of studied anti-cancer drugs with the numbers of significant protein spot changes, direction of their changes and the number of identified proteins. DNR, daunorubicin; DOXO, doxorubicin; MTX, mitoxantrone; CisPt, cisplatin; TAX, paclitaxel.

Anti-cancer drug	No. Different Spot	4–7 Up	4–7 Down	No. ID proteins	No. Different Spot	6–11 Up	6–11 Down	No. ID proteins	No. Different Spot	Total Up	Total Down	No. ID proteins
DNR	32	8	24	24	8	1	7	5	40	9	31	29
DOXO	29	15	14	21	18	13	5	10	47	28	19	31
MTX	40	24	16	30	14	9	5	10	54	33	21	40
CisPt	24	21	3	18	23	16	7	13	47	37	10	31
TAX	29	25	4	21	2	1	1	1	31	26	5	22
Total	154	93	61	114	65	40	25	39	219	133	86	153

On average, 2180 protein spots could be detected on pH 4–7 gels and 570 protein spots could be detected on pH 6–11 gels. The spot numbers indicate significantly altered protein spots after daunorubicin, doxorubicin or mitoxantrone treatments (fold change >1.2 and p-value <0.01 and fold change >1.5 and p-value <0.05). Gels were stained using Sypro Ruby and Redfin SW was used for 2-D gel image analysis.

2.3. The Proteins Significantly Changing Their Abundance after Treatment by Individual Anthracycline/Anthracenedione Drugs and Their Distribution by Biological Processes

The proteins significantly changing their abundance and identified as single protein per protein spot for DNR, DOXO and MTX treatments and their classification into biological processes are in Table 3 and depicted in Figure 3. With regard to relatively short time intervals of individual drug treatments, observed increase or decrease in protein levels may be due to impact of drug on turn-over of these proteins.

Light blue squares represent anti-cancer drugs. The nodes show identified proteins marked according to their gene names, the color code represents Gene Ontology biological process based on PANTHER classification. The node shape shows trend of change in protein level, proteins with increased levels are depicted as triangles, proteins with decreased levels as arrowheads and proteins with opposite changes between different drugs as diamonds. Detailed information about the proteins is shown in Table 3.

Table 3. The list of identified changed proteins.

3A	DNR								
Drug	**Spot No.**	**Protein name**	**Gene Name**	**UniProt No.**	**Biological process**	**pH**	**Change**	**Fold change**	***p*-value**
DNR	4	L-lactate dehydrogenase B chain	*LDHB*	P07195	3	4–7	↑	1.34	0.0048
DNR	7	Rho GDP-dissociation inhibitor 2	*ARHGDIB*	P52566	1	4–7	↑	1.69	0.008
DNR	36	Stathmin	*STMN1*	P16949	1	4–7	↑	1.75	0.0022
DNR	64	60 kD a heat shock protein, mitochondrial	*HSPD1*	P10809	5	4–7	↓	1.52	0.0023
DNR	72b	Proteasome subunit beta type-2	*PSMB2*	P49721	5	6–11	↓	1.70	0033
DNR	96b	Obg-like ATPase 1	*OLA1*	Q9NTK5	8	6–11	↑	1.34	0.0022
DNR	97	Cytochrome b-c1 complex subunit 1, mitochondrial	*UQCRC1*	P31930	3	4–7	↓	1.36	0.0041
DNR	107b	Glucose-6-phosphate 1-dehydrogenase	*G6PD*	P11413	5	6–11	↓	2.95	0.0013
DNR	124b	*S*-formylglutathione hydrolase	*ESD*	P10768	8	6–11	↓	2.22	0.009
DNR	125	Heat shock 70 kDa protein 4	*HSPA4*	P34932	4	4–7	↓	2.25	0.0076
DNR	126	Cofilin-1	*CFL1*	P23528	1	4–7	↑	2.01	0.0045
DNR	159	Succinyl-CoA: 3-ketoacid-coenzyme A transferase 1, mitochondrial	*OXCT1*	P55809	5	4–7	↓	1.67	0.0059
DNR	166	Dihydrolipoyllysine-residue acetyltransferase component of pyruvate dehydrogenase complex, mitochondrial	*DLAT*	P10515	5	4–7	↓	2.34	0.0004
DNR	220	Heterogeneous nuclear ribonucleoprotein H	*HNRNPH1*	P31943	5	4–7	↓	1.56	0.0017
DNR	221	Plastin-2	*LCP1*	P13796	1	4–7	↓	1.63	0.0093
DNR	287	DnaJ homolog subfamily A member 2	*DNAJA2*	O60884	4	4–7	↓	1.63	0.0021
DNR	346	Transitional endoplasmic reticulum ATPase	*VCP*	P55072	7	4–7	↓	2.55	0.0098
DNR	360	Mitochondrial-processing peptidase subunit alpha	*PMPCA*	Q10713	3	4–7	↓	1.66	0.0029
DNR	399	Anamorsin	*CIAPIN1*	Q6FI81	8	4–7	↓	1.47	0.0049
DNR	407	Protein phosphatase methylesterase 1	*PPME1*	Q9Y570	5	4–7	↑	1.44	0.0083
DNR	424	ATP synthase subunit beta, mitochondrial	*ATP5B*	P06576	3	4–7	↓	2.21	0.0009
DNR	573	60 kDa heat shock protein, mitochondrial	*HSPD1*	P10809	5	4–7	↓	1.72	0.0009
DNR	574	TAR DNA-binding protein 43	*TARDBP*	Q13148	5	4–7	↑	1.33	0.0065
DNR	768	Glutathione synthetase	*GSS*	P48637	5	4–7	↓	2.00	0.0019
DNR	849	Heterogeneous nuclear ribonucleoprotein F	*HNRNPF*	P52597	5	4–7	↓	1.71	0.009

Table 3. *Cont.*

3B	DOXO								
Drug	**Spot No.**	**Protein name**	**Gene Name**	**UniProt No.**	**Biological process**	**pH**	**Change**	**Fold change**	***p*-value**
DOXO	29	Heat shock 70 kDa protein 1A/1B	*HSPA1A/ HSPA1B*	P08107	4	4–7	↑	1.43	0.0073
DOXO	44b	Far upstream element-binding protein 2	*KHSRP*	Q92945	5	6–11	↑	1.53	0.0079
DOXO	61b	KH domain-containing, RNA-binding, signal transduction-associated protein 1	*KHDRBS1*	Q07666	5	6–11	↓	1.78	0.0004
DOXO	63b	EH domain-containing protein 1	*EHD1*	Q9H4M9	7	6–11	↑	1.79	0.049
DOXO	91	DNA replication licensing factor MCM7	*MCM7*	P33993	1	4–7	↑	1.56	0.0081
DOXO	115b	Elongation factor 2	*EEF2*	P13639	5	6–11	↑	1.54	0.0023
DOXO	141	Caprin-1	*CAPRIN1*	Q14444	7	4–7	↑	1.54	0.0008
DOXO	163b	Medium-chain specific acyl-CoA dehydrogenase, mitochondrial	*ACADM*	P11310	3	6–11	↓	1.45	0.0025
DOXO	170b	Far upstream element-binding protein 2	*KHSRP*	Q92945	5	6–11	↑	1.89	0.0013
DOXO	278	Spermidine synthase	*SRM*	P19623	5	4–7	↑	1.64	0.0049
DOXO	282	Ubiquitin-like modifier-activating enzyme 1	*UBA1*	P22314	1	4–7	↑	1.97	0.0062
DOXO	308	F-actin-capping protein subunit alpha-2	*CAPZA2*	P47755	1	4–7	↑	1.45	0.0098
DOXO	364	4-trimethylaminobutyraldehyde dehydrogenase	*ALDH9A1*	P49189	5	4–7	↑	1.51	0.0033
DOXO	592	Ezrin	*EZR*	P15311	1	4–7	↑	2.59	0.0071
DOXO	595	L-aminoadipate-semialdehyde dehydrogenase-phosphopantetheinyl transferase	*AASDHPPT*	Q9NRN7	8	4–7	↓	1.54	0.0009
DOXO	630	Ubiquitin-like domain-containing CTD phosphatase 1	*UBLCP1*	Q8WVY7	8	4–7	↓	1.36	0.0025
DOXO	699	Rho GDP-dissociation inhibitor 2	*ARHGDIB*	P52566	1	4–7	↓	2.00	0.0015
DOXO	787	Glutathione *S*-transferase P	*GSTP1*	P09211	4	4–7	↓	1.54	0.0089
DOXO	908	GTP-binding protein SAR1b	*SAR1B*	Q9Y6B6	7	4–7	↓	1.33	0.0073

Table 3. *Cont.*

3C	MTX								
Drug	**Spot No.**	**Protein name**	**Gene Name**	**UniProt No.**	**Biological process**	**pH**	**Change**	**Fold change**	***p*-value**
MTX	11	Elongation factor 1-gamma	*EEF1G*	P26641	5	4–7	↑	1.32	0.0056
MTX	12	Protein disulfide-isomerase A3	*PDIA3*	P30101	5	4–7	↑	1.48	0.0056
MTX	22	Heterogeneous nuclear ribonucleoprotein F	*HNRNPF*	P52597	5	4–7	↑	1.37	0.0011
MTX	24	Stress-70 protein, mitochondrial	*HSPA9*	P38646	4	4–7	↑	1.47	0.007
MTX	25	60 S acidic ribosomal protein P0	*RPLP0*	P05388	5	4–7	↑	1.3	0.0012
MTX	30b	Staphylococcal nuclease domain-containing protein 1	*SND1*	Q7KZF4	5	6–11	↑	1.53	0.024
MTX	35	T-complex protein 1 subunit beta	*CCT2*	P78371	5	4–7	↑	1.47	0.0017
MTX	36b	Peptidyl-prolyl cis-*trans* isomerase	*PPIA*	P62937	4	6–11	↓	1.75	0.0072
MTX	68	T-complex protein 1 subunit gamma	*CCT3*	P49368	5	4–7	↑	1.56	0.00014
MTX	83	Activator of 90 kDa heat shock protein ATPase homolog 1	*AHSA1*	O95433	4	4–7	↑	1.47	0.00035
MTX	109b	Heterogeneous nuclear ribonucleoproteins A2/B1	*HNRNPA2B1*	P22626	5	6–11	↓	1.87	0.0071
MTX	110b	ATP-dependent RNA helicase DDX1	*DDX1*	Q92499	5	6–11	↑	1.51	0.008
MTX	116	RuvB-like 1	*RUVBL1*	Q9Y265	5	4–7	↑	1.66	0.00004
MTX	128b	Eukaryotic translation initiation factor 2 subunit 3	*EIF2S3L*	Q2VIR3	5	6–11	↓	1.73	0.02
MTX	131	60 kDa heat shock protein, mitochondrial	*HSPD1*	P10809	5	4–7	↑	1.52	0.001
MTX	136	Transaldolase	*TALDO1*	P37837	5	4–7	↑	1.33	0.0042
MTX	223	Mitochondrial inner membrane protein	*IMMT*	Q16891	8	4–7	↑	1.58	0.0028
MTX	230	Proteasome subunit alpha type-5	*PSMA5*	P28066	5	4–7	↑	2.51	0,004
MTX	297	Heat shock 70 kDa protein 1A/1B	*HSPA1A/HSPA1B*	P08107	4	4–7	↑	1.36	0.0066
MTX	455	G-rich sequence factor 1	*GRSF1*	Q12849	5	4–7	↑	1.66	0.0016
MTX	461	Rho GDP-dissociation inhibitor 2	*ARHGDIB*	P52566	1	4–7	↓	1.46	0.0033
MTX	466	Eukaryotic translation initiation factor 3 subunit G	*EIF3G*	O75821	5	4–7	↓	1.46	0.002
MTX	615	Transformer-2 protein homolog beta	*TRA2B*	P62995	5	4–7	↓	1.93	0.0025
MTX	647	Mitochondrial inner membrane protein	*IMMT*	Q16891	8	4–7	↑	1.34	0.0006
MTX	679	Stathmin	*STMN1*	P16949	1	4–7	↓	2.26	0.0028
MTX	1050	Adenylosuccinate synthetase isozyme 2	*ADSS*	P30520	5	4–7	↑	1.52	0.00005

Table 3. *Cont.*

3D	**DNR + DOXO**								
Drug	**Spot No.**	**Protein name**	**Gene Name**	**UniProt No.**	**Biological process**	**pH**	**Change**	**Fold change**	***p*-value**
DNR	15b	Heterogeneous nuclear ribonucleoprotein H3	*HNRNPH3*	P31942	5	6–11	↓	1.88	0.04
DOXO	15b	Heterogeneous nuclear ribonucleoprotein H3	*HNRNPH3*	P31942	5	6–11	↓	2.25	0.025
DNR	279	Protein disulfide-isomerase A3	*PDIA3*	P30101	5	4–7	↓	1.50	0.0056
DOXO	279	Protein disulfide-isomerase A3	*PDIA3*	P30101	5	4–7	↓	1.59	0.004
3E	**DNR + MTX**								
Drug	**Spot No.**	**Protein name**	**Gene Name**	**UniProt No.**	**Biological process**	**pH**	**Change**	**Fold change**	***p*-value**
DNR	320	Heat shock protein 75 kDa, mitochondrial	*TRAP1*	Q12931	4	4–7	↓	1.66	0.001
MTX	320	Heat shock protein 75 kDa, mitochondrial	*TRAP1*	Q12931	4	4–7	↑	1.33	0.0045
DNR	413	NADH-ubiquinone oxidoreductase 75 kDa subunit, mitochondrial	*NDUFS1*	P28331	3	4–7	↓	1.37	0.0015
MTX	413	NADH-ubiquinone oxidoreductase 75 kDa subunit, mitochondrial	*NDUFS1*	P28331	3	4–7	↑	1.6	0.0073
DNR	642	Paraspeckle component 1	*PSPC1*	Q8WXF1	5	4–7	↓	4.11	0.0028
MTX	642	Paraspeckle component 1	*PSPC1*	Q8WXF1	5	4–7	↓	2.44	0.0077
3F	**DOXO + MTX**								
Drug	**Spot No.**	**Protein name**	**Gene Name**	**UniProt No.**	**Biological process**	**pH**	**Change**	**Fold change**	***p*-value**
DOXO	4b	Elongation factor 2	*EEF2*	P13639	5	6–11	↑	1.47	0.00038
MTX	4b	Elongation factor 2	*EEF2*	P13639	5	6–11	↑	1.47	0.00035
DOXO	25b	Peptidyl-prolyl cis-*trans* isomerase	*PPIA*	P62937	4	6–11	↓	1.85	0.0023
MTX	25b	Peptidyl-prolyl cis-*trans* isomerase	*PPIA*	P62937	4	6–11	↓	1.7	0.0025
DOXO	33b	*C*-1-tetrahydrofolate synthase, cytoplasmic	*MTHFD1*	P11586	5	6–11	↑	1.77	0.013
MTX	33b	*C*-1-tetrahydrofolate synthase, cytoplasmic	*MTHFD1*	P11586	5	6–11	↑	1.67	0.011
DOXO	37b	*C*-1-tetrahydrofolate synthase, cytoplasmic	*MTHFD1*	P11586	5	6–11	↑	1.69	0.0074
MTX	37b	*C*-1-tetrahydrofolate synthase, cytoplasmic	*MTHFD1*	P11586	5	6–11	↑	1.62	0.0122
DOXO	45	Peptidyl-prolyl cis-*trans* isomerase FKBP4	*FKBP4*	Q02790	4	4–7	↑	1.38	0.0066
MTX	45	Peptidyl-prolyl cis-*trans* isomerase FKBP4	*FKBP4*	Q02790	4	4–7	↑	1.53	0.0052

Table 3. *Cont.*

3F	**DOXO + MTX**								
Drug	**Spot No.**	**Protein name**	**Gene Name**	**UniProt No.**	**Biological process**	**pH**	**Change**	**Fold change**	***p*-value**
DOXO	46b	GMP synthase [glutamine-hydrolyzing]	*GMPS*	P49915	5	6–11	↑	1.6	0.014
MTX	46b	GMP synthase [glutamine-hydrolyzing]	*GMPS*	P49915	5	6–11	↑	1.65	0.0038
DOXO	70	Actin, cytoplasmic 1	*ACTB*	P60709	1	4–7	↓	1.38	0.0017
MTX	70	Actin, cytoplasmic 1	*ACTB*	P60709	1	4–7	↓	1.47	0.0009
DOXO	85b	DAZ-associated protein 1	*DAZAP1*	Q96EP5	6	6–11	↓	1.71	0.0011
MTX	85b	DAZ-associated protein 1	*DAZAP1*	Q96EP5	6	6–11	↓	2.22	0.0059
DOXO	140b	Far upstream element-binding protein 2	*KHSRP*	Q92945	5	6–11	↑	1.68	0.035
MTX	140b	Far upstream element-binding protein 2	*KHSRP*	Q92945	5	6–11	↑	1.61	0.0131
DOXO	153	D-3-phosphoglycerate dehydrogenase	*PHGDH*	O43175	5	4–7	↑	1.68	0.0068
MTX	153	D-3-phosphoglycerate dehydrogenase	*PHGDH*	O43175	5	4–7	↑	1.9	0.0097
DOXO	242	Splicing factor, arginine/serine-rich 3	*SFRS3*	P84103	5	4–7	↓	1.31	0.0064
MTX	242	Splicing factor, arginine/serine-rich 3	*SFRS3*	P84103	5	4–7	↓	1.58	0.0034
DOXO	526	Rab GDP dissociation inhibitor beta	*GDI2*	P50395	1	4–7	↓	2.08	0.0009
MTX	526	Rab GDP dissociation inhibitor beta	*GDI2*	P50395	1	4–7	↓	1.51	0.0052
DOXO	541	Heat shock protein 105 kDa	*HSPH1*	Q92598	4	4–7	↑	1.47	0.0028
MTX	541	Heat shock protein 105 kDa	*HSPH1*	Q92598	4	4–7	↑	1.75	0.0015
3G	**DNR + DOXO + MTX**								
Drug	**Spot No.**	**Protein name**	**Gene Name**	**UniProt No.**	**Biological process**	**pH**	**Change**	**Fold change**	***p*-value**
DOXO	437	L-lactate dehydrogenase B chain	*LDHB*	P07195	3	4–7	↓	1.83	0.0064
MTX	437	L-lactate dehydrogenase B chain	*LDHB*	P07195	3	4–7	↓	1.86	0.0048
DNR	437	L-lactate dehydrogenase B chain	*LDHB*	P07195	3	4–7	↓	2.50	0.0032

Identified proteins typical for individual treatment with 3A: daunorubicin (DNR); 3B: doxorubicin (DOXO); 3C: mitoxantrone (MTX). Proteins with overlap between DNR and DOXO are listed in 3D; between DNR and MTX in 3E; between DOXO and MTX in 3F. Proteins with overlap between all three drugs are in 3G. Proteins from basic pH 6–11 are annotated as "b" beside spot number. The Gene Ontology biological process classification using PANTHER software is indicated by numbers 1 for cellular process, 2 for developmental process, 3 for generation of precursor metabolites and energy, 4 for immune system process/response to stimulus, 5 for metabolic process, 6 for reproduction, 7 for transport and 8 for un-annotated proteins.

Figure 3. Graphical representation of identified differentially abundant proteins after doxorubicin (DOXO), daunorubicin (DNR) and mitoxantrone (MTX) treatment of CEM T-lymphoblastic leukemia cells.

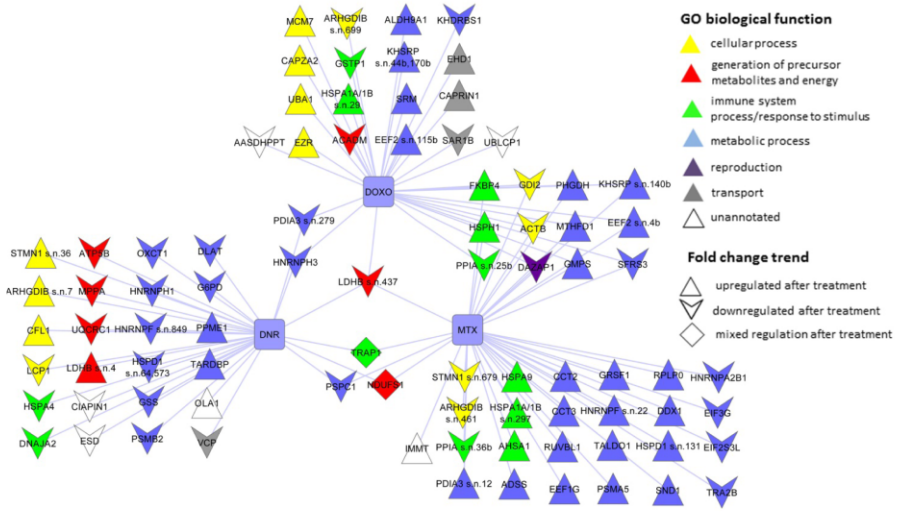

2.3.1. DNR Induced Protein Changes

Based on the evaluation criteria applied in this study we have identified 24 proteins at different levels after DNR treatment in CEM cells (Table 3A, Figure 3). Among them, five proteins (L-lactate dehydrogenase B chain, LDHB, spot no. 4; Rho GDP-dissociation inhibitor 2, ARHGDIB, spot No. 7; stathmin, STMN1, spot No. 36; 60 kDa heat shock protein, HSPD1, spots No. 64 and 573; heterogeneous nuclear ribonucleoprotein F, HNRNPF, spot No. 849) represented protein variants specifically affected by DNR whilst another protein forms of these individual proteins observed as distinct protein spots on 2DE were also regulated by DOXO or MTX (Figure 4A–E). Only for HSPD1 there were two protein forms separated by 2DE significantly changed after DNR treatment (Figure 4D). The annotations of the identified proteins in terms of their integration into biological processes according to Gene Ontology implemented in PANTHER software tool were used to classify DNR associated changes in treated cells. The proteins involved in metabolic processes represented 42% of total changes followed by 17% of proteins participating in cellular processes as well as 17% of proteins regulating generation of precursor metabolites and energy (Figure 5A). Interestingly, majority of proteins of metabolic processes were seen to decrease after DNR treatment which is opposite to what we observed for DOXO and MTX (Figure 3). The most expressed DNR induced changes in metabolic processes include decreased levels of glucose-6 phosphate 1-dehydrogenase (G6PD, spot no. 107 b), dihydrolipoyllysine-residue acetyltransferase component of pyruvate dehydrogenase complex (DLAT, spot No. 166), the important part of glycolysis, and glutathione synthetase (GSS, spot No. 768). Additionally, decrease of two heterogeneous nuclear ribonucleoproteins (HNRNPH1, spot No. 220 and a variant of HNRNPF, spot No. 849) involved in mRNA processing was observed. There were only two proteins belonging to the group of metabolic processes with increased levels after DNR treatment, protein phosphatase metylesterase 1 (PPME1, spot No. 407) and TAR DNA-binding protein 43

(TARDBP, spot No. 574). Cellular processes involved in DNR effect were represented by one decreased level of protein, plastin-2 (LCP1, spot No. 221), and three increased levels of proteins including cofilin-1 (CFL1, spot No. 126), STMN1 and ARHGDIB. Common targets of these proteins are actin cytoskeleton and microtubule filaments and their organization. The proteins of group of generation of precursor metabolites and energy appeared to be typical for DNR (Figure 5A) with their only negligible proportion observed after MTX and DOXO treatments (Figure 5B,C). This group consisted of three decreased mitochondrial proteins such as ATP synthase subunit beta (ATP5B, spot No. 424), mitochondrial-processing peptidase subunit alpha (PMPCA, spot No. 360) and cytochrome b-c1 complex subunit 1 (UQCRC1, spot No. 97) as well as increased isoform of LDHB (spot No. 4).

Figure 4. Distinct protein variants of several individual proteins after treatment of CEM T-lymphoblastic leukemia cells with doxorubicin (DOXO), daunorubicin (DNR) and mitoxantrone (MTX).

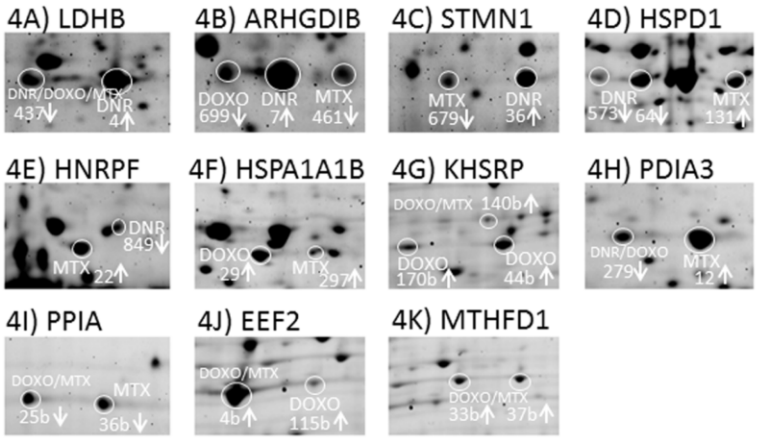

Protein variants were represented by different protein spots of the same protein and are marked with 2DE spot numbers. Arrows indicated trend of protein level changes after drug treatment. 4(A): L-lactate dehydrogenase B chain, LDHB, spot no. 4 was increased by DNR treatment and spot no. 437 was decreased by all three DNR, DOXO and MTX treatments; 4(B): Rho GDP-dissociation inhibitor 2, ARHGDIB, spot No. 7 was increased by DNR, spot No. 699 was decreased by DOXO and spot No. 461 was decreased by MTX; 4(C): stathmin, STMN1, spot No. 36 was increased by DNR and spot No. 679 was decreased by MTX; 4(D): 60 kDa heat shock protein, HSPD1, spots No. 64 and 573 were decreased by DNR and spot No. 131 was increased by MTX; 4(E): heterogeneous nuclear ribonucleoprotein F, HNRNPF, spot No. 849 was decreased by DNR and spot No. 22 was increased by MTX; 4(F): heat shock 70 kDa protein 1A/1B, HSPA1A1B, spot No. 29 was increased by DOXO and spot No. 297 was increased by MTX; 4(G): Far upstream element-binding protein 2, KHSRP spots No. 44b and 170b were increased by DOXO and spot No. 140b was increased by both DOXO and MTX treatment; 4(H): protein disulfide isomerase A3, PDIA3, spot No. 12 was increased by MTX and spot No. 279 was decreased by DNR and DOXO treatment; 4(I): peptidyl-prolyl cis-*trans* isomerase A, PPIA, spot No. 36b was decreased by MTX and spot No. 25b was decreased by both DOXO and MTX; 4(J): elongation factor 2, EEF2, spot No. 4b was increased by MTX and DOXO and spot No. 115b was

increased solely by DOXO treatment; 4(K): *C*-1-tetrafydrofolate synthase, MTHFD1, spots No. 33b and 37b were increased by DOXO and MTX treatments.

Figure 5. Distribution of anthracycline/anthracenedione regulated proteins by biological processes.

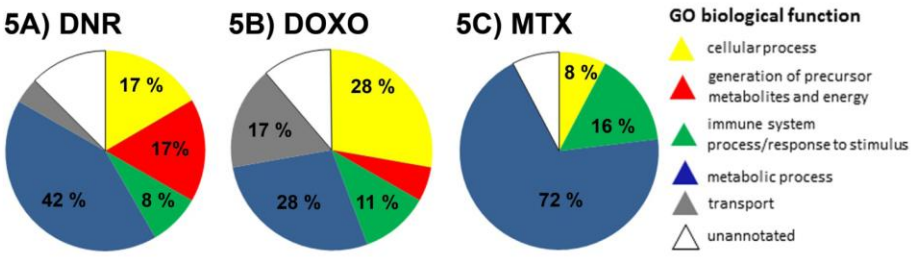

Pie charts of Gene Ontology classification of biological processes based on the contribution of proteins differentially abundant after treatment of CEM cells by: 5(A) daunorubicin (DNR); 5(B) doxorubicin (DOXO); 5(C) mitoxantrone (MTX).

2.3.2. DOXO Induced Protein Changes

In total, we found 18 proteins significantly changed after treatment of CEM cells by DOXO (Table 3B, Figure 3). Four of these proteins (Heat shock 70 kDa protein 1A/1B, HSPA1A1B, spot No. 29; Far upstream element-binding protein 2, KHSRP spots No. 44b and 170b; ARHGDIB, spot No.699 and elongation factor 2, EEF2 spot No. 115 b) were identified from the protein spots specifically influenced by DOXO although another variants of these proteins were also identified from distinct protein spots which were regulated by DNR or MTX treatment (Figure 4B,F,G,J). KHSRP was found in two evidently separated 2DE spots thus representing multiple forms of this protein (Figure 4G). As regards Gene Ontology classification of identified proteins and their incorporation into biological processes, the proteins involved in metabolic processes represented 28% of total changes and the same percentage was observed for cellular processes, followed by 17% of transport proteins and 11% of proteins from the group of immune system process and response to stimuli (Figure 5B). Metabolic processes were represented by decrease in KH domain-containing, RNA binding, signal transduction-associated protein 1 (KHDRBS1, spot No. 61b) which is an important adapter protein in signal transduction as well as regulator of RNA stability. Furthermore, we found three proteins with increased levels after DOXO treatment including KHSRP, spermidine synthase (SRM, spot No. 278), and EEF2. Among the proteins of cellular processes, there was significant decrease in ARHGDIB and increased expression of three proteins, namely ezrin (EZR, spot No. 592, ubiquitin-like modifier-activating enzyme 1 (UBA1, spot No. 282), and DNA replication licensing factor MCM7 (MCM7, spot No. 91). Transport proteins were observed as selective group of proteins responding to DOXO treatment. They were represented by lowered GTP-binding protein SAR1b (SAR1B, spot No. 908), and higher levels of EH domain-containing protein 1 (EHD1, spot No. 63b) and caprin 1 (CAPRIN1, spot No.141), stress granule associated protein.

2.3.3. MTX Induced Protein Changes

We have identified 25 proteins differentially abundant in CEM T-lymphoblastic leukemia cells followed by MTX treatment (Table 3, Figure 3). Among them there were seven proteins (protein disulfide isomerase A3, PDIA3, spot No. 12; HNRNPF, spot No. 22; peptidyl-prolyl cis-*trans* isomerase A, PPIA, spot No. 36b; HSPD1, spot No. 131; HSPA1A1B, spot No. 297; ARHGDIB, spot No. 461; *STMN1*, spot No. 679) presented as MTX specific protein variants despite distinct forms recognized after DNR or DOXO treatment (Figure 4B–F,H,I). For MTX treatment the proportion of the proteins involved in metabolic processes was the highest observed among DNR, DOXO and MTX drugs and covered 72% of total changes followed by 16% of proteins of immune system process and response to stimuli. Only 8% of proteins involved in cellular processes represented the lowest contribution of this category among DNR, DOXO and MTX drugs (Figure 5C). Amongst the proteins of metabolic processes only a few decreased proteins were observed including transformer-2 protein homolog beta (TRA2B, spot No. 615) and heterogeneous nuclear ribonucleoprotein A2/B1 (HNRNPA2B1, spot No. 109b) driving mRNA splicing and mRNA processing, as well as eukaryotic translation initiation factor 2 subunit 3 (EIF2S3L, spot No. 128b) (Figure 3). The changes of the majority of increased proteins from the metabolic group were mostly moderate with a fold change around 1.4. The most pronounced change observed was the increase in proteosome subunit alpha type (PSMA5, spot No. 230) with a fold change of 2.51, and RuvB-like 1 protein (RUVBL1, spot No. 116) as well as G-rich sequence factor (GRSF1, spot No. 455) (Table 3). Beside metabolic proteins, emerging MTX selective group of proteins of immune system process and response to stimuli was evident (Figure 5C). Majority of these proteins were increased including activator of 90 kDa heat shock protein ATPase homolog 1 (AHSA1, spot no. 83), stress-70 protein (HSPA9, spot No. 24), and HSPA1A1B. Small proportions of proteins of cellular processes were characterized by evident decrease of STMN1 and also lower level of ARHGDIB (Figure 3).

2.4. The Protein Changes Linking the Effects of Anthracycline/Anthracenedione Drugs DNR, DOXO, and MTX

In order to evaluate similarities among studied anthracycline/anthracenedione anti-cancer drugs, we looked for the overlap of the proteins changed after treatments. The highest number of such shared proteins was revealed for DOXO and MTX (Table 3, Figure 3). Three proteins, including EEF2 (spot No. 4b), PPIA (spot No. 25b) and KHSRP (spot No. 140b) were also present in another distinct spots affected exclusively either by DOXO or MTX treatment (Figure 4G,I,J. The enzyme *C*-1-tetrahydrofolate synthase (MTHFD1, spots No. 33b and 37b) was present in two spots for both DOXO as well as MTX treatments (Figure 4K). Among these twelve proteins common for DOXO and MTX (Figure 4), the fold changes of increased proteins from the category of metabolic processes ranged between 1.47 and 1.9 including EEF2, MTHFD1, GMP synthase (GMPS, spot No. 46b), D-3-phosphoglycerate dehydrogenase (PHGDH, spot No.153) and KHSRP. Only one protein from this category, splicing factor, arginine/serine-rich3 (SFRS3, spot No. 242) was decreased (Table 3). The group of proteins of immune system process and response to stimuli consisted of two functionally different proteins with isomerase activity PPIA and peptidyl-prolyl cis-*trans* isomerase FKBP4 (FKBP4, spot No. 45) with

opposite direction of protein change. Additionally, increased heat shock protein 105 kDa (HSPH1, spot No. 541) was seen to be a part of this group too (Figure 3). Small proportion of cellular processes was directed to regulation of cytoskeleton organization mediated by decreased actin (ACTB, spot No. 70) and small GTP signaling protein Rab GDP dissociation inhibitor beta (GDI2, spot No. 526). Interestingly, a decrease in one protein was observed in this study which was DAZ- associated protein 1 (DAZAP1, spot No. 85b) which belongs to the category of reproduction (Figure 3).

Compared to the overlapping of twelve different proteins for DOXO and MTX treatments, the numbers of common protein overlaps for DNR/MTX and DNR/DOXO were three and two, respectively, with only one protein common for the effect of all three drugs (Table 3 and Figure 3). The proteins common for DNR and MTX included paraspeckle component 1 (PSPC1, spot No. 642), which decreased with evidently high values of fold change for both drugs. On the contrary, two other proteins, heat shock protein 75 kDa (TRAP1, spot No. 320) and NADH-ubiquinone oxidoreductase 75 kDa subunit (NDUFS1, spot No. 413) exhibited opposite trend in protein level showing a decrease after DNR treatment and an increase induced by MTX (Table 3, Figure 3). Different abundance of two proteins of metabolic processes shared between DNR and DOXO regarded heterogeneous nuclear ribonucleoprotein H3 (HNRNPH3, spot. No. 15b) and protein disulfide-isomerase A3 (PDIA3, spot No. 279) (Table 3, Figure 3). The enzyme from the group of generation of metabolic precursors and energy, LDHB (spot No. 437) was significantly decreased after treatment with anthracyclines DNR and DOXO as well as anthracenedione MTX. Interestingly as mentioned above, this enzyme was also identified from protein spot No. 4 increased in response to DNR (Table 3, Figure 3, Figure 4A).

2.5. The Proteins Commonly Affected by Five Anti-Cancer Drugs: Anthracycline/Anthracenedione DNR, DOXO, MTX and Distinct Chemotherapeutics CisPt and TAX

Comparison of all five anti-cancer treatments is depicted in Figure S1. The response to cisplatin (CisPt) is presented by 19 unique proteins (Table S2) whilst effect of paclitaxel (TAX) is characterized by 13 proteins (Table S2). Nevertheless, the main purpose of this part of our study was selection of proteins overlapping between CisPt, TAX and anthracycline/anthracenedione drugs (Table S2) to underline common protein features of anti-cancer response. Four proteins (EHD1, spot no. 63b; Medium-chain specific acyl-CoA dehydrogenase, mitochondrial, ACADM, spot No. 163b; KHSRP, spot No. 170b; EZR, spot. No. 592) overlapped for CisPt and DOXO treatments and two proteins (4-trimethylaminobutyraldehyde dehydrogenase, ALDH9A1, spot No. 364; ARHGDIB, spot. No. 699) were shared between TAX and DOXO treatments. Another eight proteins (PPIA, spot No. 25b; CFL1, spot No. 126;, HNRNPA2B1, spot No. 109b; NDUFS1, spot No. 413; PHGDH, spot No. 153, G6PD, spot No. 107b; PPME1, spot No. 407; and TRA2B, spot No. 615) were common for one of the anthracycline/anthracenedione drugs and CisPt or TAX.

2.6. Principal Component Analysis of Quantitative Data

Besides pair comparison of protein alterations induced by each treatment, unsupervised multivariate classification (PCA) was performed to provide an overview of the variance in the whole data set including all studied drugs. PCA reduces the huge amount of data into several components named principal components (PCs) on the basis of similarities in the data set. When visualized in two

dimensional graphs, the objects/samples with similar behavior tend to "sit together" whilst distance in the position indicates dissimilarity. The first PC accounted for approximately 30% of the total variance in the data, whilst the second PC accounted for approximately 21% of total variance and finally the third PC for nearly 19% of variance (Figure 6). In the first dimension, DNR, DOXO and MTX were separated from CTRL, CisPt and TAX. In the second dimension, DNR separated mainly from DOXO and MTX. Finally, in the third dimension, DNR was more sequestered from CTRL untreated cells.

Figure 6. Multivariate principal component analysis of quantitative 2DE data to classify anti-cancer treatments.

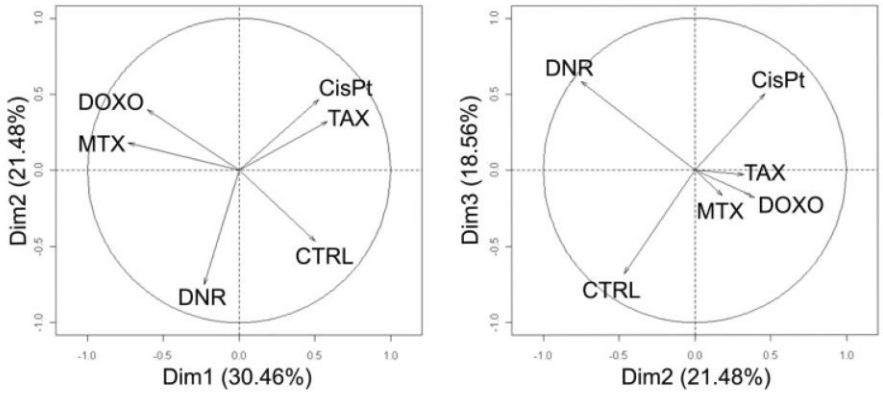

Principal component analysis was performed to obtain an overview of the variance in the data set and classify treatments according to their similarities or dissimilarities. Quantitative 2DE data of control untreated cells (CTRL), anthracyclines daunoribicin (DNR) and doxorubicine (DOXO), anthracenedione mitoxantrone (MTX), and distinct chemotherapeutics cisplatin (CisPt) and paclitaxel (TAX) were used for evaluation. In the first dimension, untreated controls, CisPt and TAX were separated from DOXO, DNR and MTX treatments, the second and third dimensions evidently distinguished DNR from DOXO and MTX as well as CisPt and TAX.

2.7. Verification of Selected Protein Changes Using Immunoblot

Several of the differentially abundant proteins were selected for verification of 2DE observations using Western blot analysis (Figure 7). Among them, significant increase of MTHFD1 after both DOXO and MTX treatments was confirmed. Further, FKBP4, another increased protein on 2DE after both DOXO and MTX treatment, was also tracked using specific antibody and significant increase reflecting a probability of 90% was confirmed for MTX whilst DOXO showed a slight increase. Using 2-DE, RUVBL1, one of the proteins typical for MTX response, was significantly increased not only after MTX treatment but a non-significant increase observed after DOXO was shown as a significant change by immunoblot. Amongst the proteins typical for DNR response the transcription factor TARDBP was verified as significantly increased after DNR treatment.

Figure 7. Western blot analysis of selected proteins.

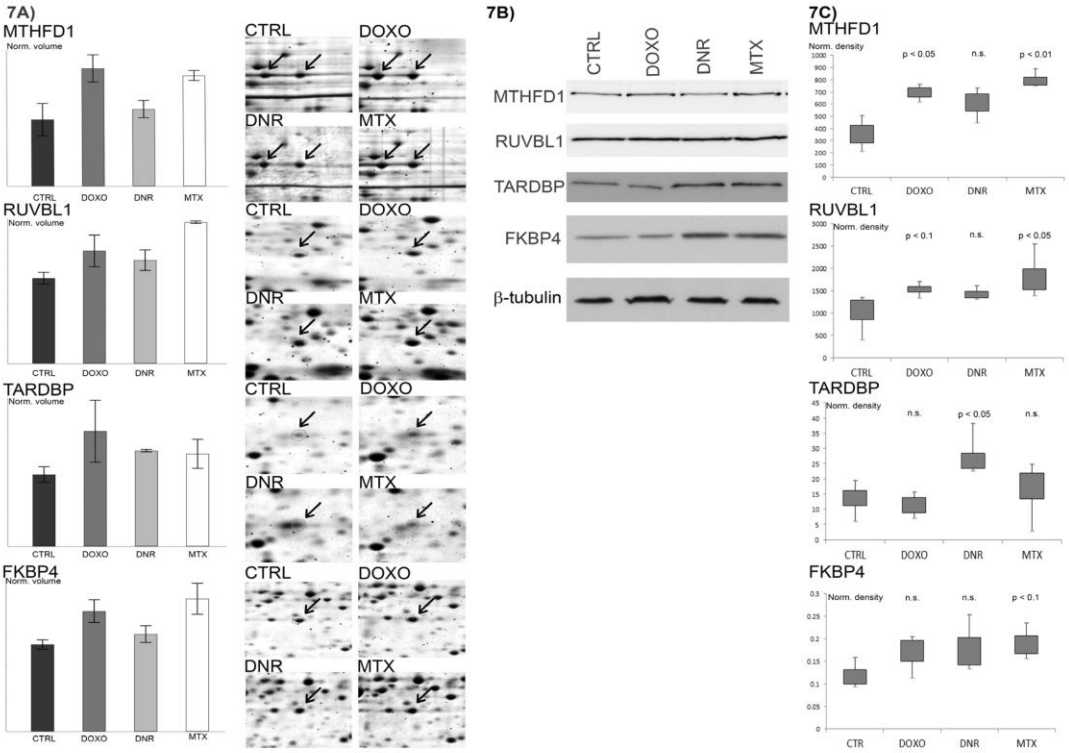

Immunoblot analysis of *C*-1-tetrahydrofolate synthase (MTHFD1), RuvB-like 1 protein (RUVBL1), TAR DNA-binding protein 43 (TARDBP) and peptidyl-prolyl cis-*trans* isomerase FKBP4 (FKBP4) in untreated CEM cells and CEM cells treated with anthracycline drugs doxorubicin (DOXO), daunorubicin (DNR) and mitoxantrone (MTX) was performed. (7A) Bar plots of normalized volume intensities of selected differentially abundant protein spots calculated and graphically represented from 2D gels by Redfin software and corresponding protein features on 2D gels of control cells and drug treatments. Significantly regulated protein spots between control cells and individual treatments are in graphs indicated by an asterisk. The arrows indicate the location of each protein feature. (7B) The whole cell lysates were examined on immunoblot using specific antibodies directed against selected proteins. β-tubulin was used as a loading control. (7C) The protein bands from immunoblot were quantified using Quantity one software for at least three replicates analyzed per protein and the density of individual band was normalized for total density in given protein line. The results were illustrated as boxplots. Significance of differences between controls and each treatment was calculated using Student's *t*-test for $p < 0.05$ and $p < 0.01$ (n.s., not significant).

3. Discussion

To gain insight into molecular mechanisms and biological processes underlying the treatments with representative anti-cancer anthracycline/anthracenedione drugs DNR, DOXO and MTX, we have used CEM T-lymphoblastic leukemia cells and investigated protein fingerprints of the drug effects

employing combination of zoomed 2DE with fluorescent protein stain and MALDI-TOF/TOF mass spectrometry. The CEM T-lymphoblastic leukemia cells have been considered as suitable model of hematological malignancies as well as tumor cells sensitive to various anti-cancer drugs [18]. Several previous studies focused on the effects of DOXO or DNR with mostly applied 24 h or 48 h treatments and low micromolar concentrations of drugs, which may correspond to relevant clinical doses [11–15]. In our study, we designed proteomic experiments focused on earlier time intervals in order to reliably monitor protein alterations that precede induction of apoptosis and minimize its impact on observed protein changes. Using individual half time to onset of apoptosis (TA_{50}), corresponding 10 times IC_{50} doses of the drugs instead of the same time interval for all treatments allowed us to optimize comparable stage of all used anti-cancer treatments. Whilst for four out of five drugs TA_{50} ranged from 120 min to 150 min, the longest 250 min interval was confirmed for DOXO and even this was still at least 6 times shorter than what was used in previously published studies [11–15].

To date, the effect of DOXO treatment on different cancer cell lines has mainly been studied by proteomic techniques [11,13,14]. To extend current observations and with the view to help translation of molecular findings toward improvements in clinical use, we focused on the effects of several clinically relevant representatives of the group of anthracycline/anthracenedione drugs. Hence, comprehensive proteome map of model T-lymphoblastic leukemia cells and its alterations after DNR, DOXO and MTX drug treatments were monitored and evaluated either by pair comparison to relevant untreated control or multivariate classification of drug treated and untreated samples.

In order to emphasise proteins specific for response toward anthracycline/anthracenedione drugs among all identified differentially abundant proteins, we performed in the same design, analysis of the effects of two additional anti-cancer drugs, CisPt and TAX, taken from distinct groups of chemotherapeutics, and compared protein alterations to those found after DNR, DOXO and MTX. As expected, using this step we marked the proteins affected and shared in anti-cancer response of such drug treatments. These proteins belong to the enzymes critical for cellular metabolism such as G6PD, the enzyme producing pentose sugars essential for nucleic acid synthesis; PHGDH, the enzyme involved in syntheses of purines and amino acids; NDUFS1, core subunit of the mitochondrial membrane respiratory chain NADH dehydrogenase (Complex I). More interestingly and corroborating our findings are the observations that many of these “promiscuous” general anti-cancer response proteins are the ones already known to play a vital role in various human cancers. For example PPME1 that demethylates protein phosphatase 2A was recently described as tumor suppressor [19]. TRA2B or HNRNPA2B1 regulating repair of double strand breaks have elevated levels in various cancers [20] and changed in levels by anti-cancer treatments as shown here. HNRNPA2B1 has been even assigned as proto-oncogene [21]. Further evidence is presented by KHSRP regulating transcription and mRNA processing which was shown to support migration in liver cancer cells [22]. Additionally, involvement of multifunctional protein PPIA in cancer progression has been described [23]. Interestingly, several cytoskeleton regulating proteins including CFL1 [24] and EZR [25] were associated with invasion and metastasis and ARHGDIB was linked to the development of chemoresistance [26]. These proteins, although non-specific as regards used drugs and functioning in various biological processes, most probably present important targets underlying anti-cancer mechanisms and possibly play role of anchor molecules which may connect different pathways in a very complex regulation of cancer cell processes. Despite their importance, the major aim of this study has been to identify specific proteins

typical for the response to anthracycline/anthracenedione drugs DNR, DOXO and MTX and to characterize similarities in the effects of these structurally very close drugs.

In total, we found several tens of proteins with significantly changed levels at early time intervals after DNR, DOXO and MTX treatments which corresponded only to 1%–2% of the total number of spots detected. According to Gene Ontology classification of biological processes the highest representation of identified proteins for all three drugs belongs to metabolic processes of nucleic acids or proteins and cellular processes involved mainly in cytoskeleton organisation. It corresponds to well-known observations that metabolic alterations on glucose consumption and biosynthetic activity of nucleotides, amino acids and lipids are the changes for sustaining cell proliferation in cancer cells. Typical evidence of this fact is the Warburg effect, the conditions when the cancer cells switch from oxidative phosphorylation to glycolysis to produce ATP and set of enzymes such as lactate dehydrogenase and pyruvate dehydrogenase play crucial role [27]. Evidently and surprisingly, we observed in our study such changes in CEM T-lymphoblastic leukemia cells at very early time intervals after anti-cancer DNR treatment. The most probable explanation of this behaviour is adaptive effort of tumor cells to make even stronger the essential mechanisms supporting cancer growth. Regulation of metabolic enzymes offers new directions for anti-cancer treatments and lactate dehydrogenase which catalyses the final step in the glycolytic cascade constitutes a relatively new anti-cancer target [28]. Nevertheless, design of the combination of the enzymes or even their isoforms and development of specific inhibitors that would eliminate robustness of cancer cells is not a simple task.

In addition to changes in energy metabolism, DNR treatment of CEM cells leads to the decrease of two heterogeneous nuclear ribonucleoproteins which are involved in RNA processing but we also observed increase of TARDBP which is homologous to the heterogeneous nuclear ribonucleoproteins. The higher level of this protein was further confirmed using Western blot. The TARDBP has been identified as a cause of neuropathology in a wide spectrum of neurodegenerative diseases, including amyotrophic lateral sclerosis. Using Drosophila model for proteinopathy associated with TARDBP, it was shown that increasing human wild-type TARDBP expression is sufficient to cause neurotoxicity *in vivo* [29]. The protein may also be involved in microRNA biogenesis, apoptosis and cell division [30]. The finding of increased level of TARDBP in CEM leukemic cells after anti-cancer DNR treatment let us hypothesise that it might significantly contribute to the toxicity toward the tumor cell and positively influence outcome of anti-cancer response. Higher levels of this protein may also result from its decreased clearance, which was shown as mediated by lower activity of ubiqutin-proteasome system and autophagosome in synergy [31]. Hence, the link between the level of TARDBP and activity of ubiqutin-proteasome system and autophagosome is another good example underlying importance of these cellular mechanisms in regulation of carcinogenesis or response of cancer cell to anti-cancer treatment.

Doxorubicin, the other member of anthracyclines, also affected metabolic and cellular biological processes in CEM leukemic cells and majority of targeted proteins were exclusively specific for this drug and increased in cells after drug treatment. Among them, the role of spermidine synthase is aimed to redox regulation of tumor cell followed by anti-cancer treatment. Overproduction of spermidine increases resistance to oxidative stress with spermidine serving as a free-radical scavenger *in vitro* as well as *in vivo* [32]. Hence, increase of spermidine synthase in DOXO treated cancer cell may present regulatory response which may increase resistance of cancer cell.

EEF2 translates growth and stress impulses to the regulation of protein synthesis by catalyzing ribosomal translocation step during translation elongation. However, phosphorylation of EEF2 by EEF2 kinase inactivates this factor which indicates that EEF2 kinase could be promising anti-cancer target. Interestingly, using pharmacological inhibition of EEF2 kinase demonstrated that anti-cancer activity of widely accepted inhibitor and anti-proliferation agent against different cancer cells was more correlated with induction of EEF2 phosphorylation than inhibition of EEF2 kinase activity. In addition, stronger induction of EEF2 phosphorylation mediated by AMPK activators and mTOR inhibitor was linked to more effective cancer cell growth inhibition. Accordingly, EEF2 phosphorylation appears to be mediated through multiple pathways thus alarming the need of combinatory inhibition of EEF2 kinase in anti-cancer therapy [33]. In our study, we identified EEF2 in two protein spots from 2DE (Figure 4J). The more basic and less abundant spot was increased after DOXO treatment and may represent non-phosphorylated form, whilst the more acidic and more abundant protein spot may be representative of phosphorylated form increased by DOXO and MTX. The presence of more abundant/phosphorylated form might contribute to anti-cancer effect of DOXO and MTX, whilst the less abundant basic/non-phosphorylated form would have a role in regulation of protein synthesis and sustaining cancer cell growth.

One of a few examples of proteins decreased in level after DOXO treatment was found to be metabolic protein KHDRBS1. In case of human breast tumors it was shown that phosphorylation of this protein regulated its intracellular localization and anti-proliferative properties were blocked by phosphorylation [34]. Therefore, in addition to quantitative changes observed in this study, it would be necessary to investigate its post-translationally modified forms and localization as regards contribution to anti-cancer effect of DOXO.

Among the proteins of cellular processes affected by DOXO, we observed increase of UBA1 controlling ubiquitin conjugation pathway, and MCM7 having a role in DNA strand elongation involved in DNA replication. MCM7 is a known component of minichromosome maintenance complex which is the putative replicative helicase in eukaryotic cells and demonstrated to be efficient and sensitive marker to assess disease progression in the uterine cervix [35], prognosis of patients with non-small cell lung cancer [36], or Hodgkin lymphoma [37]. Comprehensive comparative analysis of pre-replication complex proteins in transformed and normal cells indicated that cellular transformation was associated with an overexpression and increased chromatin association of the pre-replication complex proteins including MCM7 [38]. From this point of view, increased level of MCM7 at early time interval after anti-cancer DOXO treatment may reflect other adaptive mechanisms of cancer cell contributing to the transformation of cell.

Transport proteins appeared to be an important group of proteins responding to DOXO treatment. They included SAR1B involved in protein transport from endoplasmic reticulum to Golgi, and cytoplasmic activation/proliferation-associated protein-1, CAPRIN1, stress granule associated protein. These findings may suggest possible role of induction of endoplasmic reticulum stress associated with proteotoxic stress. Subsequently, such stress stimulates either apoptosis of cancer cell which is involved in anti-cancer effects or autophagy as a cytoprotective, stress-induced adaptive pathway following disruption of protein homeostasis [39]. CAPRIN1 may also regulate the transport and translation of mRNAs of proteins with impact on cell proliferation and negative regulation of translation. The protein is putative target of miR-16 thus linking miRNA to the regulation of cell

proliferation [40]. Overexpression of CAPRIN1 induced phosphorylation of eukaryotic translation initiation factor 2 alpha resulted in global inhibition of protein synthesis [41]. This may be synergistic with above mentioned role of phosphorylated EEF2 in suppression of protein synthesis as a part of anti-cancer effect of DOXO.

The majority of MTX induced protein alterations were moderate metabolic changes. Interesting, EIF2S3L which functions in the early steps of protein synthesis, PSMA5 and RUVBL1 with the roles in transcriptional regulation, DNA replication and probably DNA repair, were observed. Evidently, decrease of protein level mediated by decrease of EIF2S3L may play an important role in MTX anti-cancer effect. Furthermore, protein homeostasis which is controlled by ubiquitin–proteasome system as mentioned above seemed to be critical mechanisms for cancer cell. Pharmacologic inhibitors of the proteasome promote tumor cytotoxicity and clinical studies have showed improvement in patient survival. Despite success of the proteasome inhibitor bortezomib in the treatment of the hematologic malignancy such as multiple myeloma, treatment of the more complex solid tumors has been less successful [42]. Our results document that MTX similarly to DOXO exploit proteins of ubiquitin-proteasome system to trigger or modulate cancer cell stress response to anti-cancer treatment in order to induce either apoptosis or autophagy.

RUVBL1 is a highly conserved AAA(+) ATPase whose expression as well as expression of its homolog RUVBL2 was high in different cancers. In case of human hepatocellular carcinoma silencing of RUVBL2 reduced cell growth and increased apoptosis whilst overexpression enhances tumorigenicity [43]. The level of RUVBL1 was significantly increased in CEM cells treated with MTX, and Western blot analysis confirmed a significantly increased level not only after MTX but also DOXO drug treatment. The question remains whether RUVBL1 at an increased level is involved in promotion of tumorigenicity in CEM T-lymphoblastic cells similarly as described in the study on human hepatocellular carcinoma.

It was possible to see that very selective group of MTX treatment are the proteins of immune system process and response to stimuli, namely chaperones thus indicating significant contribution of protein folding and stress response in tumorigenesis and anti-cancer treatment [44]. Furthermore, these chaperone proteins may be involved in presentation of tumor antigens for direct recognition of tumor by T cells [45,46] or as autoantigens which can give raise to the production of autoantibodies [47]. As regards anthracyclines, Fucikova *et al.* [48] investigated the effectiveness of anthracyclines to induce immunogenic cell death in human tumor cell lines and primary tumor cells. The data demonstrated induction of immunogenic cell death in sensitive human tumor cells including human prostate cancer, ovarian cancer, and acute lymphoblastic leukemia cells treated by anthracyclines as anti-cancer drugs. Our findings of increased chaperone proteins after MTX treatment corroborate such published data and support the role of chaperons in tumor immunity.

This study has shown that each of the studied anti-cancer anthracycline/anthracenedione drugs possess typical proteins or protein variants which are specifically changed in level by individual drugs despite of their very close structural similarity which is currently used for their grouping within chemotherapeutic drugs. However, the design of our study allowed us to evaluate and classify proteome maps of all tested anti-cancer drugs to characterize the similarities that would link drug responses. Importantly, the observation of significant decrease of LDHB after treatment of anthracyclines DNR and DOXO as well as anthracenedione MTX thus underlies common anti-cancer

effect of this group of drugs directed to the energy metabolism of cancer cell. Nevertheless, it has been important to be aware of the fact, as shown in several examples mentioned above, that the given drug may affect preferentially certain isoform/species of an individual protein hence, in many cases the specific role of such protein isoform/species may play decisive role compared to the quantitative change at the total level of a given protein.

Furthermore, we found several proteins common in DOXO and MTX, among them mainly those directed to the regulation protein synthesis as well as purine and amino acid biosynthesis including MTHFD1 whose increase after treatment by DOXO and MTX was confirmed by Western blot. Regulation of SFRS3 appeared to be a new emerging role because it was recently described as a proto-oncogene critical for cell proliferation and tumor induction and maintenance. It was highly expressed in various cancers and its reduction, mediated by RNAi, resulted in G2/M arrest, growth retardation, and apoptosis [49]. Accordingly, decreased level of SFRS3after DOXO and MTX treatments offers a new mechanism contributing to anti-cancer activities common to anthracycline/anthracenedione drugs.

Compared to a group of proteins linking the effect of DOXO and MTX, there were only a few proteins shared between DNR and DOXO or MTX thus indicating the distinct position of DNR among the anthracycline/antracenedione drugs. This finding was further corroborated by principal component analysis showing DNR sequestered from DOXO and MTX as well as other treatments such as CisPt and TAX in the first three components covering in total 71% of variances of the whole experimental set. Interestingly, there were two proteins, PSPC1 and HNRNPH3 which were shared between DNR/MTX and DNR/DOXO treatments, respectively, with surprisingly high fold changes observed. PSPC1 is required for the formation of nuclear paraspeckles, subnuclear bodies that alter gene expression via the nuclear retention of RNAs [50]. It belongs to the family of proteins of the Drosophila behavior/human splicing (DBHS) which are predominately nuclear and influence various biological processes, including carcinogenesis. The significant increase of PSPC1 after DNR and MTX treatments points to possible important role of nuclear paraspeckles in anti-cancer activities of anthracycline/anthracenedione drugs.

4. Materials and Methods

4.1. Cell Cultures and Sample Preparation—Determination of IC_{50} and TA_{50}

Human T-lymphoblastic leukemia CEM cells (American Tissue Culture Collection, Manassas, VA, USA) were cultured at a density of 1×10^6 cells/mL in RPMI-1640 medium supplemented with 2 mM glutamine, 100 U/mL penicillin, 100 μg/mL streptomycin, and 10% of heat inactivated fetal bovine serum with or without addition of anti-cancer drug in a humidified incubator with 5% CO_2 at 37 °C. Drugs were dissolved directly in RPMI-1640 medium.

The cytotoxicity of DNR, DOXO, MTX, cisplatin (CisPt) and paclitaxel (TAX) was determined by the three-day MTT test as described previously and the inhibitory concentration corresponding to 50% of cell growth (IC_{50}) was calculated [51]. Early time interval studies, when the influence of apoptosis is minimal, facilitate reliable observation of protein changes and hence time to apoptosis induction (TA) was measured for five times IC_{50} and 10 times IC_{50} doses of the drugs using caspase 3 and/or 7 activation Magic Red™ caspase detection kit [52]. For these relatively high drug doses used, no significant

differences in TA for individual drugs were found. Hence, for proteomic analysis, the cells were treated with ten times IC_{50} doses of the drugs and harvested at half time to apoptosis induction (TA_{50}) (Table 1). Cells were washed three times in ice-cold PBS and 6×10^6 cells were lysed in 200 µL of lysis buffer containing 7 M urea, 2 M thiourea, 3% *w*/*v* CHAPS, 2% *v*/*v* Nonidet-P40, 5 mM TCEP in presence of inhibitors of proteases and phosphatases (Roche, Basel, Switzerland) according to manufacturers' directions. After centrifugation at 4 °C, 20,000× *g*, 10 min, the supernatant was collected and protein concentration was determined by the Pierce 660 nm protein assay. Samples were frozen to −80 °C for future use. At least three biological replicates were analyzed for each drug treatment.

4.2. Two-Dimensional Gel Electrophoresis (2DE)

Aliquots of samples corresponding to 100 µg of proteins and 0.5% IPG buffer 4–7 were loaded on pH 4–7 Immobiline Drystrips using active in gel rehydration (IPG strip 18 cm, pH 4–7) in buffer containing 7 M urea, 2 M thiourea, 4% CHAPS, 200 mM DeStreak, inhibitors of proteases, phosphatases (Roche, Basel, Switzerland), 0.5% IPG buffer 4–7 and a trace of bromophenol blue. Isoelectric focusing separation (IEF) was performed on IEF Cell (Bio-Rad, Hercules, CA, USA) system using the following program: 1 h to 200 V, 10 h 200 V, 30 min to 500 V, 30 min to 1000 V, 1.5 h to 5000 V, and 5000 V until total of 55 kVh was reached. After IEF separation, the gel strips were equilibrated in 50 mM Tris, pH 6.8, 6 M urea, 30% glycerol, 4% SDS, 100 mM DeStreak, and a trace of bromophenol blue for 25 min [53].

Aliquots of samples corresponding to 70 µg of proteins and 0.5% IPG buffer 6–11 were cup-loaded on pH 6–11 Immobiline DryStrips (IPG strip 18 cm, pH 6–11) passively rehydrated in buffer containing 7 M urea, 2 M thiourea, 4% CHAPS, 30 mM DTT, inhibitors of proteases, phosphatases (Roche, Basel, Switzerland), 0.5% IPG buffer 6–11 and a trace of bromophenol blue overnight. IEF was performed on IEF Cell system using the following program: 1 h to 150 V, 12 h 150 V, 1 h to 1000 V, 3 h to 8000 V, and 8000 V for 12 kVh. After IEF separation, the strips were equilibrated in 50 mM Tris, pH 6.8, 6 M urea, 30% glycerol, 8% SDS, and 1% DTT for 15 min, followed by equilibration in 50 mM Tris, pH 6.8, 6 M urea, 30% glycerol, 8% SDS, 4% IAA and a trace of bromophenol blue for 15 min.

After equilibration, both 4–7 and 6–11 IPG strips were rinsed and applied to vertical 12% SDS-PAGE (18 mm × 18 mm × 1 mm gel). SDS-PAGE was carried out at a constant current of 40 mA per gel using in series connected Protean II xi Cells (Bio-Rad, Hercules, CA, USA) allowing simultaneous run of six gels. Gels were then stained with Sypro Ruby according to manufacturers' directions. Stained gels were scanned and digitized at 50 µm resolution at Pharos FX fluorescent scanner (Bio-Rad, Hercules, CA, USA) with excitation length 488 nm and emission length 605 nm.

The images were evaluated using Redfin 3.3.2 Solo software (Ludesi, Malmo, Sweden, 2010). Pair comparison between untreated controls and each single treatment was performed for all 5 drugs. At least three biological replicates were used for each treatment or control samples. Protein spots that were statistically significant according to Student's *t*-tests with $p < 0.01$ and fold-change >1.2 as well as $p < 0.05$ and fold-change >1.5 and accepted by visual inspection were selected for identification by mass spectrometry.

4.3. Protein Identification by Mass Spectrometry

Preparative 2D gels were prepared for spot excision and in gel digestion of selected protein spots according to the protocol above with the following modifications. Protein load was 500 µg of total protein amount per pH 4–7 gels and 150 µg of total protein amount per pH 6–11 gels. Gels were stained with reverse zinc staining [54]. Protein spots were excised from gels, cut into small pieces and destained using chelating agent. After complete destaining, the gel was washed with water, shrunk by dehydration in ACN and re-swollen again in water. The supernatant was removed and the gel was partly dried in a SpeedVac concentrator. The gel pieces were then rehydrated in a cleavage buffer containing 25 mM 4-ethylmorpholine acetate, 5% ACN and trypsin (5 ng/µL), and incubated overnight at 37 °C. The digestion was stopped by addition of 5% TFA in ACN and the aliquot of the resulting peptide mixture was desalted using a GELoader microcolumn (Eppendorf, Hamburg, Germany) packed with a Poros Oligo R3™ material [55]. The purified and concentrated peptides were eluted from the microcolumn in several droplets directly onto MALDI plate using 1 µL of *R*-cyano-4-hydroxycinnamic acid (CCA) matrix solution (5 mg/mL in 50% ACN/ 0.1% TFA).

Mass spectra were measured on an Ultraflex III MALDI-TOF/TOF instrument (Bruker Daltonics, Bremen, Germany) as described before [56]. Briefly, peptide mass fingerprint spectra were acquired in the mass range 700–3500 Da and peak list in XML format created using FlexAnalysis 3.0 searched using MASCOT search engine against Swiss-Prot 2011_09 database subset of human proteins with the following search settings; peptide tolerance of 50 ppm, missed cleavage site value set to one, variable carbamidomethylation of cysteine, oxidation of methionine and protein *N*-terminal acetylation. Proteins with Mascot score over the threshold 56 calculated for the used settings were considered as identified. If the score was lower or only slightly higher than the threshold value, the identity of protein candidate was confirmed by MS/MS analysis.

4.4. Western Blot Analysis

Protein lysates prepared as described above were diluted in 2× SDS buffer (4% SDS, 50% glycerol, 140 mM mercaptoethanol, 125 mM Tris pH 6.8 and a trace of bromophenol blue) and separated by 10%, 12% or 15% SDS-PAGE. Separated proteins were transferred onto Immobilone-P membrane (Millipore, Bedford, MA, USA) using a semidry blotting system (Biometra, Gottingen, Germany). The membranes were blocked in 5% non-fat dry milk or in 5% BSA in Tris-buffered saline with 0.05% Tween 20 (TBST) pH 7.4 for 1 h and incubated overnight with the respective primary antibodies: anti-MTHFD1 (Sigma-Aldrich, St. Louis, MO, USA) (HPA000704, 1:20000 in 5% BSA); anti-RUVBL1 (Sigma-Aldrich, St. Louis, MO, USA) (HPA019947, 1:200,00 in 5% BSA); anti-TARDBP (Sigma-Aldrich, St. Louis, MO, USA) (HPA017284, 1:1000 in 5% milk); anti-FKBP4 (Sigma-Aldrich, St. Louis, MO, USA) (HPA006148, 1:200,00 in 5% BSA) and anti-β-tubulin (Sigma-Aldrich, T4026, 1:5000 in 5% milk). Peroxidase-conjugated secondary anti-mouse or anti-rabbit antibodies (Jackson Immunoresearch, Suffolk, UK) were diluted 1:100,00 in 5% non-fat dry milk in TBST and incubated for 1 h at RT. The ECL+ chemiluminescence (GE Healthcare, Uppsala, Sweden) detection system was used to detect the proteins. The exposed CL-XPosure films (Thermo Scientific, Rockford, IL, USA) were scanned by a calibrated densitometer GS-800 (Bio-Rad, Hercules, CA, USA). QuantityOne 4.6.5. (Bio-Rad, Hercules, CA, USA, 2008) software was used for analysis and quantification of Western blot results.

4.5. Data Analysis Applying Principal Component Analysis (PCA)

Statistical analyses were performed using freeware R 2.14.1. (www.r-project.org) (R Foundation, Vienna, Austria, 2011). PCA was used to determine grouping of the drugs on the basis of similarities/differences in protein patterns. For each drug, arithmetical means of ratios measured intensity/volume of the spot were taken as input data [57].

4.6. Protein Classification According to Gene Ontology

The PANTHER (Protein ANalysis THrough Evolutionary Relationships) classification software was used to assign identified proteins according to Gene Ontology to biological processes (PANTHER version 7) [58].

5. Conclusions

To help translation of molecular findings toward improvements in clinical use we focused on the effects of several clinically relevant representatives of the group of anthracycline/anthracenedione drugs on the tumor cell.

It was evident that each of the drugs of anthracycline/anthracenedione group of chemotherapeutics was capable of inducing exclusively specific protein changes in tumor cells, many of which represent possible new molecular mechanisms contributing to anti-cancer activity. On the other hand, we observed several protein changes that corresponded to the adaptive effort of cancer cells to sustain growth. The findings of drug specific protein changes induced by structurally related drugs might help in explaining their different clinical use. Additionally, protein changes common in the drugs may be exploited for further enhancement of anti-cancer activities.

In summary, together with induction of anti-cancer activities, there may be significant benefits in blocking the activation of adaptive pathways in order to improve the outcomes of a specific treatment in cancer patients undergoing therapy.

Acknowledgments

This work was supported in part by grants from the Ministry of Education, Youth and Sports LC07017 and by Institutional Research Concepts RVO 67985904 (IAPG, AS CR, v.v.i.) and RVO 61388971 (IMIC, AS CR, v.v.i.). Infrastructural part of this project was supported from the Operational Program Research and Development for Innovations (CZ.1.05/2.1.00/01.0030).

Conflict of Interest

The authors declare no conflict of interest.

References

1. Carvalho, C.; Santos, R.X.; Cardoso, S.; Correia, S.; Oliveira, P.J.; Santos, M.S.; Moreira, P.I. Doxorubicin: The good, the bad and the ugly effect. *Curr. Med. Chem.* **2009**, *16*, 3267–3285.

2. Minotti, G.; Menna, P.; Salvatorelli, E.; Cairo, G.; Gianni, L. Anthracyclines: Molecular advances and pharmacologic developments in antitumor activity and cardiotoxicity. *Pharmacol. Rev.* **2004**, *56*, 185–229.
3. Hande, K.R. Clinical applications of anticancer drugs targeted to topoisomerase II. *Biochim. Biophys. Acta* **1998**, *1400*, 173–184.
4. Nitiss, J.L. Targeting DNA topoisomerase II in cancer chemotherapy. *Nat. Rev. Cancer* **2009**, *9*, 338–350.
5. Pommier, Y.; Leo, E.; Zhang, H.; Marchand, C. DNA topoisomerases and their poisoning by anticancer and antibacterial drugs. *Chem. Biol.* **2010**, *17*, 421–433.
6. Gewirtz, D.A. A critical evaluation of the mechanisms of action proposed for the antitumor effects of the anthracycline antibiotics adriamycin and daunorubicin. *Biochem. Pharmacol.* **1999**, *57*, 727–741.
7. Kremer, L.C.; van Dalen, E.C.; Offringa, M.; Ottenkamp, J.; Voute, P.A. Anthracycline-induced clinical heart failure in a cohort of 607 children: Long-term follow-up study. *J. Clin. Oncol.* **2001**, *19*, 191–196.
8. Simunek, T.; Sterba, M.; Popelova, O.; Adamcova, M.; Hrdina, R.; Gersl, V. Anthracycline-induced cardiotoxicity: Overview of studies examining the roles of oxidative stress and free cellular iron. *Pharmacol. Rep.* **2009**, *61*, 154–171.
9. Cortes-Funes, H.; Coronado, C. Role of anthracyclines in the era of targeted therapy. *Cardiovasc. Toxicol.* **2007**, *7*, 56–60.
10. Hanash, S.; Taguchi, A. The grand challenge to decipher the cancer proteome. *Nat. Rev. Cancer* **2010**, *10*, 652–660.
11. Hammer, E.; Bien, S.; Salazar, M.G.; Steil, L.; Scharf, C.; Hildebrandt, P.; Schroeder, H.W.; Kroemer, H.K.; Volker, U.; Ritter, C.A. Proteomic analysis of doxorubicin-induced changes in the proteome of HepG2cells combining 2-D DIGE and LC-MS/MS approaches. *Proteomics* **2010**, *10*, 99–114.
12. Chen, S.T.; Pan, T.L.; Tsai, Y.C.; Huang, C.M. Proteomics reveals protein profile changes in doxorubicin-treated MCF-7 human breast cancer cells. *Cancer Lett.* **2002**, *181*, 95–107.
13. Jiang, Y.J.; Sun, Q.; Fang, X.S.; Wang, X. Comparative mitochondrial proteomic analysis of Rji cells exposed to adriamycin. *Mol. Med.* **2009**, *15*, 173–182.
14. Dong, X.; Xiong, L.; Jiang, X.; Wang, Y. Quantitative proteomic analysis reveals the perturbation of multiple cellular pathways in jurkat-T cells induced by doxorubicin. *J. Proteome Res.* **2010**, *9*, 5943–5951.
15. Moller, A.; Malerczyk, C.; Volker, U.; Stoppler, H.; Maser, E. Monitoring daunorubicin-induced alterations in protein expression in pancreas carcinoma cells by two-dimensional gel electrophoresis. *Proteomics* **2002**, *2*, 697–705.
16. Keenan, J.; Murphy, L.; Henry, M.; Meleady, P.; Clynes, M. Proteomic analysis of multidrug-resistance mechanisms in adriamycin-resistant variants of DLKP, a squamous lung cancer cell line. *Proteomics* **2009**, *9*, 1556–1566.
17. Murphy, L.; Clynes, M.; Keenan, J. Proteomic analysis to dissect mitoxantrone resistance-associated proteins in a squamous lung carcinoma. *Anticancer Res.* **2007**, *27*, 1277–1284.

18. Skalnikova, H.; Halada, P.; Dzubak, P.; Hajduch, M.; Kovarova, H. Protein fingerprints of anti-cancer effects of cyclin-dependent kinase inhibition: identification of candidate biomarkers using 2D liquid phase separation coupled to mass spectrometry. *Tech. Cancer Res. Treat* **2005**, *4*, 447–454.
19. Puustinen, P.; Junttila, M.R.; Vanhatupa, S.; Sablina, A.A.; Hector, M.E.; Teittinen, K.; Raheem, O.; Ketola, K.; Lin, S.; Kast, J.; *et al*. PME-1 protects extracellular signal-regulated kinase pathway activity from protein phosphatase 2A-mediated inactivation in human malignant glioma. *Cancer Res.* **2009**, *69*, 2870–2877.
20. Haley, B.; Paunesku, T.; Protic, M.; Woloschak, G.E. Response of heterogeneous ribonuclear proteins (hnRNP) to ionising radiation and their involvement in DNA damage repair. *Int. J. Radiat. Biol.* **2009**, *85*, 643–655.
21. He, Y.; Rothnagel, J.A.; Epis, M.R.; Leedman, P.J.; Smith, R. Downstream targets of heterogeneous nuclear ribonucleoprotein A2 mediate cell proliferation. *Mol. Carcinog.* **2009**, *48*, 167–179.
22. Malz, M.; Weber, A.; Singer, S.; Riehmer, V.; Bissinger, M.; Riener, M.O.; Longerich, T.; Soll, C.; Vogel, A.; Angel, P.; *et al.* Overexpression of far upstream element binding proteins: A mechanism regulating proliferation and migration in liver cancer cells. *Hepatology* **2009**, *50*, 1130–1139.
23. Obchoei, S.; Wongkhan, S.; Wongkham, C.; Li, M.; Yao, Q.; Chen, C. Cyclophilin A: Potential functions and therapeutic target for human cancer. *Med. Sci. Monit.* **2009**, *15*, RA221–32.
24. Wang, W.; Eddy, R.; Condeelis, J. The cofilin pathway in breast cancer invasion and metastasis. *Nat. Rev. Cancer* **2007**, *7*, 429–440.
25. Ren, L.; Hong, S.H.; Cassavaugh, J.; Osborne, T.; Chou, A.J.; Kim, S.Y.; Gorlick, R.; Hewitt, S.M.; Khanna, C. The actin-cytoskeleton linker protein ezrin is regulated during osteosarcoma metastasis by PKC. *Oncogene* **2009**, *28*, 792–802.
26. Skalnikova, H.; Martinkova, J.; Hrabakova, R.; Halada, P.; Dziechciarkova, M.; Hajduch, M.; Gadher, S.J.; Hammar, A.; Enetoft, D.; Ekefjard, A.; *et al.* Cancer drug-resistance and a look at specific proteins: Rho GDP-dissociation inhibitor 2, Y-box binding protein 1, and HSP70/90 organizing protein in proteomics clinical application. *J. Proteome Res.* **2010**, *10*, 404–415.
27. Resendis-Antonio, O.; Checa, A.; Encarnacion, S. Modeling core metabolism in cancer cells: Surveying the topology underlying the Warburg effect. *PLoS One* **2010**, *5*, e12383.
28. Granchi, C.; Roy, S.; De Simone, A.; Salvetti, I.; Tuccinardi, T.; Martinelli, A.; Macchia, M.; Lanza, M.; Betti, L.; Giannaccini, G.; *et al. N*-Hydroxyindole-based inhibitors of lactate dehydrogenase against cancer cell proliferation. *Eur. J. Med. Chem.* **2011**, *46*, 5398–5407.
29. Li, Y.; Ray, P.; Rao, E.J.; Shi, C.; Guo, W.; Chen, X.; Woodruff, E.A., III; Fushimi, K.; Wu, J.Y. A Drosophila model for TDP-43 proteinopathy. *Proc. Natl. Acad. Sci. USA* **2010**, *107*, 3169–3174.
30. Kawahara, Y.; Mieda-Sato, A. TDP-43 promotes microRNA biogenesis as a component of the Drosha and Dicer complexes. *Proc. Natl. Acad. Sci. USA* **2012**, *109*, 3347–3352.
31. Urushitani, M.; Sato, T.; Bamba, H.; Hisa, Y.; Tooyama, I. Synergistic effect between proteasome and autophagosome in the clearance of polyubiquitinated TDP-43. *J. Neurosci. Res.* **2010**, *88*, 784–797.
32. Nilsson, J.; Gritli-Linde, A.; Heby, O. Skin fibroblasts from spermine synthase-deficient hemizygous gyro male (Gy/Y) mice overproduce spermidine and exhibit increased resistance to oxidative stress but decreased resistance to UV irradiation. *Biochem. J.* **2000**, *352*, 381–387.

33. Chen, Z.; Gopalakrishnan, S.M.; Bui, M.H.; Soni, N.B.; Warrior, U.; Johnson, E.F.; Donnelly, J.B.; Glaser, K.B. 1-Benzyl-3-cetyl-2-methylimidazolium iodide (NH125) induces phosphorylation of eukaryotic elongation factor-2 (eEF2): A cautionary note on the anticancer mechanism of an eEF2 kinase inhibitor. *J. Biol. Chem.* **2011**, *286*, 43951–43958.
34. Lukong, K.E.; Larocque, D.; Tyner, A.L.; Richard, S. Tyrosine phosphorylation of sam68 by breast tumor kinase regulates intranuclear localization and cell cycle progression. *J. Biol. Chem.* **2005**, *280*, 38639–38647.
35. Lobato, S.; Tafuri, A.; Fernandes, P.A.; Caliari, M.V.; Silva, M.X.; Xavier, M.A.; Vago, A.R. Minichromosome maintenance 7 protein is a reliable biological marker for human cervical progressive disease. *J. Gynecol. Oncol.* **2012**, *23*, 11–15.
36. Liu, Y.Z.; Jiang, Y.Y.; Hao, J.J.; Lu, S.S.; Zhang, T.T.; Shang, L.; Cao, J.; Song, X.; Wang, B.S.; Cai, Y.; *et al.* Prognostic significance of MCM7 expression in the bronchial brushings of patients with non-small cell lung cancer (NSCLC). *Lung Cancer* **2012**, *77*, 176–182.
37. Marnerides, A.; Vassilakopoulos, T.P.; Boltetsou, E.; Levidou, G.; Angelopoulou, M.K.; Thymara, I.; Kyrtsonis, M.C.; Pappi, V.; Tsopra, O.; Panayiotidis, P.; *et al.* Immunohistochemical expression and prognostic significance of CCND3, MCM2 and MCM7 in Hodgkin lymhoma. *Anticancer Res.* **2011**, *31*, 3585–3594.
38. Di Paola, D.; Zannis-Hadjopoulos, M. Comparative analysis of pre-replication complex proteins in transformed and normal cells. *J. Cell. Biochem.* **2012**, *113*, 1333–1347.
39. Kumano, M.; Furukawa, J.; Shiota, M.; Zardan, A.; Zhang, F.; Beraldi, E.; Wiedmann, R.M.; Fazli, L.; Zoubeidi, A.; Gleave, M.E. Cotargeting Stress-Activated Hsp27 and Autophagy as a Combinatorial Strategy to Amplify Endoplasmic Reticular Stress in Prostate. Cancer *Mol. Cancer Therapeut.* **2012**, doi:10.1158/1535-7163.MCT-12-0072.
40. Kaddar, T.; Rouault, J.P.; Chien, W.W.; Chebel, A.; Gadoux, M.; Salles, G.; Ffrench, M.; Magaud, J.P. Two new miR-16 targets: Caprin-1 and HMGA1, proteins implicated in cell proliferation. *Biol. Cell* **2009**, *101*, 511–524.
41. Solomon, S.; Xu, Y.; Wang, B.; David, M.D.; Schubert, P.; Kennedy, D.; Schrader, J.W. Distinct structural features of caprin-1 mediate its interaction with G3BP-1 and its induction of phosphorylation of eukaryotic translation initiation factor 2alpha, entry to cytoplasmic stress granules, and selective interaction with a subset of mRNAs. *Mol. Cell Biol.* **2007**, *27*, 2324–2342.
42. Driscoll, J.J.; Woodle, E.S. Targeting the ubiquitin+proteasome system in solid tumors. *Semin. Hematol.* **2012**, *49*, 277–283.
43. Rousseau, B.; Menard, L.; Haurie, V.; Taras, D.; Blanc, J.F.; Moreau-Gaudry, F.; Metzler, P.; Hugues, M.; Boyault, S.; Lemiere, S.; *et al.* Overexpression and role of the ATPase and putative DNA helicase RuvB-like 2 in human hepatocellular carcinoma. *Hepatology* **2007**, *46*, 1108–1118.
44. Luo, B.; Lee, A.S. The critical roles of endoplasmic reticulum chaperones and unfolded protein response in tumorigenesis and anticancer therapies. *Oncogene* **2012**, doi:10.1038/onc.2012.130.
45. Calderwood, S.K.; Murshid, A.; Gong, J. Heat shock proteins: Conditional mediators of inflammation in tumor immunity. *Front. Immunol.* **2012**, *3*, 75.
46. Tsuji, T.; Matsuzaki, J.; Caballero, O.L.; Jungbluth, A.A.; Ritter, G.; Odunsi, K.; Old, L.J.; Gnjatic, S. Heat shock protein 90-mediated peptide-selective presentation of cytosolic tumor antigen for direct recognition of tumors by CD4(+) T cells. *J. Immunol.* **2012**, *188*, 3851–3858.

47. Kiyamova, R.; Garifulin, O.; Gryshkova, V.; Kostianets, O.; Shyian, M.; Gout, I.; Filonenko, V. Preliminary study of thyroid and colon cancers-associated antigens and their cognate autoantibodies as potential cancer biomarkers. *Biomarkers* **2012**, *17*, 362–371.
48. Fucikova, J.; Kralikova, P.; Fialova, A.; Brtnicky, T.; Rob, L.; Bartunkova, J.; Spisek, R. Human tumor cells killed by anthracyclines induce a tumor-specific immune response. *Cancer Res.* **2011**, *71*, 4821–4833.
49. Jia, R.; Li, C.; McCoy, J.P.; Deng, C.X.; Zheng, Z.M. SRp20 is a proto-oncogene critical for cell proliferation and tumor induction and maintenance. *Int. J. Biol. Sci.* **2010**, *6*, 806–826.
50. Passon, D.M.; Lee, M.; Rackham, O.; Stanley, W.A.; Sadowska, A.; Filipovska, A.; Fox, A.H.; Bond, C.S. Structure of the heterodimer of human NONO and paraspeckle protein component 1 and analysis of its role in subnuclear body formation. *Proc. Natl. Acad. Sci. USA* **2012**, *109*, 4846–4850.
51. Mihal, V.; Hajduch, M.; Noskova, V.; Janostakova, A.; Safarova, M.; Orel, M.; Kouzmina, G.; Stary, J.; Blazek, B.; Pospisilova, D. The analysis of correlations between drug resistance and clinical/laboratory measures found in a group of children with all treated by ALL-BFM 90 protocol. *Bull. Cancer* **2004**, *91*, 10080–10089.
52. Lee, B.W.; Johnson, G.L.; Hed, S.A.; Darzynkiewicz, Z.; Talhouk, J.W.; Mehrotra, S. DEVDase detection in intact apoptotic cells using the cell permeant fluorogenic substrate, (z-DEVD)2-cresyl violet. *Biotechniques* **2003**, *35*, 1080–1085.
53. Luche, S.; Diemer, H.; Tastet, C.; Chevallet, M.; van Dorsselaer, A.; Leize-Wagner, E.; Rabilloud, T. About thiol derivatization and resolution of basic proteins in two-dimensional electrophoresis. *Proteomics* **2004**, *4*, 551–561.
54. Hardy, E.; Castellanos-Serra, L.R. "Reverse-staining" of biomolecules in electrophoresis gels: Analytical and micropreparative applications. *Anal. Biochem.* **2004**, *328*, 1–13.
55. Gobom, J.; Nordhoff, E.; Mirgorodskaya, E.; Ekman, R.; Roepstorff, P. Sample purification and preparation technique based on nano-scale reversed-phase columns for the sensitive analysis of complex peptide mixtures by matrix-assisted laser desorption/ionization mass spectrometry. *J. Mass Spectrom.* **1999**, *34*, 105–116.
56. Jarkovska, K.; Martinkova, J.; Liskova, L.; Halada, P.; Moos, J.; Rezabek, K.; Gadher, S.J.; Kovarova, H. Proteome mining of human follicular fluid reveals a crucial role of complement cascade and key biological pathways in women undergoing *in vitro* fertilization. *J. Proteome Res.* **2010**, *9*, 1289–1301.
57. Team, RDevelopment Core. *R: A Language and Environment for Statistical Computing*; R Foundation for Statistical Computing: Vienna, Austria, 2011.
58. Thomas, P.D.; Campbell, M.J.; Kejariwal, A.; Mi, H.; Karlak, B.; Daverman, R.; Diemer, K.; Muruganujan, A.; Narechania, A. PANTHER: A library of protein families and subfamilies indexed by function. *Genome Res.* **2003**, *13*, 2129–2141.

© 2012 by the authors; licensee MDPI, Basel, Switzerland. This article is an open access article distributed under the terms and conditions of the Creative Commons Attribution license (http://creativecommons.org/licenses/by/3.0/).

PŘÍLOHA 2

research articles Journal of proteome research

Cancer Drug-Resistance and a Look at Specific Proteins: Rho GDP-Dissociation Inhibitor 2, Y-Box Binding Protein 1, and HSP70/90 Organizing Protein in Proteomics Clinical Application

Helena Skalnikova,[†,#] Jirina Martinkova,[†,#] Rita Hrabakova,[†] Petr Halada,[‡] Marta Dziechciarkova,[§] Marian Hajduch,[§] Suresh Jivan Gadher,[||] Andreas Hammar,[⊥] Daniel Enetoft,[⊥] Andreas Ekefjard,[⊥] Ola Forsstrom-Olsson,[⊥] and Hana Kovarova*[,†]

Institute of Animal Physiology and Genetics AS CR, v.v.i., Rumburska 89, 277 21 Libechov, Czech Republic, Institute of Microbiology AS CR, v.v.i., Videnska 1083, 142 20 Prague, Czech Republic, Laboratory of Experimental Medicine, Institute of Translational and Molecular Medicine, Faculty of Medicine and Dentistry, Palacky University and University Hospital, Puskinova 6, 775 20 Olomouc, Czech Republic, Millipore Bioscience, 15 Research Park Drive, St. Charles, Missouri 63304, United States, and Ludesi, Engelbrektsgatan 15, SE-211 33 Malmö, Sweden

Received May 14, 2010

Resistance to anti-cancer drugs is a well recognized problem and very often it is responsible for failure of the cancer treatment. In this study, the proteome alterations associated with the development of acquired resistance to cyclin-depedent kinases inhibitor bohemine, a promising anti-cancer drug, were analyzed with the primary aim of identifying potential targets of resistance within the cell that could pave a way to selective elimination of specific resistant cell types. A model of parental susceptible CEM T-lymphoblastic leukemia cells and its resistant counterpart CEM-BOH was used and advanced 2-D liquid chromatography was applied to fractionate cellular proteins. Differentially expressed identified proteins were further verified using immunoblotting and immunohistochemistry. Our study has revealed that Rho GDP-dissociation inhibitor 2, Y-box binding protein 1, and the HSP70/90 organizing protein have a critical role to play in resistance to cyclin-depedent kinases inhibitor. The results indicated not only that quantitative protein changes play an important role in drug-resistance, but also that there are various other parameters such as truncation, post-translational modification(s), and subcellular localization of selected proteins. Furthermore, these proteins were validated for their roles in drug resistance using different cell lines resistant to diverse representatives of anti-cancer drugs such as vincristine and daunorubicin.

Keywords: cancer • anti-cancer drugs • drug resistance • CEM T-lymphoblastic leukemia • CDK inhibitor • proteomics • Rho GDP-dissociation inhibitor 2 • Y-box binding protein 1 • Hsp70/90 organizing protein • biomarker

Introduction

Cancers represent group of unprecedentedly heterogeneous diseases that affect humans with high frequency and contribute significantly to overall morbidity and mortality. Development of resistance to cancer chemotherapeutic treatments is a major problem for successful therapy, especially in late stages of the disease.

Cancer cells can acquire drug resistance by several distinct mechanisms. One such group of mechanisms of extreme importance is represented by pharmacological and physiological parameters. Included within this group is the family of P450 enzymes in liver which controls the metabolism of drugs. Increased levels of these enzymes are observed in a variety of solid tumors and may contribute to drug resistance. The membrane proteins including channels, solute carriers, and ABC transporters are known to play a role in increased drug efflux from cancer cells. Inadequate metabolic activation of anti-cancer drug analogues of DNA precursors represents a synergistic enhancement to the drug resistance by cancer cells. Furthermore, the resistance to the drugs that directly affect structural integrity of DNA may result from the activation of DNA-repair systems which may nullify the effect of the drug. The second mechanism grouping of the factors contributing to the anti-cancer drug resistance includes altered survival pathways such as evasion of apoptosis, necrosis, mitotic catastrophe, or senescence.[1,2] Consideration has to be given to a third group represented by cancer stem cells. These cells are likely to share many of the properties of normal stem cells,

* To whom correspondence should be addressed. E-mail, kovarova@iapg.cas.cz; tel, +420 315 639 582; fax, +420 315 639 510.
[#] Both authors contributed equally to this work.
[†] Institute of Animal Physiology and Genetics AS CR, v.v.i.
[‡] Institute of Microbiology AS CR, v.v.i.
[§] Palacky University and University Hospital.
[||] Millipore Bioscience.
[⊥] Ludesi.

Published on Web 11/10/2010
10.1021/pr100468w
© 2011 American Chemical Society

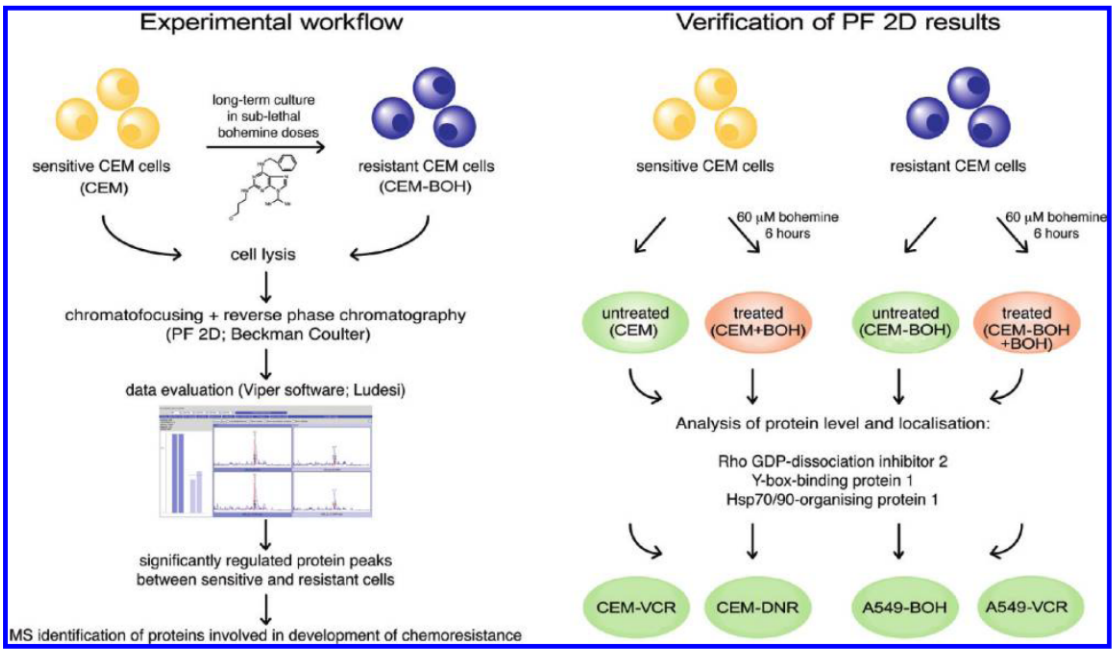

Figure 1. Schematic presentation of the experimental and verification workflows. The lysates of cell samples of parental susceptible CEM cell line and CEM-BOH cells resistant to cyclin-dependent kinases inhibitor bohemine were fractionated using 2-D liquid chromatography. The proteome maps were evaluated for differentially expressed protein peaks and identity of the proteins was determined by mass spectrometry. Selected protein changes were verified using immunoblotting and immunohistochemistry. The proteins were further validated for their roles in drug resistance using CEM and A549 cell lines resistant to vincristine or daunorubicin.

thus, mediating self-renewal and long life span including resistance to drugs and toxins through the expression of several ABC transporters, an active DNA-repair capacity, and a resistance to apoptosis.[3] Most of the above-described mechanisms were revealed using cell culture experiments and their correlation to clinical outcomes need further studies.

Recently, proteomic approaches have been applied to further our knowledge of the mechanisms underlying chemoresistance in context of overall protein expression and disease states. Such studies have been performed to date on selected cancer cell lines to address resistance to drugs including DNA damaging agents (doxorubicin, cisplatin, carboplatin, etoposide, daunorubicin, mitoxantrone) and drugs targeting microtubule dynamics (vincristine, vinblastine). Although the conventional 2-DE was utilized in most of these studies resulting predominantly in identification of abundant proteins, many particular mechanisms of resistance were identified for individually selected drugs and cancer cell lines with a commonality of several other features. Among them, the up-regulated expressions of HSP27, 14-3-3σ, and peroxiredoxins were evident and were further validated (reviewed in Zhang and Liu).[2] However, most of the proteins identified in the proteomic analyses of drug resistant cancer cells have not been verified for their expression changes using other approaches such as Western blot or for their prominent role in drug resistance using functional assays such as MTT cytotoxicity and colony formation.

Previously, we described the effects of bohemine, an inhibitor of cyclin-dependent kinases (CDKI) from the family of trisubstituted purines, on primarily sensitive T-lymphoblastic leukemia CEM cells as well as resistant lung adenoma cell line A549.[4,5] The cyclin-dependent kinases together with cyclins belong to the key molecules regulating cell cycle progression and numerous compounds that can suppress cyclin/cyclin-dependent kinases activities have been described as cytostatic drugs.[6] On the basis of the evaluation of the protein maps and possible pathways relevant to response to CDKI, the glycolytic enzymes, annexin IV, histones, and the Crkl adaptor protein implicated in many signal transduction events appeared to be the important targets. The level and phosphorylation of Crkl protein, which is the major tyrosine-phosphorylated protein in chronic myeloid leukemia, was down-regulated in CDKI treated CEM T-lymphoblastic leukemia cells. These changes were validated using immunoblot experiments and in our pilot experiments using K562 myeloid leukemia cells transplanted into SCID mice and treated/untreated with CDKI under *in vivo* conditions.[4]

In this study, the proteome alterations associated with the development of acquired resistance to CDKI bohemine were analyzed on a model of parental susceptible CEM cell line and its resistant counterpart CEM-BOH. 2-D liquid chromatography was used for protein fractionation of cell lysates. The proteome maps were evaluated for differentially expressed proteins and selected changes were further verified using immunoblotting and immunohistochemistry. Furthermore, the proteins were validated for their roles in drug resistance using different cell lines resistant to diverse representatives of anti-cancer drugs such as vincristine and daunorubicin (Figure 1).

Materials and Methods

Chemicals. Urea, Tris-base, thiourea, sodium dodecyl sulfate (SDS), *n*-octyl glucoside, Tris (2-carboxyethyl) phosphine hydrochloride, and iminodiacetic acid were obtained from Sigma-

Aldrich (St. Louis, MO). Nonidet P40, 3-3(cholamidolpropyl)-dimethylammonio-1-propane sulfonate and dithiothreitol were from USB Corporation (Cleveland, OH). Glycerol and β-glycerolphosphate were purchased from Penta (Prague, Czech Republic). Protease inhibitors cocktail was obtained from Roche (Mannheim, Germany). All other chemicals for protein fractionations were of HPLC or analytical grade and buffers were prepared using Mili-Q water system (Millipore Bedford, MA). Unless otherwise specified, all chemicals used for mass spectrometry were from Sigma (Steinheim, Germany).

Cell Cultures and Sample Preparation. The CEM (CEM-CCRF, human T-lymphoblastic leukemia cells) and A549 (human lung adenocarcinoma) cell lines were obtained from American Tissue Culture Collection (ATCC, Manassas, VA). The CEM and A549 cells were cultured in RPMI 1640 and DMEM, respectively, with 5 g/L glucose, 2 mM glutamine, 100 U/mL penicillin, 100 μg/mL streptomycin, and 10% fetal calf serum as described previously.[5] The CEM-BOH bulk cell line resistant to CDKI bohemine was derived from parental sensitive CEM cells by selective pressure of CDKI bohemine as described in previous study.[7] The process of selection started with the drug concentration equal to 10% tumor cells survival of parental CEM line and the concentration of the drug was subsequently increased to 10-fold of 50% tumor cells survival. The CEM cells resistant to vincristine (CEM-VCR) or daunorubicin (CEM-DNR) as well as A549 cells resistant to CDKI bohemine (A549-BOH) or vincristine (A549-VCR) were established using the same protocol and drug resistant lines were designated as the bulk culture and grown in the media mentioned above.[7]

For 2-D liquid chromatography fractionation on ProteomeLab PF 2D (PF 2D; Beckman Coulter, Fullerton, CA), parental sensitive CEM cells and resistant counterparts CEM-BOH were grown to approximately 80 $\times$ 10^6 cells, harvested, and washed three times with PBS. A total of 400 μL of cell suspensions was lysed in 1.6 mL of PF 2D lysis buffer containing 7.5 M urea, 2.5 M thiourea, 62.5 mM Tris, 2.5% octyl glucoside, 6.25 mM TCEP, 12.5% glycerol, and 1.25 mM protease inhibitor. The lysates were centrifuged at 20 000*g* at 4 °C for 1 h. The supernatants were stored at −80 °C for future use. Two biological replicates of each sample of CEM cells as well as CEM-BOH cells were analyzed. For SDS-PAGE followed by Western blot, parental sensitive CEM cells and their resistant counterparts CEM-BOH, CEM-VCR, and CEM-DNR as well as parental A549 cells and derived resistant cells A549-BOH or A549-VCR were grown in media as mentioned above. The cells were washed in ice-cold PBS, lysed in SDS sample buffer, and boiled and total cell protein extracts of 10^5 cells corresponding to approximately 10 μg of proteins were loaded on the gel. Additionally, CEM cells treated with 60 μM CDKI bohemine for 6 h were prepared in the same manner.

Two-Dimensional HPLC ProteomeLab PF 2D Chromatography and Image Analysis. Samples of CEM and CEM-BOH cell lines in denaturating buffer were loaded on PD10 column equilibrated with 25 mL of the start buffer (provided in PF 2D kit, Beckman Coulter, Fullerton, CA) to exchange denaturating lysis buffer to the start buffer. The protein concentration in the sample collected from PD10 column was determined by direct measurement of absorbance at 280 nm (DU 7400 spectrophotometer, Beckman Coulter, Fullerton, CA). For the first-dimension high-performance chromatofocusing fractionation (HPCF), two buffers, a start buffer pH 8.5 and an elution buffer pH 4.0, both provided in PF 2D kit were used to generate an internal linear pH gradient on the column. The HPCF column was equilibrated with 30 column volumes of start buffer and cell lysate of 3.6 mg of total protein was applied on HPCF column using 5 mL injection loop. The separation was performed at a flow rate of 0.2 mL/min. Once the pH in the column achieved a stable value of 8.5 (30 min), the linear gradient of elution buffer to pH of 4 was switched. The proteins remaining on the column at pH 4 were washed out by 1 M NaCl in 30% *n*-propanol solution. UV detection was performed at 280 nm and the pH of the effluent was monitored using a flow-through online pH probe. Fraction collection started when gradient reached pH 8.3 and individual fractions were collected in 0.3 pH intervals. In every run, pH was monitored for 150 min and UV was monitored for 220 min. In total, 15 fractions collected in the pH range 8.30−4.10 and one fraction collected in the pH > 8.30 (proteins that did not bind to the HPCF column) were collected during HPCF separation. The pH fractions were further separated on high-performance reversed phase column (HPRP) packed with C18 nonporous silica beads. Solvent A was 0.1% trifluoroacetic acid (TFA) in water and solvent B was 0.08% TFA in acetonitrile (MeCN). The separation was done at 50 °C at a flow rate 0.75 mL/min. The gradient was run from 0% to 100% B in 35 min, followed by 100% B for 4 min and 100% A for 10 min. UV absorptions were monitored at 214 nm. The fractions were collected in 0.13 min time intervals into 96-deep well plates using the fraction collector Gilson FC204 (Immunotech a.s., Prague, Czech Republic) and stored at −80 °C until further use.

2-D protein expression maps of sensitive CEM and resistant CEM-BOH cells displaying protein isoelectric point versus protein hydrophobicity were generated by ProteoVue software running on PF 2D system. ProteoVue software converts the UV peak intensity in the chromatograms from the second dimension HPRP column of each pH fraction to a band and line format and provides the mean to view and quantify protein levels. The novel Viper software version 2.3.0.0. was further used to evaluate protein maps. The above software was developed in collaboration with Ludesi (Malmö, Sweden), Beckman Coulter (Fullerton, CA), Johns Hopkins University (Baltimore, MD), and Academy of Sciences of the Czech Republic (Prague, Czech Republic). It is an analysis software for aligning, quantifying, normalizing, and comparing data in a multisample 2-D LC-experiment as described. At first, the baseline in chromatograms was detected and one sample was selected as a Master. Then, the UV profiles of fractions with corresponding pH were aligned to correct eventual pH shifts during the first-dimension separation. The second-dimension chromatograms of each consecutive pH fraction in the Master were then aligned to detect protein peaks eluting in the same retention time. The maximum span of the single protein peak in sequential pH fractions was set to 3 fractions. The second-dimension chromatograms of individual pH fractions of the samples were then aligned with the Master. Protein peaks were detected in the area of retention times from 10 to 26 min and the peak intensities were quantified and normalized to the sum of areas under the chromatograms in this retention time range for the whole sample (in all pH fractions). Additionally, for individual peak areas detected in each of the pH fractions, the Viper software allows calculation of total area for every protein peak with the same retention time that is present in several sequential pH fractions. The peaks with *p*-values in ANOVA test below 0.05 and/or peaks with fold change ≥1.6 were

Table 1. Differentially Expressed Proteins Identified in 2-D LC Experiment[a]

peak no.	protein name	UniProt no.	biological function	change	fold change	*p*-value
088	Tubulin-specific chaperone A	TBCA_HUMAN	protein folding	↓	2	0.056
115	Rho GDP-dissociation inhibitor 1	GDIR_HUMAN	Rho protein signal transduction	↑	2.02	0.22
	Tumor protein D54	TPD54_HUMAN	regulation of cell proliferation			
	Tropomyosin alpha-3 chain	TPM3_HUMAN	cellular component movement			
	Histone H2B type 1-B	H2B1B_HUMAN	nucleosome assembly			
163	Histone H2A type 1-H*	H2A1H_HUMAN	nucleosome assembly	↓	1.92	0.039
	Elongation factor 1-alpha 1	EF1A1_HUMAN	translational elongation			
200	Stress-induced-phosphoprotein 1	STIP1_HUMAN	response to stress	↑	8.18	0.008
	Macrophage-capping protein	CAPG_HUMAN	protein complex assembly			
362	Rho GDP-dissociation inhibitor 2	GDIR2_HUMAN	actin cytoskeleton organization Rho protein signal transduction	↑	2.36	0.591
365	Tropomyosin alpha-4 chain	TPM4_HUMAN	cellular component movement	↑	1.72	0.046
	Histone H4*	H4_HUMAN	nucleosome assembly			
648	60S ribosomal protein L6*	RL6_HUMAN	translation	↓	2.06	0.18
	60S ribosomal protein L4	RL4_HUMAN	translation			
	Histone H2B type 1-D	H2B1D_HUMAN	nucleosome assembly			
	Histone H4*	H4_HUMAN	nucleosome assembly			
649	Histone H2B type 1-J	H2B1J_HUMAN	nucleosome assembly	↓	2.4	0.006
	Histone H4	H4_HUMAN	nucleosome assembly			
701	Nuclease sensitive element-binding protein 1	YBOX1_HUMAN	regulation of transcription mRNA processing	↓	8.72	0.31
770	60S ribosomal protein L15	RL15_HUMAN	translation	↓	2.56	0.59
	40S ribosomal protein S8	RS8_HUMAN	translation			
780	40S ribosomal protein S24	RS24_HUMAN	translation	↓	1.82	0.107
800	40S ribosomal protein S25	RS25_HUMAN	translation	↑	1.62	0.006
	40S ribosomal protein S4, X isoform	RS4X_HUMAN	translation			
	Small nuclear ribonucleoprotein Sm D3	SMD3_HUMAN	mRNA processing, RNA splicing			
847	Nuclease sensitive element-binding protein 1	YBOX1_HUMAN	regulation of transcription mRNA processing	↓	2.68	0.13
	60S ribosomal protein L26	RL26_HUMAN	translation			
889	Histone H2A type 1-H*	H2A1H_HUMAN	nucleosome assembly	↑	1.67	0.025
1145	60S ribosomal protein L6*	RL6_HUMAN	translation	↓	2.04	0.15
	40S ribosomal protein S13	RS13_HUMAN	translation			
	60S ribosomal protein L7a	RL7A_HUMAN	translation			

[a] The arrows indicate change in the protein level in the resistant cells compared to sensitive cells. Detailed data from MS identification are supplied in the Supplemental Table 1. Asterisks (*) indicate proteins found in nonsequential fractions.

considered as significant differences and the corresponding fractions were processed by mass spectrometry (Table 1).

Protein Identification by MALDI-TOF Mass Spectrometry. The fractions from the second dimension of PF2D separation were completely dried using a SpeedVac and redissolved in 50 μL of a cleavage buffer containing 0.01% 2-mercaptoethanol, 50 mM 4-ethylmorpholine acetate, 5% MeCN, and 5 ng of sequencing grade trypsin (Promega, Madison, WI). After overnight digestion, the resulting peptides were acidified by the addition of 5 μL of 5% TFA in MeCN. A solution of α-cyano-4-hydroxycinnamic acid in aqueous 50% MeCN/0.2% TFA (5 mg/mL) was used as a MALDI matrix. A 0.5 μL of a sample was deposited on the MALDI target and allowed to air-dry at room temperature. After complete evaporation, 0.5 μL of the matrix solution was added. MALDI mass spectra were measured on an Ultraflex III instrument (Bruker Daltonics, Bremen, Germany) equipped with a Smartbeam solid state laser and LIFT technology for MS/MS analysis. The spectra were acquired in the mass range of 700−4000 Da and calibrated internally using the monoisotopic $[M + H]^+$ ions of trypsin autoproteolytic fragments (842.5 and 2211.1 Da).

Peak lists in XML data format were created using flexAnalysis 3.0 program with SNAP peak detection algorithm. No smoothing was applied and maximal number of assigned peaks was set to 50. After peak labeling, all known contaminant signals were manually removed. The peak lists were searched using MASCOT search engine against Swiss-Prot 57.6 database subset of human proteins with the following search settings: peptide tolerance of 20 ppm, missed cleavage site value set to two, variable oxidation of methionine and N-acetylation of protein N-terminus. No restriction on protein molecular weight and p*I* value was applied. Proteins with MOWSE score over the threshold 56 calculated for the used settings were considered as identified. If the score was only slightly higher than the threshold value or the sequence coverage too low, the identity of protein candidate was confirmed by MS/MS analysis. In addition to the above-mentioned MASCOT settings, fragment mass tolerance of 0.6 Da and Ultraflex III instrument (Bruker Daltonics, Bremen, Germany) equipped with a Smartbeam solid state laser and LIFT technology for MS/MS analysis was applied for MS/MS spectra searching.

The Protein Expression Analysis Using Immunoblot. The whole-cell lysates prepared as described above were used for SDS-PAGE. For electrophoretic separation of PF 2D fractions, 10% of the total volume of the first-dimension pH fractions was precipitated by trichloroacetic acid, dissolved in 15 μL of SDS sample buffer, and loaded on SDS-PAGE.

Following SDS-PAGE using 10, 12, or 15% polyacrylamide gels, separated proteins were transferred onto Immobilon P (Millipore, Bedford, MA) membranes using a semidry blotting system (Biometra, Göttingen, Germany) and transfer buffer containing 48 mM Tris, 39 mM glycine, and 20% methanol.[8] The membranes were blocked in 5% nonfat dry milk or in 5% BSA in Tris-buffered saline with 0.05% Tween 20 (TBST) pH 7.4 for 1 h and incubated overnight with the respective primary antibodies: anti-Rho-GDI2 (Rho GDP-dissociation inhibitor 2; Abcam ab13925; 1:500 in 5% BSA/TBST), anti-YB1 (Y-box binding protein 1; Abcam ab12148; 1:10 000 in 5% nonfat dry milk/TBST), anti-Hop (HSP 70/90 organizing protein; Abcam ab37752; 1:10 000 in 5% nonfat dry milk/TBST), or anti-β-tubulin (Sigma T4026; 1:1000 in 5% nonfat dry milk/TBST). Peroxidase-conjugated secondary anti-mouse and anti-rabbit IgG antibodies (Jackson Immunoresearch, Suffolk, U.K.) were diluted 1:10 000, and anti-chicken IgY (Abcam ab6753) was diluted 1:100 000 in 5% nonfat dry milk/TBST and applied as appropriate. The ECL+ chemiluminescence (GE Healthcare, Uppsala, Sweden) detection system was used to detect specific proteins. The exposed CL-XPosure films (Thermo Scientific, Rockford, IL) were scanned by a calibrated densitometer GS-800 (Bio-Rad, Hercules, CA).

Protein Expression Profiles Characterized by Immunohistochemistry. Paraffin-embedded samples of CEM cells, CEM cells treated with 60 μM CDKI bohemine for 6 h, CEM-BOH cells resistant to CDKI bohemine, and CEM-BOH cells resistant to CDKI bohemine treated with 60 μM CDKI bohemine for 6 h were cut in the sections, mounted on silane-coated slides, deparaffinized, rehydrated, and pretreated in a microwave at 650 W for 30 min in citrate buffer pH 6.0. Nonspecific binding was blocked with 5% rabbit serum in phosphate buffer solution. Sections were incubated in the primary anti-Hop antibody (Abcam ab37752; 1:500). As a secondary antibody, anti-chicken IgY (Abcam ab6753) was applied for 60 min (working dilution 1:400) followed by biotin−streptavidin−peroxidase complex (Dako, Copenhagen, Denmark). Diaminobenzidine substrate was used as a chromogen, according to the manufacturer's instructions (DAKO, Copenhagen, Denmark). Sections were counterstained with hematoxylin.

Computer Modeling of Protein Interaction Network. Interologous Interaction Database (I2D; an online database of known and predicted mammalian and eukaryotic protein−protein interactions) was used to search for possible protein−protein interaction partners for proteins identified as regulated during the development of acquired resistance to cyclin-dependent kinases inhibitor. Version 1.8 of I2D, including 254 588 source interactions and 238 553 predicted interactions (http://ophid.utoronto.ca/ophidv2.201/ppi.jsp) was used for interaction search with human selected as target organism. Protein−protein interaction network was visualized using NAViGaTOR (Network Analysis, Visualization & Graphing TORonto) software (http://ophid.utoronto.ca/navigator). In protein−protein interaction networks, nodes represent proteins and edges between nodes represent physical interactions between the proteins. NAViGaTOR allows nodes to be color-coded according to Gene Ontology (GO, a controlled vocabulary describing properties of genes) terms.

Results

Proteomic Changes Observed in CEM-BOH Cells Resistant to CDKI Bohemine Compared to Sensitive CEM Cells Using 2-D LC. The primary aim of our study was to identify differences in protein expression between CEM-BOH cells resistant to CDKI bohemine and bohemine-sensitive parental CEM cells. The lysates of cell samples were fractionated using 2-D liquid chromatography, resulting proteome maps were evaluated for differentially expressed protein peaks, and identity of the proteins was determined by mass spectrometry. Selected protein changes were verified using immunoblotting and immunohistochemistry. The proteins were further validated for their roles in drug resistance using CEM and A549 cell lines resistant to vincristine or daunorubicin (Figure 1).

The purpose of 2-D LC protein separation performed on PF 2D was to use an advanced gel-independent fractionation technique. This method has the distinct advantage over the 2-DE based approach in that it overcomes many of its drawbacks and, importantly, the fractions of intact proteins can be directly utilized for mass spectrometric analysis. The PF 2D involves 2-D separation and mapping of the total protein expression. Proteins are fractionated by isoelectric points in pH gradient using the chromatofocusing at 0.3 pH intervals in the first dimension. Each of these pH protein fractions is further separated by hydrophobicity using reversed phase in the second dimension.[9] The global information about protein expression obtained by means of PF 2D separation has been depicted using ProteoVue software that enables the construction of 2-D protein map showing pH fractions versus protein hydrophobicity. Reproducibility of the 2-D LC fractionation can be expressed by coefficient of variation which may be calculated using the values of retention time of all peaks, peak heights, or peak areas from several runs as exemplified in the study of Linke et al.[10] While the values of % of coefficient of variation (% CV) are usually low (in average 0.40) for peak retention time, they are obviously higher (around 20) for peak height or peak area. In our study, median % CV based on the values of normalized peak areas was 31. Coefficient of determination R^2 calculated for variations in peak areas between biological replicates was equal to 94% and 96% for protein patterns corresponding to CEM and CEM-BOH cells, respectively, indicating good reproducibility of separation and quantification methods.

In total, 15 fractions collected in the pH range of 8.30−4.10 and one fraction collected in the pH > 8.30 (proteins that did not bind to the HPCF column) were then separated on HPRP column (Figure 2). The 2-D protein maps of all runs performed in this study are shown in Supplemental Figure 1. The samples of CEM and CEM-BOH cells were separated in average into 1229 protein peaks and the evaluation of qualitative and quantitative differences by UV measurement between 2-D protein maps using Viper software identified 6 differentially expressed protein peaks with p-value $\leq$0.05 (Peak Nos: 163, 200, 365, 649, 800, 889) and 12 protein peaks with fold change $\geq$1.6 (Peak Nos: 88, 115, 163, 200, 362, 648, 649, 701, 770, 780, 847 and 1145) between sensitive CEM and resistant CEM-BOH cells. Nine of the differentially expressed protein peaks revealed by PF 2D approach were present at decreased level in resistant CEM-BOH cells. On the contrary, six protein bands were found in higher level in resistant CEM-BOH cells (Table 1). Relative differences in expression ranged from 1.6-fold to as much as 8.7-fold. Figure 3 demonstrates an example of differences found in fraction of pH 7.7−8.0 and other differences mentioned

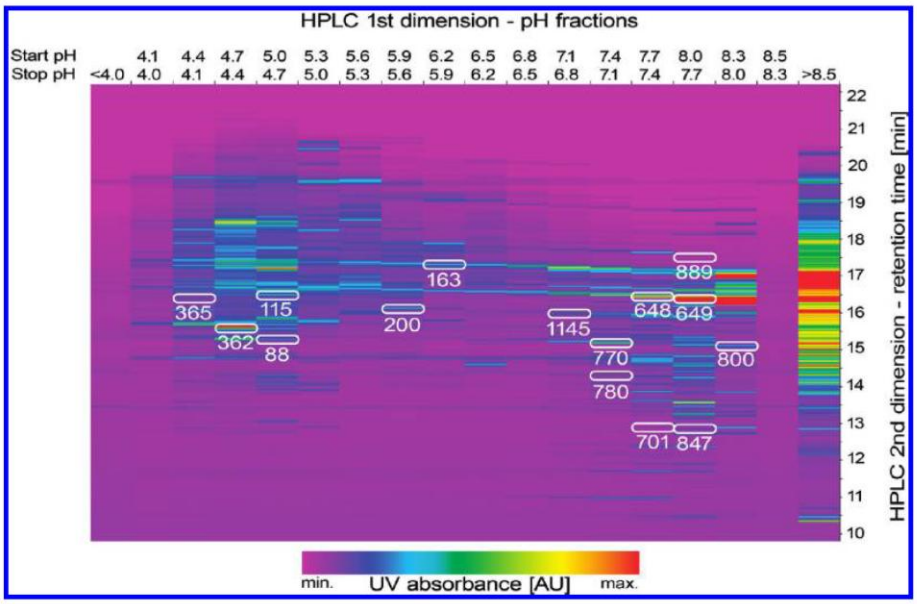

Figure 2. Two-dimensional liquid chromatography protein map of CEM cell line and set of protein peaks significantly different in resistant CEM-BOH cells compared to CEM cells. Lysates of cell samples were subjected to 2-D liquid chromatography and protein fractionation was monitored using UV detection. 2-D protein expression maps were generated by ProteoVue software and their images were evaluated using Viper software. Figure shows representative protein map from parental sensitive CEM cells and a set of protein bands significantly different in resistant CEM-BOH cells. The colors of the protein bands correspond to UV intensity and provide information about protein quantification. Regulated protein peaks are indicated by their numbers assigned by Viper software.

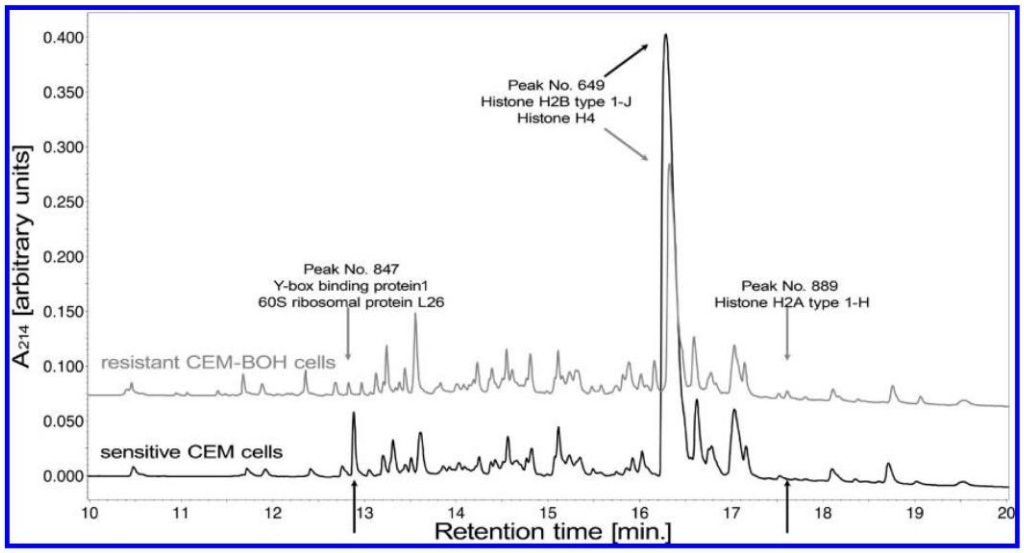

Figure 3. The UV profile of second dimension of 2-D HPLC ProteomeLabPF 2D chromatography and comparison of differences between analyzed samples. The UV chromatogram of pH fraction 7.7−8.0 separated in the second dimension on reversed phase column packed with C18 nonporous silica beads. The UV absorptions were monitored at 214 nm. Three protein peaks were found differentially expressed between sensitive CEM cells and CEM-BOH cells resistant to CDKI bohemine.

above are provided in Supplemental Figure 2). All these discriminate protein peaks were chosen for further mass spectrometry and the proteins in all of them were satisfactorily identified (Table 1). Supplementary Table 1 provides comprehensive information about the proteins (fraction numbers, protein names, database accession numbers, protein MW and p*I*, and all MS identification data including Mascot scores, sequence coverage, matched peaks, unmatched peaks, and MS/MS confirmation). Among the proteins identified in differentially regulated protein peaks in resistant CEM-BOH cells were several ribosomal proteins including the proteins of large 60S ribosomal subunit (proteins L4, L6, L7a, L15 and L26) as well as the proteins of the small 40S ribosomal subunit (S4_X isoform, S8, S13, S24, S25). Furthermore, we have detected

several histone variants, namely, histone H2A type 1-H, histone H2B type 1-B, histone H2B type 1-D, histone H2B type 1-J, and histone H4, to be differently expressed between susceptible and resistant cells. On the basis of our MS data (Supplemental Table 1), we have unambiguously distinguished ribosomal proteins according to the unique peptides that were observed for each identified protein. The only ambiguity in protein identification could be related to specific histone variants within a single core histone, namely, histone H2A and H2B where the top position with the highest score in the protein candidate list given by MASCOT was accepted without any other sequential confirmation. Nevertheless, the core histones H2A, H2B, and H4 were satisfactorily distinguished, and in our opinion, sufficient for the purpose of this study.

It was evident that many of the protein peaks collected after the second dimension contained more than one protein and this was reconfirmed by mass spectrometric analysis. However, there were also protein peaks fulfilling the criteria of one protein/one peak in a fraction: the protein peaks nos. 088 and 701 showing decrease in resistant CEM-BOH cells which corresponded to tubulin-specific chaperone A and Y-box binding protein 1; the protein peaks nos. 362 and 889 showing increase in resistant CEM-BOH cells corresponded to Rho GDP-dissociation inhibitor 2 and histone H2A type 1-H (Table 1, Figure 2).

In the subsequent work, we focused on detailed verification of the proteins (a) with highly elevated/significant increase in resistant CEM-BOH cells: Rho-GDP-dissociation inhibitor 2 (Rho GDI2) with 2.36-fold change and Hsp70/90 organizing protein (Hop; stress-induced phosphoprotein 1- STIP 1) reaching 8.18-fold change; (b) Y-box binding protein 1 (YB-1; nuclease sensitive element-binding protein 1) decreased to almost 9-fold in resistant cells.

Immunoblotting Verification of Protein Changes Typical for Resistant CEM-BOH Cells. To validate the results of the proteomic analysis, immunoblot experiments were performed to confirm the identity of the proteins Rho GDI2 and YB-1 which were increased and decreased, respectively, in resistant CEM-BOH cells compared to sensitive CEM cells on PF 2D chromatography. Furthermore, Hop protein identified as one of two unambiguously identified proteins in peak no. 200 from PF 2D with observed higher UV absorbance level in CEM-BOH cells was selected to demonstrate verification and contribution of a particular protein to UV absorbance level corresponding to protein amount.

First, monitoring of protein changes at the level of whole cell lysates was performed. The samples of untreated sensitive CEM and resistant CEM-BOH cells were completed by the cells treated with 60 μM CDKI bohemine for 6 h to monitor early response of sensitive as well as resistant cells to the drug that precedes onset of apoptosis. The results shown in Figure 4A confirmed significantly higher level of Rho GDI2 in resistant cells. The treatment by CDKI bohemine resulted in almost undetectable Rho GDI2 level in sensitive cells while in resistant cells showed high Rho GDI2 level. The level of YB-1 protein observed at 50 kDa corresponding to intact protein[11] did not reveal significant difference between the sensitive and resistant cells. In spite of this, similarly to Rho GDI2, treatment by CDKI bohemine resulted in decreased level of YB-1 in sensitive cells but not in resistant cells. The faint protein band observed at 32 kDa represented truncated form of the YB-1 protein[12] which appeared to be more evident in resistant CEM-BOH cells.

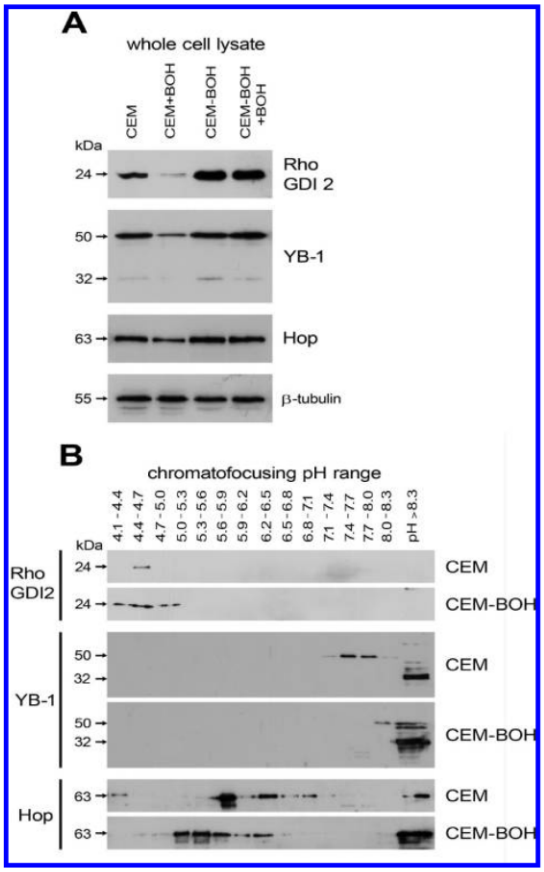

Figure 4. Immunoblot analysis of Rho GDP-dissociation inhibitor 2, Hsp70/90 organizing protein, and Y-box binding protein 1 in susceptible CEM cell line and CEM-BOH cells resistant to cyclin-dependent kinases inhibitor bohemine. (A) The whole-cell lysates were prepared from untreated sensitive CEM cell line and CEM-BOH cells resistant to cyclin-dependent kinases inhibitor bohemine (BOH). The samples of untreated cells were completed by the cells exposed by 60 μM CDKI bohemine: CEM+BOH and CEM-BOH +BOH. The lysates were examined on immunoblots using specific antibodies recognizing Rho GDP-dissociation inhibitor 2 (Rho GDI2), Hsp70/90 organizing protein (Hop), and Y-box binding protein 1 (YB-1). The β-tubulin was used as a loading control. (B) The pH fractions of the first dimension of 2-D fractionation were analyzed using Western blot to detect changes in specific isoforms of these three selected proteins. The shift in pH of YB-1 and Hop proteins between sensitive CEM cells and resistant CEM-BOH cells was detected.

Additionally, the total level of Hop did not reveal significant difference between the sensitive and resistant cells.

Second, protein changes were verified directly in pH fractions from PF 2D in order to look whether different protein forms/variants contribute to the observed alterations (Figure 4B). In case of Rho GDI2, immunoblot of PF 2D pH fractions confirmed massive elevation of the level in resistant cells with spread over several fractions that were symmetrically distributed around protein pH observed in sensitive cells. On the contrary, immunoblot of pH fractions confirmed the presence of acidic 50 kDa YB-1 protein forms (pH 7.1−8.0) in sensitive cells which were not observed in resistant cells. In resistant

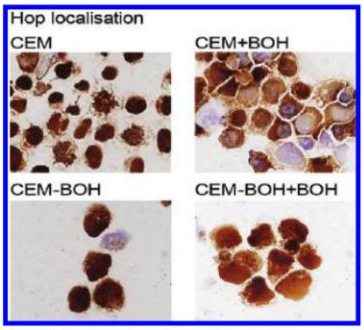

Figure 5. Subcellular localization of Hsp70/90 organizing protein in susceptible CEM cell line and CEM-BOH cells resistant to cyclin-dependent kinases inhibitor bohemine. Untreated sensitive CEM cell line, CEM-BOH cells resistant to cyclin-dependent kinases inhibitor bohemine (BOH), and both cell lines exposed by 60 μM CDKI bohemine: CEM+BOH and CEM-BOH+BOH were analyzed using immunohistochemistry (magnification 800×). Translocation of Hop from nuclei to cytoplasm was observed in sensitive CEM cells after treatment with bohemine. In resistant cells, the Hop protein was localized both in nuclei and cytoplasm and the treatment had no effect on protein level/localization.

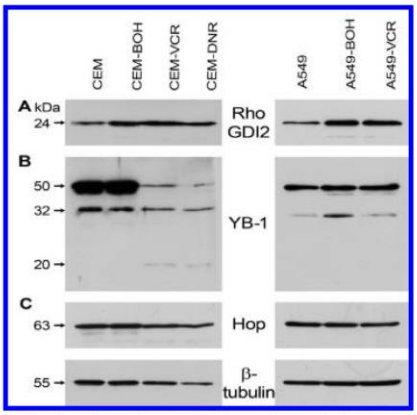

Figure 6. The level of Rho-GDP-dissociation inhibitor 2, Hsp70/90 organizing protein, and Y-box binding protein 1 in cell lines resistant to vincristine or daunorubicin. The samples of CEM cell lines resistant to vincristine (CEM-VCR) or daunorubicin (CEM-DNR) as well as A549 cell lines resistant to CDKI bohemine (A549-BOH) or vincristine (A549-VCR) were examined on immunoblots using specific antibodies recognizing Rho-GDP-dissociation inhibitor 2 (A), Y-box binding protein 1 (B), and Hsp70/90 organizing protein (C). The β-tubulin was used as a loading control.

cells, both protein forms at 50 and 32 kDa were found only in basic fraction with pH higher than 8.3. We could also observe the shift of Hop protein which was distributed in more acidic pH at 5.0−5.6 in resistant cells compared to its predominance at around pH 6.0 in susceptible counterparts. It is likely that the more acidic forms of Hop in CEM-BOH cells represent phosphorylated protein.[13]

Different Subcellular Distribution of the Hop Protein in Resistant CEM-BOH Cells. With respect to the published observations that phosphorylation of Hop protein has impact on its cellular functions as well as localization,[14,15] we used immunohistochemistry to study distribution of Hop protein in sensitive CEM and resistant CEM-BOH cells. As in the in above-mentioned immunoblot experiments, the samples of untreated sensitive CEM and resistant CEM-BOH cells were completed by the cells treated with 60 μM CDKI bohemine for 6 h.

The staining of the Hop protein was high in the nuclei of sensitive CEM cells and appeared to be closely associated to chromosomes. In comparison to this picture, the protein in resistant CEM-BOH cells was localized in both nuclei and cytoplasm. Treatment by CDKI bohemine resulted in decreased staining of Hop protein in nuclei and partial translocation to the cytoplasm in sensitive cells but did not evidently influence the expression pattern in resistant cells (Figure 5).

The Level of Rho GDI2, YB-1, and Hop Proteins in CEM and A549 Cell Lines Resistant to Bohemine, Vincristine, or Daunorubicin. To study the Rho GDI2, YB-1, and Hop proteins for their role in drug resistance, we further examined CEM cell lines resistant to vincristine (CEM-VCR) or daunorubicin (CEM-DNR) as well as representatives of solid tumor, lung adenocarcinoma cell lines A549 resistant to CDKI bohemine (A549-BOH) or vincristine (A549-VCR). Among conventional chemotherapeutic drugs, vincristine belongs to microtubule dynamics affecting drug and daunorubicin is DNA damaging agent. The resistant cell lines were derived and characterized previously.[7]

The immunoblot of whole-cell lysates confirmed increase in the level of Rho GDI2 in all resistant cell lines, including CEM-VCR and CEM-DNR cells compared to parental CEM cells and A549-VCR or A549-DNR cells compared to parental A549 cells (Figure 6A). The expression of YB-1 protein observed in both CEM and CEM-BOH cells at the 50 and 32 kDa bands was without any evident changes between sensitive and resistant cells. On the contrary, the full-length YB-1 protein band at 50 kDa was almost diminished in CEM-VCR and CEM-DNR cells and, in addition to observed 32 kDa truncated form, the appearance of 20 kDa cleaved isoform was evident. Furthermore, the presence of a 32 kDa band of truncated YB-1 protein was also typical for A549-BOH resistant cell line (Figure 6B). The total level of Hop was not different among sensitive cells and cells resistant to bohemine, vincristine, or daunorubicin (Figure 6C); however, it does not exclude the role of specific protein form or its post-translational modification in resistant cells as evidenced by 2-D fractionation mentioned above.

Computer Modeling and Simulation of Possible Interaction Network Connecting Potential Candidate Proteins Regulated during the Development of Acquired Resistance to CDKI. Identified proteins differentially regulated during the development of acquired resistance to cyclin-dependent kinases inhibitor (Protein/Swiss-Prot accession numbers provided in Table 1) were introduced into I2D database in order to identify possible interaction partners and to construct a protein−protein interaction network that enables to graphically visualize possible functional relationships among identified molecules (Figure 7). The network exposed many additional interaction proteins with a role in the development of acquired resistance to anti-cancer drugs. In total, 2060 interactions were recognized for the 26 proteins identified in this study (Supplemental Table 2). Computer modeling highlighted a high number of direct as well as mediated interactions among ribosomal proteins, histones, and elongation factor 1-alpha 1, thus, networking transcriptional and translational pathways. Furthermore, it was of interest to observe interconnection of the YB-1 and Hop proteins with this network, namely, direct interaction of Hop protein with elongation factor 1-alpha 1 and link between YB-1 and Hop proteins mediated by three interacting proteins:

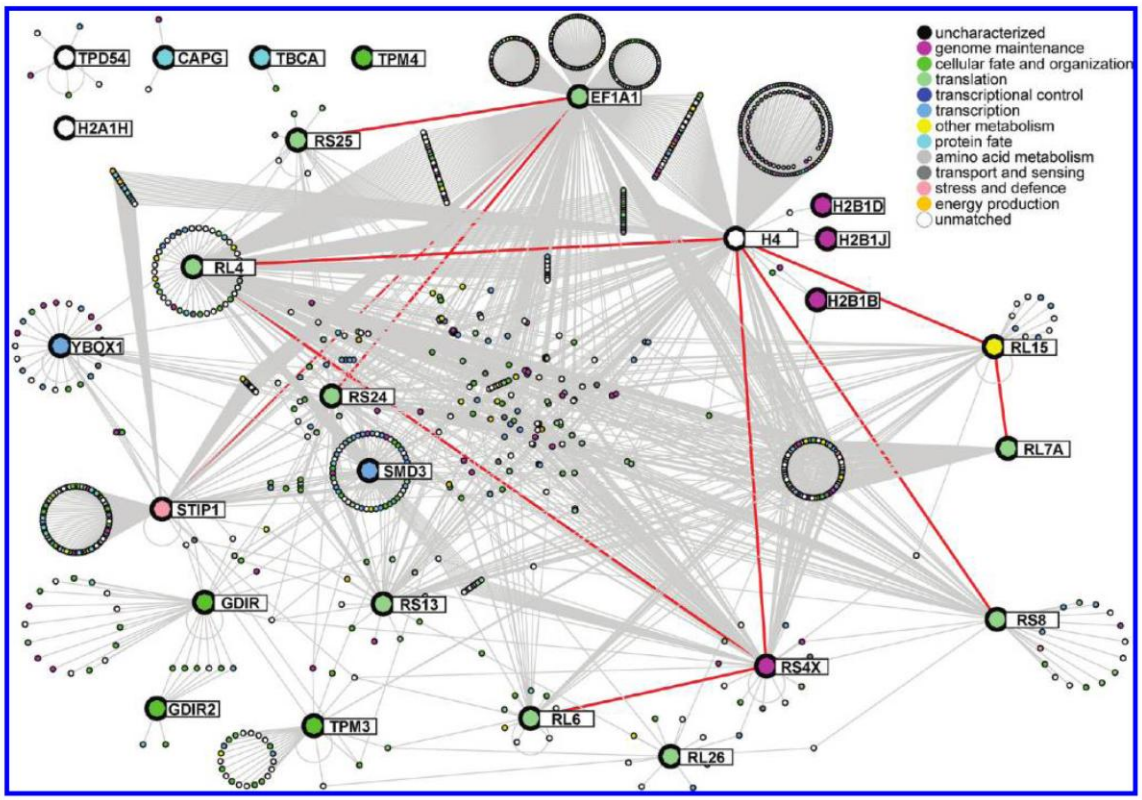

Figure 7. Computer modeling and simulation of possible interaction network connecting potential candidate proteins regulated during the development of acquired anti-cancer drug resistance. Network of possible protein−protein interactions, generated by querying I2D database and NAViGaTOR software for 26 identified proteins which were found to be regulated during the development of acquired anti-cancer drug resistance. Some interacting proteins, with direct interconnection are highlighted by red link. Color of nodes and edges represents Gene Ontology function.

Cullin-1 (CUL1; UniProt Q13616), Glycogen synthase kinase-3 beta (GSK3B; UniProt ID P49841), and S-phase kinase-associated protein 1 (SKP1A; UniProt P63208). Contrary to the above, the Rho GDI2 remains to be segregated from this interaction network.

Discussion

Resistance to anti-cancer drugs is a well-recognized problem and very often it is responsible for failure of the cancer treatment. Unfortunately, drug resistance has been observed not only to conventional chemotherapy but also to molecularly targeted anti-cancer drugs.[2] In our studies we considered selective cyclin-dependent kinases inhibitor as a promising anti-cancer drug. To date, some derivatives of this group of anti-cancer agents have been subjected to pilot clinical trials. Despite this, there are expectations of high probability of resistance development toward this type of selective drugs which may significantly contribute to failure of therapy.

Proteomic analyses of model cancer cell lines have been focused on molecular mechanisms of resistance to many different conventional anti-cancer chemotherapeutic drugs with the primary aim of identifying potential targets of resistance within the cell that would help in selective elimination of specific resistant cell types in actual disease state. The data published to date demonstrated a variety of protein alterations in drug-resistant cells that could contribute to resistance development.[2,16] The protein fractionation using 2-DE was most frequently applied in those experiments. Hence, many of the proteins on the list were relatively highly abundant proteins. Typically, it is exemplified by observed up-regulated expressions of HSP27, 14-3-3σ, and peroxiredoxins which are on the published list of the top 15 most often identified differentially expressed proteins/protein families in proteomics, regardless of the type of experiments, tissue, and even species.[17] The interpretation of such proteomic data has to be very carefully evaluated as regards specificity of these protein changes and before they are considered as relevant in a particular biological model. Hence, selection of the potential candidate proteins that may have crucial roles in molecular mechanisms of drug-resistance and verification using other independent techniques is critical and necessary. The advantage of the above-mentioned list of the top 15 proteins as suggested by Petrak et al.[17] is the possibility of short-listing of differentially expressed candidate proteins to access the more relevant potential drug targets.

To track down more specific proteins contributing to the development of resistance to CDKI, we used advanced gel-independent liquid-phase 2-D HPLC protein fractionation system that enabled in-depth study for selection of the key potential drug targets. We have used CEM T-lymphoblastic

leukemia cells, which are chemosensitive to a majority of anticancer drugs except for the glucocorticoids, and are frequently used for preparation and functional studies of drug resistant sublines.[7] Interestingly, although CEM cells have heterozygous mutations at codons 175/248 (175His/248His) of the p53 gene, the mutated protein forms complexes with DNA leading to transactivation and thus keeping pathway p53 functional.[18] In total, we have identified 26 protein species in 15 differentially expressed protein peaks between sensitive and resistant cells. A majority of the protein changes, in contrast to the previously published 2-DE-based studies, were found to belong to the ribosomal proteins and histones indicating deregulation of translational and transcriptional pathways, respectively, as well as possible epigenetic regulation. The results from our previous study showed down-regulation of three histone variants with different p*I* and hydrophobicity in response to CDKI bohemine, demonstrating that anti-mitotic and anti-cancer activities of this compound may be associated with epigenetic regulation at the level of chromatin structure.[9] In the study presented here, these activities involved in primary response to CDKI bohemine also contribute significantly to acquired resistance to anticancer drug.

Taking into consideration values of fold change and/or significance of the observed differences, it appeared evident that the best potential drug targets could be found among the proteins Rho GDI2, Hop and YB-1. As measured at the total protein levels, only the Rho GDI2 confirmed observed proteome data indicating increased level in resistant CEM-BOH cells. Despite this observation, sensitive CEM cells responded to CDKI bohemine treatment by decrease in the levels of all three candidate proteins, Rho GDI2, YB-1, and Hop, while their protein levels did not change after the treatment in CEM-BOH resistant cells. More detailed immunoblot verification after 2-D separation of cellular proteins clearly demonstrated that, in case of Hop and YB-1 proteins, the observed changes corresponded more to the presence of different protein forms or variants or modifications between susceptible and resistant cells. These findings have subsequently led us to hypothesize that upregulation of Rho GDI2 level together with the presence of more basic YB-1 protein forms and more acidic Hop variants can make CEM cells less vulnerable to anti-cancer inhibitors of CDKs.

The Rho GDI2 belongs to a family of the GDP dissociation inhibitors, which are pivotal regulators of small GTPases, including Ras1, Cdc42, and RhoA. It was shown to be preferentially expressed in hematopoietic tissues and in B- and T-cell lines and its expression in bladder,[19−21] ovarian,[22] and breast cancer cells[23,24] has been demonstrated by various researchers. Some such published studies have attempted to relate the expression of this particular protein to the invasiveness or metastatic potential within different types of tumors with resultant controversy, indicating that RhoGDI2 may act differently in progression of different tumors.[19,21,24−26] More acceptable and clearly evident seems to be the link between increased RhoGDI2 expression and anti-cancer drug resistance in several cancer cell types.[27] In relation to these findings on Rho GDI2 and its overexpression in ovarian cancer resistant to paclitaxel or in fibrosarcoma cell line resistant to mitoxantrone,[27,28] our study shows that Rho GDI2 protein level is induced in leukemia CEM cells and lung adenocarcinoma A549 cells resistant to CDKI bohemine, vincristine, and daunorubicin. The mechanism by which overexpressed Rho GDI2 could most likely contribute to drug resistance would be due to an anti-apoptotic effect. This is supported by the fact that Rho GDIs form complexes with Rho, Ras or Cdc42, Rho GDI2 thereby blocking the apoptotic signal pathway mediated by Ras and c-Jun kinases.[27] Rho GDI2 thus represents a very promising potential marker of resistance to several different cytostatic drugs by various cancers. Such a multidrug resistance marker could be crucial in the determination of drug regimens for patients undergoing cytostatic chemotherapy and may have a significant bearing on the final outcome.

The YB-1 protein, which is the member of the cold shock domain protein family, has several pleiotropic functions in the regulation of gene transcription and translation, DNA repair, and cellular responses to environmental stimuli.[29] YB-1 activity and subcellular distribution may be regulated by its phosphorylation[11] and its proteolysis mediated by proteasome cleavage.[12] Sutherland et al.[30] showed that phosporylation by Akt kinase may induce nuclear translocation of YB-1. Furthermore, the YB-1 protein is transcriptionally activated via newly discovered transcriptional factor Twist, which also directly transactivates Akt2 gene in T-cell leukemias.[31] Akt2 kinase survival pathway is associated with chemoresistance against multiple cytotoxic and targeted therapies. The studies of truncated YB-1 forms revealed that its localization in nuclei of human cancers including breast, ovarian, prostate, colon, osteosarcoma, and synovial sarcoma could be a marker for poor patient outcome and multiple drug resistance.[12,29,32−34] We detected truncated form of YB-1 in leukemia CEM cells resistant to CDKI bohemine, vincristine, and daunorubicin and in lung adenocarcinoma A549 cells resistant to CDKI bohemine. This profile is in agreement with involvement of proteolytic clevage of YB-1 form in multidrug resistance. Furthermore, our study showed that the presence of more basic YB-1 form(s) is typical for CEM cell resistant to CDKI. The modifications causing this pH shift may include changes in protein phosphorylations but truncations or deletions cannot be excluded.[35]

Human Hop is a co-chaperone mediating the association of the molecular chaperones Hsp70 and Hsp90.[36] The best characterized function of Hop protein is its participation in steroid receptor signaling including glucocorticoid response (reviewed in Daniel et al.).[37] More recent findings suggest that Hop can not only associate with Hsp70 and 90 and modulate their activities, but also interact with several other proteins as mentioned above as well as the prion proteins.[15,37] There is evidence that murine homologue mSTI and human Hop may be phosphorylated and this modification affects protein localization.[14,38] In our study, the Hop in resistant CEM-BOH cells was more acidic than in parental CEM cells sensitive to CDKI bohemine but resistant to glucocorticoid dexamethasone suggesting that in CEM-BOH resistant cells Hop may undergo enhanced phosphorylation. Further findings from immunohistochemistry revealed that Hop is localized in nucleus as well as cytoplasm in CEM-BOH resistant cells in contrast to its prevailing accumulation in nucleus in CEM cells. Hence, the shift to more acidic forms appears to be associated with protein translocation to cytoplasm and development of resistance of CEM cells to anti-cancer CDKI bohemine. Interestingly, Longshaw et al.[14] showed that inhibition of cdc2 kinase triggered by CDKI olomoucine, belonging to the same group of anticancer compounds as bohemine, resulted in the nuclear accumulation of mSTI in mouse fibroblasts. On the basis of our findings, it is possible to hypothesize that Hop shuttling induced by CDKI bohemine and associated with development of resistance to this drug in CEM cells which are also resistant

to glucocorticoids may influence steroid receptor signaling via modulation of expression and/or post-translational modification of Hop co-chaperone.

Cancer, the world's second largest killer, has the highest need for new innovative treatments to increase the numbers of patients cured, and to decrease chemoresistant failures resulting in mortality. Drug resistance to synthetic CDK inhibitors is a poorly understood phenomenon and our results demonstrate that, unlike with other anti-cancer drugs, trisubstituted purine analogues represented by bohemine and roscovitine do not induce expression of multidrug resistance proteins. Moreover, roscovitine showed higher efficacy in P-glycoprotein overexpressing cells[39] highlighting these small molecules for therapy of multidrug resistant cancers. Collectively, our study has revealed that Y-box binding protein 1 and the HSP70/90 organizing protein have a critical role to play and interact with the protein nodes of transcriptional and translational networks that are also regulated by CDKI bohemine during the development of acquired resistance to this anti-cancer drug. To add to this, another important role may also be assigned to the Rho-GDP-dissociation inhibitor 2 due to an anti-apoptotic effect and potential effect in multidrug resistance.

Conclusion

While there is plenty of evidence for pre-eminence in basic research on chemoresistance for different cancers, there seems to be a profound lack of translational research (converting basic discoveries into innovative cures) for the benefit of cancer patients. Additionally, cancer related research and treatment costs are spiralling unless action is taken to improve research outcome on chemoresistance which in turn may impact survival rates as well as push down mortality rates. In particular, uptake of novel technologies and lack of specific biomarkers of the disease are proving to be key barriers to improvement. We have endeavored to work with several proteomic technologies and for a quest for proteins as specific biomarkers that may facilitate better and early diagnosis or as a handle for rapidly assessing chemoresistance to single or multidrug treatment.

The results presented in this study indicate that not only qualitative/quantitative protein changes play an important role in drug-resistance, but that there are various other parameters that too, may have a significant influence on the outcome. More importantly, truncation and/or post-translational modification(s) of selected proteins may alter their subcellular localization as well as their key role in controlling response of cancer cells to anti-cancer treatment. Additionally, simulation of possible interaction network could be used to extrapolate both the functional interpretation as well as the validity of such proteomic findings.

Further studies on these identified proteins are needed and may help to resolve many of the discrepancies between drug treatment for various cancers and poor outcome due to chemoresistance to the drugs in cancer medicine.

Abbreviations: A549-BOH, human A549 cells resistant to bohemine; A549-VCR, human A549 cells resistant to vincristine; CDKI, inhibitor of cyclin-dependent kinases; CEM-DNR, human CEM cells resistant to daunorubicin; CEM-VCR, human CEM cells resistant to vincristine; Hop, Hsp70/90 organizing protein (stress-induced phosphoprotein 1); HPCF, high-performance chromatofocusing fractionation; HPRP, high-performance reverse phase fractionation; MeCN, acetonitrile; SDS, sodium dodecyl sulfate; Rho GDI2, Rho GDP-dissociation inhibitor 2; TBST, Tris-buffered saline with 0.05% Tween 20; TFA, trifluoroacetic acid; YB-1, Y-box binding protein 1 (nuclease sensitive element-binding protein 1).

Acknowledgment. This study was supported by the Czech Ministry of School and Education (grant number LC07017) and Institutional Research Concepts AV0Z50450515 (IAPG AS CR,v.v.i.) and AV0Z50200510 (IMIC AS CR, v.v.i.), Grant Agency of the Czech Republic GACR 301/08/1649. Infrastructural part of this project (Institute of Molecular and Translational Medicine) was supported from the Operational Program Research and Development for Innovations (project CZ.1.05/2.1.00/01.0030).

Supporting Information Available: Supplemental Figure 1, 2-D liquid chromatography protein maps of sensitive CEM and resistant CEM-BOH cells; Supplemental Figure 2, the UV profiles of the second dimension HPRP fractionations of pH fractions with significant UV differences in protein peaks found between sensitive CEM cells and resistant CEM-BOH counterparts; Supplemental Table 1, table of differentially expressed proteins identified in 2-D HPLC experiment including mass spectrometry data; Supplemental Table 2, I2D protein−protein Interaction search results. This material is available free of charge via the Internet at http://pubs.acs.org.

References

(1) Raguz, S.; Yague, E. Resistance to chemotherapy: new treatments and novel insights into an old problem. *Br. J. Cancer* **2008**, *99* (3), 387–91.
(2) Zhang, J. T.; Liu, Y. Use of comparative proteomics to identify potential resistance mechanisms in cancer treatment. *Cancer Treat. Rev.* **2007**, *33* (8), 741–56.
(3) Dean, M.; Fojo, T.; Bates, S. Tumour stem cells and drug resistance. *Nat. Rev. Cancer* **2005**, *5* (4), 275–84.
(4) Hajduch, M., Skalnikova, H., Halada, P., Vydra, D., Dzubak, P., Dziechciarkova, M., Strnad, M., Radioch, D., Kovarova, H., Cyclin-dependent kinase inhibitors and cancer: usefulness of proteomic approaches in assessment of the molecular mechanisms and efficacy of novel therapeutics. In *Clinical Proteomics: From Diagnosis to Therapy*; Van Eyk, J. E., Dunn, M. J., Eds.; Wiley-VCH: Weinheim, 2007; pp 177−202.
(5) Kovarova, H.; Hajduch, M.; Korinkova, G.; Halada, P.; Krupickova, S.; Gouldsworthy, A.; Zhelev, N.; Strnad, M. Proteomics approach in classifying the biochemical basis of the anticancer activity of the new olomoucine-derived synthetic cyclin-dependent kinase inhibitor, bohemine. *Electrophoresis* **2000**, *21* (17), 3757–64.
(6) Dobashi, Y.; Takehana, T.; Ooi, A. Perspectives on cancer therapy: cell cycle blockers and perturbators. *Curr. Med. Chem.* **2003**, *10* (23), 2549–58.
(7) Noskova, V.; Dzubak, P.; Kuzmina, G.; Ludkova, A.; Stehlik, D.; Trojanec, R.; Janostakova, A.; Korinkova, G.; Mihal, V.; Hajduch, M. In vitro chemoresistance profile and expression/function of MDR associated proteins in resistant cell lines derived from CCRF-CEM, K562, A549 and MDA MB 231 parental cells. *Neoplasma* **2002**, *49* (6), 418–25.
(8) Towbin, H.; Staehelin, T.; Gordon, J. Electrophoretic transfer of proteins from polyacrylamide gels to nitrocellulose sheets: procedure and some applications. *Proc. Natl. Acad. Sci. U.S.A.* **1979**, *76* (9), 4350–4.
(9) Skalnikova, H.; Halada, P.; Dzubak, P.; Hajduch, M.; Kovarova, H. Protein fingerprints of anti-cancer effects of cyclin-dependent kinase inhibition: identification of candidate biomarkers using 2-D liquid phase separation coupled to mass spectrometry. *Technol. Cancer Res. Treat.* **2005**, *4* (4), 447–54.
(10) Linke, T.; Ross, A. C.; Harrison, E. H. Proteomic analysis of rat plasma by two-dimensional liquid chromatography and matrix-assisted laser desorption ionization time-of-flight mass spectrometry. *J. Chromatogr., A* **2006**, *1123* (2), 160–9.
(11) Bader, A. G. YB-1 activities in oncogenesis: transcription and translation. *Curr. Cancer Ther. Rev.* **2006**, *2* (1), 31–9.
(12) Sorokin, A. V.; Selyutina, A. A.; Skabkin, M. A.; Guryanov, S. G.; Nazimov, I. V.; Richard, C.; Th'ng, J.; Yau, J.; Sorensen, P. H.; Ovchinnikov, L. P.; Evdokimova, V. Proteasome-mediated cleavage

of the Y-box-binding protein 1 is linked to DNA-damage stress response. *EMBO J.* **2005**, *24* (20), 3602–12.
(13) Honore, B.; Leffers, H.; Madsen, P.; Rasmussen, H. H.; Vandekerckhove, J.; Celis, J. E. Molecular cloning and expression of a transformation-sensitive human protein containing the TPR motif and sharing identity to the stress-inducible yeast protein STI1. *J. Biol. Chem.* **1992**, *267* (12), 8485–91.
(14) Longshaw, V. M.; Chapple, J. P.; Balda, M. S.; Cheetham, M. E.; Blatch, G. L. Nuclear translocation of the Hsp70/Hsp90 organizing protein mSTI1 is regulated by cell cycle kinases. *J. Cell Sci.* **2004**, *117* (Pt. 5), 701–10.
(15) Odunuga, O. O.; Longshaw, V. M.; Blatch, G. L. Hop: more than an Hsp70/Hsp90 adaptor protein. *BioEssays* **2004**, *26* (10), 1058–68.
(16) Petrak, J.; Toman, O.; Simonova, T.; Halada, P.; Cmejla, R.; Klener, P.; Zivny, J. Identification of molecular targets for selective elimination of TRAIL-resistant leukemia cells. From spots to in vitro assays using TOP15 charts. *Proteomics* **2009**, *9* (22), 5006–15.
(17) Petrak, J.; Ivanek, R.; Toman, O.; Cmejla, R.; Cmejlova, J.; Vyoral, D.; Zivny, J.; Vulpe, C. D. Deja vu in proteomics. A hit parade of repeatedly identified differentially expressed proteins. *Proteomics* **2008**, *8* (9), 1744–9.
(18) Park, D. J.; Nakamura, H.; Chumakov, A. M.; Said, J. W.; Miller, C. W.; Chen, D. L.; Koeffler, H. P. Transactivational and DNA binding abilities of endogenous p53 in p53 mutant cell lines. *Oncogene* **1994**, *9* (7), 1899–906.
(19) Gildea, J. J.; Seraj, M. J.; Oxford, G.; Harding, M. A.; Hampton, G. M.; Moskaluk, C. A.; Frierson, H. F.; Conaway, M. R.; Theodorescu, D. RhoGDI2 is an invasion and metastasis suppressor gene in human cancer. *Cancer Res.* **2002**, *62* (22), 6418–23.
(20) Seraj, M. J.; Harding, M. A.; Gildea, J. J.; Welch, D. R.; Theodorescu, D. The relationship of BRMS1 and RhoGDI2 gene expression to metastatic potential in lineage related human bladder cancer cell lines. *Clin. Exp. Metastasis* **2000**, *18* (6), 519–25.
(21) Theodorescu, D.; Sapinoso, L. M.; Conaway, M. R.; Oxford, G.; Hampton, G. M.; Frierson, H. F., Jr. Reduced expression of metastasis suppressor RhoGDI2 is associated with decreased survival for patients with bladder cancer. *Clin. Cancer Res.* **2004**, *10* (11), 3800–6.
(22) Tapper, J.; Kettunen, E.; El-Rifai, W.; Seppala, M.; Andersson, L. C.; Knuutila, S. Changes in gene expression during progression of ovarian carcinoma. *Cancer Genet. Cytogenet.* **2001**, *128* (1), 1–6.
(23) Jiang, W. G.; Watkins, G.; Lane, J.; Cunnick, G. H.; Douglas-Jones, A.; Mokbel, K.; Mansel, R. E. Prognostic value of rho GTPases and rho guanine nucleotide dissociation inhibitors in human breast cancers. *Clin. Cancer Res.* **2003**, *9* (17), 6432–40.
(24) Schunke, D.; Span, P.; Ronneburg, H.; Dittmer, A.; Vetter, M.; Holzhausen, H. J.; Kantelhardt, E.; Krenkel, S.; Muller, V.; Sweep, F. C.; Thomssen, C.; Dittmer, J. Cyclooxygenase-2 is a target gene of rho GDP dissociation inhibitor beta in breast cancer cells. *Cancer Res.* **2007**, *67* (22), 10694–702.
(25) Cho, H. J.; Baek, K. E.; Park, S. M.; Kim, I. K.; Choi, Y. L.; Nam, I. K.; Hwang, E. M.; Park, J. Y.; Han, J. Y.; Kang, S. S.; Kim, D. C.; Lee, W. S.; Lee, M. N.; Oh, G. T.; Kim, J. W.; Lee, C. W.; Yoo, J. RhoGDI2 expression is associated with tumor growth and malignant progression of gastric cancer. *Clin. Cancer Res.* **2009**, *15* (8), 2612–9.
(26) Zhao, J.; Chang, A. C.; Li, C.; Shedden, K. A.; Thomas, D. G.; Misek, D. E.; Manoharan, A. P.; Giordano, T. J.; Beer, D. G.; Lubman, D. M. Comparative proteomics analysis of Barrett metaplasia and esophageal adenocarcinoma using two-dimensional liquid mass mapping. *Mol. Cell. Proteomics* **2007**, *6* (6), 987–99.
(27) Goto, T.; Takano, M.; Sakamoto, M.; Kondo, A.; Hirata, J.; Kita, T.; Tsuda, H.; Tenjin, Y.; Kikuchi, Y. Gene expression profiles with cDNA microarray reveal RhoGDI as a predictive marker for paclitaxel resistance in ovarian cancers. *Oncol. Rep.* **2006**, *15* (5), 1265–71.
(28) Sinha, P.; Hutter, G.; Kottgen, E.; Dietel, M.; Schadendorf, D.; Lage, H. Search for novel proteins involved in the development of chemoresistance in colorectal cancer and fibrosarcoma cells in vitro using two-dimensional electrophoresis, mass spectrometry and microsequencing. *Electrophoresis* **1999**, *20* (14), 2961–9.
(29) Kuwano, M.; Oda, Y.; Izumi, H.; Yang, S. J.; Uchiumi, T.; Iwamoto, Y.; Toi, M.; Fujii, T.; Yamana, H.; Kinoshita, H.; Kamura, T.; Tsuneyoshi, M.; Yasumoto, K.; Kohno, K. The role of nuclear Y-box binding protein 1 as a global marker in drug resistance. *Mol. Cancer Ther.* **2004**, *3* (11), 1485–92.
(30) Sutherland, B. W.; Kucab, J.; Wu, J.; Lee, C.; Cheang, M. C.; Yorida, E.; Turbin, D.; Dedhar, S.; Nelson, C.; Pollak, M.; Leighton Grimes, H.; Miller, K.; Badve, S.; Huntsman, D.; Blake-Gilks, C.; Chen, M.; Pallen, C. J.; Dunn, S. E. Akt phosphorylates the Y-box binding protein 1 at Ser102 located in the cold shock domain and affects the anchorage-independent growth of breast cancer cells. *Oncogene* **2005**, *24* (26), 4281–92.
(31) Tanji, H.; Ishikawa, C.; Sawada, S.; Nakachi, S.; Takamatsu, R.; Matsuda, T.; Okudaira, T.; Uchihara, J. N.; Ohshiro, K.; Tanaka, Y.; Senba, M.; Uezato, H.; Ohshima, K.; Duc Dodon, M.; Wu, K. J.; Mori, N. Aberrant expression of the transcription factor Twist in adult T-cell leukemia. *Blood* **2010**, *116* (8), 1386.
(32) Bargou, R. C.; Jurchott, K.; Wagener, C.; Bergmann, S.; Metzner, S.; Bommert, K.; Mapara, M. Y.; Winzer, K. J.; Dietel, M.; Dorken, B.; Royer, H. D. Nuclear localization and increased levels of transcription factor YB-1 in primary human breast cancers are associated with intrinsic MDR1 gene expression. *Nat. Med.* **1997**, *3* (4), 447–50.
(33) Fujita, T.; Ito, K.; Izumi, H.; Kimura, M.; Sano, M.; Nakagomi, H.; Maeno, K.; Hama, Y.; Shingu, K.; Tsuchiya, S.; Kohno, K.; Fujimori, M. Increased nuclear localization of transcription factor Y-box binding protein 1 accompanied by up-regulation of P-glycoprotein in breast cancer pretreated with paclitaxel. *Clin. Cancer Res.* **2005**, *11* (24 Pt. 1), 8837–44.
(34) Oda, Y.; Ohishi, Y.; Saito, T.; Hinoshita, E.; Uchiumi, T.; Kinukawa, N.; Iwamoto, Y.; Kohno, K.; Kuwano, M.; Tsuneyoshi, M. Nuclear expression of Y-box-binding protein-1 correlates with P-glycoprotein and topoisomerase II alpha expression, and with poor prognosis in synovial sarcoma. *J. Pathol.* **2003**, *199* (2), 251–8.
(35) Zhu, K.; Zhao, J.; Lubman, D. M.; Miller, F. R.; Barder, T. J. Protein pI shifts due to posttranslational modifications in the separation and characterization of proteins. *Anal. Chem.* **2005**, *77* (9), 2745–55.
(36) Lassle, M.; Blatch, G. L.; Kundra, V.; Takatori, T.; Zetter, B. R. Stress-inducible, murine protein mSTI1. Characterization of binding domains for heat shock proteins and in vitro phosphorylation by different kinases. *J. Biol. Chem.* **1997**, *272* (3), 1876–84.
(37) Daniel, S., Soti, C., Csermely, P., Bradley, G., Blatch, G. L. Hop: An Hsp70/Hsp90 co-chaperone that functions within and beyond Hsp70/Hsp90 protein folding pathways. In *Networking of Chaperones by Co-Chaperones*; Blatch, G. L., Ed.; Springer: New York, 2007; pp 26−37.
(38) Daniel, S.; Bradley, G.; Longshaw, V. M.; Soti, C.; Csermely, P.; Blatch, G. L. Nuclear translocation of the phosphoprotein Hop (Hsp70/Hsp90 organizing protein) occurs under heat shock, and its proposed nuclear localization signal is involved in Hsp90 binding. *Biochim. Biophys. Acta* **2008**, *1783* (6), 1003–14.
(39) Cappellini, A.; Chiarini, F.; Ognibene, A.; McCubrey, J. A.; Martelli, A. M. The cyclin-dependent kinase inhibitor roscovitine and the nucleoside analog sangivamycin induce apoptosis in caspase-3 deficient breast cancer cells independent of caspase mediated P-glycoprotein cleavage: implications for therapy of drug resistant breast cancers. *Cell Cycle* **2009**, *8* (9), 1421–5.

PR100468W

PŘÍLOHA 3

Journal of proteome research

Article

pubs.acs.org/jpr

Cancer Cell Resistance to Aurora Kinase Inhibitors: Identification of Novel Targets for Cancer Therapy

Rita Hrabakova,[†] Madhu Kollareddy,[‡] Jirina Tyleckova,[†] Petr Halada,[§] Marian Hajduch,[‡] Suresh Jivan Gadher,[∥] and Hana Kovarova*[,†]

[†]Institute of Animal Physiology and Genetics, AS CR, v.v.i., Laboratory of Biochemistry and Molecular Biology of Germ Cells, Rumburska 89, 277 21 Libechov, Czech Republic

[‡]Institute of Molecular and Translational Medicine, Laboratory of Experimental Medicine, Palacky University and University Hospital in Olomouc, Faculty of Medicine and Dentistry, Hnevotinska 5, 775 15 Olomouc, Czech Republic

[§]Institute of Microbiology, AS CR, v.v.i., Laboratory of Molecular Structure Characterisation, Videnska 1083, 142 20 Prague, Czech Republic

[∥]Life Technologies, Frederick, Maryland 21704, United States

S *Supporting Information*

ABSTRACT: Drug resistance is the major obstacle to successful cancer therapy. Our study focuses on resistance to Aurora kinase inhibitors tested as anticancer drugs in clinical trials. We have used 2D electrophoresis in the pH ranges of 4−7 and 6−11 followed by protein identification using MALDI-TOF/TOF to compare the protein composition of HCT116 colon cancer cells either sensitive to CYC116 and ZM447439 inhibitors or resistant toward these drugs. The analysis also included $p53^{+/+}$ and $p53^{-/-}$ phenotypes of HCT116 cells. Our findings demonstrate that platelet-activating factor acetylhydrolase and GTP-binding nuclear protein Ran contribute to the development of resistance to ZM447439 only where resistance is related to p53. On the other hand, serine hydroxymethyltransferase was found to promote the tumor growth in cells resistant to CYC116 without the influence of p53. Computer modeling of interaction networks highlighted a direct link of the p53-independent mechanism of resistance to CYC116 with autophagy. Importantly, serine hydroxymethyltransferase, serpin B5, and calretinin represent the target proteins that may help overcome resistance in combination therapies. In addition, serpin B5 and calretinin appear to be candidate biomarkers that may be accessible in patients for monitoring of cancer therapy with ease.

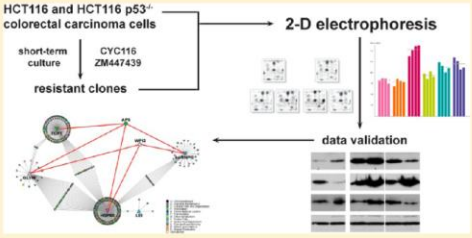

KEYWORDS: *Aurora kinase inhibitors, resistance, p53, apoptosis, autophagy, platelet-activating factor acetylhydrolase, Ran, serine hydroxymethyltransferase, serpin B5, calretinin*

INTRODUCTION

Despite significant progress in the development of anticancer drugs, there is still a need for novel therapeutic strategies that would overcome development of drug resistance and improve the outcome of cancer patient therapy. Extensive efforts have been made to develop the therapy directed toward specific genetic alterations present predominantly or exclusively in tumors but not in normal cells. Aurora kinases (AURKs), which are comprised of three family members, Aurora-A, Aurora-B, and Aurora-C, are essential regulators of mitotic events including G2/M transition, spindle organization, chromosome segregation, and cytokinesis. Because AURKs are frequently overexpressed in human cancers, they have emerged as attractive therapeutic targets.[1] Accordingly, inhibitors of AURKs with potent antiproliferative and antiapoptotic effects have evolved, too.[2]

In the present study, we have taken into account an experimental and well-characterized AURK inhibitor ZM447439, 4-(4-(*N*-benzoylamino)anilino)-6-methoxy-7-(3-(1-morpholino)propoxy)quinazoline, which has been found to inhibit AURK-A and AURK-B,[3] and a novel AURK inhibitor CYC116, ([4-(2-amino-4-methyl-thiazol-5-yl)pyrimidin-2-yl]-(4-morpholin-4-ylphenyl)-amine]), which inhibits not only AURK-A, AURK-B and AURK-C, but also angiogenesis promoter VEGFR2 (vascular endothelial growth factor receptor 2).[2,4]

A major obstacle to successful cancer therapy is the presence of dormant and/or drug resistant cells, which may later evoke disease relapse. In response to anticancer treatment, changes in different cellular processes are triggered as tumors struggle to survive where mechanisms of extreme importance including pharmacological, physiological, and altered survival pathway parameters come into play. For instance, the overexpression of

Received: August 30, 2012

ACS Publications © XXXX American Chemical Society

dx.doi.org/10.1021/pr300819m | *J. Proteome Res.* XXXX, XXX, XXX−XXX

drug transport pumps can lead to the increased drug efflux, which usually manifests as multidrug resistance.[5] Additionally, activated DNA repair and impaired apoptosis have been implicated in the development of drug resistance.[6,7] Cancer stem cell phenomenon and epigenetic regulation that simultaneously influence expression of multiple genes might also contribute to the acquisition of drug resistance.[8,9] Nevertheless, molecular mechanisms of drug resistance have not yet been fully elucidated in spite of numerous studies carried out to date.

Previous studies have described mutations in p53 tumor suppressor gene in over 50% of human malignancies including colorectal cancer.[10] Some forms and/or combinations of p53 mutants may also enhance resistance of tumor cells to anticancer drugs.[11] In response to genotoxic stress and hypoxia, p53 transcriptionally activates upstream genes important for cell cycle arrest, DNA repair, or apoptosis[12] and can also induce apoptosis by nontranscriptional inhibition of bcl-2 and bcl-xl proteins at the mitochondrial membrane level.[13] Additionally, there is an important interaction between p53 and AURK, and deregulation of functional balance might trigger chromosome instability and carcinogenesis.[14]

Interaction of p53 with AURK-A suppresses its oncogenic activity.[15] On the other hand, AURK-A phosphorylates p53, resulting in p53 protein turnover and its transcriptional activity.[16] It has been shown that pharmacological inhibition of AURK-A provides a growth advantage to cells that have suffered from p53 loss or alternatively may lead to complete loss of wild-type p53 activity.[14] It remains obscure how p53 affects the development of resistance to AURK inhibitors in cancer cells.

Currently, proteomic approaches represent promising tools in our understanding of the molecular mechanisms of various diseases and a quest for disease biomarkers as well as specific targets for novel drugs. We have used 2D electrophoresis in pH ranges of 4−7 and 6−11 to compare sensitive and resistant HCT116 human colon cancer cells with $p53^{+/+}$ (wild-type) and $p53^{-/-}$ phenotypes. Using MALDI-TOF/TOF, we have identified proteins that may contribute to the acquisition of resistance toward CYC116 and ZM447439 AURK inhibitors. Such protein alterations have also been examined in CCRF-CEM human T-lymphoblastic leukemia cells carrying p53 mutations[17] and A549 human lung adenocarcinoma cells with p53 wild-type phenotype[18] resistant to diverse anticancer drugs. On the basis of our findings, we propose novel targets for drugs, which may prevent or overcome the drug resistance and highlight candidate markers that could be used to monitor anticancer therapy in patients.

■ EXPERIMENTAL SECTION

Chemicals

Unless otherwise stated, all chemicals were obtained from Sigma-Aldrich (St. Louis, MO).

Cell Culture and Sample Preparation

HCT116 $p53^{+/+}$ (wild-type) and HCT116 $p53^{-/-}$ cell lines derived from a human colon carcinoma were purchased from Horizon Discovery Ltd. (Cambridge, United Kingdom) and cultured in DMEM supplemented with 10% FCS (PAN-Biotech GmbH, Aidenbach, Germany), penicillin (Biotika, Prague, Czech Republic), and streptomycin at 37 °C and 5% CO_2. Cells resistant to AURK inhibitors were derived by short-term exposure of parental sensitive cells directly to 1 μM (cytotoxic dose above IC_{50} for both inhibitors) CYC116 (Cyclacel Ltd., Dundee Technopole, Dundee, Scotland, United Kingdom) or ZM447439 (AstraZeneca Pharmaceuticals Ltd., London, United Kingdom). After 5 weeks, several colonies were isolated, and a MTT-based proliferation assay was performed as described previously[19] to confirm resistance to AURK inhibitors. The resistance was evaluated as a fold increase calculated by dividing mean IC_{50} values of respective resistant clones and parental $p53^{+/+}$ and $p53^{-/-}$ sensitive cells.

In the present study, two clones resistant to CYC116 with wild-type $p53^{+/+}$ alleles (R1.2 and R1.3), two clones resistant to CYC116 with mutated $p53^{-/-}$ alleles (R2.1 and R2.2), two clones resistant to ZM447439 with wild-type $p53^{+/+}$ alleles (R3.1 and R3.2), and two clones resistant to ZM447439 with mutated $p53^{-/-}$ alleles (R4.2 and R4.3) were analyzed. Clones exhibited high resistance with a fold increase of IC_{50} as follows: 82 and 63 for R1.2 and R1.3, 64 and 41 for R2.1 and R2.2, 83 for both R3.1 and R3.2, and 38 and 39 for R4.2 and R4.3, respectively. All clones were maintained at 1 μM concentration of AURK inhibitors.

The CCRF-CEM (human T-lymphoblastic leukemia cells) and A549 (human lung adenocarcinoma) cell lines were obtained from American Tissue Culture Collection (ATCC, Manassas, VA). The CCRF-CEM and A549 cells were cultured at 37 °C and 5% CO_2 in RPMI 1640 and DMEM, respectively, with 5 g/L glucose, 2 mM glutamine, 10% FCS (PAN-Biotech GmbH), penicillin (Biotika), and streptomycin. The CCRF-CEM cells resistant to daunorubicin, vincristine, or cytarabine as well as A549 cells resistant to vincristine or paclitaxel were established as described previously[20] and grown in the media mentioned above.

Cells were grown to 80% confluency in Petri dish, rinsed with cold PBS, and solubilized in 500 μL of extraction buffer consisting of 7 M urea, 2 M thiourea, 3% w/v CHAPS (Carl Roth GmbH, Karlsruhe, Germany), 2% v/v Nonidet 40, 5 mM TCEP, protease inhibitor cocktail (complete Mini, Roche, Mannheim, Germany), and phosphatase inhibitor cocktail (PhosSTOP, Roche, Mannheim, Germany). Cell lysates were left for 30 min at room temperature to optimize protein extraction and centrifuged at 20000*g* at 4 °C for 1 h, and the clarified protein extracts were kept at −80 °C until used. The protein concentration of each sample was estimated using the Pierce 660 nm protein assay kit (Thermo Scientific, Rockford, IL) according to the manufacturer's protocol.

2-DE and Evaluation of Protein Spot Differences

2-DE was carried out using Protean IEF Cell (Bio-Rad, Hercules, CA) for the first dimension and Protean II xi Cell (Bio-Rad) for the second dimension. Polyacrylamide gel strips with an IPG of 4−7 and 6−11 (180 mm × 3 mm × 0.5 mm, GE Healthcare, Uppsala, Sweden) were loaded with 100 and 70 μg of proteins, respectively. For the pH range 4−7, protein extracts were diluted to 130 μL with extraction buffer and dissolved in 230 μL of rehydration buffer: 7 M urea, 2 M thiourea, 4% CHAPS, 200 mM DeStreak reagent (GE Healthcare, Uppsala, Sweden), 2% IPG buffer pH 4−7 (GE Healthcare), protease inhibitor cocktail, phosphatase inhibitor cocktail, and a trace of bromophenol blue. Proteins were loaded into IPG strips using overnight in gel rehydration at 50 V, and IEF was performed at the following voltages: 200 V for 10 h, 600 V for 30 min, 1000 V for 30 min, and 5000 V for the time period necessary to reach 50000 Vh in total. After IEF separation, IPG strips were equilibrated in 50 mM Tris-HCl, pH 6.8 (Carl Roth GmbH), 6 M urea, 30% glycerol (Penta, Prague, Czech Republic), 4% SDS, and 100 mM DeStreak reagent for 25 min.

dx.doi.org/10.1021/pr300819m | J. Proteome Res. XXXX, XXX, XXX−XXX

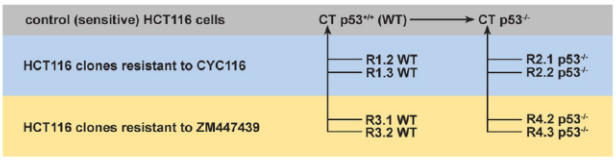

Figure 1. Clones resistant to CYC116 or ZM447439 AURK inhibitors analyzed using 2-DE. Wild-type (WT) $p53^{+/+}$ resistant cells were compared to sensitive HCT116 $p53^{+/+}$ cells, and resistant cells carrying $p53^{-/-}$ alleles were compared to sensitive HCT116 $p53^{-/-}$ cells.

For the pH range 6−11, IPG strips were passively rehydrated overnight without sample in 340 μL of rehydration buffer with 0.5% IPG buffer, pH 6−11 (GE Healthcare), and 30 mM DTT instead of DeStreak reducing agent. Protein extracts were diluted to 150 μL with extraction buffer supplemented by 65 mM DTT and 0.5% IPG buffer, pH 6−11. After 15 min, free thiol groups were alkylated by 30 mM iodoacetamide, a trace of bromophenol blue was added, and cup-loading was applied. IEF was performed at the following voltages: 150 V for 12 h, 1000 V for 1 h, 8000 V for 3 h, and 8000 V for the time period necessary to reach 20000 Vh in total. After IEF separation, IPG strips were equilibrated for 20 min as described above but with 8% SDS and without reducing agent (DeStreak).

For preparative gels, IPG strips were loaded with 500 and 130 μg of total protein for pH 4−7 and pH 6−11, respectively. Prior to the second dimension, the focused proteins were reduced (1% DTT) and alkylated (4% iodoacetamide) in two 15 min steps via equilibration.

The equilibrated proteins were transferred from the IPG strips onto a 10% SDS-PAGE gels (180 mm × 180 mm × 1 mm). SDS-PAGE was carried out at a constant current of 40 mA per gel until the bromophenol blue line reached the bottom of the gel. Analytical gels were stained with SYPRO Ruby protein gel stain (Bio-Rad) and digitized at 500 DPI resolution using a Pharos FX scanner (Bio-Rad). Protein spots on preparative gels were visualized by reverse staining using a zinc salt.[21]

For further evaluation, 2-DE gel images were subjected to REDFIN Solo analysis (http://www.ludesi.com/, Ludesi, Malmo, Sweden).[22] All resistant clones were compared in pairs with relevant (sensitive) control either HCT116 $p53^{+/+}$ (wild-type) or HCT116 $p53^{-/-}$ cell line (Figure 1), and differential expression of proteins was determined by applying the criteria of significance with $p < 0.05$ and fold-change values > ±1.20. The calculations (Student's t test) were performed by REDFIN software from the mean normalized volumes of four biological replicates, which were grown and processed independently.

Enzymatic In-Gel Digestion

Spots showing a significant expression change ($p < 0.05$) were excised from zinc-stained preparative gels and cut into small pieces. To complex zinc ions, gel pieces were incubated for 5 min in 50 mM Tris-HCl pH 8.3 (Carl Roth GmbH), 200 mM glycine, and 30% acetonitrile (Merck Millipore, Bilerica, MA). The gel pieces became transparent, and after complete destaining, the chelating solution was removed, and gels were rinsed twice with 50 mM Tris-HCl, pH 8.3 (Carl Roth GmbH). Then, gels were washed with water, shrunk by dehydration in acetonitrile, and reswollen in water. The washing step was repeated three times, and gels were partly dried in a SpeedVac concentrator. Gels were rehydrated in a cleavage buffer containing 25 mM 4-ethylmorpholine, 5% acetonitrile, and trypsin (3.3 ng/μL; Promega, Madison, WI) and incubated overnight at 37 °C. The digestion was stopped by the addition of 5% trifluoroacetic acid in acetonitrile, and the aliquot of the resulting peptide mixture was desalted using a GELoader microcolumn (Eppendorf, Prague, Czech Republic) packed with a Poros Oligo R3 material.[23] The purified and concentrated peptides were eluted from the microcolumn in several droplets directly onto MALDI plate using 1 μL of α-cyano-4-hydroxycinnamic acid matrix solution (5 mg/mL in 50% acetonitrile and 0.1% trifluoroacetic acid).

Protein Identification by MALDI-TOF/TOF Mass Spectrometry

MALDI mass spectra were measured on an Ultraflex III MALDI-TOF/TOF instrument (Bruker Daltonics, Bremen, Germany) equipped with a smartbeam solid state laser and LIFT technology for MS/MS analysis. PMF spectra were acquired in the mass range of 700−4000 Da and calibrated internally using the monoisotopic $[M + H]^+$ ions of trypsin autoproteolytic fragments (842.5 and 2211.1 Da). For PMF database searching, peak lists in XML data format were created using the flexAnalysis 3.0 program with SNAP peak detection algorithm. No smoothing was applied, and a maximal number of assigned peaks was set to 50. After peak labeling, all known contaminant signals were removed.

The peak lists were searched using in-house MASCOT search engine against the Swiss-Prot 2011_09 database subset of human proteins with the following search settings: peptide tolerance of 30 ppm, missed cleavage site value set to one, variable carbamidomethylation of cysteine, oxidation of methionine, and protein N-terminal acetylation. No restrictions on protein molecular weight and pI value were applied. Proteins with a Mascot score over the threshold 56 calculated for the used settings were considered as identified. If the score was lower or only slightly higher than the threshold value, the identity of protein candidate was confirmed by MS/MS analysis. In addition to the above-mentioned MASCOT settings, a fragment mass tolerance of 0.6 Da and instrument type MALDI-TOF/TOF were applied for MS/MS spectra searching.

Classification of Protein Changes in HCT116 Resistant Cells and Computer Modeling of Interaction Networks

To assign the roles in biological processes, differentially expressed proteins were searched against the PANTHER 7.0 (http://www.pantherdb.org/).[24] Stringent criteria were further applied to select protein changes overlapping among resistant clones and alterations present exclusively in all four clones resistant to CYC116 or in all four clones resistant to ZM447439, irrespective of p53, as well as those present in all four $p53^{+/+}$ clones or in all four $p53^{-/-}$ clones resistant to both AURK inhibitors were searched. In addition, protein changes present in two clones either $p53^{+/+}$ or $p53^{-/-}$ and typical for CYC116 or ZM447439 were also evaluated. Furthermore, selection of candidate biomarkers of resistance to AURK inhibitors was performed according to the presence of significant protein

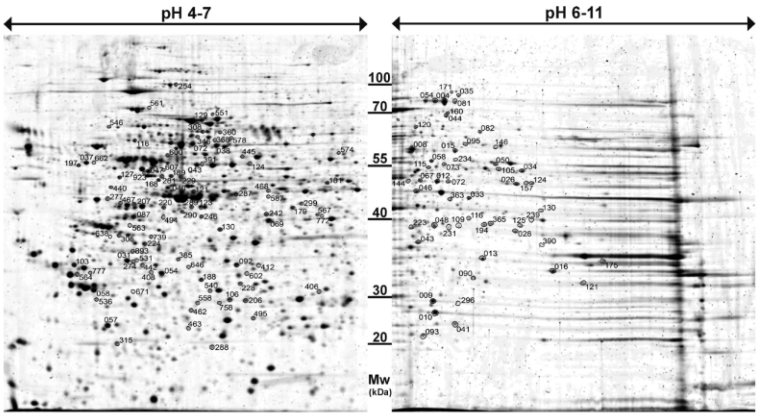

Figure 2. Significantly regulated protein spots in HCT116 cells resistant to AURK inhibitors. Representative maps of 2-DE gels in pH 4–7 and 6–11 show the protein spots significantly regulated in resistant cells ($p < 0.05$) with numbers generated by REDFIN software. Spot numbers of pH 4–7 and 6–11 are in tables marked with N (neutral) and B (basic), respectively.

changes in at least five out of eight HCT116 resistant clones irrespective of inhibitor used and p53 phenotype.

To enhance observed proteomic data, selected identified proteins were introduced into the Interologous Interaction Database 1.95 of known and predicted mammalian and eukaryotic protein–protein interactions (http://ophid.utoronto.ca/ophidv2.201/index.jsp).[25] Protein–protein interaction networks were visualized using NAVIGaTOR 2.2.1 (http://ophid.utoronto.ca/navigator/).

Western Blot Analysis

Cell lysates were dissolved in SDS sample buffer, and 5 μg of the protein extracts was separated in 12% SDS-PAGE gels using Mini Protean II Cell (Bio-Rad). Proteins were then transferred to Immobilon-P membranes (Merck Millipore) using a semidry blotting system (Biometra, Gottingen, Germany) and transfer buffer containing 48 mM Tris, pH 9.2, 39 mM glycine (Carl Roth GmbH), and 20% methanol (Lach-Ner, Neratovice, Czech Republic). The membranes were blocked for 1 h with 5% nonfat dry milk in TBS, pH 7.4, with 0.05% Tween 20 and incubated overnight with primary antibodies directed against β-tubulin (anti-β-tubulin, 1:20000, Sigma, St. Louis, MO); platelet-activating factor acetylhydrolase IB subunit β (anti-PAFAH1B2, 1:1000, Abcam, Cambridge, United Kingdom); GTP-binding nuclear protein Ran (anti-Ran, 1:4000, Abcam); serine hydroxymethyltransferase (anti-SHMT2, 1:6000, Sigma Prestige Antibodies, St. Louis, MO); serpin B5 (anti-SERPINB5, 1:1000, Aviva Systems Biology, San Diego, CA); calretinin (anti-CALB2, 1:6000, Sigma Prestige Antibodies); and voltage-dependent anion-selective channel protein 2 (anti-VDAC2, 1:3000, Aviva Systems Biology). Peroxidase-conjugated secondary antibodies were diluted in 5% nonfat dry milk/TBS, pH 7.4, with 0.05% Tween 20 and applied as appropriate. Antimouse IgG antibody (Jackson Immunoresearch, Suffolk, UK) and antirabbit IgG antibody (Jackson Immunoresearch, Suffolk, UK) were diluted 1:10000, and antichicken IgY (Abcam) was diluted 1:100000. The ECL+ chemiluminiscence detection system (GE Healthcare) was used to detect specific protein bands on Western blot, and membranes were then exposed to CL-XPosure films (Thermo Scientific, Rockford, IL) in three independent experiments.

RESULTS

Overview of Proteome Changes in p53$^{+/+}$ and p53$^{-/-}$ HCT116 Cells Resistant to AURK Inhibitors

To characterize changes in protein expression involved in the development of drug resistance to AURK inhibitors, sensitive and resistant HCT116 cells with or without p53 were lysed, extracted proteins were separated by 2-DE in pH gradients 4–7 and 6–11, and protein spots were visualized by fluorescent SYPRO Ruby protein gel stain. Using REDFIN software, 984 and 390 protein spots in pH 4–7 and pH 6–11, respectively, were detected and matched in all gels of all analyzed samples (eight resistant clones, two sensitive parental cells, and four biological replicates of each sample). As shown in Figure 1, gels corresponding to the clones R1.2 and R1.3 resistant to CYC116 and carrying p53$^{+/+}$ were compared to sensitive HCT116 p53$^{+/+}$ counterparts, and CYC116 resistant clones R2.1 and R2.2 carrying p53$^{-/-}$ alleles were compared to sensitive HCT116 p53$^{-/-}$ cells. Similarly, the gels corresponding to cells resistant to ZM447439 (R3.1, R3.2, R4.2, and R4.3) were analyzed.

A statistical comparison revealed 144 significantly different protein spots with minimal fold-change ±1.20 and present in at least one of all eight resistant clones (Figure 2 and Supplementary Table 1 in the Supporting Information). Among these proteins, 51 (35%) were up-regulated and 63 (44%) were down-regulated in cells resistant to AURK inhibitors. The remaining 30 proteins (21%) have shown distinct regulation among resistant clones. Identified proteins from 144 spots represented 127 unique proteins, and 82 and 45 proteins were found in pH ranges 4–7 and 6–11, respectively. Fifteen proteins were present in two spots (031N, 274N; 037N, 662N; 129N, 467N; 168N, 281N; 197N, 495N; 290N, 739N; 305N, 638N; 360N, 095B; 564N, 777N; 012B, 067B; 028B, 125B; 034B, 105B; 035B, 171B; 044B, 160B; and 124B, 157B), two proteins were present in three spots (043N, 124N, 391N; and 004B, 054B, 081B), and there were only two spots each

dx.doi.org/10.1021/pr300819m | J. Proteome Res. XXXX, XXX, XXX–XXX

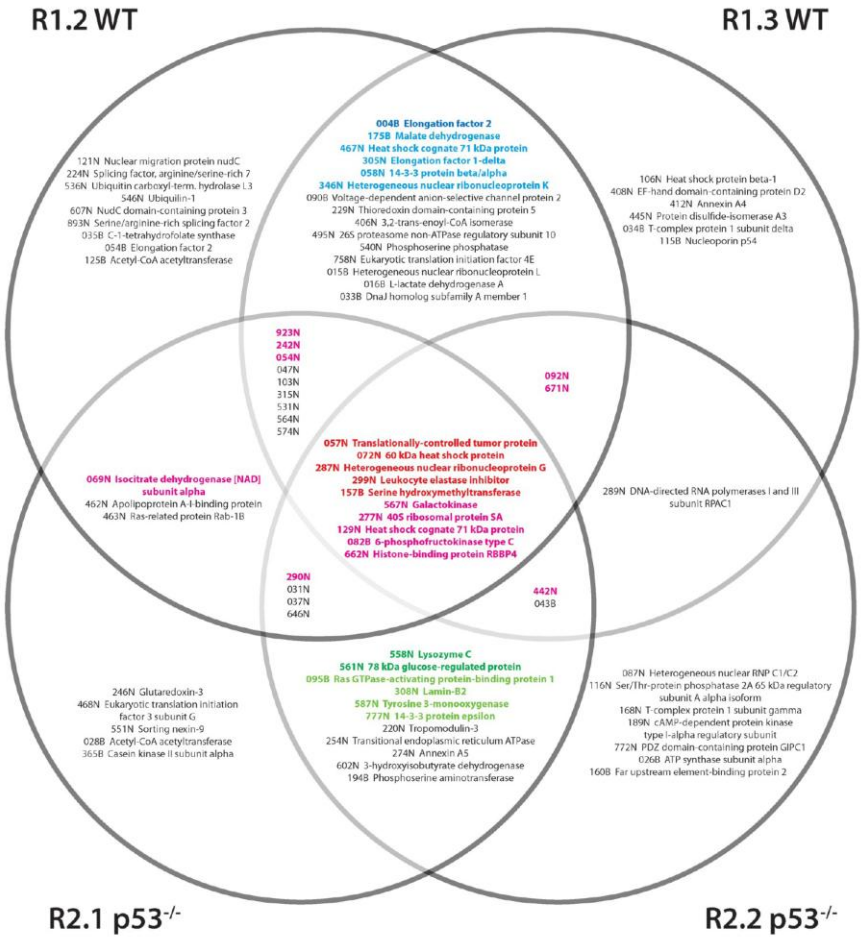

Figure 3. Venn diagram of proteins differentially expressed in HCT116 cells resistant to CYC116 and the overlap between cell types. In the diagram, the proteins in red color highlight p53-independent changes specific for CYC116 resistance (Table 1). The changes related to p53 phenotype are indicated in blue (WT) and green ($p53^{-/-}$) colors where the light shade represents CYC116 specific changes (Table 3), while the dark shade further indicates the protein(s) also overlapping with the ZM447439 (Table 2). The black color indicates the proteins regulated in at least one resistant clone (Supplementary Table 1 in the Supporting Information). The magenta color displays the proteins regulated in at least five out of total eight resistant clones without any selectivity to a specific kind of AURK inhibitor or p53 phenotype (Figure 6).

containing two proteins (197N, 146B), thus indicating high resolution of protein fractionation applied in this study. Mass spectrometric data of all identified proteins are presented in Supplementary Table 2 in the Supporting Information.

Involvement of identified proteins in biological processes classified by PANTHER database 7.0 according to Gene Ontology is provided in the Supplementary Table 3 in the Supporting Information. The majority of identified proteins are involved in metabolic processes of proteins, lipids, carbohydrates, and nucleic acids; however, this study also revealed proteins participating in signal transduction, cell cycle, developmental processes, transport, and the immune system.

Overlap of Protein Alterations among HCT116 Resistant Cells

Figures 3 and 4 show Venn diagrams of proteins differentially expressed in individual HCT116 resistant cells and the overlap between the cell types. It was evident that the number of significant protein changes shared among HCT116 resistant cells was not too high. The highest overlap was observed between cells resistant to CYC116 carrying $p53^{+/+}$ (clones R1.2 and R1.3) and $p53^{-/-}$ (clones R2.1 and R2.2). These p53-independent changes specific for CYC116 resistant cells (Figure 3 and Table 1) included a decrease in translationally controlled tumor protein (spot 057N), 60 kDa heat shock protein (spot 072N), and heterogeneous nuclear ribonucleoprotein G (spot 287N) and an

dx.doi.org/10.1021/pr300819m | J. Proteome Res. XXXX, XXX, XXX−XXX

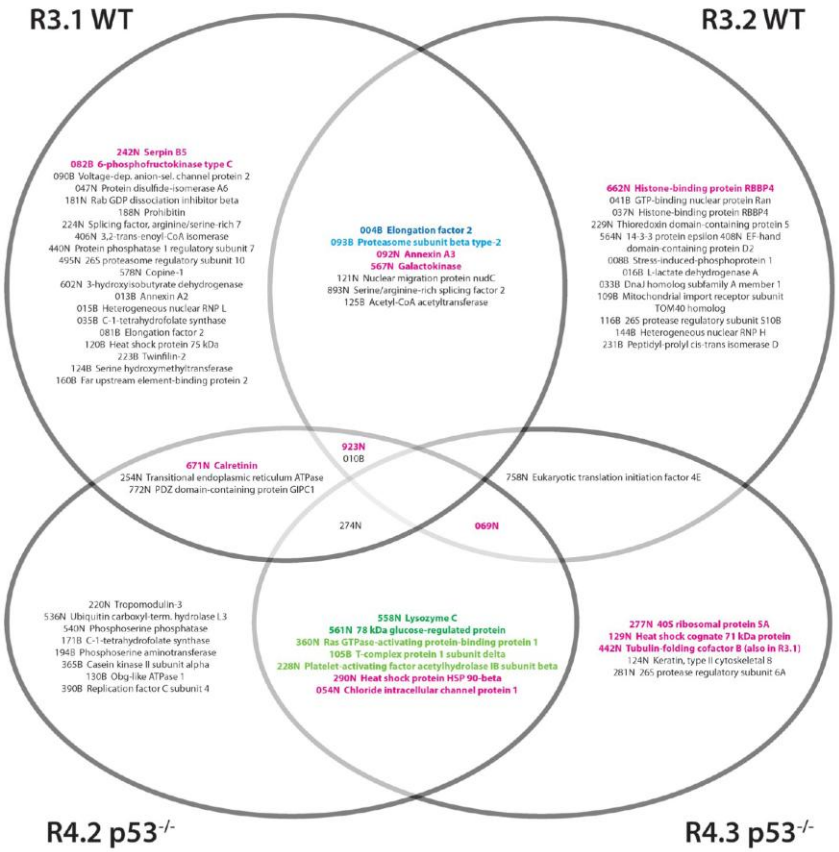

Figure 4. Venn diagram of proteins differentially expressed in HCT116 cells resistant to ZM447439 and the overlap between cell types. In this diagram, the changes related to p53 phenotype are indicated in blue (WT) and green ($p53^{-/-}$) where the lighter shade of color represents ZM447439 specific changes (Table 3) and the dark shade further indicates the protein(s) also overlapping with the CYC116 (Table 2). The black color indicates the proteins regulated in at least one resistant clone (Supplementary Table 1 in the Supporting Information). The magenta color displays the proteins regulated in at least five out of total eight resistant clones without any selectivity to a specific kind of AURK inhibitor or p53 phenotype (Figure 6).

Table 1. Protein Changes Typical for Individual AURK Inhibitors Irrespective of p53 Phenotype[a]

		CYC116				ZM447439[b]			
		$p53^{+/+}$		$p53^{-/-}$		$p53^{+/+}$		$p53^{-/-}$	
spot no.	protein name	R1.2	R1.3	R2.1	R2.2	R3.1	R3.2	R4.2	R4.3
057N	translationally controlled tumor protein	−1.86	−1.67	−2.82	−1.76				
072N	60 kDa heat shock protein	−1.63	−1.32	−1.57	−1.25				
287N	heterogeneous nuclear ribonucleoprotein G	−3.07	−2.23	−2.00	−1.90				
299N	leukocyte elastase inhibitor	1.89	1.91	2.98	2.50				
157B	serine hydroxymethyltransferase	1.46	1.82	1.43	1.31				

[a]Fold-change values for proteins significantly regulated in HCT116 resistant cells. [b]No p53-independent protein changes typical for ZM447439 resistant cells were found.

increase in leukocyte elastase inhibitor (spot 299N) and serine hydroxymethyltransferase (spot 157B). On the contrary, we did not find any overlap between cells resistant to ZM447439 carrying $p53^{+/+}$ (clones R3.1 and R3.2) and $p53^{-/-}$ (clones R4.2 and R4.3) (Figure 4 and Table 1).

We also observed that both CYC116 and ZM447439 resistant cells were characterized by differential expression of elongation factor 2 (spot 004B) exclusively in all four $p53^{+/+}$ clones (R1.2, R1.3, R3.1, and R3.2; Figures 3 and 4), while all four $p53^{-/-}$ clones (clones R2.1, R2.2, R4.2, and R4.3; Figures 3 and 4)

Table 2. Protein Changes Common to Both AURK Inhibitors Dependent on p53 Phenotype

		CYC116				ZM447439			
		$p53^{+/+}$		$p53^{-/-}$		$p53^{+/+}$		$p53^{-/-}$	
spot no.	protein name	R1.2	R1.3	R2.1	R2.2	R3.1	R3.2	R4.2	R4.3
004B	elongation factor 2	−1.72	−1.31			−1.93	−1.48		
558N	lysozyme C			1.33	1.43			1.63	1.33
561N	78 kDa glucose-regulated protein			−1.90	−1.80			−1.76	−2.10

Table 3. Protein Changes Typical for Individual AURK Inhibitors Related to p53 Phenotype[a]

		CYC116				ZM447439			
		$p53^{+/+}$		$p53^{-/-}$		$p53^{+/+}$		$p53^{-/-}$	
spot no.	protein name	R1.2	R1.3	R2.1	R2.2	R3.1	R3.2	R4.2	R4.3
175B	malate dehydrogenase	2.56	1.82						
467N	heat shock cognate 71 kDa protein	1.61	2.05						
305N	elongation factor 1-δ	1.43	1.50						
058N	14-3-3 protein β/α	−1.20	−1.67						
346N	heterogeneous nuclear ribonucleoprotein K	−1.33	−1.48						
095B	Ras GTPase-activating protein-binding protein 1			1.29	1.41				
308N	lamin-B2			−2.03	−4.60				
587N	tyrosine 3-monooxygenase			−1.38	−1.51				
777N	14-3-3 protein ε			−1.83	−1.71				
093B	proteasome subunit β type-2					1.84	2.08		
360N	Ras GTPase-activating protein-binding protein 1							1.93	1.82
105B	T-complex protein 1 subunit δ							1.23	1.27
228N	platelet-activating factor acetylhydrolase IB subunit β							−2.13	−2.19

[a]Fold-change values for proteins significantly regulated in HCT116 resistant cells.

exhibited variant levels of lysozyme C (spot 558N) and 78 kDa glucose-regulated protein (spot 561N) (Table 2).

Protein Changes in HCT116 Resistant Cells Typical for Individual AURK Inhibitors Related to p53 Phenotype

As mentioned above, we selected the group of proteins significantly changed in p53-independent manner in cells resistant to CYC116 only. In addition to these, there were other proteins typical for cells resistant to CYC116 with protein alterations related to p53 phenotype. Three proteins, namely, malate dehydrogenase (spot 175B), heat shock cognate 71 kDa protein (spot 467N), and elongation factor 1-δ (spot 305N) were significantly increased as well as two proteins, 14-3-3 protein β/α (spot 058N) and heterogeneous nuclear ribonucleoprotein K (spot 346N), were significantly decreased in two clones resistant to CYC116 carrying $p53^{+/+}$ (clones R1.2 and R1.3; Figure 3 and Table 3) but not in the clones carrying $p53^{-/-}$ (clones R2.1 and R2.2). Conversely, Ras GTPase-activating protein-binding protein 1 (spot 095N) was typically increased, while lamin-B2 (spot 308N), tyrosine 3-monooxygenase (spot 587N), and 14-3-3 protein epsilon (spot 777N) were decreased in HCT116 cells resistant to CYC116 carrying $p53^{-/-}$ (clones R2.1 and R2.2; Figure 3 and Table 3) but not in the clones $p53^{+/+}$ (clones R1.2 and R1.3).

As compared to what we could observe in cells resistant to CYC116, the number of protein alterations related to p53 phenotype typical for cells resistant to ZM447439 was limited to four proteins only. Proteasome subunit β type-2 (spot 93B) was significantly higher in $p53^{+/+}$ clones (clones R3.1 and R3.2; Figure 4 and Table 3) but not in the clones carrying $p53^{-/-}$ (clones R4.2 and R4.3), three proteins with an increased level of Ras GTPase-activating protein-binding protein 1 (spot 360N) and T-complex protein 1 subunit δ (spot 105B) and decreased level of platelet-activating factor (PAF) acetylhydrolase IB subunit β (spot 228N) were changed in $p53^{-/-}$ clones resistant to ZM447439 (clones R4.2 and R4.3; Figure 4 and Table 3) but not in the clones $p53^{+/+}$ (clones R3.1 and R3.2).

Computer Modeling of Possible Interaction Networks in HCT116 Resistant Cells

UniProtKB accessions of the proteins from Table 1 were introduced into Interologous Interaction Database to identify possible interaction partners, and Figure 5 depicts their interaction network generated by NAVIGaTOR software. In total, 435 interactions were recognized for translationally controlled tumor protein (TCPT), 60 kDa heat shock protein (HSP60), heterogeneous nuclear ribonucleoprotein G (hnRNPG), leukocyte elastase inhibitor (LEI), and serine hydroxymethyltransferase (GLYM) (Supplementary Table 4 in the Supporting Information). Computer modeling highlighted a high number of mediated interactions among these proteins and revealed interconnectivity via autophagy protein 5 (AP5, ATG5_HUMAN) and WD repeat domain phosphoinositide-interacting protein 2 (WPI2, WIPI2_HUMAN), indicating their possible role in resistance to CYC116.

Quest for Candidate Biomarkers of Resistance to AURK Inhibitors

In a quest for common candidate markers of resistance to AURK inhibitors, the proteins significantly changing their levels ($p < 0.05$) in at least five out of total eight resistant clones without any selectivity to a specific kind of inhibitor or p53 phenotype were searched. On the basis of these criteria, 13 selected proteins (Figure 6) including 26S protease regulatory subunit 6B (PRS6B, spot 923N), serpin B5 (SPB5, spot 242N), annexin A3 (ANXA3, spot 092N), calretinin (CALB2, spot 671N), heat shock protein HSP 90-β (HSP90B, spot 290N), and galactokinase (GALK1, spot 567N) were found to represent the proteins that were up-

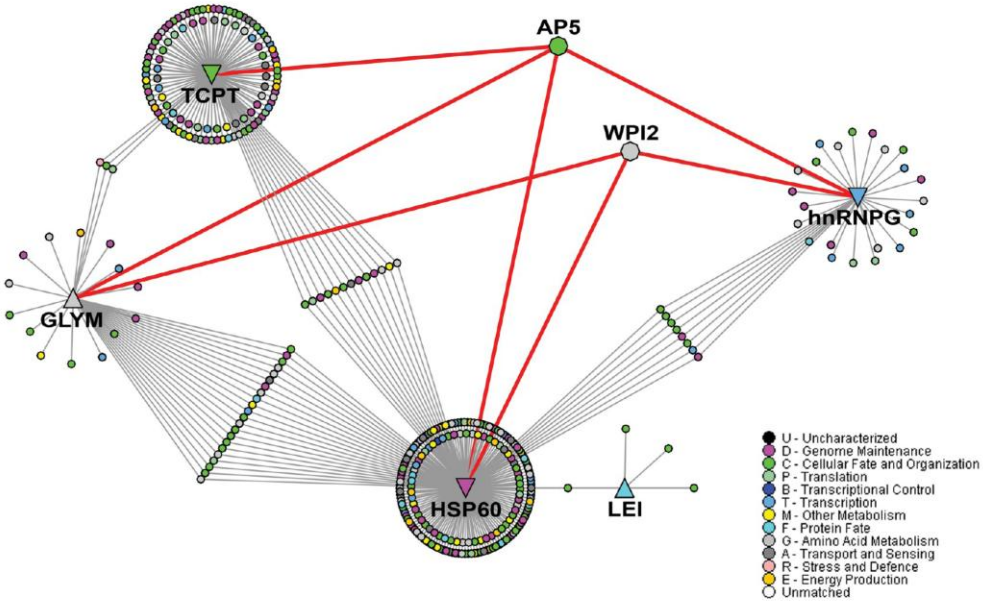

Figure 5. p53-independent interaction network in CYC116 resistant cells. Computer modeling of possible protein−protein interactions in HCT116 cells resistant to CYC116 depicts a high number of mediated interactions among proteins from Table 1 (translationally controlled tumor protein, TCPT; 60 kDa heat shock protein, HSP60; heterogeneous nuclear ribonucleoprotein G, hnRNPG; leukocyte elastase inhibitor, LEI; and serine hydroxymethyltransferase, GLYM) and highlighted by red link interconnections via autophagy protein 5 (AP5) and WD repeat domain phosphoinositide-interacting protein 2 (WPI2). The network generated by NAVIGaTOR software is best interpreted as follows: nodes represent proteins, and edges between nodes represent physical interactions between proteins. Proteins regulated specifically in all HCT116 clones resistant to CYC116 are indicated by a triangle (up- or down-regulated), and interacting proteins retrieved by Interologous Interaction Database and NAVIGaTOR software are indicated by an ellipse. The color of nodes represents Gene Ontology functionality.

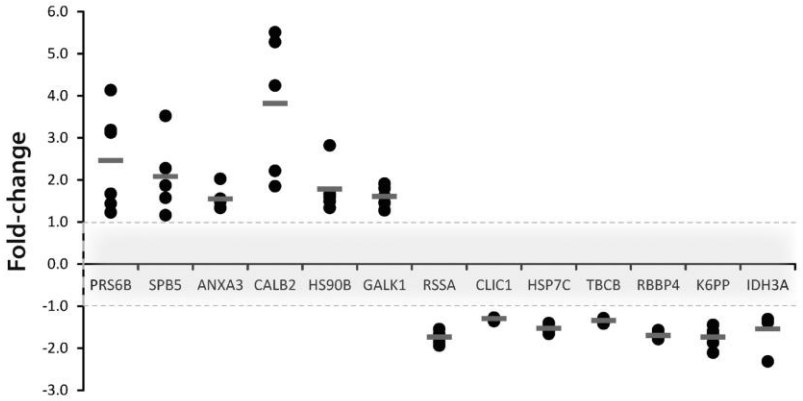

Figure 6. Biomarker candidates. Fold-change values for proteins significantly regulated in at least five out of eight resistant clones as compared to the corresponding control (fold-change > ±1.0, $p < 0.05$) are shown in the dot-plot graph. 26S protease regulatory subunit 6B (PRS6B, $n = 6$), serpin B5 (SPB5, $n = 5$), annexin A3 (ANXA3, $n = 5$), calretinin (CALB2, $n = 5$), heat shock protein HSP 90-β (HSP90B, $n = 5$), galactokinase (GALK1, $n = 6$), 40S ribosomal protein SA (RSSA, $n = 5$), chloride intracellular channel protein (CLIC1, $n = 5$), heat shock cognate 71 kDa protein (HSP7C, $n = 5$), tubulin-folding cofactor B (TBCB, $n = 5$), histone-binding protein RBBP4 (RBBP4, $n = 5$), 6-phosphofructokinase type C (K6PP, $n = 5$), and isocitrate dehydrogenase [NAD] subunit α (IDH3A, $n = 5$).

regulated in resistant clones; 40S ribosomal protein SA (RSSA, spot 277N), chloride intracellular channel protein (CLIC1, spot 054N), heat shock cognate 71 kDa protein (HSP7C, spot 129N), tubulin-folding cofactor B (TBCB, spot 442N), histone-binding

dx.doi.org/10.1021/pr300819m | J. Proteome Res. XXXX, XXX, XXX−XXX

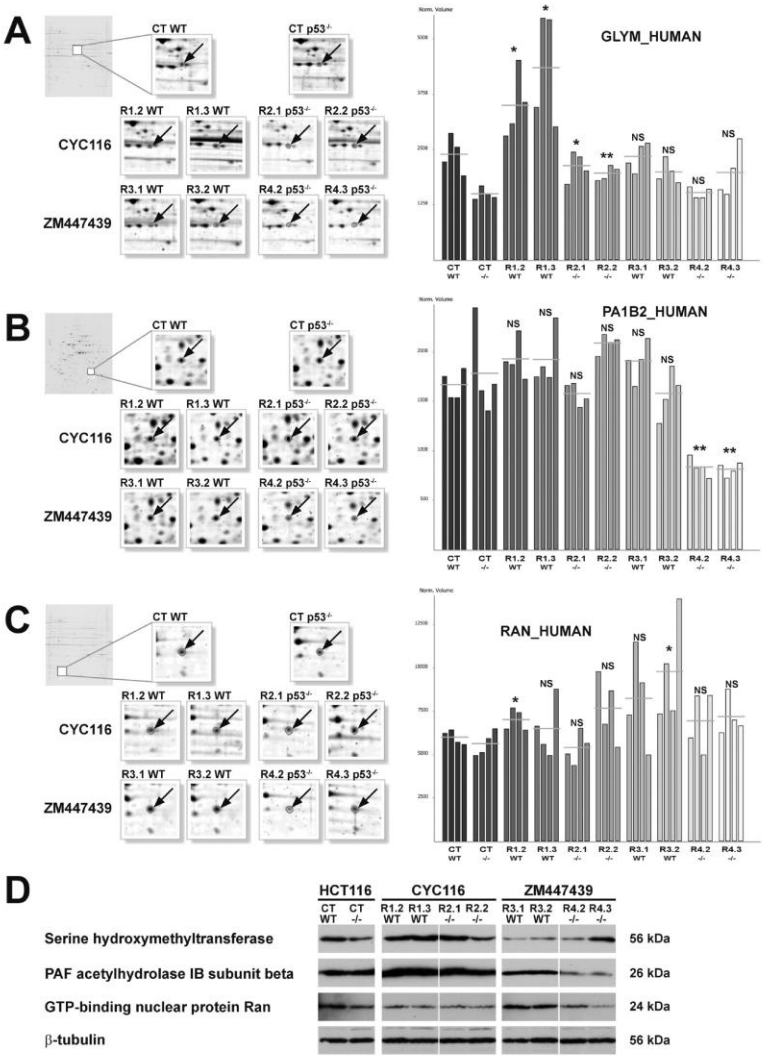

Figure 7. Protein changes in HCT116 resistant cells typical for individual AURK inhibitors. Significantly regulated protein spots between HCT116 sensitive (CT, control) cells and cells resistant to AURK inhibitors are indicated by arrows in the zoomed 2D gel images on the left with graphs on the right, generated by REDFIN software depicting normalized spot volumes in four individual gels. (A) Serine hydroxymethyltransferase, GLYM_HUMAN; (B) PAF acetylhydrolase IB subunit β, PA1B2_HUMAN; (C) GTP-binding nuclear protein Ran, RAN_HUMAN (NS, not significant; $^{*}p < 0.05$, $^{**}p < 0.01$, and $^{***}p < 0.001$, as compared to corresponding sensitive cell line HCT116 with wild-type $p53^{+/+}$ (WT) or mutated $p53^{-/-}$). (D) Western blot analysis of serine hydroxymethyltransferase, PAF acetylhydrolase IB subunit β, and GTP-binding nuclear protein Ran. Sensitive and resistant cells were examined using specific antibodies, and β-tubulin was used as a loading control.

protein RBBP4 (RBBP4, spot 662N), 6-phosphofructokinase type C (K6PP, spot 082B), and isocitrate dehydrogenase [NAD] subunit α (IDH3A, spot 069N) were the proteins down-regulated in resistant clones.

Verification of Selected Proteomic Data

Among significantly reproducible protein changes in HCT116 cells resistant to CYC116 and ZM447439 AURK inhibitors, 2-fold and higher changes were reached by translationally controlled tumor protein, heterogeneous nuclear ribonucleo-protein G, leukocyte elastase inhibitor, and 78 kDa glucose-regulated protein (Tables 1 and 2); malate dehydrogenase, heat shock cognate 71 kDa protein, lamin-B2, proteasome subunit β type-2, and PAF acetylhydrolase IB subunit β (Table 3); 26S protease regulatory subunit 6B, serpin B5, annexin A3, calretinin,

dx.doi.org/10.1021/pr300819m | J. Proteome Res. XXXX, XXX, XXX−XXX

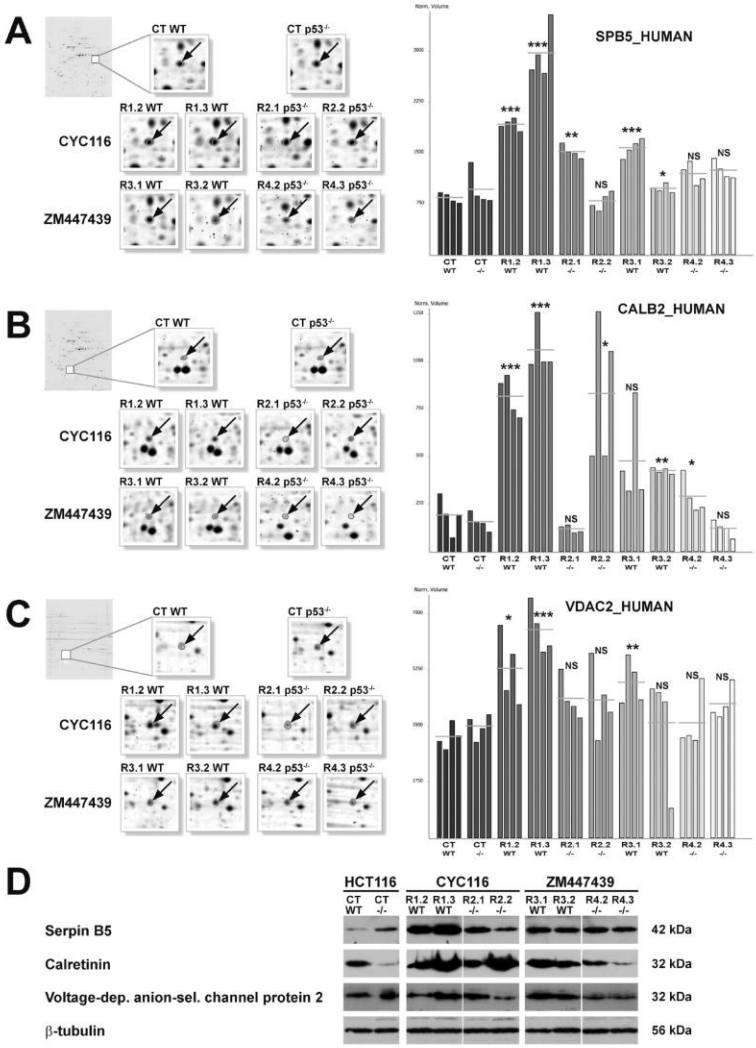

Figure 8. Apoptosis-related protein changes in HCT116 resistant cells. Significantly regulated protein spots between HCT116 sensitive (CT, control) cells and cells resistant to AURK inhibitors are indicated by arrows in the zoomed 2D gel images on the left with graphs on the right, generated by REDFIN software depicting normalized spot volumes in four individual gels. (A) Serpin B5, SPB5_HUMAN; (B) Calretinin, CALB2_HUMAN; (C) voltage-dependent anion-selective channel protein 2, VDAC2_HUMAN (NS, not significant; $*p < 0.05$, $**p < 0.01$, and $***p < 0.001$, as compared to corresponding sensitive cell line HCT116 with wild-type $p53^{+/+}$ (WT) or mutated $p53^{-/-}$). (D) Western blot analysis of serpin B5, calretinin, and voltage-dependent anion-selective channel protein 2. Sensitive and resistant cells were examined using specific antibodies, and β-tubulin was used as a loading control.

heat shock protein HSP 90-β, 6-phosphofructokinase type C, and isocitrate dehydrogenase [NAD] subunit α (Figure 6). While this may reflect the importance of these proteins in the regulation of resistance development, the role of many other less prominent protein alterations should not be ignored. To this end, we selected proteins representing some of the above-mentioned groups for verification by Western blot analysis.

Leukocyte elastase inhibitor and serine hydroxymethyltransferase are the proteins whose expression was typically increased in cells resistant to CYC116 inhibitor. The level of serine hydroxymethyltransferase (spot 157B, GLYM_HUMAN), a potential target enzyme for cancer therapy,[26] showed increase on 2-DE and Western blot in all clones resistant to CYC116 (Figure 7), confirming its independence on p53 phenotype. Interestingly,

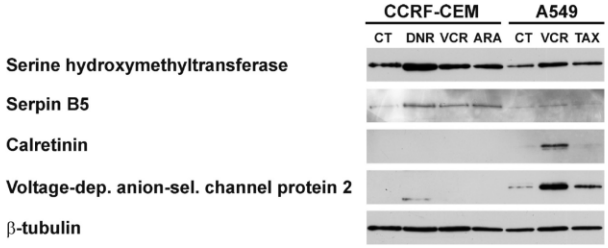

Figure 9. Protein changes in different cancer cells resistant to various anticancer drugs. The expression levels of serine hydroxymethyltransferase, serpin B5, calretinin, and voltage-dependent anion-selective channel protein 2 were measured by Western blotting in CCRF-CEM and A549 cells (CT, control) and cells resistant to daunorubicin (DNR), vincristine (VCR), cytarabine (ARA), and paclitaxel (TAX). β-tubulin was used as a loading control.

PAF acetylhydrolase IB subunit β (spot 228N, PA1B2_HUMAN) was the typical down-regulated protein in $p53^{-/-}$ HCT116 cells resistant to ZM447439 only, and Western blotting allowed verification of this protein (Figure 7). Additionally, GTP-binding nuclear protein Ran (spot 041B, RAN_HUMAN) typical for $p53^{+/+}$ HCT116 cells resistant to ZM447439 was included in the verification for its role in the translocation of p53 through the nuclear pore complex.[27] Despite the fact that significant up-regulation of this protein was observed in only one clone with 2-DE analysis, Western blotting confirmed up-regulation of the protein in both ZM447439 resistant HCT116 $p53^{+/+}$ clones (Figure 7).

Among significant protein changes in at least five out of total eight clones resistant to AURK inhibitors, serpin B5 and calretinin, previously described in regulating apoptosis,[28,29] showed visible overexpression in HCT116 cells. In seven out of eight resistant clones, considerable increase in serpin B5 (spot 242N, SPB5_HUMAN) and calretinin (spot 671N, CALB2_HUMAN) levels were observed, thus further detailing the information obtained using 2-DE (Figure 8). The changes in voltage-dependent anion-selective channel protein 2 (spot 090B, VDAC2_HUMAN), a crucial component in mitochondrial apoptosis,[30] were less pronounced in 2-DE with significantly increased level in majority of $p53^{+/+}$ HCT116 resistant clones detected by Western blot in clones R3.1, R3.2, and R1.3 but not in R1.2 (Figure 8).

Involvement of Selected Proteins in Cancer Cell Resistance to Individual Anticancer Agents

To assess the role of selected proteins from this study in the development of resistance to different chemotherapeutics in different cancer cells, T-lymphoblastic leukemia CCRF-CEM cells carrying p53 mutations and A549 lung adenocarcinoma cells with p53 wild-type phenotype resistant to anticancer drugs with diverse structures and mechanistic targets[20] were examined. Using these cells, no changes in PAF acetylhydrolase and GTP-binding nuclear protein Ran were found (data not shown). However, the different levels of serine hydroxymethyltransferase, serpin B5, calretinin, and voltage-dependent anion-selective channel protein 2 in resistant cells as compared to corresponding controls were examined (Figure 9). Serine hydroxymethyltransferase and serpin B5 were up-regulated in CCRF-CEM cells resistant to daunorubicin, vincristine and cytarabine and in A549 cells resistant to vincristine. Calretinin and voltage-dependent anion-selective channel protein 2 were detectable only in A549 cells showing a noticeable increase in cells resistant to vincristine.

DISCUSSION

The efficiency of specific regimens in cancer therapy can be improved by selective inhibition of AURKs.[2] Despite great expectations from such an approach, the development of resistance toward this type of cancer treatment has to be thoroughly investigated to avoid potential therapy failure. The published data demonstrate a variety of molecular mechanisms leading to the induction of resistance to anticancer drugs including the occurrence of drug-resistant Aurora B mutants after treatment by AURK inhibitors.[5−9,31] Nevertheless, there is a need to better describe such mechanisms and to translate these findings into clinical laboratory with predominant focus on expressed proteins that could be used as markers for therapy monitoring as well as targets for novel anticancer drugs.

In the present study, we considered CYC116 AURK inhibitor, which has been tested in phase I clinical evaluation,[2] and a model inhibitor ZM447439. By short-term culture in high doses of CYC116 and ZM447439, resistant cells were established, and 2D electrophoresis followed by MALDI-TOF/TOF was performed to comprehensively compare sensitive and resistant HCT116 colon cancer cells. The different levels of metabolic proteins such as isocitrate dehydrogenase, phosphoserine aminotransferase, and 40S ribosomal protein SA were identified, which have been already described in a number of proteomic studies of various drug-resistant cancer cell lines[32] and may reflect general response of cells to toxicity. The proteins directly involved in tumor progression and apoptosis were identified in our study, and important changes observed have become a focus of interest.

We identified several candidates; however, most protein changes were observed in individual resistant clones. Combining clones with the same p53 phenotype resistant to the single AURK inhibitor has led to the elimination of proteins expressed differently as a result of sporadic response to anticancer treatment. Because of the low overlap of expression changes between resistant cells, we hypothesize that colon cancer cells resort to different mechanisms to resist cell death induced by CYC116 and ZM447439. CYC116, which is highly effective at lower concentrations as compared to ZM447439,[2,3] was found to be a more specific and with amplified response in resistant cells.

Unlike ZM447439, CYC116 resistant cells expressed several proteins differently regardless of p53. Although these proteins are mainly involved in metabolism of proteins and nucleic acids, computer modeling revealed a high number of mediated interactions among these proteins, linking a variety of biological processes. Interestingly, direct interconnections with autophagy protein 5 and WD repeat domain phosphoinositide-interacting

protein 2 were observed, highlighting a possible role of autophagy process in p53-independent mechanisms of resistance to CYC116 AURK inhibitor. Autophagy, a lysosome-dependent degradation of cytoplasmic organelles and long-lived proteins, is frequently activated in cancer cells.[33] Recently, autophagy has been linked to drug resistance in cancer therapy, and, together with apoptosis, it has a critical role to play in determining cellular fate of tumor cells.[34−37] In HCT116 cells, regulation of translationally controlled tumor protein, 60 kDa heat shock protein, heterogeneous nuclear ribonucleoprotein G, leukocyte elastase inhibitor, and serine hydroxymethyltransferase and their direct interactions with two autophagy participating proteins appear to control the development of resistance to CYC116 AURK inhibitor.

Serine hydroxymethyltransferase plays a pivotal role in channelling metabolites between amino acid and nucleotide metabolism, as it reversibly catalyzes the conversion of serine into glycine while hydroxymethyl group is transferred to 5,6,7,8-tetrahydrofolate. The resultant compound is the sole precursor of purine biosynthesis, which is required for cell division. Hence, serine hydroxymethyltransferase have been indicated as a potential target enzyme for cancer therapy.[26] With regards to the revealed up-regulation of this enzyme in all HCT116 clones resistant to CYC116 and also in CCRF-CEM and A549 resistant cells with no apparent impact of p53 phenotype, we propose serine hydroxymethyltransferase as a target molecule that may resolve the problem of drug resistance to cancer therapy.

Recently, it was shown that inhibition of AURK was needed for efficient cell cycle arrest, which was mediated by induced p53 up-regulation via ATM/ATR protein kinases.[38] Other studies have indicated that inhibition of AURKs may provide a growth advantage to cells that have suffered from p53 loss.[14] Our study, using HCT116 colon cancer cells with and without p53, allowed us to characterize the impact of p53 phenotype on protein differences associated with resistance to AURK inhibitors. Elongation factor 2 was down-regulated specifically in $p53^{+/+}$ cells resistant to both CYC116 and ZM447439 AURK inhibitors. Yin et al. demonstrated that via association with elongation factor 2, p53 is involved in protein translation.[39] Accordingly, p53 might regulate translation in HCT116 cells and contribute to the development of resistance to AURK inhibitors. HCT116 cells with loss of p53 resistant to both CYC116 and ZM447439 AURK inhibitors were characterized by differential expression of lysozyme C and 78 kDa glucose-regulated protein. Lysozyme C, a protein specifically up-regulated in all $p53^{-/-}$ resistant cells, is known to protect cells against oxidative stress.[40] Therefore, such a protective mechanism may contribute to the resistance to AURK inhibitors in these cells. The second protein specifically regulated in all $p53^{-/-}$ resistant cells, 78 kDa glucose-regulated protein, has been previously associated with cancer and resistance to therapy.[41−43] Contrary to what was expected, the level of this antiapoptotic protein was lower in HCT116 resistant cells.

Among the proteins specifically regulated in cells resistant to ZM447439, two proteins were associated with the development of drug resistance with respect to p53 background. While PAF acetylhydrolase was specifically down-regulated in $p53^{-/-}$ resistant cells, the increased level of GTP-binding nuclear protein Ran was observed only in $p53^{+/+}$ resistant cells. PAF (1-*O*-alkyl-2-acetyl-*sn*-glyceryl-3-phosphorylcholine) deacetylation catalyzed by PAF acetylhydrolase induces the loss of PAF lipid messenger activity.[44] Such an inactivation has been demonstrated to affect tumor growth, vascularization, and cell motility.[45] More interestingly, elevated PAF acetylhydrolase levels have been detected in the tumor tissues of patients with colorectal cancer as compared with healthy individuals.[46] These findings subsequently led us to hypothesize that in colon cancer cells, the decreased level of PAF acetylhydrolase may contribute to resistance development in cells that lack p53. Ran, a member of the ras oncogene family, is known to mediate nucleocytoplasmic transport of small RNAs and proteins, and its activity is essential for mitotic spindle assembly.[47] Previous studies suggested Ran as a promising molecular target for RNA interference-based therapeutics against a variety of tumors,[48,49] and these researchers proved that silencing of Ran induced colorectal cancer cells to undergo apoptosis. Our study extended the above-mentioned observation showing that Ran-mediated regulation of apoptosis depends on p53 expression.

Mutated p53 can enhance resistance to anticancer drugs also by up-regulation of multidrug resistance protein 1 (MDR1).[50] MDR1, also known as P-glycoprotein, is a member of ATP-binding cassette transporters located on cell membrane responsible for a tissue-specific excretion of cytotoxic agents out of tumor cells.[51] In the present study, resistant cell lines of different histogenetic origin and p53 phenotype were analyzed. Consistently with previous studies, CCRF-CEM resistant cells with p53 mutations show an increased expression and activity of MDR1 and p53 wild-type A549 cells highly express LRP (lung resistance-related protein), both manifesting a stable multidrug resistance.[20] Further studies on such multidrug resistance in HCT116 resistant cells would add to our findings.

Regulation of apoptosis plays a pivotal role in the development of drug resistance in cancer therapy.[52] In the present study, we found a higher level of proteins associated with apoptotic cell death, such as serpin B5, calretinin, and voltage-dependent anion-selective channel protein 2 in HCT116 cell resistant to AURK inhibitors. Serpin B5, the so-called maspin, has been proved to suppress the growth of various tumors including breast, prostatic, and cervical carcinomas,[53−55] while promoting the growth of tumors in the colon.[28] Previous studies also linked serpin B5 to resistance in cancer therapy, which suggested that the protein could be a target for novel anticancer drugs.[56−58] We found that serpin B5 up-regulated in HCT116 cells resistant to AURK inhibitors and also in CCRF-CEM cells and A549 resistant cells, indicating its role in the development of resistance in a p53-independent manner.

Because of the unequivocal role of calcium in apoptosis, a relationship between calretinin and resistance to drug-induced cell death has been hypothesized.[59] This protein, which is expressed in poorly differentiated colon carcinomas,[60] plays a key role in processes such as message targeting and intracellular calcium buffering. The expression of calretinin in our study was substantially increased in cells resistant to AURK inhibitors and also in A549 cells resistant to vincristine but not in CCRF-CEM cells. Similar to calretinin, voltage-dependent anion-selective channel protein 2 was not detectable in CCRF-CEM cells; however, a higher level was demonstrated in $p53^{+/+}$ cells resistant to AURK inhibitors and in A549 cells resistant to vincristine. Voltage-dependent anion-selective channel protein 2 forms a channel through the mitochondrial outer membrane and acts as a crucial component in mitochondrial apoptosis.[30]

Options in cancer therapy are often limited to regimes based on statistical evaluation. Hence, there is a particular need for biomarkers to aid early detection of drug resistance. Taking into consideration that serpin B5 and calretinin were up-regulated with the highest fold-changes in almost all resistant cells used in

our study, they ultimately represent the most promising molecules for cancer therapy monitoring. Moreover, serpin B5 with secreted annotation could be released by tumors into the bloodstream, where it can be noninvasively assessed during defined therapy, adding to signature of biomarkers useful in cancer treatment.

CONCLUSIONS

Characterization of mechanisms leading to the development of drug resistance in cancer therapy is crucial to identifying targets for novel anticancer drugs, which may selectively eliminate resistant cells in specific disease stage. We have shown that serine hydroxymethyltransferase, PAF acetylhydrolase, GTP-binding nuclear protein Ran, serpin B5, calretinin, and voltage-dependent anion-selective channel protein 2 contribute to the development of drug resistance to AURK inhibitors. Following verification of observed protein changes, the overexpression of serine hydroxymethyltransferase, serpin B5, calretinin, and voltage-dependent anion-selective channel protein 2 was evident also in leukemia CCRF-CEM and lung adenocarcinoma A549 cells resistant to distinct anticancer drugs, suggesting that targeting these proteins may overcome the problem of drug resistance in cancer therapy. The study outlined here has been the key "stepping-stone" to current ongoing studies on selected proteins and their levels in cancer patient samples with focus on their functionality as novel targets for cancer therapy. After further validation, monitoring of calretinin and serpin B5 levels may have a profound impact in cancer treatment in clinics. We believe that these in-depth studies will stimulate future research, ultimately leading to improved understanding of drug resistance in cancer therapy and, in particular, to the clarification of proteins functionality.

ASSOCIATED CONTENT

Supporting Information

Supplementary Table 1, regulated proteins in HCT116 cells resistant to AURK inhibitors; Supplementary Table 2, mass spectrometric data of identified proteins; Supplementary Table 3, involvement of regulated proteins in biological processes; and Supplementary Table 4, I2D protein−protein interaction search results. This material is available free of charge via the Internet at http://pubs.acs.org.

AUTHOR INFORMATION

Corresponding Author

*Tel: +420 315 639 582. Fax: +420 315 639 510. E-mail: kovarova@iapg.cas.cz.

Author Contributions

The manuscript was written with contributions from all authors. All authors have given approval to the final version of the manuscript.

Notes

The authors declare no competing financial interest.

ACKNOWLEDGMENTS

We greatly acknowledge Jaroslava Supolikova for skillful technical assistance. This work was supported in part by the Ministry of Education, Youth and Sports (Grant LC07017) and by Institutional Research Projects RVO67985904 (IAPG, AS CR, v.v.i.) and RVO61388971 (IMIC, AS CR, v.v.i.). An infrastructural part of this project was supported from the Operational Program Research and Development for Innovations (CZ.1.05/2.1.00/01.0030).

ABBREVIATIONS

AURK, Aurora kinase; PAF, platelet-activating factor; MDR1, multidrug resistance protein 1

REFERENCES

(1) Kollareddy, M.; Dzubak, P.; Zheleva, D.; Hajduch, M. Aurora kinases: Structure, functions and their association with cancer. *Biomed. Pap. Med. Fac. Univ. Palacky Olomouc Czech Repub.* **2008**, *152* (1), 27−33.

(2) Kollareddy, M.; Zheleva, D.; Dzubak, P.; Brahmkshatriya, P. S.; Lepsik, M.; Hajduch, M. Aurora kinase inhibitors: Progress towards the clinic. *Invest. New Drugs* **2012**, *30*, 2411−2432.

(3) Ditchfield, C.; Johnson, V. L.; Tighe, A.; Ellston, R.; Haworth, C.; Johnson, T.; Mortlock, A.; Keen, N.; Taylor, S. S. Aurora B couples chromosome alignment with anaphase by targeting BubR1, Mad2, and Cenp-E to kinetochores. *J. Cell Biol.* **2003**, *161* (2), 267−280.

(4) Wang, S.; Midgley, C. A.; Scaerou, F.; Grabarek, J. B.; Griffiths, G.; Jackson, W.; Kontopidis, G.; McClue, S. J.; McInnes, C.; Meades, C.; Mezna, M.; Plater, A.; Stuart, I.; Thomas, M. P.; Wood, G.; Clarke, R. G.; Blake, D. G.; Zheleva, D. I.; Lane, D. P.; Jackson, R. C.; Glover, D. M.; Fischer, P. M. Discovery of N-phenyl-4-(thiazol-5-yl)pyrimidin-2-amine aurora kinase inhibitors. *J. Med. Chem.* **2010**, *53* (11), 4367−4378.

(5) Gottesman, M. M.; Fojo, T.; Bates, S. E. Multidrug resistance in cancer: role of ATP-dependent transporters. *Nat. Rev. Cancer* **2002**, *2* (1), 48−58.

(6) Elsaleh, H.; Powell, B.; McCaul, K.; Grieu, F.; Grant, R.; Joseph, D.; Iacopetta, B. P53 alteration and microsatellite instability have predictive value for survival benefit from chemotherapy in stage III colorectal carcinoma. *Clin. Cancer Res.* **2001**, *7* (5), 1343−1349.

(7) Youn, C. K.; Kim, M. H.; Cho, H. J.; Kim, H. B.; Chang, I. Y.; Chung, M. H.; You, H. J. Oncogenic H-Ras up-regulates expression of ERCC1 to protect cells from platinum-based anticancer agents. *Cancer Res.* **2004**, *64* (14), 4849−4857.

(8) Dean, M. Cancer stem cells: Implications for cancer causation and therapy resistance. *Discovery Med* **2005**, *5* (27), 278−82.

(9) Glasspool, R. M.; Teodoridis, J. M.; Brown, R. Epigenetics as a mechanism driving polygenic clinical drug resistance. *Br. J. Cancer* **2006**, *94* (8), 1087−92.

(10) Hollstein, M.; Sidransky, D.; Vogelstein, B.; Harris, C. C. p53 mutations in human cancers. *Science* **1991**, *253* (5015), 49−53.

(11) Gasco, M.; Crook, T. p53 family members and chemoresistance in cancer: what we know and what we need to know. *Drug Resist. Updates* **2003**, *6* (6), 323−328.

(12) Vousden, K. H.; Lu, X. Live or let die: The cell's response to p53. *Nat. Rev. Cancer* **2002**, *2* (8), 594−604.

(13) Moll, U. M.; Wolff, S.; Speidel, D.; Deppert, W. Transcription-independent pro-apoptotic functions of p53. *Curr. Opin. Cell Biol.* **2005**, *17* (6), 631−636.

(14) Mao, J. H.; Wu, D.; Perez-Losada, J.; Jiang, T.; Li, Q.; Neve, R. M.; Gray, J. W.; Cai, W. W.; Balmain, A. Crosstalk between Aurora-A and p53: Frequent deletion or downregulation of Aurora-A in tumors from p53 null mice. *Cancer Cell* **2007**, *11* (2), 161−173.

(15) Chen, S. S.; Chang, P. C.; Cheng, Y. W.; Tang, F. M.; Lin, Y. S. Suppression of the STK15 oncogenic activity requires a transactivation-independent p53 function. *EMBO J.* **2002**, *21* (17), 4491−4499.

(16) Katayama, H.; Sasai, K.; Kawai, H.; Yuan, Z. M.; Bondaruk, J.; Suzuki, F.; Fujii, S.; Arlinghaus, R. B.; Czerniak, B. A.; Sen, S. Phosphorylation by aurora kinase A induces Mdm2-mediated destabilization and inhibition of p53. *Nat. Genet.* **2004**, *36* (1), 55−62.

(17) Cheng, J.; Haas, M. Frequent mutations in the p53 tumor suppressor gene in human leukemia T-cell lines. *Mol. Cell. Biol.* **1990**, *10* (10), 5502−5509.

(18) Zhang, L.; Zhang, J.; Hu, C.; Cao, J.; Zhou, X.; Hu, Y.; He, Q.; Yang, B. Efficient activation of p53 pathway in A549 cells exposed to L2,

a novel compound targeting p53-MDM2 interaction. *Anticancer Drugs* **2009**, *20* (6), 416−424.
(19) Dzubak, P.; Hajduch, M.; Gazak, R.; Svobodova, A.; Psotova, J.; Walterova, D.; Sedmera, P.; Kren, V. New derivatives of silybin and 2,3-dehydrosilybin and their cytotoxic and P-glycoprotein modulatory activity. *Bioorg. Med. Chem.* **2006**, *14* (11), 3793−3810.
(20) Noskova, V.; Dzubak, P.; Kuzmina, G.; Ludkova, A.; Stehlik, D.; Trojanec, R.; Janostakova, A.; Korinkova, G.; Mihal, V.; Hajduch, M. In vitro chemoresistance profile and expression/function of MDR associated proteins in resistant cell lines derived from CCRF-CEM, K562, A549 and MDA MB 231 parental cells. *Neoplasma* **2002**, *49* (6), 418−425.
(21) Hardy, E.; Castellanos-Serra, L. R. "Reverse-staining" of biomolecules in electrophoresis gels: analytical and micropreparative applications. *Anal. Biochem.* **2004**, *328* (1), 1−13.
(22) Stastna, M.; Behrens, A.; McDonnell, P. J.; Van Eyk, J. E. Analysis of protein composition of rabbit aqueous humor following two different cataract surgery incision procedures using 2-DE and LC-MS/MS. *Proteome Sci.* **2011**, *9* (1), 8.
(23) Gobom, J.; Nordhoff, E.; Mirgorodskaya, E.; Ekman, R.; Roepstorff, P. Sample purification and preparation technique based on nano-scale reversed-phase columns for the sensitive analysis of complex peptide mixtures by matrix-assisted laser desorption/ionization mass spectrometry. *J. Mass Spectrom.* **1999**, *34* (2), 105−116.
(24) Thomas, P. D.; Campbell, M. J.; Kejariwal, A.; Mi, H.; Karlak, B.; Daverman, R.; Diemer, K.; Muruganujan, A.; Narechania, A. PANTHER: A library of protein families and subfamilies indexed by function. *Genome Res.* **2003**, *13* (9), 2129−2141.
(25) Brown, K. R.; Jurisica, I. Online predicted human interaction database. *Bioinformatics* **2005**, *21* (9), 2076−2082.
(26) Agrawal, S.; Kumar, A.; Srivastava, V.; Mishra, B. N. Cloning, expression, activity and folding studies of serine hydroxymethyltransferase: A target enzyme for cancer chemotherapy. *J. Mol. Microbiol. Biotechnol.* **2003**, *6* (2), 67−75.
(27) Sorokin, A. V.; Kim, E. R.; Ovchinnikov, L. P. Nucleocytoplasmic transport of proteins. *Biochemistry (Moscow)* **2007**, *72* (13), 1439−1457.
(28) Payne, C. M.; Holubec, H.; Crowley-Skillicorn, C.; Nguyen, H.; Bernstein, H.; Wilcox, G.; Bernstein, C. Maspin is a deoxycholate-inducible, anti-apoptotic stress-response protein differentially expressed during colon carcinogenesis. *Clin. Exp. Gastroenterol.* **2011**, *4*, 239−253.
(29) Stevenson, L.; Allen, W. L.; Proutski, I.; Stewart, G.; Johnston, L.; McCloskey, K.; Wilson, P. M.; Longley, D. B.; Johnston, P. G. Calbindin 2 (CALB2) regulates 5-fluorouracil sensitivity in colorectal cancer by modulating the intrinsic apoptotic pathway. *PLoS One* **2011**, *6* (5), e20276.
(30) Roy, S. S.; Ehrlich, A. M.; Craigen, W. J.; Hajnoczky, G. VDAC2 is required for truncated BID-induced mitochondrial apoptosis by recruiting BAK to the mitochondria. *EMBO Rep.* **2009**, *10* (12), 1341−1347.
(31) Girdler, F.; Sessa, F.; Patercoli, S.; Villa, F.; Musacchio, A.; Taylor, S. Molecular basis of drug resistance in aurora kinases. *Chem. Biol.* **2008**, *15* (6), 552−562.
(32) Zhang, J. T.; Liu, Y. Use of comparative proteomics to identify potential resistance mechanisms in cancer treatment. *Cancer Treat. Rev.* **2007**, 33 (8), 741−756.
(33) Mizushima, N.; Klionsky, D. J. Protein turnover via autophagy: implications for metabolism. *Annu. Rev. Nutr.* **2007**, *27*, 19−40.
(34) Han, W.; Sun, J.; Feng, L.; Wang, K.; Li, D.; Pan, Q.; Chen, Y.; Jin, W.; Wang, X.; Pan, H.; Jin, H. Autophagy inhibition enhances daunorubicin-induced apoptosis in K562 cells. *PLoS One* **2011**, *6* (12), e28491.
(35) Ma, X. H.; Piao, S.; Wang, D.; McAfee, Q. W.; Nathanson, K. L.; Lum, J. J.; Li, L. Z.; Amaravadi, R. K. Measurements of tumor cell autophagy predict invasiveness, resistance to chemotherapy, and survival in melanoma. *Clin. Cancer Res.* **2011**, *17* (10), 3478−3489.
(36) Qadir, M. A.; Kwok, B.; Dragowska, W. H.; Le, K. H.; Bally, D.; Gorski, M. B.; Macroautophagy, S. M. inhibition sensitizes tamoxifen-resistant breast cancer cells and enhances mitochondrial depolarization. *Breast Cancer Res. Treat.* **2008**, *112* (3), 389−403.
(37) Yoon, J. H.; Ahn, S. G.; Lee, B. H.; Jung, S. H.; Oh, S. H. Role of autophagy in chemoresistance: regulation of the ATM-mediated DNA-damage signaling pathway through activation of DNA-PKcs and PARP-1. *Biochem. Pharmacol.* **2012**, *83* (6), 747−757.
(38) Dreier, M. R.; Grabovich, A. Z.; Katusin, J. D.; Taylor, W. R. Short and long-term tumor cell responses to Aurora kinase inhibitors. *Exp. Cell Res.* **2009**, *315* (7), 1085−1099.
(39) Yin, X.; Fontoura, B. M.; Morimoto, T.; Carroll, R. B. Cytoplasmic complex of p53 and eEF2. *J. Cell Physiol.* **2003**, *196* (3), 474−482.
(40) Liu, H.; Zheng, F.; Cao, Q.; Ren, B.; Zhu, L.; Striker, G.; Vlassara, H. Amelioration of oxidant stress by the defensin lysozyme. *Am. J. Physiol. Endocrinol. Metab.* **2006**, *290* (5), E824−E832.
(41) Chang, Y. J.; Huang, Y. P.; Li, Z. L.; Chen, C. H. GRP78 Knockdown Enhances Apoptosis via the Down-Regulation of Oxidative Stress and Akt Pathway after Epirubicin Treatment in Colon Cancer DLD-1 Cells. *PLoS One* **2012**, *7* (4), e35123.
(42) Zhang, L. H.; Zhang, X. Roles of GRP78 in physiology and cancer. *J. Cell Biochem.* **2010**, *110* (6), 1299−1305.
(43) Zhou, H.; Zhang, Y.; Fu, Y.; Chan, L.; Lee, A. S. Novel mechanism of anti-apoptotic function of 78-kDa glucose-regulated protein (GRP78): Endocrine resistance factor in breast cancer, through release of B-cell lymphoma 2 (BCL-2) from BCL-2-interacting killer (BIK). *J. Biol. Chem.* **2011**, *286* (29), 25687−25696.
(44) Tjoelker, L. W.; Stafforini, D. M. Platelet-activating factor acetylhydrolases in health and disease. *Biochim. Biophys. Acta* **2000**, *1488* (1−2), 102−123.
(45) Biancone, L.; Cantaluppi, V.; Del Sorbo, L.; Russo, S.; Tjoelker, L. W.; Camussi, G. Platelet-activating factor inactivation by local expression of platelet-activating factor acetyl-hydrolase modifies tumor vascularization and growth. *Clin. Cancer Res.* **2003**, *9* (11), 4214−4220.
(46) Denizot, Y.; Truffinet, V.; Bouvier, S.; Gainant, A.; Cubertafond, P.; Mathonnet, M. Elevated plasma phospholipase A2 and platelet-activating factor acetylhydrolase activity in colorectal cancer. *Mediators Inflammation* **2004**, *13* (1), 53−54.
(47) Clarke, P. R.; Zhang, C. Spatial and temporal coordination of mitosis by Ran GTPase. *Nat. Rev. Mol. Cell Biol.* **2008**, *9* (6), 464−477.
(48) Honma, K.; Takemasa, I.; Matoba, R.; Yamamoto, Y.; Takeshita, F.; Mori, M.; Monden, M.; Matsubara, K.; Ochiya, T. Screening of potential molecular targets for colorectal cancer therapy. *Int. J. Gen. Med.* **2009**, *2*, 243−257.
(49) Xia, F.; Lee, C. W.; Altieri, D. C. Tumor cell dependence on Ran-GTP-directed mitosis. *Cancer Res.* **2008**, *68* (6), 1826−1833.
(50) Thottassery, J. V.; Zambetti, G. P.; Arimori, K.; Schuetz, E. G.; Schuetz, J. D. p53-dependent regulation of MDR1 gene expression causes selective resistance to chemotherapeutic agents. *Proc. Natl. Acad. Sci. U.S.A.* **1997**, *94* (20), 11037−11042.
(51) Bush, J. A.; Li, G. Regulation of the Mdr1 isoforms in a p53-deficient mouse model. *Carcinogenesis* **2002**, *23* (10), 1603−1607.
(52) Pommier, Y.; Sordet, O.; Antony, S.; Hayward, R. L.; Kohn, K. W. Apoptosis defects and chemotherapy resistance: molecular interaction maps and networks. *Oncogene* **2004**, *23* (16), 2934−2949.
(53) Lovric, E.; Gatalica, Z.; Eyzaguirre, E.; Kruslin, B. Expression of maspin and glutathionine-S-transferase-pi in normal human prostate and prostatic carcinomas. *Appl. Immunohistochem. Mol. Morphol.* **2010**, *18* (5), 429−432.
(54) Yeom, S. Y.; Jang, H. L.; Lee, S. J.; Kim, E.; Son, H. J.; Kim, B. G.; Park, C. Interaction of testisin with maspin and its impact on invasion and cell death resistance of cervical cancer cells. *FEBS Lett.* **2010**, *584* (8), 1469−1475.
(55) Zou, Z.; Anisowicz, A.; Hendrix, M. J.; Thor, A.; Neveu, M.; Sheng, S.; Rafidi, K.; Seftor, E.; Sager, R. Maspin, a serpin with tumor-suppressing activity in human mammary epithelial cells. *Science* **1994**, *263* (5146), 526−529.
(56) Ben Shachar, B.; Feldstein, O.; Hacohen, D.; Ginsberg, D. The tumor suppressor maspin mediates E2F1-induced sensitivity of cancer cells to chemotherapy. *Mol. Cancer Res.* **2010**, *8* (3), 363−372.
(57) Feng, X. P.; Yi, H.; Li, M. Y.; Li, X. H.; Yi, B.; Zhang, P. F.; Li, C.; Peng, F.; Tang, C. E.; Li, J. L.; Chen, Z. C.; Xiao, Z. Q. Identification of

biomarkers for predicting nasopharyngeal carcinoma response to radiotherapy by proteomics. *Cancer Res.* **2010**, *70* (9), 3450−3462.
(58) Nam, E.; Park, C. Maspin suppresses survival of lung cancer cells through modulation of Akt pathway. *Cancer Res. Treat.* **2010**, *42* (1), 42−47.
(59) Boyer, J.; Allen, W. L.; McLean, E. G.; Wilson, P. M.; McCulla, A.; Moore, S.; Longley, D. B.; Caldas, C.; Johnston, P. G. Pharmacogenomic identification of novel determinants of response to chemotherapy in colon cancer. *Cancer Res.* **2006**, *66* (5), 2765−2777.
(60) Haner, K.; Henzi, T.; Pfefferli, M.; Haner, K.; Salicio, V.; Schwaller, B. A bipartite butyrate-responsive element in the human calretinin (CALB2) promoter acts as a repressor in colon carcinoma cells but not in mesothelioma cells. *J. Cell Biochem.* **2010**, *109* (3), 519−531.

PŘÍLOHA 4

FEBS Letters 583 (2009) 1772–1784

journal homepage: www.FEBSLetters.org

Minireview

Challenges in cancer research and multifaceted approaches for cancer biomarker quest

Jirina Martinkova [a], Suresh Jivan Gadher [b], Marian Hajduch [c], Hana Kovarova [a,*]

[a] Institute of Animal Physiology and Genetics, Academy of Sciences of the Czech Republic, v.v.i., Rumburska 89, 27721 Libechov, Czech Republic
[b] Millipore Bioscience, 15 Research Park Drive, St. Charles, MO 63304, USA
[c] Laboratory of Experimental Medicine, Department of Pediatrics, Faculty of Medicine and Dentistry, Palacky University in Olomouc, Puskinova 6, 775 20 Olomouc, Czech Republic

ARTICLE INFO

Article history:
Received 2 February 2009
Revised 18 March 2009
Accepted 18 March 2009
Available online 25 March 2009

Edited by Miguel De la Rosa

Keywords:
Cancer research
Proteomics
Genomics
Transcriptomics
Cancer biomarker
Anti-cancer therapy

ABSTRACT

Recent advances in cancer biology have subsequently led to the development of new molecularly targeted anti-cancer agents that can effectively hit cancer-related proteins and pathways. Despite better insight into genomic aberrations and diversity of cancer phenotypes, it is apparent that proteomics too deserves attention in cancer research. Currently, a wide range of proteomic technologies are being used in quest for new cancer biomarkers with effective use. These, together with newer technologies such as multiplex assays could significantly contribute to the discovery and development of selective and specific cancer biomarkers with diagnostic or prognostic values for monitoring the disease state. This review attempts to illustrate recent advances in the field of cancer biomarkers and multifaceted approaches undertaken in combating cancer.
© 2009 Federation of European Biochemical Societies. Published by Elsevier B.V. All rights reserved.

1. Cancer biology

Cancers represent group of unprecedentedly heterogeneous diseases that affect humans with high frequency and contribute significantly to overall morbidity and mortality. Currently there are only limited anti-cancer therapies available with highly variable efficacy, which reflects an unsatisfactory cure rates. The on-set of carcinogenesis is usually initiated with DNA alteration in the target cell that mostly arise as a result of combination of several factors including genetics, environmental, dietary, immune and as well as several others still to be discovered. The DNA alterations may include a single point nucleotide exchange, deletion, amplification, translocation, chromosomal rearrangement, methylation or other events that can then lead to the activation of oncogenes and inactivation of tumor suppressor genes. Usually, an accumulation of DNA alterations irreversibly transforms normal cell into dysplastic and cancerous one. Previously, it was assumed that dysregulation of limited amount of oncogenes or tumor-suppressor genes caused cancers, however, more recently the alterations of many other genes directly or indirectly involved in the carcinogenesis and tumor progression process have been demonstrated. The integration of known cancer genes into protein transduction and signalling networks reveals their characteristic interactions within networks and shows that cancer genes often function as 'network hub proteins' which are involved in many cellular processes and form focal nodes mediating cross-talk between different signalling pathways [1–3]. Hence such disruptions in cellular communication significantly contribute to cancer development and progression. The

Abbreviations: MAP, mitogen-activated protein; PI3K, phosphatidylinositol-3 kinase; mTOR, mammalian target of rapamycin; Prom1, Prominin 1; EGFRs, epidermal growth factor receptors; VEGFR, vascular endothelial growth factor receptor; PDGFRs, platelet-derived growth factor receptors; SCF, stem cell factor; Erk, extracellular-regulated kinase; Mek, MAP Erk kinase; MAPK, MAP kinase; PKB, protein kinase B; Her-2, human epidermal growth factor receptor 2; ER, estrogen receptor; PR, progesterone receptor; DASL, cDNA-mediated annealing, selection, extension, and ligation; FFPE, formalin fixed paraffin-embedded; miRNAs, microRNAs; 1-D and 2-D gel electrophoresis, one- and two-dimensional gel electrophoresis; 2-D HPLC, two-dimensional high pressure liquid chromatography; DIGE, difference in gel electrophoresis; MS, mass spectrometry; MALDI, matrix assisted laser desorption ionisation; TOF, time-of-flight; SELDI, surface enhanced laser desorption ionisation; SILAC, stable isotope labeling by amino acids in cell culture; ICPL, isotope-coded protein labels; iTRAQ, isobaric tags for relative and absolute quantification; AQUA, absolute quantification; MRM, multiple reaction monitoring; FT-ICR, Fourier transformation-ion cyclotron resonance; GIST, gastrointestinal stromal tumor; MudPIT, multidimensional protein identification technology; NCI-60, the US National Cancer Institute 60 human tumor cell line anti-cancer drug screen; SSRP1, structure specific recognition protein 1; RALBP1, Ral binding protein 1; HSP27, heat shock 27 kDa protein; CDKI, cyclin-dependent kinase inhibitor

* Corresponding author. Fax: +420 315 639 510.
E-mail address: kovarova@iapg.cas.cz (H. Kovarova).

0014-5793/$36.00 © 2009 Federation of European Biochemical Societies. Published by Elsevier B.V. All rights reserved.
doi:10.1016/j.febslet.2009.03.042

molecular alterations are frequently found in processes mediated by growth factors, hormones and cytokines via their receptors. In order to understand cancers better, the roles of tyrosine kinase receptors and signal transduction pathways such as the epidermal growth factor receptors, platelet-derived growth factor receptors, vascular endothelial growth factor receptors, the Ras/Raf/mitogen-activated protein (MAP)-kinase, phosphatidylinositol-3 kinase (PI3K)/Akt/mammalian target of rapamycin (mTOR) and other pathways have been studied and therapeutically targeted in different cancers [4–6]. In 2000 Hanahan and Weinberg [7] outlined the basic principles of a malignant process and proposed that human cancers should demonstrate a minimal set of capabilities that are necessary to progress to a malignant tumor state: (1) growing uncontrollably; (2) insensitivity to anti-growth signals; (3) evading apoptosis; (4) acquiring limitless replicative potential; (5) ability to form and sustain new blood vessels, e.g. angiogenesis; and (6) invasion and metastasis. The identification of altered genes and signalling pathways and their targets could lead to substantial improvement in prevention, diagnosis, prognosis and tailored therapy of cancers.

Recent studies have revealed that apart from the genetic abnormality of many cancer-related genes/proteins, epigenetic regulation of genes is also critically important in the process of carcinogenesis. The mechanisms of epigenetic control of genes involve changes of gene expression patterns mediated by modifications of DNA and/or histones, without the direct alteration of nucleotide sequence of the genes. Those modifications include several processes, mainly the DNA methylation and the covalent modifications such as acetylation, methylation, phosphorylation and ubiquitination of specific amino acid residues of the N-termini of the core histones [8]. Among these modifications, histone acetylation/deacetylation plays a central role in epigenetic regulation of gene expression. Typically, high acetylation level of the chromatin hallmarks the active transcription of the genes, whereas transcriptionally inactive chromatin is usually characterised by low acetylation level of histones. It has been discovered that the occurrence of many cancers is accompanied by a genome-wide histone hypoacetylation and indeed, histone deacetylase inhibitors have significant and clinically proven anti-tumor activity [9,10].

The other key question in current cancer biology is the origin and role of cancer stem cells. Cancer stem cells are remarkably similar to normal stem cells in respect to their ability to self-renew and be multipotent [11–13], but until now it was not clear whether cancer stem cells are the direct progeny of mutated stem cells or more mature cells that re-acquire stem cell characteristics during tumor formation. Using an inducible Cre, nuclear LacZ reporter allele knocked into the Prominin1 locus (Prom1(C-L), Zhu et al. [14] showed that Prom1(+) enterocyte precursor cells located at the base of crypts in the small intestine represent small intestinal stem cell. Furthermore, lineage-tracing studies of adult Prom1(+/C-L) mice after activation of endogenous Wnt signalling pathway demonstrated disruption of crypt architecture with neoplastic transformation and importantly only progeny of Prom1(+) cells retaining Prom1 dependent reporter gene expression marked the fraction of cells that are susceptible to neoplastic transformation. Stem cells are typically expressing the multi-drug resistance proteins and transporters [15]. Indeed, the cancer stem cells are capable of resisting chemotherapy and/or radiotherapy, and they may be responsible for failure of anti-cancer treatments. Hence, the understanding of cancer stem cells properties could help to eliminate them and to prevent re-growth of cancer [16,17].

2. Anti-cancer therapies

Most of currently used conventional anti-cancer treatments include surgery, radiotherapy and chemotherapy. Unlike first two local and/or loco regional therapeutic modalities, chemotherapy has systemic effects and it can eliminate disseminated tumor cells, which are the ultimate reason for tumor recurrence and treatment failure even in potentially curable stages. The chemotherapy in oncology is focused on application of cytostatic and/or cytotoxic drugs with potential to kill malignant cells. Such drugs may be obtained using chemical synthesis or isolated and/or derivatised from plants or different fungi and such cytotoxic and cytostatic drugs are known to frequently induce DNA damage and/or block cellular division. These effects are mediated via a broad spectrum of mechanisms and these in turn target both the tumor and rapidly proliferating normal tissues. Indeed, dose of anti-cancer drugs is a balancing act between achieving concentrations that are effective towards the malignancy and that result in acceptable side effects. The differences in proliferation rates, expression of specific targets and multi-drug resistance proteins between cancer and healthy cells together with various concentrations and metabolism of individual cytostatic drugs in body organs or tissues are major determinants of drug effects. In spite of all precautionary efforts, frequency of secondary side effects and toxicity remains high. Neutropenia is one common example of a side effect of many anti-cancer agents and is related to an increased risk of infection and mortality [18]. This also reflects the general situation that therapeutic standards are based on average efficacy determined by controlled clinical trials involving large cohort of patients and generally extended to the whole population. However, for many patients, the gold standard treatment translates into very low response rate, individual efficacy is far from the mean and this becomes evident only a few months after drug administration. Currently approved anti-cancer drugs are sorted into several groups according to known mechanisms inducing DNA damage and cellular death and include: (i) alkylating cytostatic agents (melphalan, chlorambucil, cyclophosphamide and ifosfamide, derivatives of nitrosourea – carmustine and lomustine, busulfan, dacarbazine, temozolomide and procarbazine); (ii) anti-metabolites (methotrexate, 5-fluorouracil and its derivative capecitabine, cytosinarabinoside, gemcitabine, mercaptopurine, fludarabine, cladribine, hydroxyurea); (iii) anti-cancer antibiotics (doxorubicine, idarubicine, epirubicine, mitoxantron, bleomycine, mitomycin C); (iv) plant alkaloids (vinca alkaloids – vincristine, vinblastine and vinorelbine, podofylotoxin alkaloids – etoposide and teniposide, camptothecin analogs – topotecan and irinotecan, taxanes – paclitaxel and docetaxel); and (v) other drugs (platinum compounds – cisplatin, carboplatin, oxaliplatin; L-asparaginase; amsacrin and others).

Recent advances in our understanding of cancer biology including cancer-related genes, proteins and signalling pathways have opened up a window for tailored and personalised anti-cancer therapy. The ultimate goal would be tailored drug therapies using active dosage firmly directed at specific tumors with a defined molecular profile. Molecular processes in cancer cells include specific alterations in signalling pathways and protein interaction regulatory network such as over-expression and mutations of cellular receptors and other downstream effectors. Such emerging knowledge subsequently has led to the development of new molecular targeted anti-cancer agents that hit effectively cancer-related proteins and pathways. Several approaches have been applied including inhibition of growth factor receptors and receptor tyrosine kinases (EGFRs, VEGFR, PDGFRs, stem cell factor (SCF), c-Kit and chimeric Bcr-Abl protein) [19–21], inhibition of intracellular effectors that mediate intracellular oncogenic signaling such as Ras-Raf- Mek-Erk MAPK or AKT (PKB) and mTOR downstream effectors of the PI3K pathway [22], and other agents targeting integrins involved in angiogenesis and invasion, selective inhibitors of histone deacetylases, ubiquitin–proteasome system and matrix metalloproteinases [5,23].

Although the most of the molecular targeted agents have presented cytostatic activity with favorable degree of cytotoxicity as monotherapies, only modest effects or failure in survival benefit have been observed in advanced tumors. Therefore, several strategies using combination therapy have been suggested to explore possible combination of two or more agents that may target the same pathway more effectively or two different pathways, where the additional one, such as angiogenesis, may complement original target to increase treatment efficacy. Other possible therapeutic strategies include the use of molecular multi-target agents or multi-modality treatment like a combination of molecularly targeted agents with conventional chemotherapy [24–28].

3. Impact of genomics and transcriptomics on classification of cancers and prediction of response to anti-cancer therapy

Today, many cancers are diagnosed and confirmed by pathologists. Anatomic staging plays a significant role in making a diagnosis and treatment decision and classical pathological indexes such as grading are used to make prognosis and predict development of metastatic disease or help guide selection of a primary therapy. However, results of recent studies have shown that the use of these morphology-based tools is not sufficient enough in accurate identification and classification of many different disease subtypes in cancer patients. Several approaches are now available to detect genomic changes leading to tumor genesis such as fluorescence in situ hybridisation, comparative genomic hybridisation and single nucleotide polymorphism analysis including samples isolated by laser-capture micro-dissection. Furthermore, integrating genomic and transcriptomic data may significantly enhance characterisation of molecular fingerprints associated with specific cancer phenotypes [29–31]. Transcriptomic studies are focused on changes in mRNA abundance and alterations in alternative splicing [32]. Analysis of mRNA expression using cDNA microarray permits high throughput gene expression profiling and represents a powerful screening technique allowing analysis of the activation state of cancer-related genes and characterisation of molecular signatures differentially expressed or spliced genes between normal and cancer tissue. This molecular approach has allowed the subdivision and classification of cancers into more homogeneous subgroups with specific features [29,33–36]. For example Sorlie et al. [37] identified set of 456 genes that could classify breast tumor into molecular subtypes (luminal type A and B, Her-2/neu positive, basal-like and normal breast-like subtype) and validated these results on independent cohort of patients with locally advanced breast cancer. They also showed that those molecular subtypes can be clinically distinguished based on estrogen/progesterone receptor (ER/PR) and Her-2/neu gene positivity: ER/PR positive luminal subtypes A and B; ER+PR negative but Her-2/neu positive; ER-PR-Her-2/neu-triple negative basal-like; and human epidermal growth factor receptor 2 (Her-2) negative normal breast-like cancers. However, this study also provided additional molecular features that did not reflect clinical criteria such as lymph node stage, age and menopausal status of patients, thus underlying significant contribution of molecular transcriptional profiling in objective classification of cancers.

Despite the usefulness of microarray data in characterisation of tumor subtypes, recent studies have focused on monitoring of anti-cancer therapy and prediction of tumor response. The work has been done to ascertain expression patterns for commonly used chemotherapy like antimetabolite 5-fluorouracil [38], mitotic poison docetaxel [39], estrogen receptor antagonist tamoxifen [40] and chemotherapy regimens using combined fluorouracil, doxorubicine and cyclophosphamide in neoadjuvant settings [41]. More recently, this type of studies have been also extended to prediction of therapeutic outcome in targeted anti-cancer therapies [42]. The microarray analysis has also been a valuable tool for demonstrating the importance of tumor milieu. Using this technology, it has been possible to demonstrate significant changes in expression of cancer-related genes in cancer cells grown in a 3-D matrix as compared to 2-D culture when treated with anti-cancer drugs and compared to control untreated cells. Findings from such studies have highlighted the importance of cellular architecture, phenotypic variations, and extracellular matrix barrier to drug transport in cellular response to selected compounds. Combination of all these parameters contributes to the overall drug efficacy for that particular cancer or tumor [43]. These studies are aimed at the discovery of multigenic biomarkers with higher probability to better describe complex biology systems. Disease and/or therapy specific transcriptional profiles are followed by extensive validations in order to demonstrate clinical relevance. Whilst microarray technologies are extremely useful and hold their place in research and possibly in diagnostic arenas, there are still some associated limitations that restrict their full use in the clinical environment. Once these have been resolved, microarray technology will be at the forefront of clinical and scientific research. Besides the obvious technical problems associated with platform standardisation (reference RNA and housekeeping genes), reproducibility (printing fluctuation, spot variations, gene oligonucleotide tags and processing), image analysis data processing (need for new bioinformatics and biostatistical tools), there are two major caveats – essential requirement for freshly-frozen tumor tissue or cells and lack of knowledge on specific functions of many genes [34]. Inconvenient sample collection, processing and storage of frozen samples for microarray studies restrict their use for relatively small sample sets. Additionally, the resulting classifier genes require extensive validation by other techniques including qRT-PCR or DASL (cDNA mediated annealing, selection, extension and ligation). Indisputable advantage of qRT-PCR or DASL is that they can be performed using formalin fixed paraffin-embedded (FFPE) tumor tissue samples that present priceless source of clinical samples for investigation. The qRT-PCR utilises amplicons which are specifically designed on DNA fragments usually less than 100 bp thus providing high efficiency and making it suitable for examination of gene expression variation in fixed samples containing chemically modified and fragmented RNA. Compared to microarray analysis, qRT-PCR is amenable to analysis of a high number of samples in retrospective studies. The DASL assay has been developed to combine the advantages of microarray and qRT-PCR technologies. Assay allows sensitive and reproducible gene expression profiling for parallel analysis of several hundreds of mRNA transcripts on the BeadArray platform. Since this assay can be performed on FFPE samples, this technology may be especially useful for determining cancer prognosis or therapy response taking advantages of retrospective investigations of samples with known clinical outcome [44–46].

Recent work has revealed a class of microRNAs (miRNAs), a small non-protein coding RNAs which function as negative gene regulators at the post-transcriptional level. miRNAs regulate multiple gene targets and are capable of controlling wide range of biological processes including growth, differentiation and apoptosis. Hence, disregulation of miRNAs may contribute to many diseases that are known to arise from imbalance in regulation of these cellular processes. It has been shown that mutations and disruption in miRNAs biogenesis are also involved in cancer [47,48]. Studies by Lu et al. reported express profiling analysis of 217 mammalian miRNAs in 334 samples of a variety of human cancers. Expression miRNAs profiles grouped tumors according to tissue of origin and their comparison in tumor versus normal tissue reflected the degree of cell differentiation [49]. The authors introduced a novel bead-based flow cytometric miRNA profiling method taking advantage of Luminex xMAP technology where up to 100 distinct

sets of color-codes beads can be utilised. Each bead set is coated with a reagent specific to a particular bioassay, allowing the capture and detection of specific analytes from a sample. Within the Luminex compact analyser, lasers excite the internal dyes that identify each microsphere particle and also any reporter dye captured during the assay. Many readings are made on each bead set, further validating the results. This method applied to miRNA, couples oligonucleotides that are complementary to appropriate miRNAs onto beads. Purified miRNAs from cell or tissue samples are hybridised to the oligo-bound beads. Bead-based hybridisation has the theoretical advantage that it might more closely approximate hybridisation in solution, and as such, the specificity could be expected to be superior to chip microarray hybridisation. This multiplex method also set the stage for future protein/nucleic acid co-detection (http://www.luminexcorp.com/technology/index.html). Hence this technology together with novel antibodies and various specific biomarkers panel such as cancers, cellular signalling, cytokines, chemokines, growth factors, endocrines and metabolic markers, represents a powerful complete solution for 'in-depth' studies on various cancers and other diseases.

4. Proteomics in cancer research

Despite better understanding of genomic aberrations of cancer cells and advances in characterising diversity of cancer phenotypes via transcriptomics, it is obvious that proteomics deserves attention in cancer research. Compared to genomic and transcriptomic classifiers, proteomic features appear to be more realistic platforms for identification of cancer-related alterations in molecules and signalling pathways and could therefore significantly contribute to our understanding of cancerogenic developments. There are several major reasons why one should focus on cancer proteomes: (i) there is generally a poor correlation between transcriptional levels of many genes and relative abundances of corresponding proteins; (ii) due to differential splicing and translation each gene may encode several different protein variants with different properties; (iii) the key proteins driving malignant behavior of cancer cells can undergo post-translational modifications including phosphorylation and glycosylation; and (iv) proteomes are capable of monitoring dynamic changes, hence they can be used to follow up the course of the disease and any response to drug therapy. However, comprehensive studies on cancer proteomes present an important challenge and involvement of (i) extreme heterogeneity of tissue cell populations which are part of the cancer itself or host response to developing malignancy; (ii) broad dynamic range of protein abundances in proximal body fluids and serum/blood plasma which present a rich source for biomarker identification; and (iii) the need for validation of molecular changes in independent cohort of cancer patients using independent techniques and functional assays. With these aspects in mind, applications of proteomics to cancer research require careful consideration of currently available or emerging novel proteomic technologies in order to provide results that can be relevant for biological and functional interpretation. More importantly, to move forward in the fight against cancers, the proteomic findings need to be successfully translated into clinical oncology [50].

A variety of approaches that can be utilised in cancer proteomics require proper sample preparation including sample-enrichment strategies focused on subcellular or organelle fractionations, phosphoproteins and glycoproteins, specific protein tagging or tissue micro-dissection. Following proteomic analyses of cancer tissues, cells and/or body fluids are subjected to global profiling and/or comparative functional analysis. Protein separation-based approaches most frequently explore gel-based techniques (1-D and 2-D gel electrophoresis), however, gel-free liquid phase chromatographic approaches (2-D HPLC) offer some advantages and provide results complementary to gel-based fractionation [51]. The major bottleneck of classical 2-DE based approach suffers from very low dynamic range of quantification using various staining procedures and only moderate reproducibility. The use of fluorescence protein labelling and running the mixture of two different samples in one gel known as difference in gel electrophoresis (DIGE) technique has provided researchers with improved tool to look closer at the biomarkers of interest but did not completely solve the problems associated with gel-based techniques as well as protein sample complexity or high dynamic range of protein abundances in contrast to rather low dynamic range of protein detection and quantification [52].

Mass spectrometry (MS) now permits the identification of many proteins with high sensitivity that is mostly dependent on ionisation efficiency of a given peptide. Sensitivity is high for purified peptides whilst it decreases with the complexity of the samples. Thus, the quality of protein fractionation has high impact on protein identification coverage – in complex protein mixtures it is difficult to detect low abundant peptides/proteins in the presence of highly abundant ones. This situation is typical for many body fluids and tissues as well as detection of post-translationally modified peptides in the presence of unmodified counterparts. At this stage, mass spectrometry is not quantitative but allows relative comparison between same peptides/proteins in a set of different samples. MALDI-TOF (matrix assisted laser desorption ionisation-time-of-flight) is now routinely used for the identification of proteins. The SELDI (surface enhanced laser desorption ionisation) with TOF mass spectrometer combines effective sample prefractionation based on capturing different types of proteins such as hydrophobic, hydrophilic, ionic, ligands, antibodies and others on selective types of surfaces with mass analysis. This chip-based procedure is a relatively straightforward technology that is easily applicable in the clinical environment. The limitation has been the low mass accuracy which cannot be used for assignment of protein/peptide identifications.

Hence, a need for newer technologies was highlighted for progress in the field of cancer biomarker discovery. Modern mass spectrometry-based quantification methods have gained popularity over the last 5 years. The determination of protein abundances in samples is performed using stable isotope labelling techniques including stable isotope labelling by amino acids in cell culture (SILAC) or isotope-coded protein labels (ICPL) prior protein fractionation. In addition, an improved approach using amine-reactive isobaric tags for relative and absolute quantitation (iTRAQ) has been developed with potential usefulness. This technique is based on chemically tagging the N-terminus of peptides generated from protein digests that have been isolated for instance from cells cultured under different experimental conditions or other biological materials [53,54]. A specific way to introduce isotope label into peptide is the use of trypsin-catalysed incorporation of ^{18}O during protein digestion. The incorporated labels create specific mass tags that can be recognised by mass spectrometry and at the same time provide the basis for quantification. Unlike relative quantification, absolute quantification (AQUA) can be achieved using internal standard by adding known quantity of stable isotope-labeled standard proteotypic peptide to a protein digest and subsequent comparison of mass spectrometric signals of standard labeled peptide and corresponding endogenous peptide in digest. The specific modification of AQUA is a method called multiple reaction monitoring (MRM) in which the mass spectrometer monitors not only intact peptide mass but also one or more specific fragmentations of those peptides. The combination of retention time, peptide mass and fragment mass eliminates ambiguities in peptide assignment and allows for higher range of quantification. Also, targeted fragmentation of selected ions allows parallel quantification of hundreds of candidate genes in the sample in very short period of

time. Development of hybrid methods coupling MRM assay with protein enrichment by immuno-depletion or enrichment of the peptides by antibody capture and further improvements may be capable of extending MRM method to full dynamic range of plasma proteins. With this view in mind, MRM measurement of plasma peptide may provide a rapid and specific assay platform for high throughput biomarker validation [55,56].

Due to problems posed by isotope labelling methods such as removal of contaminating reagents, sample loss, costs and reproducibility, label-free methodologies for quantitation were introduced. One of the label-free method is the protein microarray methodology. Each array can contain hundreds or thousands of immobilised proteins or antibodies, where the specificity of the protein or antibody, respectively, is crucial [57]. Microarrays are versatile tools for examining large number of samples for biomarkers studies in various environments such as drug development and clinical trials. Protein and tissue microarray technologies provide a high-throughput platform for protein expression investigations including tissue sections, thus allowing analysis of several hundreds of samples simultaneously (Fig. 1). Moreover, the advent of digital slide technology has afforded an unparalleled opportunity for archiving valuable histopathological and immunohistochemical specimens. Such digital images offer a unique opportunity to provide a paradigm shift in relation to interpretation of such data via the use of automated image analysis algorithms [58,59].

Currently, proteomic analyses have been extended to whole tissue sections by using MALDI imaging. This approach allows detection of proteins in situ in the tissue sections and analysis of their spatial distribution. Each MALDI imaging data set containing large number of mass spectra may be evaluated using hierarchical clustering that is helpful in classification and interpretation of complex human tissue [60].

Recently, direct tissue proteomic approach, which represents modified shotgun proteomic tool enabling identification of proteins by micro-reverse phase LC–MS/MS isolated from FFPE tissue was introduced [61]. The successful application of direct tissue proteomics needs improved extraction protocols from FFPE tissue samples, but it offers retrospective investigation of biomarkers in well characterised clinical samples. The combination of this technology with laser-capture micro-dissection is expected to facilitate mapping of global signalling networks, which would be a powerful and more informative than individual markers in diagnostics, disease prognosis and tailored cancer therapy.

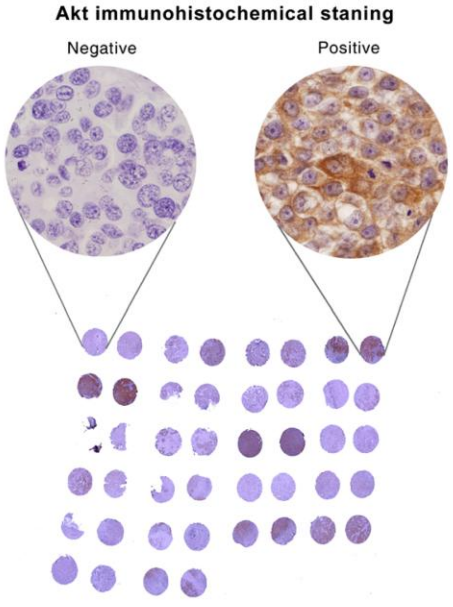

Fig. 1. Biomarker validation in tissue microarrays, example of pan anti-Akt kinase staining using primary rabbit polyclonal antibodies (11E7, Cell Signaling, USA).

5. Contribution to cancer biomarkers development

The application of a wide range of proteomic methods to the discovery of new cancer protein biomarkers would help to identify early markers of disease as well as help with prognosis, prediction and monitoring of patient response to a particular therapeutic intervention (Table 1). Such markers of disease could be released directly by cancer cells or may represent a part of host's response to malignancy. These types of diagnostic candidates could be expected to be detected in body fluids and hence detection is vitally important. The cellular proteins are often shed into extracellular fluids including tissue interstitial fluids and blood plasma. Whilst tissue interstitial fluids are in direct contact with tissue/cells via transfer of molecules, the composition of blood plasma results from the communication with tissue interstitial fluids. On the other hand, the blood plasma influences the composition of other body fluids. It is important to realise that relative concentration of biomarkers is highest in tissue interstitial fluids, which in turn drain into lymph and lymph vessels from different tissues finally merging and draining into the blood. As a result, the final concentration of biomarkers in blood would be significantly lower compared to interstitial fluids. Hence, various body fluids represent more or less enriched source of biomarkers [62]. Application of SELDI-TOF in the analysis of serum in a variety of cancers has been most frequently used [63]. In order to develop a new workflow for biomarker candidate identification, Lopez et al. [64] evaluated high-throughput carrier protein-bound affinity enrichment of serum samples coupled with high-resolution MALDI orthogonal TOF-MS, discriminant analysis of the resulting mass spectral patterns, and sequence identification of the discriminating ions to search for putative early protein/peptide biomarkers in ovarian cancer serum samples. This approach yielded a number of discriminating peptides, and provided three marker sets (9, 4, and 7 markers) that enabled classification of samples from cancer patients and healthy controls. Peptide fragments associated with the coagulation cascade provided the highest classification power. Among other candidates were identified lower intensity peptides corresponding to casein kinase 2, transgelin, keratin 2, glycosyl transferase (LARGE), and diamino oxidase. The sets of the discriminating carrier-protein bound fragments differentiated samples from patients with ovarian cancer and from apparently healthy controls with sensitivities and specificities of up to 93% and 97%, respectively. Using various proteomic approaches, the quest for cancer biomarkers in plasma is currently underway for particular cancers including breast, melanoma, lung, and pancreatic [65,66]. Among different proteomic technologies, serum glycomics approach is very attractive because the glycosylation of proteins is known to change in tumor cells during the development of cancer and these glycosylation changes correlate with increasing tumor burden and poor prognosis. Whilst currently used antibody-based immunochemical tests for cancer biomarkers of ovarian (CA125), breast (CA27.29 or CA15-3), pancreatic, gastric, and colonic (CA19-9) carcinomas target highly glycosylated mucin proteins, recent developments in MALDI-Fourier transformation-ion cyclotron resonance (FT-ICR) MS have allowed more detailed analysis of free glycan species resulting in glycan profiles containing distinct glycan features that may correspond to glycan "signatures of cancer" [67,68]. However, to further enhance the research progress it is essential to overcome limitations

Table 1
Proteomic technologies advancing cancer biomarker research.

Methodologies	Technology type with abbreviation	Research applications and usefulness	Cancer research area	Ref.
Gel-based methods	2-D-DIGE	Diagnostic biomarkers	Colorectal cancer	[87]
			Pancreatic adenocarcinoma	[88]
			Non-small-cell lung cancer	[89]
		Diagnostic and prognostic biomarkers	Bone and soft-tissue sarcoma	[90]
			Bladder cancer	[91]
		Screening of resistance biomarkers	Ovarian cancer	[92,93]
		Prognostic biomarkers	Hepatocellular carcinoma	[94]
			Lung adenocarcinoma	[95]
	2-D-PAGE	Diagnostic biomarkers	Papillary thyroid cancer	[96]
		Prognostic biomarkers	Gastrointestinal stromal tumor	[71]
Mass spectrometry-based methods – with isotope labeling	iTRAQ-2-D-LC-MS/MS	Prognostic biomarkers involved in metastatic processes	Breast cancer	[97]
		Diagnostic and prognostic biomarkers	Prostate cancer	[98]
		Diagnostic biomarkers	Head and neck spinocellular carcinoma	[99]
			Hepatocellular carcinoma	[100]
	ICAT-MS/MS	Diagnostic biomarkers in pancreatic juice	Pancreatic cancer	[101]
	SILAC-LTQ-FT-MS/MS	Diagnostic biomarkers	Hepatocellular carcinoma	[102]
	SILAC-LC-MS/MS	Diagnostic biomarkers	Pancreatic cancer	[103]
	^{18}O labeling MS	Diagnostic biomarkers	Cholangiocarcinoma	[104]
	$^{12}C6$- or $^{13}C6$-NBS labeling followed by MALDI-QIT-TOF	Diagnostic glycoprotein biomarkers in patient serum	Lung adenocarcinoma	[105]
Mass spectrometry-based methods - label-free	LC–MS/MS and MRM	Diagnostic biomarkers	Mouse model of breast cancer	[106]
	1-D-LC/MS/MS	Diagnostic biomarkers	Non-small-cell lung cancer	[107]
	LC–MS based	Prognostic biomarkers	FFPE archival melanoma tissues	[108]
	SELDI-TOF-MS	Diagnostic biomarkers in patient serum (mostly distinguish cancer patients from healthy individuals)	Laryngeal squamous cell carcinoma	[109]
			Lung cancer	[110]
			Gastric cancer	[111]
			Classifications of chronic hepatitis B, liver cirrhosis and hepatocellular carcinoma	[112]
			Renal cell carcinoma	[113]
		Diagnostic biomarkers in pancreatic juice	Malignant intraductal papillary mucinous neoplasm	[114]
		Diagnostic biomarkers in tissues	Renal cell carcinoma	[115]
		Biomarkers for prediction of clinical responsiveness to treatment	TRAIL and etoposide treated breast cancer and non-transformed cells	[116]
	MALDI imaging	Diagnostic biomarkers	Prostate cancer development	[117]
			Prostate cancer	[118]
Array-based methods	Antibody arrays	Diagnostic biomarkers	Esophageal adenocarcinoma	[119]
			Microarrays designed to detect circulating auto-antibodies against 51 tumor-associated antigens	
			Helicobacter pylori infection and gastric adenocarcinoma	[120]
			Ovarian cancer	[73]
		Diagnosis and prediction of therapy response	Bladder cancer	[121]
		Biomarkers monitoring therapeutic response	Her-2 (erbB-2) oncogene-dependent breast cancer	[122]
	Lectin glycoarrays	Diagnostic biomarkers	Colorectal cancer	[67]
	Tissue arrays	Prognostic significance	AQUA to analyze tumor-specific expression of vascular endothelial growth factor, VEGFR-1, VEGFR-2, and neuropilin-1 in breast cancer	[123]
			Use of combined biomarkers of oncogenic HPV and tumor suppressors of p53, pRb, and p21 in advanced TSCC provides prognostic molecular classification.	[124]
			E2-inducible histone variant H2A.Z, is significantly associated with lymph node metastasis and decreased breast cancer survival	[125]
Fluorescent-coded bead-based methods	Luminex®xMAP® technology	Diagnostic applications in clinical labs. Technology allows multi-analyte profiling with the ability to build internal controls into the various assays and offers multi-format and multiplexing capabilities for identifying either genetic or protein-based markers	Search for cancer markers in various cancers, offering great sensitivity to traditional ELISA-based systems, but with additional advantages including extended dynamic range and smaller sample size	[126]

Above are some examples of very recent studies utilising various proteomic technologies. More studies are recorded on Pubmed database – www.ncbi.nlm.nih.gov/pubmed/).

Table 2
Examples of most recent studies focused on response to anti-cancer treatment.

Anti-cancer agents	Methods	Cell lines	Up-regulated proteins	Down-regulated proteins	Ref.
Alkaloids					
Etoposide + TRAIL	SELDI-TOF-MS	MDA-MB231, ZR-75-1 and MCF-10A		Protein S100A6, ubiquitin	[116]
Vincristine	2-D-MALDI/TOF-MS	MCF-7	Heat shock 27 kDa protein	Heat shock 27 kDa protein	[80]
Vincristine	2-D-MALDI/TOF-MS	CEM	Class I β-tubulin, Actin (fragments), lamin B1	UV excision repair protein RAD23 homolog B, 40S ribosomal protein SA, heterogeneous nuclear ribonucleoprotein K, heterogeneous nuclear ribonucleoprotein F, p59 protein, ADP sugar pyrophosphatase, 14-3-3β, 14-3-3ε and 14-3-3τ protein, translationally-controlled tumor protein, L-plastin, lamin B1, 26S proteasome, α-tubulin 1, α-tubulin 4	[127]
Alkylating agents					
Temozolomid	2-D-LC/MS	U87-MG	Vimentin, RhoA	47-kDa mannose 6-phosphate receptor-binding protein	[77]
Anti-cancer antibiotics					
Daunorubicin	2-D-MALDI/TOF-MS	EPP85-181P		T-complex protein subunit α, transfer RNA-Trp-synthetase, T-complex protein subunit β, cytokeratin19, cytokeratin7, elongation factor 1χ, heterogeneous nuclear ribonucleoprotein, erythrocyte cytosolic protein of 51 kDa, differentiation-related gene product, heat shock protein 60, glucose regulated protein of 78 kDa Grp 78, heat shock 27 kDa protein	[78]
Doxorubicine	2-D-MALDI/TOF-MS	MCF-7	Macrophage migration inhibitory factor	heat shock 27 kDa protein	[79]
Antimetabolites					
5-Fluorouracil	2-D-MALDI/TOF-MS	HeLa	Glutathione-S-transferase, MAP kinase 13, amino-methyltransferase, eukaryotic translation initiation factor 3 subunit 3 and 4H, protein kinase C inhibitor protein-1, heterogeneous nuclear ribonucleoproteins C1/C2, homeobox protein BarH-like 2, ubiquitously expressed transcript protein, cell death activator CIDE-B, NADH-ubiquinone oxidoreductase, PDGF-associated protein, serine–threonine protein phosphatase 2B catalytic subunit, adenosylsuccinate synthase, acyl-CoA dehydrogenase, telomeric repeat-binding factor 2, histone H1.3, cation-dependent mannose-6-phosphate receptor, Apo- 1/CD 95 (Fas), caspase-3, caspase-8, and NADP-dependent leukotriene B4 12-hydroxy dehydrogenase	Mitotic checkpoint protein BUB3, 60S ribosomal protein L3, nuclear ubiquitous casein and cyclin-dependent kinase substrate, cytohesin 3, myc proto-oncogene protein, endoplasmic reticulum protein ERp29 precursor, translation initiation factor eIF-2B, D-β-hydroxybutyrate dehydrogenase, protocadherin α 5 precursor, snRNA-activating protein complex 43-kDa subunit, Src substrate cortactin, transforming protein P21A	[128]
5-Fluorouracil + Cisplatin	2-D-MALDI/TOF-MS	HeLa	Cullin homolog 4B, pre-mRNA-splicing factor PRP17 (cell division cycle 40 homolog), engulfment and cell motility protein 2, RAC-beta serine/threonine protein kinase, TRAF family-associated NF-jB I-activator, G-substrate, peptidyl-prolyl cis–trans isomerase E, synaptosomalassociated protein 29, glutathione-s-transferase, mitogen-activated protein kinase 13, amino-methyltransferase, eukaryotic translation initiation factor 3 subunit 3, eukaryotic translation initiation factor 4H, protein kinase C inhibitor protein-1, heterogeneous nuclear ribonucleoproteins C1/C2, homeobox protein BarH-like 2, UXT protein, cell death activator CIDE-B, NADH–ubiquinone oxidoreductase 42-kDa subunit, NADP-dependent leukotriene B4 12-hydroxy dehydrogenase, PDGF-associated protein, serine–threonine protein phosphatase 2B catalytic subunit, adenylosuccinate synthetase, acyl-coA dehydrogenase and telomeric repeat-binding factor 2	Regulator of G-protein signaling 13, ubiquitin carboxyl-terminal hydrolase 14, mitotic spindle assembly checkpoint protein MAD2B, 60S ribosomal protein L3, mitotic checkpoint protein BUB3, nuclear ubiquitous casein and cyclin-dependent kinase substrate, cytohesin 3 (ARF nucleotide-binding site opener 3), translation initiation factor eIF-2B b subunit, myc proto-oncogene protein, protocadherin a-5 precursor, snRNA-activating protein complex 43-kDa subunit, D-b-hydroxybutyrate dehydrogenase, endoplasmic reticulum protein ERp29 precursor, squamous cell carcinoma antigen 2 (leupin), src substrate cortactin (oncogene EMS1), and transforming protein P21A (c-K-ras).	[129]
Others:					
Cisplatin	2-D-MALDI/TOF-MS	HeLa	G-substrate, NADPH: nicotinamide adenine dinucleotide phosphate-dependent carbonyl reductase 3, serine/threonine/tyrosine interacting protein, cytochrome P450 4A11 precursor, regulator of G-protein signaling 13, TRAF-interacting protein, zinc finger protein 90, peptidyl-prolyl cis–trans isomerase E, heterogeneous nuclear ribonucleoprotein A1, partitioning defective-6 homolog a, prothrombin precursor, and cyclin-dependent kinase inhibitor p27 (p27Kip1)	Tumor necrosis factor α-induced protein 3, myc proto-oncogene, ubiquitin carboxyl-terminal hydrolase 14, potassium voltage-gated channel subfamily G member 1 aldose reductase, mitotic spindle assembly checkpoint protein MAD2B, Rho guanine nucleotide exchange factor 6, aldose reductase, proliferating cell nuclear antigen, and mitochondrial processing peptidase α subunit	[130]

(*continued on next page*)

Table 2 (*continued*)

Anti-cancer agents	Methods	Cell lines	Up-regulated proteins	Down-regulated proteins	Ref.
Cisplatin	SILAC-SDS/PAGE-MALDI/TOF-MS	Jurkat T cells	Actin, adenine phosphoribosyltransferase, elongation factor 2, eukaryotic initiation factor 4A-I, microsomal signal peptidase 25 kDa, p21-Rac2, peroxiredoxin 1, phosphomevalonate kinase, pre mRNA splicing factor SRp30C, RNA-binding protein 4, tetratricopeptide repeat domain 9C, transmembrane protein 33, tubulin α-ubiquitous chain, tubulin β	Core-binding factor beta subunit, heterogeneous nuclear ribonucleoprotein G, heterogeneous nuclear ribonucleoprotein K, heterogeneous nuclear ribonucleoprotein I, heterogeneous nuclear ribonucleoprotein H, heterogeneous nuclear ribonucleoproteins A2/B1, interleukin enhancer binding factor 2, lamina-associated polypeptide 2 isoforms β/χ, 54 kDa nuclear RNA- and DNA-binding protein, probable rRNA processing protein EBP2, Rho GDP-dissociation inhibitor 2, spectrin α chain	[83]
Cisplatin	2-D-MALDI/TOF-MS	A431	14-3-3 ξ/δ and ε, heat shock cognate 71 kDa protein, tropomyosin α 3 and 4 chain, F-actin capping protein, actin, microtubule associated protein RP/EB1, annexin V, proteasome activator complex, 60 kDa heat shock protein	Calmodulin, heat shock cognate 71 kDa protein, protein disulfide isomerase A3, stathmin, peroxiredoxin, peptidyl-prolyl cis–trans isomerase	[131]
Bohemine	2-D-MALDI/TOF-MS-ESI-MS/MS	CEM		α Enolase, triosephosphate isomerase, eucaryotic initiation factor 5A, α and β subunits of Rho GDP-dissociation inhibitor 1	[85]
Bohemine	2-D-MALDI/TOF-MS	A549	α-enolase, phosphoglycerate mutase, triosephosphate isomerase, annexin I, annexin IV, actin, cytoplasmic 1, PDZ and LIM domain protein I, endoplasmic reticulum protein disulfide isomerase A3 (ER60), 60 kDa heat shock protein, mitochondrial	Glucose-6-phosphate 1-dehydrogenase G6PD, isomerase A3	[84]
Bohemine	LC-PF2D-MALDI/TOF-MS	CEM	60 kDa heat shock protein	crk-like protein, Histone H3.3, nuclease sensitive element binding protein 1, Histone H2B.a,	[51]
Trichostatin A	2-D-MALDI/TOF-MS	PaCa44	Programmed cell death protein (TFAR19), stathmin, chromatin assembly factor 1 subunit C, growth factor receptor bound protein 2, cytochrome c oxidase polypeptide Vb, ARP2/3 complex 16 kDa subunit, programmed cell death protein 5, peroxiredoxin 1, UEV protein (ubiquitin conjugating E2 enzyme variant), thioredoxin, hint protein, deduced protein product shows significant homology to coactosin	Nucleophosmin, translationally-controlled tumor protein, 60 kDa heat shock protein, Tropomyosin α 4 chain, calreticulin precursor, tropomyosin α 3 chain, heterogeneous nuclear ribonucleoproteins A2/B1, glyceraldehyde 3-phosphate dehydrogenase, ATP synthase beta-chain, 60S acidic ribosomal protein PO	[132]
Gemcitabine + Trichostatin A	2-D-PAGE-MALDI/TOF and Q/TOF-MS	T3M4			[133]
Trichostatin A			S100A11 protein, peroxiredoxin I, guanine nucleotide-binding protein β subunit-like protein	Stress 70 protein mitochondrial	
Gemcitabine			S100A11 protein, peroxiredoxin I	Stress 70 protein mitochondrial, tubulin β chain	
Trichostatin A + Gemcitabine			Peroxiredoxin I, superoxide dismutase, thioredoxin, glutathione-S-transferase, 14-3-3 protein α, stathmin	heat shock protein HSP 90-alpha, stress 70 protein mitochondrial, cytokeratin type II CK8	

associated with serum protein profiling or quantification and improve knowledge about cancer tissue and its secretome.

The identification of new diagnostic or prognostic biomarkers characterising risk of cancer development and/or tumor progression or drug targets is mostly based on direct analysis of cancer cells and tissues and often utilises some of the above described proteomic methods. Large-scale proteomic analysis of 64 human ovarian cancer tissue samples presenting benign, borderline and malignant stages based on histological evaluation was performed using DIGE with each sample run in duplicate. Evaluation of protein quantitative data using non-supervised clustering distinguished between normal and malignant tissue samples, however, application of supervised methods allowed objective classification into four groups – normal ovaries, benign, borderline and malignant. Additionally, protein spot changes significantly contributing to this classification were reported to represent potential diagnostic tumor markers. Among those candidates, cytokeratin 19-type1, ErbB3, prohibitin, adenylosuccinate lyase and integrin alpha-5 were verified via tissue microarrays and others are currently under development to be tested for diagnostic purposes in tissue as well as blood samples [69]. Application of DIGE with large format of 2-D electrophoretic separation for laser microdissected tissue was utilised by group of Kondo [70] to investigate proteomic signatures of several types of malignancies including lung, pancreatic, colorectal, hepatocellular and cholangiocellular carcinomas, malignant mesotheliomas and soft-tissue sarcomas. Interestingly, they identified 43 protein spots whose intensity was statistically different between gastrointestinal stromal tumor (GIST) with good and poor prognosis. Mass spectrometric protein identification showed eight of the 43 spots derived from pfetin, a potassium channel protein, and four of the eight pfetin spots had a high discriminative power between the two groups. Western blotting and real-time PCR showed that pfetin expression and tumor metastasis were inversely related. The prognostic performance of pfetin was also examined by immunohistochemistry on 210 GIST cases. The 5-year metastasis-free survival rate was 93.9% versus 36.2% for patients with pfetin-positive versus pfetin-negative tumors, respectively ($P < 0.0001$). Univariate and multivariate analyses revealed that pfetin expression was a powerful prognostic factor among the clinicopathologic variables examined, including risk classification and c-kit- or platelet-derived growth factor receptor A mutation status. These results may also provide novel therapeutic strategies to prevent metastasis of GIST [71].

To obtain new insight into cancer cell invasion and migration, multidimensional protein identification technology (MudPIT) has been used in six established ovarian cancer cell lines. Within whole cell extracts MudPIT identified proteins that mapped to 2245 unique genes. Unsupervised cluster analysis partitioned the cell lines in a manner that reflected their motile/invasive capacity. A compar-

ison of protein expression profiles between cell lines of high versus low motile/invasive capacity revealed 300 proteins that were differentially expressed, of which 196 proteins were significantly up-regulated in group with high invasive capacity. Western blot analysis for selected proteins confirmed the expression profiles revealed by MudPIT, demonstrating the fidelity of this high-throughput analysis. Protein network modeling indicated a functional interplay between proteins up-regulated in group of high motile/invasive capacity cell lines characterised and increased expression of several key members of the actin cytoskeleton, extracellular matrix and focal adhesion pathways. These proteomic expression profiles could prove to be essential in the development of more effective strategies that target pivotal cell signalling pathways used by cancer cells during local invasion and distant metastasis [72].

Many cancer patients produce antibodies against tumor-associated antigens. The humoral immune response represents a form of biological amplification of signals that are otherwise weak because of very low concentrations of antigen, especially in the early stages. Hence, it is interesting to employ protein microarrays to identify these antigens. In one typical study, protein microarrays containing 5005 human proteins and auto-antibodies from 30 cancer patients were used to identify proteins that are aberrantly expressed in ovarian tissue. The differential reactivity of four antigens was tested by using immunoblot analysis and tissue microarrays. Lamin A/C, structure specific recognition protein 1 (SSRP1), and Ral binding protein 1 (RALBP1) were found to exhibit increased expression in the cancer tissue relative to controls. The combined signals from multiple antigens proved to be a robust test to identify malignant ovarian tissue and proteins aberrantly expressed in different disease states [73].

6. Focus on prediction of efficacy and monitoring of anti-cancer therapies

Clinical importance of biomarkers suitable for monitoring therapeutic response is of growing importance. Assessment of an individual patient and tumor predisposition to drugs is prerequisite to successful application of targeted anti-cancer therapy. This approach is needed namely for clinicians to stratify the patients and make proper decision about chemotherapeutic drugs that would be most effective and with minimal side effects. It is expected that proteomic profiling will help to answer the questions of tumor drug sensitivity/resistance and knowledge of molecular mechanisms that underly cancer drug response would significantly contribute to achieving this aim. In order to predict cancer drug response by proteomic profiling, Ma et al. [74] used reverse-phase protein microarrays covering 60 human cancer cell lines (NCI-60 panel) to measure protein expression levels by 52 antibodies. The specificity of each of the antibodies was verified by Western blotting. The NCI-60 panel contains 2–9 cell lines per each histological tumor type including leukemias, melanomas, and carcinomas of ovaries, renal, breast, prostate, colon, lung and central nervous system [75]. The drug activities of 118 agents were measured by growth inhibition within 48 h. In order to establish the classifiers that would be independent of tissue of origin, a combination of several algorithms were used. The results showed that it was feasible to used this data set (60 cell lines $\times$ 52 targets $\times$ 118 drugs) to generate significant chemosensitivity classifiers for 118 evaluated agents with statistical significance level $P < 0.02$. The range of drug responses was classified into three categories: sensitive, resistant and intermediate. It is important to stress, that this type of proteomic studies are focused on prediction of response without any analyses of molecular mechanisms underlying response to the drug.

The era of chemotherapy began in 1940s with the first uses of nitrogen mustards, which are nonspecific DNA alkylating agents, and later antifolates. In the early 1950s other anti-tumor drugs like anti-metabolites and vinca alkaloids came into clinical trials and use. In 1955 began systematic drug screening at the National Cancer Institute and new screening approach based on use of 60 cell lines derived from different human cancer types was introduced in 1989 [76]. The following are examples of several recent studies focused on more detail proteomic analyses of response to selected conventional chemotherapeutic drugs. The effect of alkylating agent temozolomide alone or in combination with radiotherapy on the protein expression profile of human U87-MG glioma cells in vitro was investigated by Trog et al. [77]. Using comparative analysis of protein expression pattern they found upregulation of vimentin, an extracellular matrix component, induced by temozolomide treatment. Interestingly, vimentin contributes to the mechanism of tumor progression supporting its pro-invasive and pro-angiogenic activity. Hence, potential molecular target, which in fact contributes to expansion of the cancer is promoted by treated glioma cells. This finding demonstrates usefulness of proteomic studies for uncovering possible mechanisms that interfere with successful therapy. Anti-cancer antibiotics are known to cause DNA damage (intercalation into DNA bases, interference with DNA unwinding via inhibition of topoisomerases I and/or II) and to affect tumor cell growth. 2-D gel electrophoresis was used to investigate the response of pancreatic tumor cells after exposure to daunorubicin. Identified up-regulated proteins after drug exposure participate in a variety of cellular processes probably due to activation of various signalling pathways in response to daunorubicin [78]. Human breast tumor cell line MCF-7 was used to investigate protein profile changes after doxorubicin treatment. Three isoforms of heat shock 27 kDa protein (HSP27) were found to be significantly decreased [79]. Interestingly, in investigation performed by Casado et al. [80] cellular response to plant vinca alkaloid vincristine on MCF7 cells also revealed vincristine dependent regulation of specific isoforms of anti-apoptotic protein HSP27. Since there was no effect on HSP27 mRNA they suggested that vincristine was implicated in the protein post-translational modification with up-regulation of Ser 82 phosphorylation. However, such data should be interpreted carefully, as HSP27 is highly abundant protein and it is one of the most frequently responsive protein molecules in human samples [81].

The use of combination of conventional chemotherapeutic agent vinblastine with targeted agent rapamycin (mTOR inhibitor) was studied at the protein level on the EA.hy926 endothelial cell line using 2-D gel electrophoresis coupled to MALDI mass spectrometry protein identification. Some of the regulated proteins were involved in the processes of angiogenesis, proliferation, migration and apoptosis. The authors verified proteomic data for several proteins using Western blots and also applied the computer modelling for generating a network of molecules that have common function and share similar target pathways to show that observed protein changes merged into synergistic antiangiogenic activity of vinblastine and rapamycin [82]. Platinum cytostatics belong to the group of potent and clinically important metal-based anti-cancer drugs. One of the most recent studies concerning molecular effects of cisplatin on cancer cells was published by Schmidt et al. [83]. The authors performed quantitative analysis of protein changes after cisplatin-induced apoptosis in Jurkat T cells to identify proteins related to the mechanism of cisplatin function. SILAC was used for quantitative proteome analysis of control versus apoptotic cells after cisplatin treatment. The time point for full activation of apoptosis was chosen for experiments. It was interesting that 8 of 26 identified apoptosis-related proteins contained at least one RNA-binding motif.

In our studies we considered selective cyclin-dependent kinase inhibitor (CDKI) as a promising anti-cancer drug. We applied complementary proteomic approaches to analyse responses of CEM T-lymphoblastic leukemia and A549 lung adenocarcinoma lines as representatives of haematological malignancy and solid tumor, respectively. Based on the evaluation of the protein maps and possible pathways relevant to responses to CDKI, the glycolytic enzymes, annexin IV and the crkl adaptor protein appear to be important targets. Collectively, our proteomic findings underline the importance of cell cycle control in both the cellular signaling and metabolic pathways. Initial confirmation studies focused directly on the crkl protein have proved the validity of the proteomic results, but the potential utility of CDKI warrants further study and validation using different types of tumor models [51,84,85].

The analysis of known cell signalling networks or pathways for a patient can be currently obtained from a biopsy specimen of given individual using reverse-phase protein microarrays. In this approach, the entire cellular proteome is immobilised and subsequent immunodetection reveals phosphorylation status of signalling proteins. Therefore it is suitable for monitoring of multiple pharmacodynamic biomarkers of response to molecular targeted agents. Boyd et al. [86] applied this protocol to examine phosphorylation status of 100 proteins in a panel of 30 breast cancer cell lines and showed distinct pathways activation in different subtypes that were not obvious from previous gene expression studies. It was shown that inhibitors of epidermal growth factor receptor and mitogen-activated protein kinase/extracellular signal-regulated kinase result in compensatory up-regulation of the phosphatidylinositol-3-kinase/Akt signalling pathway indicating that combined inhibition of both pathways should translate into synergistic tumor killing.

Many of the above mentioned studies were followed up at various time interval when apoptotic process occur. However, more interesting and specific would be the characterisation of earlier protein changes that precede the on-set of apoptosis. More studies on the molecular mechanisms underlying the effect of individual conventional, targeted and developmental chemotherapeutics, or their combinations are urgently needed. In fact, the number of publications covering this issue is low (Table 2). Furthermore, monitoring molecular mechanisms in earlier time intervals after drug exposure may be beneficial for detecting relevant proteins that are responsible for primary changes in signalling networks and subsequently lead later to irreversible anti-cancer processes including cell division cycle block, induction of apoptosis, and interference with cancer-related angiogenesis, invasion and metastasis.

Acknowledgements

We acknowledge support of grants from the Czech Ministry of School and Education (MSM6198959216 and LC07017) and Institutional Research Concept AV0Z50450515.

References

[1] Skvortsov, S., Skvortsova, I., Stasyk, T., Schiefermeier, N., Neher, A., Gunkel, A.R., Bonn, G.K., Huber, L.A., Lukas, P., Pleiman, C.M. and Zwierzina, H. (2007) Antitumor activity of CTFB, a novel anticancer agent, is associated with the down-regulation of nuclear factor-kappaB expression and proteasome activation in head and neck squamous carcinoma cell lines. Mol. Cancer Ther. 6, 1898–1908.
[2] Skvortsova, I., Skvortsov, S., Stasyk, T., Raju, U., Popper, B.A., Schiestl, B., von Guggenberg, E., Neher, A., Bonn, G.K., Huber, L.A. and Lukas, P. (2008) Intracellular signaling pathways regulating radioresistance of human prostate carcinoma cells. Proteomics 8, 4521–4533.
[3] Huang, W., Yu, L.F., Zhong, J., Wu, W., Zhu, J.Y., Jiang, F.X., and Wu, Y.L. (2008) Stat3 is involved in angiotensin ii-induced expression of MMP2 in gastric cancer cells. Dig. Dis. Sci. (December 11, Epub ahead of print).
[4] Chong, P.K., Lee, H., Kong, J.W., Loh, M.C., Wong, C.H. and Lim, Y.P. (2008) Phosphoproteomics, oncogenic signaling and cancer research. Proteomics 8, 4370–4382.
[5] Sathornsumetee, S., Reardon, D.A., Desjardins, A., Quinn, J.A., Vredenburgh, J.J. and Rich, J.N. (2007) Molecularly targeted therapy for malignant glioma. Cancer 110, 13–24.
[6] Prasad, N.K. (2009) SHIP2 phosphoinositol phosphatase positively regulates EGFR-Akt pathway, CXCR4 expression, and cell migration in MDA-MB-231 breast cancer cells. Int. J. Oncol. 34, 97–105.
[7] Hanahan, D. and Weinberg, R.A. (2000) The hallmarks of cancer. Cell 100, 57–70.
[8] Smith, L.T., Otterson, G.A. and Plass, C. (2007) Unraveling the epigenetic code of cancer for therapy. Trends Genet. 23, 449–456.
[9] Hake, S.B., Xiao, A. and Allis, C.D. (2004) Linking the epigenetic 'language' of covalent histone modifications to cancer. Br. J. Cancer. 90, 761–769.
[10] Pan, L.N., Lu, J. and Huang, B. (2007) HDAC inhibitors: a potential new category of anti-tumor agents. Cell Mol. Immunol. 4, 337–343.
[11] Weissman, I.L., Anderson, D.J. and Gage, F. (2001) Stem and progenitor cells: origins, phenotypes, lineage commitments, and transdifferentiations. Annu. Rev. Cell Dev. Biol. 17, 387–403.
[12] Molofsky, A.V., Pardal, R. and Morrison, S.J. (2004) Diverse mechanisms regulate stem cell self-renewal. Curr. Opin. Cell Biol. 16, 700–707.
[13] Dalerba, P., Cho, R.W. and Clarke, M.F. (2007) Cancer stem cells: models and concepts. Annu. Rev. Med. 58, 267–284.
[14] Zhu, L., Gibson, P., Currle, D.S., Tong, Y., Richardson, R.J., Bayazitov, I.T., Poppleton, H., Zakharenko, S., Ellison, D.W. and Gilbertson, R.J. (2009) Prominin 1 marks intestinal stem cells that are susceptible to neoplastic transformation. Nature 457 (7229), 603–607.
[15] Trumpp, A. and Wiestler, O.D. (2008) Mechanisms of disease: cancer stem cells-targeting the evil twin. Nat. Clin. Pract. Oncol. 5, 337–347.
[16] Bao, S., Wu, Q., Li, Z., Sathornsumetee, S., Wang, H., McLendon, R.E., Hjelmeland, A.B. and Rich, J.N. (2008) Targeting cancer stem cells through L1CAM suppresses glioma growth. Cancer Res. 68, 6043–6048.
[17] Dubrovska, A., Kim, S., Salamone, R.J., Walker, J.R., Maira, S.M., Garcia-Echeverria, C., Schultz, P.G. and Reddy, V.A. (2009) The role of PTEN/Akt/PI3K signaling in the maintenance and viability of prostate cancer stem-like cell populations. Proc. Natl. Acad. Sci. USA 106, 268–273.
[18] Wallin, J.E., Friberg, L.E. and Karlsson, M.O. (2009) A tool for neutrophil guided dose adaptation in chemotherapy. Comput. Meth. Programs Biomed. 93 (3), 283–291.
[19] Longo, R. and Gasparini, G. (2008) Anti-VEGF therapy: the search for clinical biomarkers. Expert Rev. Mol. Diagn. 8, 301–314.
[20] Tortora, G., Ciardiello, F. and Gasparini, G. (2008) Combined targeting of EGFR-dependent and VEGF-dependent pathways: rationale, preclinical studies and clinical applications. Nat. Clin. Pract. Oncol. 5, 521–530.
[21] Sarmiento, R., Bonginelli, P., Cacciamani, F., Salerno, F. and Gasparini, G. (2008) Gastrointestinal stromal tumors (GISTs): from science to targeted therapy. Int. J. Biol. Markers 23, 96–110.
[22] Eyler, C.E., Foo, W.C., LaFiura, K.M., McLendon, R.E., Hjelmeland, A.B. and Rich, J.N. (2008) Brain cancer stem cells display preferential sensitivity to Akt inhibition. Stem Cells 26, 3027–3036.
[23] Gasparini, G., Longo, R., Torino, F., Gattuso, D., Morabito, A. and Toffoli, G. (2006) Is tailored therapy feasible in oncology? Crit. Rev. Oncol. Hematol. 57, 79–101.
[24] Sathornsumetee, S. and Rich, J.N. (2008) Designer therapies for glioblastoma multiforme. Ann. NY Acad. Sci. 1142, 108–132.
[25] Sathornsumetee, S., Rich, J.N. and Reardon, D.A. (2007) Diagnosis and treatment of high-grade astrocytoma. Neurol. Clin. 25, 1111–1139. x.
[26] Longo, R., Torino, F. and Gasparini, G. (2007) Targeted therapy of breast cancer. Curr. Pharm. Des. 13, 497–517.
[27] Gasparini, G., Gion, M., Mariani, L., Papaldo, P., Crivellari, D., Filippelli, G., Morabito, A., Silingardi, V., Torino, F., Spada, A., Zancan, M., De Sio, L., Caputo, A., Cognetti, F., Lambiase, A. and Amadori, D. (2007) Randomized Phase II Trial of weekly paclitaxel alone versus trastuzumab plus weekly paclitaxel as first-line therapy of patients with Her-2 positive advanced breast cancer. Breast Cancer Res. Treat. 101, 355–365.
[28] O'Reilly, M.S. (2002) Targeting multiple biological pathways as a strategy to improve the treatment of cancer. Clin. Cancer Res. 8, 3309–3310.
[29] Hanash, S. (2004) Integrated global profiling of cancer. Nat. Rev. Cancer 4, 638–644.
[30] Pollack, J.R., Sorlie, T., Perou, C.M., Rees, C.A., Jeffrey, S.S., Lonning, P.E., Tibshirani, R., Botstein, D., Borresen-Dale, A.L. and Brown, P.O. (2002) Microarray analysis reveals a major direct role of DNA copy number alteration in the transcriptional program of human breast tumors. Proc. Natl. Acad. Sci. USA 99, 12963–12968.
[31] Wu, R., Lin, L., Beer, D.G., Ellenson, L.H., Lamb, B.J., Rouillard, J.M., Kuick, R., Hanash, S., Schwartz, D.R., Fearon, E.R. and Cho, K.R. (2003) Amplification and overexpression of the L-MYC proto-oncogene in ovarian carcinomas. Am. J. Pathol. 162, 1603–1610.
[32] Grosso, A.R., Martins, S. and Carmo-Fonseca, M. (2008) The emerging role of splicing factors in cancer. EMBO Rep. 9, 1087–1093.
[33] Perou, C.M., Sorlie, T., Eisen, M.B., van de Rijn, M., Jeffrey, S.S., Rees, C.A., Pollack, J.R., Ross, D.T., Johnsen, H., Akslen, L.A., Fluge, O., Pergamenschikov, A., Williams, C., Zhu, S.X., Lonning, P.E., Borresen-Dale, A.L., Brown, P.O. and Botstein, D. (2000) Molecular portraits of human breast tumours. Nature 406, 747–752.

[34] Collins, F.S., Green, E.D., Guttmacher, A.E. and Guyer, M.S. (2003) A vision for the future of genomics research. Nature 422, 835–847.
[35] Ntzani, E.E. and Ioannidis, J.P. (2003) Predictive ability of DNA microarrays for cancer outcomes and correlates: an empirical assessment. Lancet 362, 1439–1444.
[36] Simon, R. (2003) Diagnostic and prognostic prediction using gene expression profiles in high-dimensional microarray data. Br. J. Cancer 89, 1599–1604.
[37] Sorlie, T., Perou, C.M., Tibshirani, R., Aas, T., Geisler, S., Johnsen, H., Hastie, T., Eisen, M.B., van de Rijn, M., Jeffrey, S.S., Thorsen, T., Quist, H., Matese, J.C., Brown, P.O., Botstein, D., Eystein Lonning, P. and Borresen-Dale, A.L. (2001) Gene expression patterns of breast carcinomas distinguish tumor subclasses with clinical implications. Proc. Natl. Acad. Sci. USA 98, 10869–10874.
[38] Maxwell, P.J., Longley, D.B., Latif, T., Boyer, J., Allen, W., Lynch, M., McDermott, U., Harkin, D.P., Allegra, C.J. and Johnston, P.G. (2003) Identification of 5-fluorouracil-inducible target genes using cDNA microarray profiling. Cancer Res. 63, 4602–4606.
[39] Iwao-Koizumi, K., Matoba, R., Ueno, N., Kim, S.J., Ando, A., Miyoshi, Y., Maeda, E., Noguchi, S. and Kato, K. (2005) Prediction of docetaxel response in human breast cancer by gene expression profiling. J. Clin. Oncol. 23, 422–431.
[40] Jansen, M.P., Foekens, J.A., van Staveren, I.L., Dirkzwager-Kiel, M.M., Ritstier, K., Look, M.P., Meijer-van Gelder, M.E., Sieuwerts, A.M., Portengen, H., Dorssers, L.C., Klijn, J.G. and Berns, E.M. (2005) Molecular classification of tamoxifen-resistant breast carcinomas by gene expression profiling. J. Clin. Oncol. 23, 732–740.
[41] Ayers, M., Symmans, W.F., Stec, J., Damokosh, A.I., Clark, E., Hess, K., Lecocke, M., Metivier, J., Booser, D., Ibrahim, N., Valero, V., Royce, M., Arun, B., Whitman, G., Ross, J., Sneige, N., Hortobagyi, G.N. and Pusztai, L. (2004) Gene expression profiles predict complete pathologic response to neoadjuvant paclitaxel and fluorouracil, doxorubicin, and cyclophosphamide chemotherapy in breast cancer. J. Clin. Oncol. 22, 2284–2293.
[42] Kunz, M. (2008) Genomic signatures for individualized treatment of malignant tumors. Curr. Drug. Discov. Technol. 5, 9–14.
[43] Horning, J.L., Sahoo, S.K., Vijayaraghavalu, S., Dimitrijevic, S., Vasir, J.K., Jain, T.K., Panda, A.K. and Labhasetwar, V. (2008) 3-D tumor model for in vitro evaluation of anticancer drugs. Mol. Pharm. 5, 849–862.
[44] Abramovitz, M., Ordanic-Kodani, M., Wang, Y., Li, Z., Catzavelos, C., Bouzyk, M., Sledge Jr, G.W., Moreno, C.S. and Leyland-Jones, B. (2008) Optimization of RNA extraction from FFPE tissues for expression profiling in the DASL assay. Biotechniques 44, 417–423.
[45] Bibikova, M., Yeakley, J.M., Wang-Rodriguez, J. and Fan, J.B. (2008) Quantitative expression profiling of RNA from formalin-fixed, paraffin-embedded tissues using randomly assembled bead arrays. Meth. Mol. Biol. 439, 159–177.
[46] Ravo, M., Mutarelli, M., Ferraro, L., Grober, O.M., Paris, O., Tarallo, R., Vigilante, A., Cimino, D., De Bortoli, M., Nola, E., Cicatiello, L. and Weisz, A. (2008) Quantitative expression profiling of highly degraded RNA from formalin-fixed, paraffin-embedded breast tumor biopsies by oligonucleotide microarrays. Lab. Invest. 88, 430–440.
[47] Esquela-Kerscher, A. and Slack, F.J. (2006) Oncomirs – microRNAs with a role in cancer. Nat. Rev. Cancer 6, 259–269.
[48] Negrini, M., Ferracin, M., Sabbioni, S. and Croce, C.M. (2007) MicroRNAs in human cancer: from research to therapy. J. Cell Sci. 120, 1833–1840.
[49] Lu, J., Getz, G., Miska, E.A., Alvarez-Saavedra, E., Lamb, J., Peck, D., Sweet-Cordero, A., Ebert, B.L., Mak, R.H., Ferrando, A.A., Downing, J.R., Jacks, T., Horvitz, H.R. and Golub, T.R. (2005) MicroRNA expression profiles classify human cancers. Nature 435, 834–838.
[50] Kelloff, G.J. and Sigman, C.C. (2005) New science-based endpoints to accelerate oncology drug development. Eur. J. Cancer. 41, 491–501.
[51] Hajduch, M., Skalnikova, H., Halada, P., Vydra, D., Dzubak, P., Dziechciarkova, M., Strnad, M., Radioch, D. and Kovarova, H. (2007) Cyclin-dependent kinase inhibitors and cancer: usefulness of proteomic approaches in assessment of the molecular mechanisms and efficacy of novel therapeutics in: Clinical Proteomics (Eyk, J.E. and Dunn, M.J., Eds.), pp. 177–202, Wiley–VCH.
[52] Meyer, H.E. and Stuhler, K. (2007) High-performance proteomics as a tool in biomarker discovery. Proteomics 7 (Suppl. 1), 18–26.
[53] Ross, P.L., Huang, Y.N., Marchese, J.N., Williamson, B., Parker, K., Hattan, S., Khainovski, N., Pillai, S., Dey, S., Daniels, S., Purkayastha, S., Juhasz, P., Martin, S., Bartlet-Jones, M., He, F., Jacobson, A. and Pappin, D.J. (2004) Multiplexed protein quantitation in *Saccharomyces cerevisiae* using amine-reactive isobaric tagging reagents. Mol. Cell Proteomics 3, 1154–1169.
[54] Skalnikova, H., Rehulka, P., Chmelik, J., Martinkova, J., Zilvarova, M., Gadher, S.J. and Kovarova, H. (2007) Relative quantitation of proteins fractionated by the ProteomeLab PF 2D system using isobaric tags for relative and absolute quantitation (iTRAQ). Anal. Bioanal. Chem. 389, 1639–1645.
[55] Bantscheff, M., Schirle, M., Sweetman, G., Rick, J. and Kuster, B. (2007) Quantitative mass spectrometry in proteomics: a critical review. Anal. Bioanal. Chem. 389, 1017–1031.
[56] Hu, Z., Hood, L. and Tian, Q. (2007) Quantitative proteomic approaches for biomarker discovery. Proteomics Clin. Appl. 1, 1036–1041.
[57] Spurrier, B., Honkanen, P., Holway, A., Kumamoto, K., Terashima, M., Takenoshita, S., Wakabayashi, G., Austin, J. and Nishizuka, S. (2008) Protein and lysate array technologies in cancer research. Biotechnol. Adv. 26, 361–369.
[58] Pollard, H.B., Srivastava, M., Eidelman, O., Jozwik, C., Rothwell, S.W., Mueller, G.P., Jacobowitz, D.M., Darling, T., Guggino, W.B., Wright, J., Zeitlin, P.L. and Paweletz, C.P. (2007) Protein microarray platforms for clinical proteomics. Proteomics Clin. Appl. 1, 934–952.
[59] Hober, S. and Uhlen, M. (2008) Human protein atlas and the use of microarray technologies. Curr. Opin. Biotechnol. 19, 30–35.
[60] Deininger, S.O., Ebert, M.P., Futterer, A., Gerhard, M., and Rocken, C. (2008) MALDI imaging combined with hierarchical clustering as a new tool for the interpretation of complex human cancers. J. Proteome Res. (October 23, Epub ahead of print).
[61] Rezaul, K., Wilson, L.L. and Han, D.K. (2008) Direct tissue proteomics in human diseases: potential applications to melanoma research. Expert Rev. Proteomics 5, 405–412.
[62] Ahn, S.M. and Simpson, R.J. (2007) Body fluid proteomics: prospects for biomarker discovery. Proteomics Clin. Appl. 1, 1004–1015.
[63] Yip, T.T. and Lomas, L. (2002) SELDI ProteinChip array in oncoproteomic research. Technol. Cancer Res. Treat. 1, 273–280.
[64] Lopez, M.F., Mikulskis, A., Kuzdzal, S., Golenko, E., Petricoin 3rd, E.F., Liotta, L.A., Patton, W.F., Whiteley, G.R., Rosenblatt, K., Gurnani, P., Nandi, A., Neill, S., Cullen, S., O'Gorman, M., Sarracino, D., Lynch, C., Johnson, A., Mckenzie, W. and Fishman, D. (2007) A novel, high-throughput workflow for discovery and identification of serum carrier protein-bound peptide biomarker candidates in ovarian cancer samples. Clin. Chem. 53, 1067–1074.
[65] Hanash, S.M., Pitteri, S.J. and Faca, V.M. (2008) Mining the plasma proteome for cancer biomarkers. Nature 452, 571–579.
[66] Maurya, P., Meleady, P., Dowling, P. and Clynes, M. (2007) Proteomic approaches for serum biomarker discovery in cancer. Anticancer Res. 27, 1247–1255.
[67] Qiu, Y., Patwa, T.H., Xu, L., Shedden, K., Misek, D.E., Tuck, M., Jin, G., Ruffin, M.T., Turgeon, D.K., Synal, S., Bresalier, R., Marcon, N., Brenner, D.E. and Lubman, D.M. (2008) Plasma glycoprotein profiling for colorectal cancer biomarker identification by lectin glycoarray and lectin blot. J. Proteome Res. 7, 1693–1703.
[68] Kirmiz, C., Li, B., An, H.J., Clowers, B.H., Chew, H.K., Lam, K.S., Ferrige, A., Alecio, R., Borowsky, A.D., Sulaimon, S., Lebrilla, C.B. and Miyamoto, S. (2007) A serum glycomics approach to breast cancer biomarkers. Mol. Cell Proteomics 6, 43–55.
[69] Bengtsson, S., Krogh, M., Szigyarto, C.A., Uhlen, M., Schedvins, K., Silfversward, C., Linder, S., Auer, G., Alaiya, A. and James, P. (2007) Large-scale proteomics analysis of human ovarian cancer for biomarkers. J. Proteome Res. 6, 1440–1450.
[70] Kondo, T. (2008) Tissue proteomics for cancer biomarker development: laser microdissection and 2D-DIGE. BMB Rep. 41, 626–634.
[71] Suehara, Y., Kondo, T., Seki, K., Shibata, T., Fujii, K., Gotoh, M., Hasegawa, T., Shimada, Y., Sasako, M., Shimoda, T., Kurosawa, H., Beppu, Y., Kawai, A. and Hirohashi, S. (2008) Pfetin as a prognostic biomarker of gastrointestinal stromal tumors revealed by proteomics. Clin. Cancer Res. 14, 1707–1717.
[72] Sodek, K.L., Evangelou, A.I., Ignatchenko, A., Agochiya, M., Brown, T.J., Ringuette, M.J., Jurisica, I. and Kislinger, T. (2008) Identification of pathways associated with invasive behavior by ovarian cancer cells using multidimensional protein identification technology (MudPIT). Mol. Biosyst. 4, 762–773.
[73] Hudson, M.E., Pozdnyakova, I., Haines, K., Mor, G. and Snyder, M. (2007) Identification of differentially expressed proteins in ovarian cancer using high-density protein microarrays. Proc. Natl. Acad. Sci. USA 104, 17494–17499.
[74] Ma, Y., Ding, Z., Qian, Y., Shi, X., Castranova, V., Harner, E.J. and Guo, L. (2006) Predicting cancer drug response by proteomic profiling. Clin. Cancer Res. 12, 4583–4589.
[75] Nishizuka, S., Charboneau, L., Young, L., Major, S., Reinhold, W.C., Waltham, M., Kouros-Mehr, H., Bussey, K.J., Lee, J.K., Espina, V., Munson, P.J., Petricoin 3rd, E., Liotta, L.A. and Weinstein, J.N. (2003) Proteomic profiling of the NCI-60 cancer cell lines using new high-density reverse-phase lysate microarrays. Proc. Natl. Acad. Sci. USA 100, 14229–14234.
[76] Chabner, B.A. and Roberts Jr, T.G. (2005) Timeline: chemotherapy and the war on cancer. Nat. Rev. Cancer 5, 65–72.
[77] Trog, D., Fountoulakis, M., Friedlein, A. and Golubnitschaja, O. (2006) Is current therapy of malignant gliomas beneficial for patients? Proteomics evidence of shifts in glioma cells expression patterns under clinically relevant treatment conditions. Proteomics 6, 2924–2930.
[78] Moller, A., Malerczyk, C., Volker, U., Stoppler, H. and Maser, E. (2002) Monitoring daunorubicin-induced alterations in protein expression in pancreas carcinoma cells by two-dimensional gel electrophoresis. Proteomics 2, 697–705.
[79] Chen, S.T., Pan, T.L., Tsai, Y.C. and Huang, C.M. (2002) Proteomics reveals protein profile changes in doxorubicin-treated MCF-7 human breast cancer cells. Cancer Lett. 181, 95–107.
[80] Casado, P., Zuazua-Villar, P., del Valle, E., Martinez-Campa, C., Lazo, P.S. and Ramos, S. (2007) Vincristine regulates the phosphorylation of the antiapoptotic protein HSP27 in breast cancer cells. Cancer Lett. 247, 273–282.
[81] Petrak, J., Ivanek, R., Toman, O., Cmejla, R., Cmejlova, J., Vyoral, D., Zivny, J. and Vulpe, C.D. (2008) Deja vu in proteomics. A hit parade of repeatedly identified differentially expressed proteins. Proteomics 8, 1744–1749.
[82] Campostrini, N., Marimpietri, D., Totolo, A., Mancone, C., Fimia, G.M., Ponzoni, M. and Righetti, P.G. (2006) Proteomic analysis of anti-angiogenic effects by a combined treatment with vinblastine and rapamycin in an endothelial cell line. Proteomics 6, 4420–4431.

[83] Schmidt, F., Hustoft, H.K., Strozynski, M., Dimmler, C., Rudel, T. and Thiede, B. (2007) Quantitative proteome analysis of cisplatin-induced apoptotic Jurkat T cells by stable isotope labeling with amino acids in cell culture, SDS–PAGE, and LC-MALDI-TOF/TOF MS. Electrophoresis 28, 4359–4368.
[84] Kovarova, H., Halada, P., Man, P., Dzubak, P. and Hajduch, M. (2002) Application of proteomics in the search for novel proteins associated with the anti-cancer effect of the synthetic cyclin-dependent kinases inhibitor, bohemine. Technol. Cancer Res. Treat. 1, 247–256.
[85] Kovarova, H., Hajduch, M., Korinkova, G., Halada, P., Krupickova, S., Gouldsworthy, A., Zhelev, N. and Strnad, M. (2000) Proteomics approach in classifying the biochemical basis of the anticancer activity of the new olomoucine-derived synthetic cyclin-dependent kinase inhibitor. Bohemine. Electrophoresis 21, 3757–3764.
[86] Boyd, Z.S., Wu, Q.J., O'Brien, C., Spoerke, J., Savage, H., Fielder, P.J., Amler, L., Yan, Y. and Lackner, M.R. (2008) Proteomic analysis of breast cancer molecular subtypes and biomarkers of response to targeted kinase inhibitors using reverse-phase protein microarrays. Mol. Cancer Ther. 7, 3695–3706.
[87] Kim, H.J., Kang, H.J., Lee, H., Lee, S.T., Yu, M.H., Kim, H., and Lee, C. (2009) Identification of S100A8 and S100A9 as serological markers for colorectal cancer. J. Proteome Res. (February 2, Epub ahead of print).
[88] Tian, M., Cui, Y.Z., Song, G.H., Zong, M.J., Zhou, X.Y., Chen, Y. and Han, J.X. (2008) Proteomic analysis identifies MMP-9, DJ-1 and A1BG as overexpressed proteins in pancreatic juice from pancreatic ductal adenocarcinoma patients. BMC Cancer 8, 241.
[89] Hoagland 4th, L.F., Campa, M.J., Gottlin, E.B., Herndon 2nd, J.E. and Patz Jr., E.F. (2007) Haptoglobin and posttranslational glycan-modified derivatives as serum biomarkers for the diagnosis of nonsmall cell lung cancer. Cancer 110, 2260–2268.
[90] Kawai, A., Kondo, T., Suehara, Y., Kikuta, K. and Hirohashi, S. (2008) Global protein-expression analysis of bone and soft tissue sarcomas. Clin. Orthop. Relat. Res. 466, 2099–2106.
[91] Orenes-Pinero, E., Corton, M., Gonzalez-Peramato, P., Algaba, F., Casal, I., Serrano, A. and Sanchez-Carbayo, M. (2007) Searching urinary tumor markers for bladder cancer using a two-dimensional differential gel electrophoresis (2D-DIGE) approach. J. Proteome Res. 6, 4440–4448.
[92] Di Michele, M., Della Corte, A., Cicchillitti, L., Del Boccio, P., Urbani, A., Ferlini, C., Scambia, G., Donati, M.B. and Rotilio, D. (2009) A proteomic approach to paclitaxel chemoresistance in ovarian cancer cell lines. Biochim. Biophys. Acta 1794, 225–236.
[93] Cicchillitti, L., Di Michele, M., Urbani, A., Ferlini, C., Donati, M.B., Scambia, G., and Rotilio, D. (2009) Comparative proteomic analysis of paclitaxel sensitive A2780 epithelial ovarian cancer and its resistant counterpart A2780TC1 by 2D-DIGE: the role of ERp57. J. Proteome Res. (February 2, Epub ahead of print).
[94] Orimo, T., Ojima, H., Hiraoka, N., Saito, S., Kosuge, T., Kakisaka, T., Yokoo, H., Nakanishi, K., Kamiyama, T., Todo, S., Hirohashi, S. and Kondo, T. (2008) Proteomic profiling reveals the prognostic value of adenomatous polyposis coli-end-binding protein 1 in hepatocellular carcinoma. Hepatology 48, 1851–1863.
[95] Liu, Y.F., Xiao, Z.Q., Li, M.X., Li, M.Y., Zhang, P.F., Li, C., Li, F., Chen, Y.H., Yi, H., Yao, H.X. and Chen, Z.C. (2009) Quantitative proteome analysis reveals annexin A3 as a novel biomarker in lung adenocarcinoma. J. Pathol. 217, 54–64.
[96] Giusti, L., Iacconi, P., Ciregia, F., Giannaccini, G., Donatini, G.L., Basolo, F., Miccoli, P., Pinchera, A. and Lucacchini, A. (2008) Fine-needle aspiration of thyroid nodules: proteomic analysis to identify cancer biomarkers. J. Proteome Res. 7, 4079–4088.
[97] Bouchal, P., Roumeliotis, T., Hrstka, R., Nenutil, R., Vojtesek, B. and Garbis, S.D. (2009) Biomarker discovery in low-grade breast cancer using isobaric stable isotope tags and two-dimensional liquid chromatography-tandem mass spectrometry (iTRAQ-2DLC-MS/MS) based quantitative proteomic analysis. J. Proteome Res. 8, 362–373.
[98] Garbis, S.D., Tyritzis, S.I., Roumeliotis, T., Zerefos, P., Giannopoulou, E.G., Vlahou, A., Kossida, S., Diaz, J., Vourekas, S., Tamvakopoulos, C., Pavlakis, K., Sanoudou, D. and Constantinides, C.A. (2008) Search for potential markers for prostate cancer diagnosis, prognosis and treatment in clinical tissue specimens using amine-specific isobaric tagging (iTRAQ) with two-dimensional liquid chromatography and tandem mass spectrometry. J. Proteome Res. 7, 3146–3158.
[99] Ralhan, R., Desouza, L.V., Matta, A., Chandra Tripathi, S., Ghanny, S., Datta Gupta, S., Bahadur, S. and Siu, K.W. (2008) Discovery and verification of head-and-neck cancer biomarkers by differential protein expression analysis using iTRAQ labeling, multidimensional liquid chromatography, and tandem mass spectrometry. Mol. Cell Proteomics 7, 1162–1173.
[100] Chaerkady, R., Harsha, H.C., Nalli, A., Gucek, M., Vivekanandan, P., Akhtar, J., Cole, R.N., Simmers, J., Schulick, R.D., Singh, S., Torbenson, M., Pandey, A. and Thuluvath, P.J. (2008) A quantitative proteomic approach for identification of potential biomarkers in hepatocellular carcinoma. J. Proteome Res. 7, 4289–4298.
[101] Chen, R., Pan, S., Yi, E.C., Donohoe, S., Bronner, M.P., Potter, J.D., Goodlett, D.R., Aebersold, R. and Brentnall, T.A. (2006) Quantitative proteomic profiling of pancreatic cancer juice. Proteomics 6, 3871–3879.
[102] Sun, Y., Mi, W., Cai, J., Ying, W., Liu, F., Lu, H., Qiao, Y., Jia, W., Bi, X., Lu, N., Liu, S., Qian, X. and Zhao, X. (2008) Quantitative proteomic signature of liver cancer cells: tissue transglutaminase 2 could be a novel protein candidate of human hepatocellular carcinoma. J. Proteome Res. 7, 3847–3859.
[103] Gronborg, M., Kristiansen, T.Z., Iwahori, A., Chang, R., Reddy, R., Sato, N., Molina, H., Jensen, O.N., Hruban, R.H., Goggins, M.G., Maitra, A. and Pandey, A. (2006) Biomarker discovery from pancreatic cancer secretome using a differential proteomic approach. Mol. Cell Proteomics 5, 157–171.
[104] Kristiansen, T.Z., Harsha, H.C., Gronborg, M., Maitra, A. and Pandey, A. (2008) Differential membrane proteomics using 18O-labeling to identify biomarkers for cholangiocarcinoma. J. Proteome Res. 7, 4670–4677.
[105] Ueda, K., Katagiri, T., Shimada, T., Irie, S., Sato, T.A., Nakamura, Y. and Daigo, Y. (2007) Comparative profiling of serum glycoproteome by sequential purification of glycoproteins and 2-nitrobenzensulfenyl (NBS) stable isotope labeling: a new approach for the novel biomarker discovery for cancer. J. Proteome Res. 6, 3475–3483.
[106] Whiteaker, J.R., Zhang, H., Zhao, L., Wang, P., Kelly-Spratt, K.S., Ivey, R.G., Piening, B.D., Feng, L.C., Kasarda, E., Gurley, K.E., Eng, J.K., Chodosh, L.A., Kemp, C.J., McIntosh, M.W. and Paulovich, A.G. (2007) Integrated pipeline for mass spectrometry-based discovery and confirmation of biomarkers demonstrated in a mouse model of breast cancer. J. Proteome Res. 6, 3962–3975.
[107] Pan, J., Chen, H.Q., Sun, Y.H., Zhang, J.H. and Luo, X.Y. (2008) Comparative proteomic analysis of non-small-cell lung cancer and normal controls using serum label-free quantitative shotgun technology. Lung 186, 255–261.
[108] Huang, S.K., Darfler, M.M., Nicholl, M.B., You, J., Bemis, K.G., Tegeler, T.J., Wang, M., Wery, J.P., Chong, K.K., Nguyen, L., Scolyer, R.A. and Hoon, D.S. (2009) LC/MS-based quantitative proteomic analysis of paraffin-embedded archival melanomas reveals potential proteomic biomarkers associated with metastasis. PLoS ONE. 4, e4430.
[109] Cheng, L., Zhou, L., Tao, L., Zhang, M., Cui, J. and Li, Y. (2008) SELDI-TOF MS profiling of serum for detection of laryngeal squamous cell carcinoma and the progression to lymph node metastasis. J. Cancer Res. Clin. Oncol. 134, 769–776.
[110] Han, K.Q., Huang, G., Gao, C.F., Wang, X.L., Ma, B., Sun, L.Q. and Wei, Z.J. (2008) Identification of lung cancer patients by serum protein profiling using surface-enhanced laser desorption/ionization time-of-flight mass spectrometry. Am. J. Clin. Oncol. 31, 133–139.
[111] Lim, J.Y., Cho, J.Y., Paik, Y.H., Chang, Y.S. and Kim, H.G. (2007) Diagnostic application of serum proteomic patterns in gastric cancer patients by ProteinChip surface-enhanced laser desorption/ionization time-of-flight mass spectrometry. Int. J. Biol. Markers 22, 281–286.
[112] Cui, J., Kang, X., Dai, Z., Huang, C., Zhou, H., Guo, K., Li, Y., Zhang, Y., Sun, R., Chen, J., Li, Y., Tang, Z., Uemura, T. and Liu, Y. (2007) Prediction of chronic hepatitis B, liver cirrhosis and hepatocellular carcinoma by SELDI-based serum decision tree classification. J. Cancer Res. Clin. Oncol. 133, 825–834.
[113] Engwegen, J.Y., Mehra, N., Haanen, J.B., Bonfrer, J.M., Schellens, J.H., Voest, E.E. and Beijnen, J.H. (2007) Validation of SELDI-TOF MS serum protein profiles for renal cell carcinoma in new populations. Lab. Invest. 87, 161–172.
[114] Shirai, Y., Sogawa, K., Yamaguchi, T., Sudo, K., Nakagawa, A., Sakai, Y., Ishihara, T., Sunaga, M., Nezu, M., Tomonaga, T., Miyazaki, M., Saisho, H. and Nomura, F. (2008) Protein profiling in pancreatic juice for detection of intraductal papillary mucinous neoplasm of the pancreas. Hepatogastroenterology 55, 1824–1829.
[115] Holcakova, J., Hernychova, L., Bouchal, P., Brozkova, K., Zaloudik, J., Valik, D., Nenutil, R. and Vojtesek, B. (2008) Identification of alphaB-crystallin, a biomarker of renal cell carcinoma by SELDI-TOF MS. Int. J. Biol. Markers 23, 48–53.
[116] Leong, S., Christopherson, R.I. and Baxter, R.C. (2007) Profiling of apoptotic changes in human breast cancer cells using SELDI-TOF mass spectrometry. Cell Physiol. Biochem. 20, 579–590.
[117] Chaurand, P., Rahman, M.A., Hunt, T., Mobley, J.A., Gu, G., Latham, J.C., Caprioli, R.M. and Kasper, S. (2008) Monitoring mouse prostate development by profiling and imaging mass spectrometry. Mol. Cell Proteomics 7, 411–423.
[118] Schwamborn, K., Krieg, R.C., Reska, M., Jakse, G., Knuechel, R. and Wellmann, A. (2007) Identifying prostate carcinoma by MALDI-Imaging. Int. J. Mol. Med. 20, 155–159.
[119] Kilic, A., Schuchert, M.J., Luketich, J.D., Landreneau, R.J., Lokshin, A.E., Bigbee, W.L. and El-Hefnawy, T. (2008) Use of novel autoantibody and cancer-related protein arrays for the detection of esophageal adenocarcinoma in serum. J. Thorac. Cardiovasc. Surg. 136, 199–204.
[120] Ellmark, P., Ingvarsson, J., Carlsson, A., Lundin, B.S., Wingren, C. and Borrebaeck, C.A. (2006) Identification of protein expression signatures associated with *Helicobacter pylori* infection and gastric adenocarcinoma using recombinant antibody microarrays. Mol. Cell Proteomics 5, 1638–1646.
[121] Sanchez-Carbayo, M., Socci, N.D., Lozano, J.J., Haab, B.B. and Cordon-Cardo, C. (2006) Profiling bladder cancer using targeted antibody arrays. Am. J. Pathol. 168, 93–103.
[122] Vazquez-Martin, A., Colomer, R. and Menendez, J.A. (2007) Protein array technology to detect HER2 (erbB-2)-induced 'cytokine signature' in breast cancer. Eur J. Cancer 43, 1117–1124.
[123] Ghosh, S., Sullivan, C.A., Zerkowski, M.P., Molinaro, A.M., Rimm, D.L., Camp, R.L. and Chung, G.G. (2008) High levels of vascular endothelial growth factor and its receptors (VEGFR-1, VEGFR-2, neuropilin-1) are associated with worse outcome in breast cancer. Hum. Pathol. 39, 1835–1843.

[124] Chung, Y.L., Lee, M.Y., Horng, C.F., Jian, J.J., Cheng, S.H., Tsai, S.Y., Hsieh, C.I., Yen, L.K. and Lin, C.Y. (2009) Use of combined molecular biomarkers for prediction of clinical outcomes in locally advanced tonsillar cancers treated with chemoradiotherapy alone. Head Neck 31, 9–20.
[125] Hua, S., Kallen, C.B., Dhar, R., Baquero, M.T., Mason, C.E., Russell, B.A., Shah, P.K., Liu, J., Khramtsov, A., Tretiakova, M.S., Krausz, T.N., Olopade, O.I., Rimm, D.L. and White, K.P. (2008) Genomic analysis of estrogen cascade reveals histone variant H2A.Z associated with breast cancer progression. Mol. Syst. Biol. 4, 188.
[126] Mor, G., Visintin, I., Lai, Y., Zhao, H., Schwartz, P., Rutherford, T., Yue, L., Bray-Ward, P. and Ward, D.C. (2005) Serum protein markers for early detection of ovarian cancer. Proc. Natl. Acad. Sci. USA 102, 7677–7682.
[127] Verrills, N.M., Walsh, B.J., Cobon, G.S., Hains, P.G. and Kavallaris, M. (2003) Proteome analysis of vinca alkaloid response and resistance in acute lymphoblastic leukemia reveals novel cytoskeletal alterations. J. Biol. Chem. 278, 45082–45093.
[128] Yim, E.K., Lee, K.H., Bae, J.S., Namkoong, S.E., Um, S.J. and Park, J.S. (2004) Proteomic analysis of antiproliferative effects by treatment of 5-fluorouracil in cervical cancer cells. DNA Cell Biol. 23, 769–776.
[129] Yim, E.K., Lee, S.B., Lee, K.H., Kim, C.J. and Park, J.S. (2006) Analysis of the in vitro synergistic effect of 5-fluorouracil and cisplatin on cervical carcinoma cells. Int. J. Gynecol. Cancer 16, 1321–1329.
[130] Yim, E.K., Lee, K.H., Kim, C.J. and Park, J.S. (2006) Analysis of differential protein expression by cisplatin treatment in cervical carcinoma cells. Int. J. Gynecol. Cancer 16, 690–697.
[131] Castagna, A., Antonioli, P., Astner, H., Hamdan, M., Righetti, S.C., Perego, P., Zunino, F. and Righetti, P.G. (2004) A proteomic approach to cisplatin resistance in the cervix squamous cell carcinoma cell line A431. Proteomics 4, 3246–3267.
[132] Cecconi, D., Scarpa, A., Donadelli, M., Palmieri, M., Hamdan, M., Astner, H. and Righetti, P.G. (2003) Proteomic profiling of pancreatic ductal carcinoma cell lines treated with trichostatin-A. Electrophoresis 24, 1871–1878.
[133] Cecconi, D., Donadelli, M., Scarpa, A., Milli, A., Palmieri, M., Hamdan, M., Areces, L.B., Rappsilber, J. and Righetti, P.G. (2005) Proteomic analysis of pancreatic ductal carcinoma cells after combined treatment with gemcitabine and trichostatin A. J. Proteome Res. 4, 1909–1916.

PŘÍLOHA 5

Anal Bioanal Chem (2007) 389:1639–1645
DOI 10.1007/s00216-007-1547-x

TECHNICAL NOTE

Relative quantitation of proteins fractionated by the ProteomeLab™ PF 2D system using isobaric tags for relative and absolute quantitation (iTRAQ)

Helena Skalnikova · Pavel Rehulka · Josef Chmelik · Jirina Martinkova · Michaela Zilvarova · Suresh Jivan Gadher · Hana Kovarova

Received: 3 July 2007 / Revised: 3 August 2007 / Accepted: 6 August 2007 / Published online: 28 August 2007
© Springer-Verlag 2007

Abstract We describe an optimised protocol for application of isobaric tags for relative and absolute quantitation (iTRAQ) and tandem mass spectrometry to obtain relative quantitative data from peptides derived from tryptic digestions of proteins fractionated by using the 2D liquid-phase ProteomeLab™ PF 2D technique. This methodology is suitable for the quantitation of proteins from a pool of co-eluting proteins which are often difficult to identify for the purpose of candidate protein selection for biologically relevant qualitative/quantitative changes under experimental conditions or in disease states. iTRAQ quantitation also facilitates the possibility of result to result comparison using other methodologies such as UV protein quantitation via the ProteomeLab™ PF 2D technique. The optimised protocol outlined here allows relative quantitation by MALDI-TOF/TOF mass spectrometry with high sensitivity and without the need to perform 2D HPLC separation of labelled peptides. The overall outcome is the simplification in the data complexity and the ease of use of the labelling protocol.

Keywords 2D liquid chromatography · Human T-lymphoblastic leukemia cell proteins · iTRAQ · ProteomeLab™ PF 2D · Relative quantitation

This study is dedicated to Dr. Josef Chmelik in memory of his contribution and constant inspiration.

H. Skalnikova · J. Martinkova · M. Zilvarova · H. Kovarova
Institute of Animal Physiology and Genetics,
Academy of Sciences of the Czech Republic,
Rumburska 89,
277 21 Libechov, Czech Republic

P. Rehulka · J. Chmelik
Institute of Analytical Chemistry,
Academy of Sciences of the Czech Republic,
Veveri 97,
602 00 Brno, Czech Republic

S. J. Gadher
Beckman Coulter International S.A.,
1260 Nyon, Switzerland

H. Kovarova (✉)
Department of Reproductive and Developmental Biology,
Institute of Animal Physiology and Genetics,
Academy of Sciences of the Czech Republic,
Rumburska 89,
277 21 Libechov, Czech Republic
e-mail: kovarova@iapg.cas.cz

Introduction

Current proteomic approaches for analyses of complex protein mixtures from tissues, cells or various biological fluids rely on 2D separation techniques. One such unique system is the liquid-phase 2D HPLC fractionation system known as the ProteomeLab™ PF 2D system (Beckman Coulter, Fullerton, CA, USA) and this has been developed to separate complex protein mixtures by chromatofocusing in the first dimension followed by high-resolution non-porous silica reversed-phase chromatography (RPLC) in the second dimension [1, 2]. It has been utilised recently for the analysis of a variety of samples including serum, cancer cells and plants [3–5]. Sensitive UV detectors are used to quantify the proteins during fractionation, and individual fractions are collected in a liquid phase. Specific software (ProteoVue and DeltaVue) implemented in the system allows construction of 2D protein maps and comparison of protein expression profiles of the analysed samples to select candidate proteins for biologically relevant qualita-

tive and/or quantitative changes. Past research has shown that UV-based quantitation has limitations when several proteins appear in one fraction despite the high resolving power of the ProteomeLab™ PF 2D system [4]. In such situations, iTRAQ methodology coupled to mass spectrometry can play an important role in evaluating not only the protein identities but also protein quantitation. Recent advances in mass-spectrometry-based proteomics methodologies facilitate determination of protein abundance in samples using stable isotope labelling techniques prior to protein fractionation including stable isotope labelling by amino acids in cell culture (SILAC) [6] and isotope-coded protein labels (ICPL) [7]. In addition, an improved approach using amine-reactive isobaric tags for relative and absolute quantitation (iTRAQ) has been developed that offers great potential [8]. This technique is based on chemically tagging the N-terminus of peptides generated from protein digests that have been isolated from cells cultured under different experimental conditions. Two labelled peptide samples are then combined, fractionated by 2D HPLC and analysed by tandem mass spectrometry. A database search of the fragmented peptides results in the identification of the labelled peptides and hence their corresponding proteins. Fragmentation of the tag attached to the peptide generates a low molecular mass 'reporter ion' that is unique to the tag used to label each of the digests. Measurement of the intensity of these reporter ions enables relative quantitation of the peptides in each digest and hence the proteins from which they initially originate. Currently there are four available tags producing reporter ions with *m/z* 114, 115, 116 and 117, enabling four different samples to be multiplexed together in one experiment. Additionally, an eight-plex iTRAQ chemistry protocol for simultaneous analysis of eight different samples (with reporter ions at *m/z* 113, 114, 115, 116, 117, 118, 119 and 121) is expected to be commercially available soon.

We report here an optimised protocol for application of iTRAQ and tandem mass spectrometry to obtain relative quantitative data from peptides derived by tryptic digestions of proteins fractionated by the 2D liquid-phase ProteomeLab™ PF 2D technique. This novel approach together with our 'fine-tuned' protocol facilitates further examination of fractions containing co-eluting proteins and in turn the determination of selective protein(s) responsible for quantitative changes.

Experimental

The iTRAQ 3-Assay Duplex Trial Kit was from Applied Biosystems (Foster City, CA, USA, cat. No. 4369561). Untreated human T-lymphoblastic leukemia CEM cell line (control) or CEM cells exposed to cyclin-dependent kinases inhibitor (CDKI) under experimental conditions were used as a source of protein samples and their protein expression patterns were obtained from the ProteomeLab™ PF 2D fractionation as described previously [4].

To obtain sufficient material for subsequent MS/MS analysis, 3 mg of total cellular proteins was injected onto the chromatofocusing column and 500 μL of the first dimension fractions (instead of 200 μL) was injected onto the RPLC. Proteins were eluted with a linear gradient of 0–100% solvent B (0.08% trifluoroacetic acid (TFA) in acetonitrile (ACN)) in solvent A (0.1% TFA in HPLC grade water) with a run time of 35 min. Second dimension fractions were collected in 0.1- to 0.15-min intervals ensuring that no more than one peak detected in the UV chromatogram was present per fraction. The fraction volumes were between 75 and 112 μL and protein amount per peak measured by UV ranged between 0.01 and 0.5 μg. The selected fractions of two experimental samples, i.e. control and CDKI-treated (Fig. 1a), as judged by UV intensities and significant quantitative difference, were individually labelled with two iTRAQ reagents, *m/z* 114 and 117, respectively. These were then mixed in a 1:1 ratio for subsequent quantitation.

The fractions were dried down to a volume of approximately 2 μL using a SpeedVac (Concentrator 5301, Eppendorf, Hamburg, Germany). Proteins were dissolved by adding 8 μL of dissolution buffer (TEAB, 0.05% triethylammonium bicarbonate buffer, pH 8.5, provided in the iTRAQ kit) with 1 M urea (Sigma–Aldrich, Steinheim, Germany, cat. No. U0631), vortexed and the pH of the sample was checked to make sure that it was equal to the dissolution buffer pH (pH 8.5). The disulphide bonds were reduced by addition of 1 μL of reducing reagent (50 mM TCEP, provided in the iTRAQ kit), incubated at 35 °C for 90 min and cysteines were modified for 10 min at room temperature by addition of 0.5 μL of cysteine blocking reagent (MMTS, 200 mM methyl methane-thiosulfonate in isopropanol, provided in the iTRAQ kit). The proteins were then digested overnight at 35 °C with 25 ng sequencing grade "modified trypsin" (Promega, Madison, WI, USA, cat. No. V5113) instead of 25 μg of "unmodified trypsin" provided in the iTRAQ kit. The reason for substituting 'unmodified trypsin' with 'modified trypsin' was that in our hands 'unmodified trypsin' caused autolysis with resultant tryptic peptides which interfered with subsequent mass spectrometric analysis. The "modified trypsin" used was a better option as it was rendered resistant to proteolytic digestion due to its structural reductive methylation modification and hence was suitable for 'follow-on' investigative studies. The subsequent digests were sonicated, acidified to pH<4 and diluted to an approximate volume of 50 μL by addition of 2% TFA to an approximate TFA concentration of 1%. Prior to the iTRAQ labelling, the samples were purified

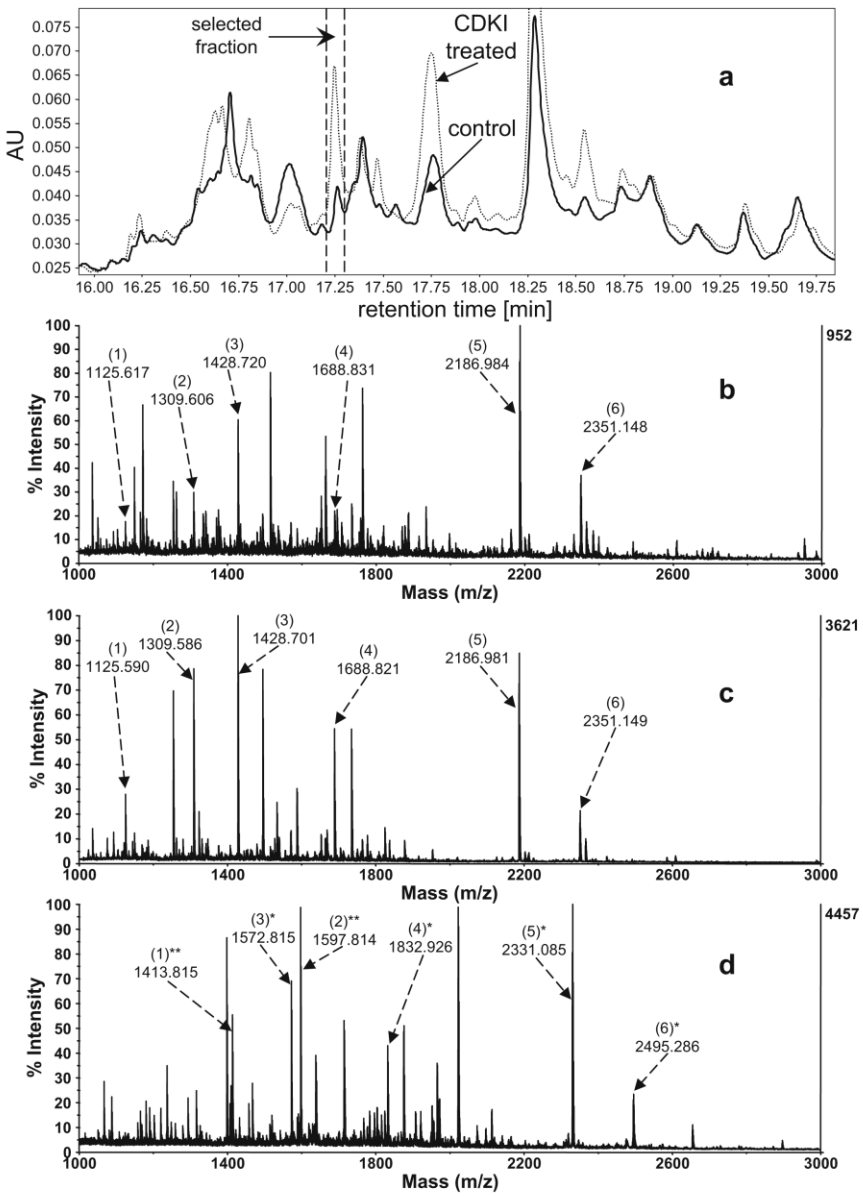

Fig. 1 **a** An example of PF 2D chromatogram from the second dimension (RPLC) with a marked protein peak showing quantitative difference that was subjected to further iTRAQ analysis. MS spectra of unlabelled tryptic peptides of the control (**b**) and CDKI-treated samples (**c**). After labelling (**d**), the relative molecular weight of the peptide increases by 144.1 Da (labelled N-terminus) and by additional 144.1 Da for each labelled lysine residue present in the peptide sequence (total mass increment for double labelled peptide is 288.2)

with POROS R2 (Applied Biosystems, Foster City, CA, USA) packed microcolumns 8–9 mm in length, in order to remove urea, salts and other reagents [9]. The POROS R2 microcolumns have higher binding capacity than commercially available ZipTip C_{18} pipette tips (Millipore, Bedford, MA, USA, cat. No. ZTC18S096) and allow the peptides to be eluted in lower volumes than the standard sized ZipTip C_{18} pipette tips. The microcolumns were wetted by 2×10 μL 100% ACN, equilibrated by 2×10 μL 5% ACN in 0.1% TFA and then the sample was passed through the column. During the sample loading, the unbound peptides (flow-through, 50 μL) were collected. After the washing step (2× 10 μL 0.1% TFA) the bound peptides were eluted by 5 μL of 60% ACN in 0.1% TFA. The column was re-equilibrated and 50 μL of unbound peptides were repeatedly loaded on the column, washed and eluted in 5 μL of 60% ACN in 0.1% TFA to the same tube. Hence, a volume of 10 μL of the eluate was collected in total, minimising sample loss and ensuring good quantitation. A 1-μL aliquot of the purified sample was spotted as two spots on the MALDI target covered with CHCA matrix (Sigma–Aldrich, Steinheim, Germany, cat. No. 145505) by deposition of 0.5 μL of

Table 1 Workflow of optimised protocol for application of iTRAQ and tandem mass spectrometry to obtain relative quantitative data from peptides derived by tryptic digestions of proteins fractionated by the 2D liquid-phase ProteomeLab™ PF 2D technique

Step	Standard iTRAQ procedure	Optimised iTRAQ procedure
Purification	Acetone precipitation	RPLC fractions dried down to 2 μL
Dissolution	20 μL 0.5 M triethylammoniumbicarbonate with 0.1% SDS	8 μL 0.5 M triethylammoniumbicarbonate with 1 M urea
Reduction	5 mM TCEP, 60 °C, 1 h	5 mM TCEP, 35 °C, 1.5 h
Alkylation	10 mM MMTS, RT, 10 min	10 mM MMTS, RT, 10 min
Digestion	Trypsin 25 μg	Modified trypsin 25 ng
Purification + concentration	None	Poros R2 microcolumns, completely dry by SpeedVac, added 1 μL of 0.5 M triethylammonium bicarbonate
Labelling	70 μL ethanol + Whole tube of iTRAQ reagent + Sample (24 μL) Total>100 μL	9 μL ethanol + 1 μL of iTRAQ reagent + Sample (1 μL) Total 11 μL
Combination of samples to be quantified		
Purification	Cation exchange chromatography followed by desalting on RPLC	Poros R2 microcolumns, elution with 3 μL of 60% ACN/ 0.1%TFA directly on MALDI target (6 spots of 0.5 μL each)
Procurement of MS/MS spectra followed by result analysis		

Table 2 Summary of six identified peptides sequences and their relative abundance ratios

Peptide no.	Experimental precursor mass		Peptide sequence	Number of iTRAQ labels	Cluster area		Ratio CDKI-treated/control
	Unlabelled CDKI treated sample	iTRAQ-labelled mixture			Ion 114	Ion 117	
1	1,125.590	1,413.815	(R)FANYIDKVR(F)	2	2,802	6,593	2.35
2	1,309.586	1,597.814	(K)NLQEAEEWYK(S)	2	1,575	3,855	2.45
3	1,428.701	1,572.815	(R)SLYASSPGGVYATR(S)	1	364	934	2.57
4	1,688.821	1,832.926	(R)VEVERDNLAEDIMR(L)	1	1,598	3,276	2.05
5	2,186.981	2,331.085	(R)EMEENFAVEAANYQDTIGR(L)	1	1,191	2,539	2.13
6	2,351.149	2,495.286	(K)LQEEMLQREEAENTLQSFR(Q)	1	240	487	2.03

5 g L^{-1} CHCA solution in 60% ACN in 0.1% TFA. MALDI-TOF MS and MS/MS spectra were obtained with a 4700 Proteomics Analyzer (Applied Biosystems, Framingham, MA) to check the digest quality prior to labelling and to identify protein(s) present in the analysed samples. The remaining 9 μL of desalted peptides was completely dried down by SpeedVac. A 1-μL aliquot of dissolution buffer was added to ensure basic pH for the labelling reaction and the samples were briefly mixed to dissolve the peptides. A 1-μL aliquot of iTRAQ reagent (*m*/*z* 114 for control sample and *m*/*z* 117 for CDKI-treated sample) was mixed with 9 μL of ethanol and added to the peptide sample. The labelling was performed using a thermomixer (Thermomixer Comfort, Eppendorf, Hamburg, Germany) for 90 min at room temperature (final total volume of the labelling reaction was 11 μL). After labelling, the contents of both sample tubes (control and CDKI-treated) were mixed together in 1:1 ratio and excess of organic solvent was removed by SpeedVac by drying down to approximately 2 μL. The mixed sample was acidified by adding 20 μL of 0.5% TFA and the peptide mixture was purified by using the POROS R2 microcolumn in the same way as described previously. The microcolumn was eluted using 3 μL of 60% ACN in 0.1% TFA and directly spotted as four to six spots on a MALDI plate coated with CHCA matrix as described previously. Thus, the whole PF 2D fraction was concentrated on four to six MALDI spots, providing sufficient concentration of labelled peptide for acquisition of MS/MS spectra. The above optimised workflow is tabulated for ease of use and for comparison with the manufacturer's protocol (Table 1).

MALDI-TOF MS and MS/MS spectra of iTRAQ-labelled samples were measured using the MALDI-TOF/TOF instrument 4700 Proteomics Analyzer. Regularly updated external calibration both in the MS and MS/MS positive ion mode was used throughout all MS measurements. Resolution of the time-ion selector for the MS/MS analysis was set to 200. MS/MS spectra were acquired using a 1-keV collision energy and nitrogen was used as a collision gas with an indicated collision gas pressure at about 10^{-6} Torr. Approximately 2,500 and 5,000 laser shots were collected in MS and MS/MS measurements, respectively. A maximum of ten precursor ions from each MS spectra were selected for subsequent MS/MS analysis. MS and MS/MS spectra were analysed both in the 4000 Series Explorer or Data Explorer v. 4.6 program (Applied Biosystems, Framingham, MA, USA). Protein identifications were performed using the GPS Explorer v. 3.6 program (Applied Biosystems, Framingham, MA, USA) connected to the local Mascot search engine (Matrix-Science, London, UK, v. 1.9.05) or by direct submission of MS peak lists to the corresponding database searching program in the Mascot web interface. The following parameters were used for database searching: database—SwissProt (v. 24.10.2006); taxonomy—all entries; enzyme—trypsin; allowed missed cleavages—1; fixed modifications—MMTS (C); variable modifications—oxidation (M); peptide tolerance—30 ppm; MS/MS tolerance—150 mmu;

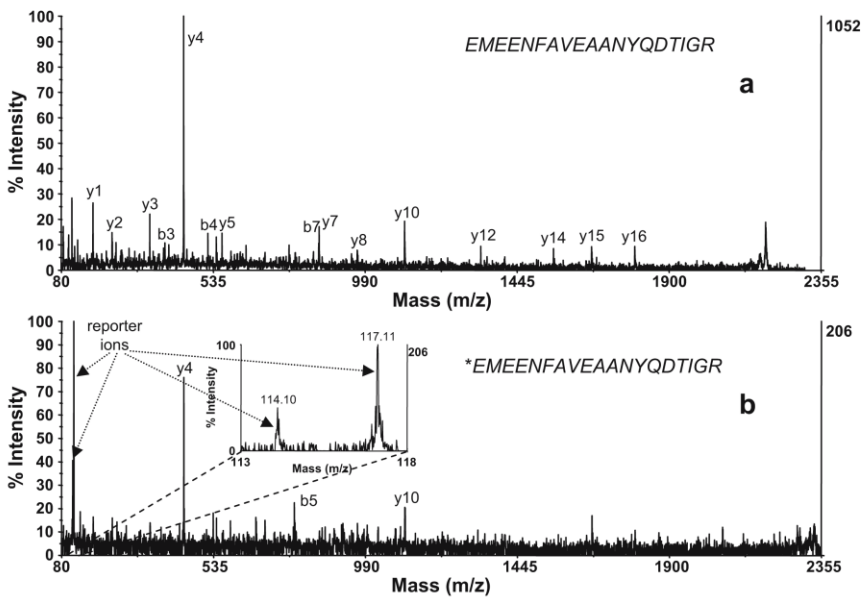

Fig. 2 **a** MS/MS spectrum of the unlabelled tryptic peptide from CDKI-treated sample detected at *m*/*z* 2,186.981 that is shown in Fig. 1c. The same peptide was also detected at *m*/*z* 2186.984 in the control sample (Fig. 1b, corresponding MS/MS data not shown). **b** MS/MS spectrum of the iTRAQ singly labelled tryptic peptide from the mixture of control (tag 114) and CDKI-treated (tag 117) samples detected at *m*/*z* 2,331.085 that is shown in Fig. 1d. The *inset* depicts *m*/*z* range with detected reporter ions 114 and 117. The sequence of fragmented peptide is shown together with denoted *b*- and *y*-type ions

peptide charge—(+1); monoisotopic masses; instrument—MALDI-TOF/TOF. In the case of analysis of iTRAQ-labelled peptides, additional settings to fixed modifications were iTRAQ (N-term), iTRAQ (K); and to variable modifications—iTRAQ (Y).

Results and discussion

The iTRAQ 3-Assay Duplex Trial Kit (Applied Biosystems, Foster City, CA, USA, cat. No. 4369561) is primarily designed for labelling and quantitation of 5–100 μg of complex protein mixtures from tissues or cell lysates. However, the protein amount available from various recent protein fractionation technologies like the ProteomeLab™ PF 2D is usually much lower in collected fractions and ranges from approximately 0.01 to 0.5 μg of proteins depending on the initial load on the system and on the complexity of the sample. At first, iTRAQ labelling was performed according to manufacturer's instructions using tryptic digests of 0.05, 0.5, 5 and 50 μg of bovine serum albumin (Sigma, Steinheim, Germany, cat. no. A-7511). At low protein amounts (0.05 and 0.5 μg) no specific peptide signal in MALDI-TOF MS spectra was detected, probably due to the presence of substances such as SDS, TCEP, trypsin autolysis products or iTRAQ reagents, which may be the cause of interference with ionization and MS measurement (data not shown). For even lower amounts of protein ranging from microgram to nanogram amounts, these chemicals present in the digest may not be completely removed by reversed-phase and/or cation exchange chromatography as recommended by the manufacturer's protocol (Applied Biosystems iTRAQ™ Reagents Chemistry Reference Guide, 2004 -http://docs.appliedbiosystems.com/

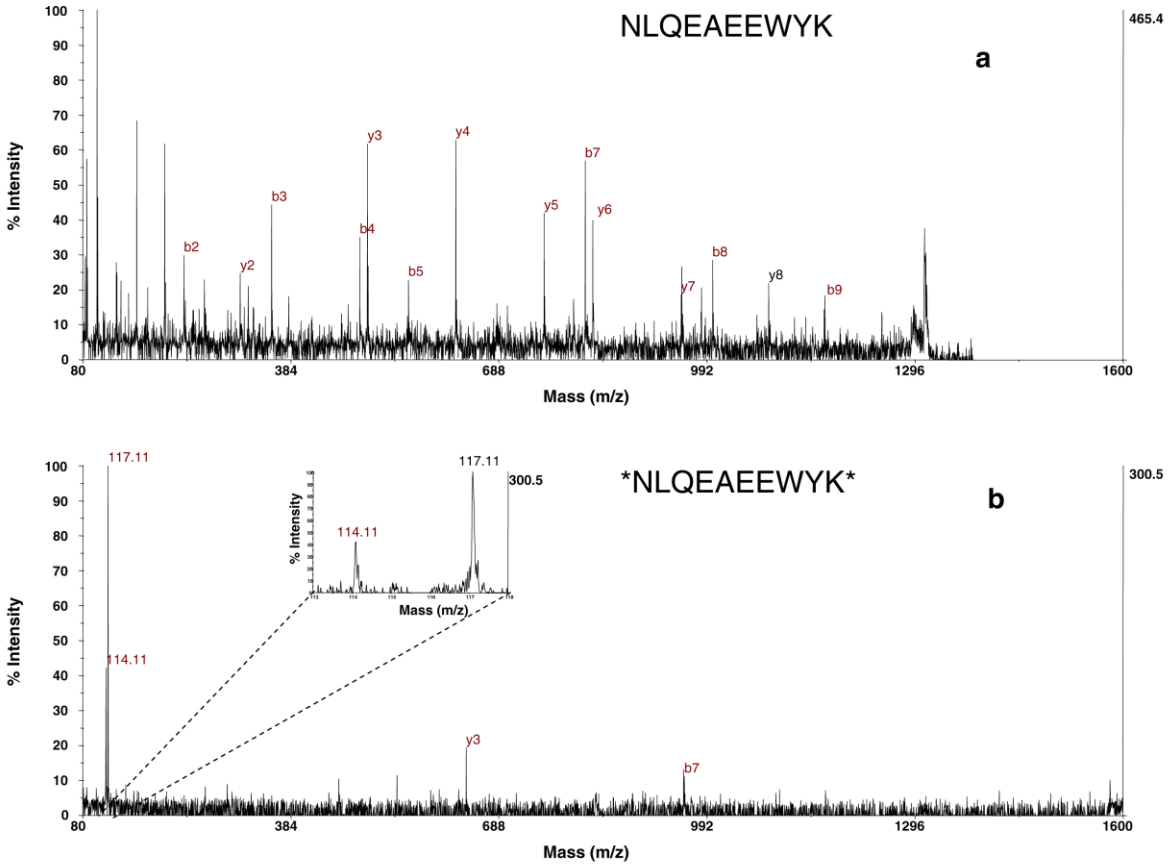

Fig. 3 **a** MS/MS spectrum of the unlabelled tryptic peptide from CDKI-treated sample detected at *m/z* 1,309.586 that is shown in Fig. 1c. The same peptide was also detected at *m/z* 1,309.606 in the control sample (Fig. 1b, corresponding MS/MS data not shown). **b** MS/MS spectrum of the iTRAQ doubly labelled tryptic peptide from the mixture of control (tag 114) and CDKI-treated (tag 117) samples detected at *m/z* 1,597.814 that is shown in Fig. 1d. The *inset* depicts *m/z* range with detected reporter ions 114 and 117. The sequence of fragmented peptide is shown together with denoted *b*- and *y*-type ions

pebiodocs/04350831.pdf). Hence, we optimised the iTRAQ labelling protocol supplied by the manufacturer for this range of protein amounts (low level microgram to nanogram quantities). The key necessary modifications of the standard iTRAQ labelling protocol were the use of 1 M urea instead of 0.1% SDS and the scaling down of the reagent volumes within the assay system. The amount of reagent was decreased by tenfold, whilst the amount of protein was scaled down by a factor of at least 200 or more. A relatively high concentration of iTRAQ reagent is important because of its reactivity toward water in TEAB buffer present within the assay.

To demonstrate the feasibility of such an approach, protein expression patterns obtained from the ProteomeLab™ PF 2D fractionation of human T-lymphoblastic leukemia CEM cell line were used in our experiments. The individual PF 2D fractions (p*I* 4.9–5.2 and retention time 17.2–17.3 min) of two samples and their individual mass spectra before iTRAQ labelling, and mass spectrum of iTRAQ-labelled peptide mixture are shown in Fig. 1. Six peptides were selected for subsequent MS/MS fragmentation analyses. The peptides at *m*/*z* 1,572.815, 1,832.926, 2,331.085 and 2,495.286 were singly iTRAQ modified with a mass increment of 144.1, while the peptides found at *m*/*z* 1,413.815 and 1,597.814 were doubly modified showing a mass increment of 288.2 in comparison to their unmodified state (Fig. 1d, Table 2). MALDI-TOF/TOF fragmentation mass spectra of the peptide EMEENFAVEAANYQDTIGR from both unlabelled sample (*m*/*z* 2,186.981) and iTRAQ single-labelled sample (*m*/*z* 2,331.085) are shown in Fig. 2a and b, respectively. The inset in Fig. 2b shows the low *m*/*z* region of the tandem mass spectrum where the ion signals of reporter ions of two iTRAQ reagents (114 and 117) appear. The experimentally determined ratio of CDKI-treated (*m*/*z* 117) and control (*m*/*z* 114) sample for this peptide was 2.13. Another example of fragmentation MS/MS spectra of iTRAQ double-labelled peptide is shown in Fig. 3. In spite of purification on POROS R2 microcolumns after iTRAQ labelling, we noted lower intensities of *b*- and *y*-type ions in MS/MS spectra and less confident protein identification by database searching compared to the data obtained from the samples before iTRAQ labelling. Therefore, the complementary MS/MS spectrum of unlabelled precursor ion may significantly support the reliability of identification. The summary of six identified peptide sequences and the relative abundance ratios are shown in Table 2. All six peptides corresponded to vimentin (SwissProt database accession number P08670) and the ratio between reporter ions was close for each peptide, thus confirming that the peptides originate from the same protein and showing overexpression of this protein (vimentin) in CDKI-treated sample. Average increase in the level of vimentin calculated from the measurement of six peptides was 2.26±0.20. This was in good agreement with the 1.94-fold increase calculated from UV detection reported by 32 Karat software in the PF 2D system for protein peak analysed by iTRAQ. The essential aspect of the iTRAQ quantitation is the selection of only a singly parent ion for MS/MS resulting in accurate quantitation. Additionally, iTRAQ quantification ratio may reflect the combined expression changes of more than one peptide in the case of the multiplexed nature of the fragmentation spectrum [10].

In the ICPL method, labelling of amino groups of intact proteins before fractionation by isotopic tags shifts their p*I* values to acidic pH, which is not compatible with chromatofocusing in pH range 8.5–4 of the ProteomeLab™ PF 2D system. However, the use of iTRAQ-labelled peptides from the protein digests after HPLC protein fractionation by the ProteomeLab™ PF 2D system suffers no negative influence on the proteins as judged by the 2D protein maps and is a suitable method for quantitation of proteins in fractions containing co-eluted proteins. In addition, the results from the iTRAQ quantitation may be compared with the data from UV protein quantitation thus providing a ‘double-check’ approach. The optimised labelling protocol allows relative quantitation by MALDI-TOF/TOF MS with high sensitivity without the necessity of using 2D HPLC separation of labelled peptides and with resultant simplification of data complexity.

Acknowledgement This research was supported by Czech Science Foundation (#301/05/0418), the Ministry of School, Youth and Sports of the Czech Republic (LC07017) and Institutional Research Concepts IAPG # AV0Z50450515 and # UZFG/06/17.

References

1. Yan F, Subramanian B, Nakeff A, Barder TJ, Parus SJ, Lubman DM (2003) Anal Chem 75:2299–2308
2. Lubman DM, Kachman MT, Wang H, Gong S, Yan F, Hamler RL, O’Neil KA, Zhu K, Buchanan NS, Barder TJ (2002) J Chromatogr B 782:183–196
3. Sheng S, Chen D, Van Eyk J (2006) Mol Cell Proteomics 5:26–34
4. Skalnikova H, Halada P, Dzubak P, Hajduch M, Kovarova H (2005) Technol Cancer Res Treat 4:447–454
5. Pirondini A, Visioli G, Malcevschi A, Marmiroli N (2006) J Chromatogr B 83:91–100
6. Ong SE, Blagoev B, Kratchmarova I, Kristensen DB, Steen H, Pandey A, Mann M (2002) Mol Cell Proteomics 1:376–386
7. Schmidt A, Kellermann J, Lottspeich F (2005) Proteomics 5:4–15
8. Ross PL, Huang YN, Marchese JN, Williamson B, Parker K, Hattan S, Khainovski N, Pillai S, Dey S, Daniels S, Purkayastha S, Juhasz P, Martin S, Bartlet-Jones M, He F, Jacobson A, Pappin DJ (2004) Mol Cell Proteomics 3:1154–1169
9. Gobom J, Nordhoff E, Mirgorodskaya E, Ekman R, Roepstorff P (1999) J Mass Spectrometry 34:105–116
10. Hu J, Qian J, Borisov O, Pan S, Li Y (2006) Proteomics 3:4321–4334

PŘÍLOHA 6

research articles Journal of proteome research

Proteome Mining of Human Follicular Fluid Reveals a Crucial Role of Complement Cascade and Key Biological Pathways in Women Undergoing *in Vitro* Fertilization

Karla Jarkovska,[†] Jirina Martinkova,[†] Lucie Liskova,[†] Petr Halada,[‡] Jiri Moos,[§,||] Karel Rezabek,[||] Suresh Jivan Gadher,[⊥] and Hana Kovarova*[,†]

Institute of Animal Physiology and Genetics AS CR, v.v.i., Libechov, Czech Republic, Institute of Microbiology AS CR, v.v.i., Prague, Czech Republic, Assisted Reproduction Centre, Department of Obstetrics and Gynecology, General Teaching Hospital, Prague, Czech Republic, Sigma-Aldrich spol. s.r.o., Prague, Czech Republic, and Millipore Bioscience, 15 Research Park Drive, St. Charles, Missouri 63304

Received September 8, 2009

In vitro fertilization (IVF) is fraught with problems and currently proteomics approaches are being tried out to examine the microenvironment of the follicle in order to assess biological and immunological parameters that may affect its development. Additionally, better understanding of reproductive process may help increase IVF birth rate per embryo transfer and at the same time avoid spontaneous miscarriages or life threatening conditions such as ovarian hyperstimulation syndrome. The primary aim of this study was to search for specific differences in protein composition of human follicular fluid (HFF) and plasma in order to identify proteins that accumulate or are absent in HFF. Depletion of abundant proteins combined with multidimensional protein fractionation allowed the study of middle- and lower-abundance proteins. Paired comparison study examining HFF with plasma/serum from women undergoing successful IVF revealed important differences in the protein composition which may improve our knowledge of the follicular microenvironment and its biological role. This study showed involvement of innate immune function of complement cascade in HFF. Complement inhibition and the presence of C-terminal fragment of perlecan suggested possible links to angiogenesis which is a vital process in folliculogenesis and placental development. Differences in proteins associated with blood coagulation were also found in the follicular milieu. Several specific proteins were observed, many of which have not yet been associated with follicle/oocyte maturation. These proteins together with their regulatory pathways may play a vital role in the reproductive process.

Keywords: Human follicular fluid • plasma • assisted reproduction • IVF • proteomics • biomarkers • complement cascade • angiogenesis • blood coagulation

Introduction

Application of powerful proteomic technologies in reproductive medical research may significantly contribute to the comprehensive understanding of reproductive processes. Additionally, it may lead to the discovery and selection of specific biomarkers with diagnostic and prognostic values for a wide range of fertility problems and pregnancy related complications.[1]

Assisted reproduction refers to a number of advanced techniques that aid fertilization. Among these, the most used is *in vitro* fertilization (IVF) followed by embryo implantation into the woman's uterus. IVF was originally developed to help women with damaged or absent fallopian tubes which prevented the sperm from meeting the egg. It is now used to treat various fertility issues, and its effectiveness has improved in the past few years, but the chance of pregnancy is still only around 40%.[2] Controlled ovarian hyperstimulation is a key factor in the success of IVF. In the course of ovarian stimulation, the competent follicles start to grow, granulosa cells begin to divide, follicular basal lamina expands and the antrum fills up with follicular fluid (FF). FF provides a special microenvironment containing regulatory molecules which are important for the maturation of oocytes. The composition of FF results from the combination of secretions from the granulosa and thecal cells with minor contribution from the oocytes as well as from the transfer of blood plasma constituents that cross blood follicular barrier via theca capillaries.[3] FF is the resultant byproduct during aspiration of oocytes from mature ovarian follicle, and hence, it has been utilized in various studies focused on oocyte quality, fertilization success or pregnancy complications.

In 1993, Spitzer et al. for the first time used 2-DE to compare complex protein patterns of FF from mature and immature

* To whom correspondence should be addressed. E-mail: kovarova@iapg.cas.cz. Phone: +420 315 639 582. Fax: +420 315 639 510.
[†] Institute of Animal Physiology and Genetics AS CR v.v.i.
[‡] Institute of Microbiology AS CR v.v.i.
[§] Department of Obstetrics and Gynecology, General Teaching Hospital.
[||] Sigma-Aldrich spol. s.r.o.
[⊥] Millipore Bioscience.

10.1021/pr900802u © 2010 American Chemical Society

Published on Web 01/08/2010

human follicles.[4] Since then, improved and advanced proteomic approaches have been applied to further reproductive research. The study performed by Anahory et al. aimed at profiling of human follicular fluid (HFF) of women undergoing IVF resulted in identification of three new proteins (thioredoxin peroxidase 1, transthyretin and retinol-binding protein) present in HFF.[5] In a similarly designed study, Lee et al. identified four other proteins, named hormone sensitive lipase, unnamed protein product 1, unnamed protein product 2, and apolipoprotein A-IV that were not yet reported in HFF.[6] Direct mass spectrometry (MS) based technique SELDI-TOF was applied by Schweigert et al. to compare peptide and protein profiles in serum and HFF of women undergoing IVF.[7] Among 186 individual MS signals, four were identified as haptoglobin alpha1- and alpha 2-chains, haptoglobin 1 and transthyretin. Specific peptide patterns were also analyzed by Liu et al. who reported peptide peaks that correlated with different developmental stages. Two proteins, apolipoprotein A-I and collagen type IV were verified using Western blot analysis.[8] Taking together such findings from these proteomic studies, it was evident that only limited information had been uncovered and that not all components of HFF had been identified. More importantly, their physiological roles in reproduction or pathologies in case of infertility remained unknown. In 2006, Angelucci et al. performed an in-depth study to determine the composition of HFF from women undergoing IVF for male associated infertility and to compare it with the plasma samples of the same women. Many proteins were identified in relatively high levels in HFF including mainly acute phase proteins and several proteins with antioxidant functionalities.[9] Subsequent studies utilized HFF of women with recurrent spontaneous abortion[10] or women that were less than 32 years old and failed to become pregnant after IVF.[11] The results indicated that coagulation factors may play an important role in response to IVF and maintaining normal pregnancy. More recently, Hanrieder et al. utilized combination of isoelectric focusing and reversed phase nanochromatography coupled with nano-LC MALDI TOF/TOF to analyze HFF samples of women undergoing IVF. This study revealed significantly increased numbers of proteins that had not been previously reported in HFF using proteomic techniques.[12] A majority of all identified proteins were plasma matched proteins mostly represented by acute phase proteins but some low copy proteins including sex hormone binding globulin and inhibin A were also found.

The primary aim of this study was to search for specific differences in protein composition of HFF and plasma in order to identify proteins that accumulate or are absent in HFF. These proteins may hold a key to the reproductive process and further evaluation may identify them as potential biomarkers of follicle/oocyte quality and successful IVF during assisted reproduction. To achieve this goal, we carried out for the first time the depletion of the 12 most abundant plasma/HFF matched proteins in paired samples of HFF and plasma obtained from women undergoing successful IVF. Following removal of abundant proteins, the samples were analyzed using combination of 2-D gel-based and 2-D liquid chromatography protein fractionation techniques. The protein identity of evaluated alterations in protein patterns was determined using MS and proteomic data were verified by specific immunoblot or biochemical assay (Figure 1). A majority of protein changes were found to belong to complement cascade and its regulatory proteins. Some other specific biological processes such as acute phase response, transport, lipid metabolism and blood coagulation were involved to a lesser extent.

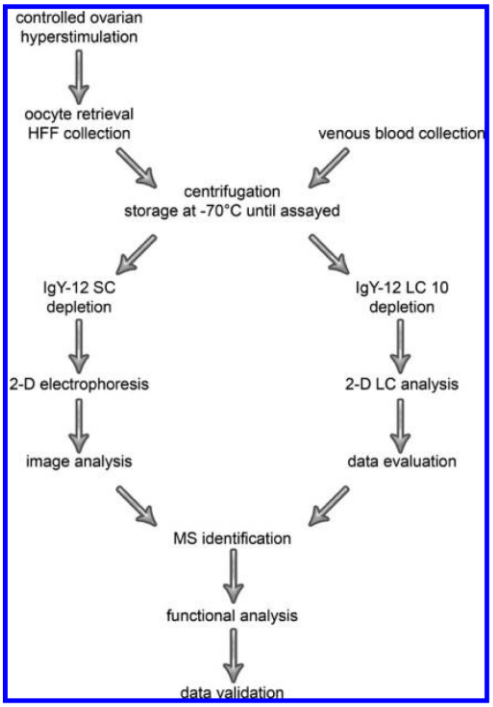

Figure 1. Schematic presentation of the IgY-12, 2-DE and 2-D HPLC workflows. The paired samples of follicular fluid and blood were retrieved from women undergoing controlled ovarian stimulation. The samples were depleted of the 12 most abundant plasma/HFF matched proteins and processed for 2-DE and 2-D HPLC analyses as indicated in the workflows. Subsequently, proteomic data were verified by specific immunoblot or biochemical assay.

Materials and Methods

Chemicals. IgY-12 High Capacity SC Spin Column kit, IgY-12 High Capacity LC10 Proteome Partitioning kit and ProteomeLab PF 2D kit (includes chromatofocusing column, high-resolution reverse-phase column, start buffer and eluent buffer) were purchased from Beckman Coulter (Fullerton, CA). Amicon Ultra-15 Centrifugal Filter Device was from Millipore (Millipore Bedford, MA). Acrylamide, bis-acrylamide, urea, Tris-base, thiourea, SDS, bromophenol blue, amonium persulfate (APS), TEMED, *n*-octyl glucoside, Tris, (2-carboxyethyl) phosphine hydrochloride (TCEP), and iminodiacetic acid were obtained from Sigma-Aldrich (St. Louis, MO). Nonidet-40, 3-3(cholamidolpropyl)-dimethylammonio-1-propane sulfonate (CHAPS) and DTT were from USB Corporation (Cleveland, OH). Glycerol and β-glycerolphosphate were purchased from Penta (Prague, Czech Republic). Protease inhibitors cocktail were obtained from Roche (Mannheim, Germany). Immobiline DryStrip (18 cm, 3−10 NL), Ampholine pH 3−10, and PD-10 desalting columns were from GE Healthcare (Uppsala, Sweden). Silver Quest staining kit was purchased from Invitrogen (Carlsbad, CA). All other chemicals for protein fractionations were of HPLC or analytical grade and buffers were prepared using Mili-Q

water system (Millipore Bedford, MA). Unless otherwise specified, all chemicals used for MS were from Sigma (Steinheim, Germany).

Follicular Fluid and Plasma. Women undergoing stimulation for IVF were recruited for the study at the Centre of Assisted Reproduction, Department of Obstetric and Gynecology, General Teaching Hospital in Prague. In total, 38 women with the Body Mass Index ranged from 19.8 to 29.3 and age between 24 and 38 years were involved in the study. Paired HFF and plasma samples obtained from 12 women were used for proteomic analyses including Western blot (4 paired samples for 2-DE, 2 paired samples for 2-D HPLC and 8 paired samples for Western blot consisting of 2 samples used for 2-D analyses and 6 additional samples). In addition, paired samples of 29 women (including 3 paired samples from above-mentioned set) were analyzed for complement activity and concentrations of complement C3 and C4 components. All female patients gave their informed consent prior to sample collection. All samples used in this study were derived from the women with successful (100% rate) IVF. Patients suffering from the severe form of ovarian hyperstimulation syndrome (OHSS)[13] resultant from ovarian stimulation were excluded from the study.

To achieve stimulation, standard treatment protocol was applied including controlled ovarian follicle-stimulating hormone (FSH) hyperstimulation using gonadotropin-releasing hormone (GnRH) short antagonists and GnRH long agonists with human chorionic gonadotropin (hCG) administration to induce follicular/egg maturation. Oocyte transvaginal ultrasound retrieval was performed 36 h after hCG administration according to the strict procedure approved by Assisted Reproduction Centre. Each follicular fluid sample was obtained from puncture of dominant ovarian follicles (in diameter from 14 to 22 mm). Only macroscopically clear fluids, indicating lack of contamination, were considered in the study. After oocyte isolation, HFF was centrifuged to remove cellular components and debris and then transferred to sterile polypropylene tubes and frozen at −70 °C until further analysis.[14] In parallel, patient paired samples of venous blood (5 mL) were taken on the day of oocyte retrieval, collected in sterile plastic tubes containing EDTA as anticoagulant, cleared by centrifugation, and the resulting plasma samples were frozen at −20 °C and kept at −70 °C until assayed. Alternatively, for complement components C3, C4 and complement activity analyses, samples of blood were allowed to clot, cleared by centrifugation and the resulting sera were frozen at −20 °C and kept at −70 °C until assayed.

Depletion of Major Abundant Proteins and Sample Preparation. Protein concentrations in samples of HFF or plasma were determined using BCA Protein Assay kit (Thermo Scientific, Rockford, IL). Depletion of the 12 most abundant proteins (albumin, IgG, transferin, fibrinogen, IgA, α2-macroglobulin, IgM, α1-antitrypsin, haptoglobin, α1-acidic glycoprotein and apolipoproteins A-I a A-II) in plasma or HFF was carried out using multiple affinity ProteomeLab IgY-12 columns (Beckman Coulter, Fullerton, CA) as per manufacturer's instructions with a few modifications. Briefly, for follow-up 2-DE analysis, IgY-12 SC Spin Column with binding capacity of 10 μL of plasma was used. The 10 μL aliquots of original HFF samples and plasma were diluted in 490 μL of dilution buffer containing 0.15 M NaCl in 10 mM Tris-HCl, pH 7.4, and protease plus phosphatase inhibitors were added. The diluted sample was loaded onto affinity column and flow-through fraction was collected after 30 min by centrifugation. For each sample of HFF and plasma, the number of IgY-12 depletion cycles was adjusted according to sample protein concentration. With average concentrations of 50 and 75 mg/mL, 3 and 2 depletion cycles were obviously needed for HFF and plasma, respectively. The proteins in pools of flow-through fractions for each sample were precipitated by addition of 0.15% sodium deoxycholate for 10 min and 72% trichloroacetic acid (TCA) for 30 min (both in 1/10 of total volume). After washing with ice-cold acetone, pellets were resolubilized in 150 μL of the sample buffer containing 9 M urea, 3% (w/v) CHAPS, 2% (v/v) Nonidet 40, 70 mM DTT, pH 3−10 ampholytes (0.5% w/v), 10 mM beta-glycerol phosphate, 5 mM sodium fluoride, 0.1 mM sodium orthovanadate, and protease inhibitors.

For follow-up 2-D HPLC PF 2D analysis, we used pool of flow-through fractions collected from 6 and 4 cycles of ProteomeLab IgY-12 LC 10 column (binding capacity 250 μL) for HFF and plasma, respectively. For every cycle, an aliquot of sample containing 20 mg of proteins was diluted to final volume of 625 μL using dilution buffer containing 0.15 M NaCl in 10 mM Tris-HCl, pH 7.4. The diluted sample was cleaned using 0.45 μm membrane spin filters and loaded onto IgY-12 LC 10 column. Standard liquid chromatography protocol provided by manufacturer was carried out. Flow-through fractions of the same sample were pooled, concentrated using Amicon Ultra-15 centrifugal filter devices to 0.5 mL and diluted in denaturating buffer containing 7.5 M urea, 2.5 M thiourea, 12.5% glycerol, 62.5 mM Tris-HCl, 2.5% *n*-octylglucoside, and 1.25 mM EDTA to final volume of 2.5 mL.

Two-Dimensional Gel Electrophoresis and Image Analysis. Aliquots of samples of depleted HFF or plasma corresponding to 100 μg of protein were loaded in the first-dimension isoelectric focusing separation using active in gel rehydration of Immobiline DryStrips (IPG strip 18 cm 3−10 NL) in rehydration buffer containing 5 M urea, 2 M thiourea, 2% CHAPS, 2 mM TCEP, 40 mM Tris-base, and 0.003% bromophenol blue. Isoelectric focusing (IEF) was performed on IEF Cell (Bio-Rad, Hercules, CA) system using the following program: 1 h to 200 V, 1 h to 500 V, 1 h to 1000 V, 1 h to 3000 V, 1 h to 5000 V, and 5000 V until total of 55 kVh was reached. After IEF separation, the gel strips were equilibrated in 50 mM Tris-HCl, pH 8.8, 6 M urea, 30% glycerol, 4% SDS, and 65 mM DTT for 15 min and then in the same buffer, except that the DTT was replaced by 4% iodacetamide and bromophenol blue, for 15 min. After equilibration, IPG strips were rinsed and applied to vertical 12%T acrylamide SDS-PAGE (18 × 18 × 1 mm gel). SDS-PAGE was carried out at a constant current of 40 mA per gel using two in series connected Protean II xi Cells (Bio-Rad, Hercules, CA) allowing simultaneous run of four gels. Gels were then stained with mass spectrometry compatible silver staining SilverQuest kit (Invitrogen, Carlsbad, CA). Stained gels were scanned and digitized at 400 dpi resolution using a GS800 scanner (Bio-Rad, Hercules, CA).

The images were evaluated using PDQuest version 7.1 software (Bio-Rad, Hercules, CA). 2-DE gels of four patient-paired samples of follicular fluids and plasma were included in the analysis. After automatic spot detection and matching, manual editing was performed and the results were in good agreement with those of the visual inspection. The relative abundance of each resolved protein spot was then quantified by fitting Gaussian curves in the *X* and *Y* dimension and performing additional modeling to create the final Gaussian spot and express a ppm value. Data were normalized, that is,

expressed as percentages of all valid spots, to account for any differences in protein loading and gel staining. Normalized data were analyzed using statistical procedures available within the PDQuest version 7.1 package which provides the table to determine minimum/maximal number of gels/samples per class of HFF or plasma to control procedure. The protein spots that were statistically significant with $P < 0.05$ according to Student's t tests were selected for identification by mass spectrometry.

Two-Dimensional HPLC ProteomeLab PF 2D Chromatography and Image Analysis. Samples of depleted HFF or plasma in denaturating buffer were loaded on PD10 column equilibrated with 25 mL of the start buffer to exchange denaturing lysis buffer to the start buffer. The protein concentration in the sample collected from PD10 column was determined by direct measurement of absorbance at 280 nm (DU 7400 spectrophotometer, Beckman, Fullerton, CA). For the first-dimension chromatofocusing fractionation (HPCF) two buffers, a start buffer pH 8.5 and an elution buffer pH 4.0 both provided in the PF 2D kit were used to generate an internal linear pH gradient on the column. The HPCF column was equilibrated with 30 column volumes of start buffer and depleted sample of 2 mg of total protein was applied on HPCF column using 5 mL injection loop. The separation was performed at flow rate of 0.2 mL/min. Once the pH in the column achieved a stable pH at 8.5 (30 min), the linear gradient of elution buffer to pH of 4 was switched. The proteins remaining on the column at pH 4 were washed out by 1 M NaCl in 30% *n*-propanol solution. UV detection was performed at 280 nm and the pH of the effluent was monitored using a flow-through online pH probe. Fraction collection started when gradient reached pH 8.3 and individual fractions were collected in 0.3 pH intervals or with maximum time 8.5 min when the pH did not change. In every run, pH was monitored for 150 min, and UV was monitored for 220 min. The percentage of protein recovery from the column within pH gradient 8.5−4 was about 45%, while the remaining part of the loaded proteins was collected in either basic (flow-through) or acidic (wash out) fractions. In total, 35 fractions were collected during HPCF separation including the basic as well as acidic proteins out of the pH gradient. The pI fractions containing any proteins detected at 280 nm were further separated on reversed phase column packed with nonporous silica beads (HPRP). Solvent A was 0.1% trifluoroacetic acid (TFA) in water and solvent B was 0.08% TFA in acetonitrile (MeCN). The separation was done at 50 °C at a flow rate 0.75 mL/min. The gradient was run from 0% to 100% B in 30 min, followed by 100% B for 4 min and 100% A for 10 min. UV absorptions were monitored at 214 nm. The fractions were collected in 0.25 min time intervals into 96-deep well plates using the fraction collector Gilson FC204 (Immunotech a.s., Prague, Czech Republic) and stored at −80 °C until further use.

2-D protein expression maps of HFF and plasma displaying protein isoelectric point versus protein hydrophobicity were generated by ProteoVue software running on PF 2D system. ProteoVue software converts the UV peak intensity in the chromatograms from the second-dimension HPRP column of each p*I* fraction to a band and line format and provides the mean to view and quantify protein levels. The Viper software version 2.2.0 (Ludesi, Sweden) was used for PF 2D data evaluation of four patient pairs of HFF and plasma. The profiles of the second dimension were matched and quantitative data were analyzed using analysis of variance (ANOVA) statistical test implemented in Viper software. Only statistically significant (p-value < 0.05) protein peaks with reproducible profile were selected for mass spectrometric identification.

Enzymatic In-Gel Digestion. Silver nitrate stained protein spots were excised from the gel, cut into small pieces and washed with freshly prepared solution of 30 mM potassium ferricyanide and 100 mM sodium thiosulfate (mixed in 1:1 ratio). After complete destaining, the gel was washed with water, shrunk by dehydration in MeCN and reswelled again in water. The supernatant was removed and the gel was partly dried in a SpeedVac concentrator. The gel pieces were then rehydrated in a cleavage buffer containing 25 mM 4-ethylmorpholine acetate, 5% MeCN and trypsin (5 ng/μL; Promega, Madison, WI), and incubated overnight at 37 °C. The digestion was stopped by addition of 5% TFA in MeCN and the aliquot of the resulting peptide mixture was desalted using a GELoader microcolumn (Eppendorf, Hamburg, Germany) packed with a Poros Oligo R3 material.[15] The purified and concentrated peptides were eluted from the microcolumn in several droplets directly onto MALDI plate using 1 μL of α-cyano-4-hydroxycinnamic acid (CCA) matrix solution (5 mg/mL in 50% MeCN/0.1% TFA).

The fractions from 2-D HPLC were dried completely using the SpeedVac concentrator and dissolved in 50 μL of the above-mentioned cleavage buffer. The digestion and desalting was performed as described for 2-DE protein spots.

MALDI Mass Spectrometry. Mass spectra were measured on an Ultraflex III MALDI-TOF/TOF instrument (Bruker Daltonics, Bremen, Germany) equipped with a smartbeam solid state laser and LIFT technology for MS/MS analysis. PMF spectra were acquired in the mass range of 700−4000 Da and calibrated internally using the monoisotopic $[M + H]^+$ ions of trypsin autoproteolytic fragments (842.5 and 2211.1 Da).

Protein Identification. For PMF database searching, peak lists in XML data format were created using flexAnalysis 3.0 program with SNAP peak detection algorithm. No smoothing was applied and maximal number of assigned peaks was set to 50. After peak labeling, all known contaminant signals were removed. The peak lists were searched using in-house MASCOT search engine against Swiss-Prot 57.0 database subset of human proteins with the following search settings: peptide tolerance of 30 ppm, missed cleavage site value set to two, variable carbamidomethylation of cysteine, oxidation of methionine and protein N-terminal acetylation. No restrictions on protein molecular weight and p*I* value were applied. Proteins with MOWSE score over the threshold 56 calculated for the used settings were considered as identified. If the score was lower or only slightly higher than the threshold value, the identity of protein candidate was confirmed by MS/MS analysis. In addition to the above-mentioned MASCOT settings, fragment mass tolerance of 0.6 Da and instrument type MALDI-TOF-TOF was applied for MS/MS spectra searching.

Immunoblot and Quantitative Analysis. Aliquots of the total nondepleted protein extracts of HFF and blood plasma (15 μg) were separated in 12% SDS-PAGE gels using Protean II xi Cell (Bio-Rad). Proteins were then transferred to Immobilon P (Millipore, Bedford, MA) membranes using a semidry blotting system (Biometra, Göttingen, Germany) and transfer buffer containing 48 mM Tris, 39 mM glycine and 20% methanol. The membranes were blocked for 1 h with 5% skimmed milk in Tris-buffered saline with 0.05% Tween 20 (TBST pH 7.4) and incubated overnight with primary antibodies raised against complement factor H (Santa Cruz Biot., CA, sc-59174; 1:500); clusterin (Abcam Inc., Cambridge, MA, ab16077; 1:2000) and

perlecan (C-terminus; Santa Cruz Biot., CA, sc-25848; 1:2000). Peroxidase-conjugated secondary anti-mouse or anti-rabbit IgG antibodies (Jackson Immunoresearch, Suffolk, U.K.), as appropriate, were diluted 1:10 000 in 5% skimmed milk in TBST, and the ECL+ chemiluminiscence (GE Healthcare, Uppsala, Sweden) detection system was used to detect specific proteins. The exposed CL-XPosure films (Thermo Scientific, Rockford, IL) were scanned by a calibrated densitometer GS-800 (Bio-Rad, Hercules, CA). The proteins bands of each sample were quantified as Trace Quantity (the quantity of a band as measured by the area under its intensity profile curve, units are intensity × mm) using Quantity One software (Bio-Rad, Hercules, CA).

Further immunoanalysis of clusterin and perlecan was carried out by separating nondepleted lysates of HFF samples containing 150 and 100 μg of protein, respectively, in 2-DE gels. Immobiline DryStrips 3−10 NL 13 cm were used to analyze microheterogeneity of clusterin and IPG 4−7 were used for perlecan analysis. Gels were then stained using SYPRO Ruby Protein Gel Stain kit (Bio-Rad, Hercules, CA) and stained gels were scanned and digitized at 800 dpi resolution using a Pharos FX scanner(Bio-Rad, Hercules, CA). Transfer of the proteins to membranes for immunodetection was performed as described above. Protein quantification was performed using ImageMaster Platinum 6.0 (GE Healthcare, Uppsala, Sweden) and data were expressed as relative spot volume of all spots representing a given protein.

Measurement of Total Complement Activity and Concentrations of C3 and C4 Components. The total hemolytic complement activity CH100 was assayed by hemaglutination method using Hemolytic Complement kit (The Binding Site Ltd., Birmingham, U.K.). The concentrations of C3 and C4 complement components in serum and follicular fluid were analyzed using the protein analysis system BNII (Siemens Healthcare Diagnostics, Inc., Deerfield, IL) and diagnostic kits Human C3C and C4C (Siemens Healthcare Diagnostics, Inc., Deerfield, IL). All the diagnostic kits were processed according to the manufacturer's instructions.

Results

The controlled ovarian hyperstimulation results in relatively synchronized maturation of several dominant follicles/oocytes, thus, reducing otherwise high impact of biological variation in samples for proteomic analyses. The paired samples of HFF and plasma obtained from women undergoing IVF and depleted of the 12 most abundant plasma matched proteins as described below were utilized in this study to search for relevant differences in protein composition of HFF and plasma.

Removal of Highly Abundant Proteins for Follow-Up Proteomic Analyses. To overcome limitations of commonly used proteomic techniques related to high dynamic range of protein concentration in a variety biological fluids and access rather middle- or low-abundance proteins (μg/mL to pg/mL), both HFF and plasma samples were depleted of the 12 most abundant proteins. Separation on IgY-12 SC removed around 90% of total loaded protein amount. Using column capacity of 10 μL of plasma resulted in yield of 75 and 50 μg of protein on average in flow-through fractions from plasma and HFF, respectively. Hence, to apply 100 μg of depleted proteins on analytical 2-DE gels, two and three IgY-12 spin column cycles were needed for each sample of plasma and FF, respectively. The removal of the 12 most abundant proteins was monitored using 2-DE fractionation of flow-through and bound fractions (Supplementary Figure 1) and determination of their protein content. The effectiveness of high capacity IgY-12 LC10 column with loading capacity up to 250 μL of plasma was slightly higher with removal of 95−98% of original protein amount. One cycle provided in average 630 and 930 μg of proteins of FF and plasma, respectively. In total, we performed six depletion cycles for FF and four for blood plasma to obtain 2 mg of depleted proteins of each individual sample for one run of 2-D LC PF 2D analysis.

Proteomic Changes Observed in Depleted Human Follicular Fluid Compared to Plasma Using Two Different Approaches: 2-DE and 2-D LC. A typical 2-DE separation performed in the pH 3−10 and the 10−200 kDa range resulted in separation of 477 ± 61 and 433 ± 73 protein spots on average in HFF and plasma, respectively, depleted of the 12 most abundant proteins (Figure 2A,B). Eight gels of four patient-paired samples were used for comparative analysis of protein profiles. A statistical comparison between the two groups of gels using Student's t test implemented in PDQuest software version 7.1 (Bio-Rad) identified 16 protein spots that were significantly ($p < 0.05$) increased or decreased in HFF compared to plasma (Figure 2A,B). Moreover, evaluation of the protein spots that appeared solely on gels from HFF or plasma (considered as qualitative changes based on the criterion of minimum differences being 10-fold stronger than background signals) did not reveal any protein spots that were typical of HFF. Most of the 16 quantitatively altered protein spots were decreased in HFF, but three spots, nos. 0103, 2004, and 2006, were significantly increased (Figure 2C). The protein identity in 11 of these 16 discriminate protein spots from silver nitrate-stained gels was satisfactorily determined using mass spectrometry. An abbreviated list of identified differentially expressed proteins and their functions is presented in Table 1. Comprehensive information about the proteins (SSP numbers, protein names, database accession numbers, protein MW, protein pI value and all MS identification data including Mascot scores, sequence coverage, matched peaks, unmatched peaks, and MS/MS confirmation) is presented in Supplementary Table 1. The presence of fibrinogen beta chain most probably results from incomplete removal of this protein in the course of depletion of major abundant proteins.

The purpose of 2-D LC PF 2D experiments was to complement observations from 2-DE using an advanced gel-independent fractionation technique. This method has the distinct advantage over the 2-DE based approach in that it overcomes many of its drawbacks and, importantly, the fractions of intact proteins can be directly utilized for mass spectrometric analysis. The PF 2D involves 2-D separation and mapping of the total protein expression. Proteins are fractionated by isoelectric points in pH gradient using the chromatofocusing at 0.3 pH intervals in the first dimension. Each of these pI protein fractions is further separated by hydrophobicity using nonporous silica reverse phase chromatography in the second dimension.[16] The global information about protein expression obtained by means of PF 2D separation has been depicted using ProteoVue software that enables the construction of 2-D protein map showing pI fractions versus protein bands according to their hydrophobicity (Figure 3A). In total, the samples of depleted HFF and plasma were separated on average into 1175 protein peaks and evaluation of qualitative and quantitative differences between 2-D protein maps using Viper software identified 96 differentially expressed protein bands with p-value ≤0.05 between HFF and plasma. Twelve of them with area

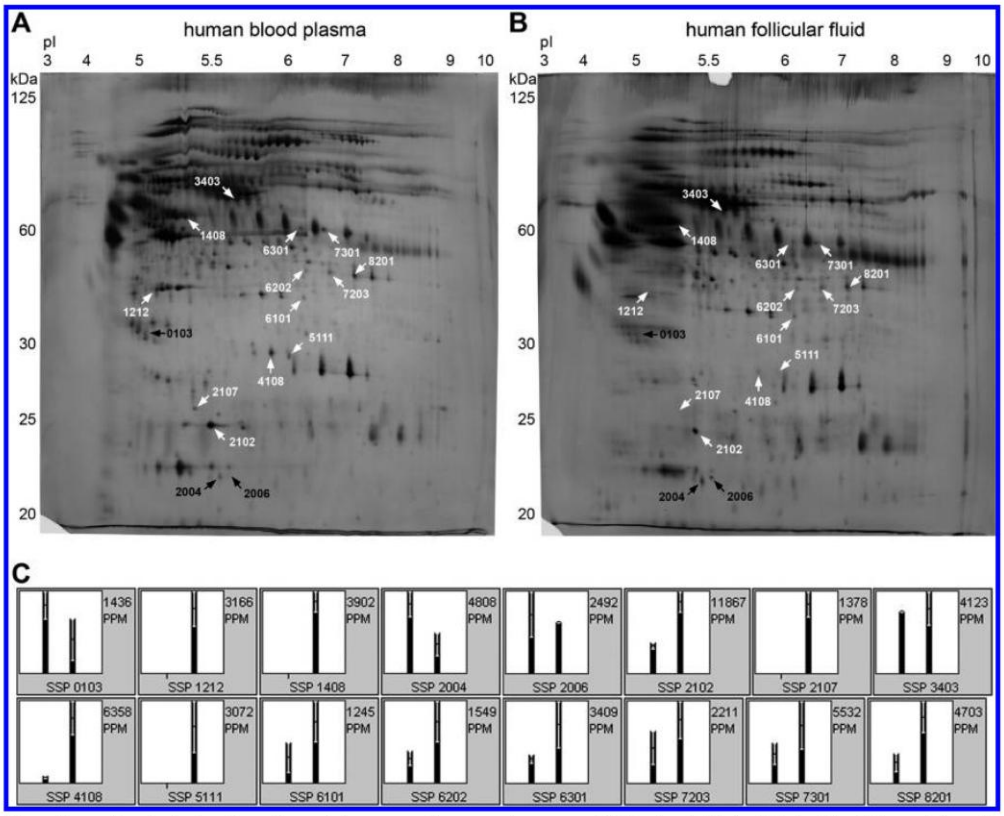

Figure 2. Two-dimensional electrophoretic protein maps of human plasma and follicular fluid depleted of the 12 most abundant plasma matched proteins and set of protein spots significantly different in follicular fluid. Protein lysates of paired samples of depleted human plasma and follicular fluid were subjected to 2-DE, followed by silver staining and image analysis using PDQuest software. The gels from eight liquid samples were evaluated. Panels (A) and (B) show representative gels from depleted plasma and follicular fluid, respectively, and protein spots that were differentially expressed ($P < 0.05$). Regulated proteins are indicated by their SSP numbers assigned by PDQuest software, black numbers indicate higher protein level in follicular fluid and white numbers denote lower level in follicular fluid compared to plasma. Panel (C) shows relative volume intensities of identified regulated protein spots calculated and graphically presented by PDQuest software. Left columns correspond to follicular fluid and right columns to blood plasma.

under curve higher than 1×10^{-5} at 214 nm were chosen for further mass spectrometry and the proteins in 6 of these discriminate protein bands were satisfactorily identified (Figure 3A,B). A summary of differentially expressed proteins and their functions is presented in Table 2. Supplementary Table 2 provides comprehensive information about the proteins (fraction numbers, protein names, database accession numbers, protein MW and all MS identification data including Mascot scores, sequence coverage, matched peaks, unmatched peaks, and MS/MS confirmation). Some of the protein bands collected after the second dimension contained more than one protein and this was reconfirmed by mass spectrometric analysis (Table 2). Most of the differentially expressed protein bands revealed by PF 2D approach and identified were present at significantly increased level in HFF (Figure 3B). These protein bands included apolipoprotein A-IV, alpha-1 antichymotrypsin, antithrombin-III, complement component C9, hemopexin, transthyretin, histidine-rich glycoprotein and complement factor H. The protein band no. 509 showing highly elevated increase in HFF and fulfilling the criteria of one protein/one band in a fraction corresponded to complement component C9 (Figure 3B and Table 2).

Immunoblotting Verification of Protein Changes Typical for Human Follicular Fluid. To validate the results of the proteomic analyses, immunoblot experiments were performed to confirm the identity of the proteins that were increased in HFF compared to plasma on 2-DE gels: clusterin and perlecan. Furthermore, complement factor H that was identified as one of three unambiguously identified proteins in band no. 1021 from 2-D LC with observed higher UV absorbance level in HFF was selected to demonstrate need of verification and contribution of a particular protein to UV absorbance level corresponding to protein amount. Eight paired samples of nondepleted HFF and plasma including six independent samples not previously used in proteomic analyses were separated using 1-D SDS-PAGE followed by protein transfer and specific immunodetection. The results shown in Figure 4 confirmed significantly higher level of clusterin in HFF versus plasma, while the level of complement factor H was lower in HFF. The total level of C-terminal fragment(s) of perlecan did not reveal significant difference between HFF and plasma.

Table 1. The List of Identified Significantly Different Proteins ($p < 0.05$) between HFF and Plasma Selected Using 2-DE[a]

spot no.	protein name	Swiss-Prot no.	upregulation/ fold change	functionality
0103	Clusterin precursor[b]	CLUS_HUMAN	HFF 2.69	Apoptosis Complement pathway Immune response Innate immunity
2006	Basement membrane-specific heparan sulfate proteoglycan core protein precursor (HSPG)[b]	PGBM_HUMAN	HFF 4.55	Cell adhesion
2102	Serum amyloid P-component precursor	SAMP_HUMAN	Plasma 2.61	Acute-phase response Chaperone-mediated protein complex assembly Protein folding
2107	Complement C4-A precursor[b]	CO4A_HUMAN	Plasma >100	Complement activation, alternative pathway Complement activation, classical pathway
4108	Ficolin-3 precursor	FCN3_HUMAN	Plasma 25.15	Complement activation, lectin pathway Signal transduction
5111	Ficolin-3 precursor	FCN3_HUMAN	Plasma >100	Complement activation, lectin pathway Signal transduction
6101	Complement C4-A precursor[b]	CO4A_HUMAN	Plasma 2.47	Complement activation, alternative pathway Complement activation, classical pathway
6301	Fibrinogen beta chain precursor	FIBB_HUMAN	Plasma 4.82	Platelet activation Protein polymerization Response to calcium ion Signal transduction
7203	Complement C3 precursor[b]	CO3_HUMAN	Plasma 3.54	Complement alternate pathway Complement pathway Immune response Inflammatory response Innate immunity
7301	Fibrinogen beta chain precursor	FIBB_HUMAN	Plasma 3.98	Platelet activation Protein polymerization Response to calcium ion Signal transduction
8201	Complement C3 precursor[b]	CO3_HUMAN	Plasma 3.24	Complement alternate pathway Complement pathway Immune response Inflammatory response Innate immunity

[a] The table shows SSP number, protein name, Swiss-Prot no., regulation/fold of the change and functionality based on search in UniProt/Gene Ontology/Biological Process. [b] Fragments only.

The microheterogeneity of clusterin that appeared as an approximate 37 kDa smear on immunoblots from reducing SDS-PAGE was better observed using 2-D immunoblotting of nondepleted samples. This was most likely related to the presence of two chains and their glycosylation as also observed by other researchers.[17] It was evident that protein forms with lower molecular weight and more basic p*I* corresponded to less glycosylated forms and these were observed to be present at higher level in FF (Figure 5A). Similarly, five protein spots corresponding to C-terminal truncated forms of perlecan were immunodetected using specific antibody raised against C-terminal part of the protein. On the basis of the measurements from 3 paired samples of HFF and plasma using Student's *t* test, relative volumes of two most basic spots, nos. 4 and 5, were significantly changed with $p < 0.06$ and $p < 0.02$, respectively, in HFF versus plasma (Figure 5). The level of immunodetected spot no. 4 was higher in HFF with ratio to plasma level corresponding to mean value of 3.96. The opposite was observed in plasma where the immunodetected form of spot no. 5 was higher with mean ratio levels of FF/plasma being 0.24.

Decreased Total Hemolytic Activity of Complement Cascade and Levels of C3 and C4 Component in Human Follicular Fluid Compared to Serum. On the basis of proteomic analyses presented above, many components of the complement cascade (complement C4-A, complement C3, complement component C9) as well as its regulatory proteins (clusterin, complement factor H, ficolin-3) were found in relatively different abundance in HFF compared to plasma. To demonstrate outcome of this dysregulation and possible impact on activity of complement cascade, we analyzed paired samples of HFF and serum for total complement activity as well as for native concentrations of two major complement components, C3 and C4, in order to justify functionality of this important immune process in the microenvironment of the growing follicle. The analysis performed with 29 paired samples showed significantly lower total hemolytic activity in HFF as compared to serum (43% decrease in average with significance of $P < 10^{-13}$, Student's *t* test, Table 3). In correlation with this observation the concentrations of complement components C3 and C4 were also significantly lower in FF compared to serum and their FF/serum ratios were 0.595 and 0.565, respectively (Table 3).

Discussion

Currently, couples having difficulties conceiving, resort to Assisted Reproductive Technology such as IVF in order to achieve pregnancy by artificial means. In IVF cycles, the serum levels of FSH and luteinizing hormone (LH) are determined by the amount of exogeneously administered hCG and by degree of pituitary suppression reducing the endogenous gonadotropin secretion which is regulated by administration of GnRH antagonist and later in final stage of follicular maturation by GnRH agonist. Recent studies demonstrated that administration of GnRH agonist results in less systemic inflam-

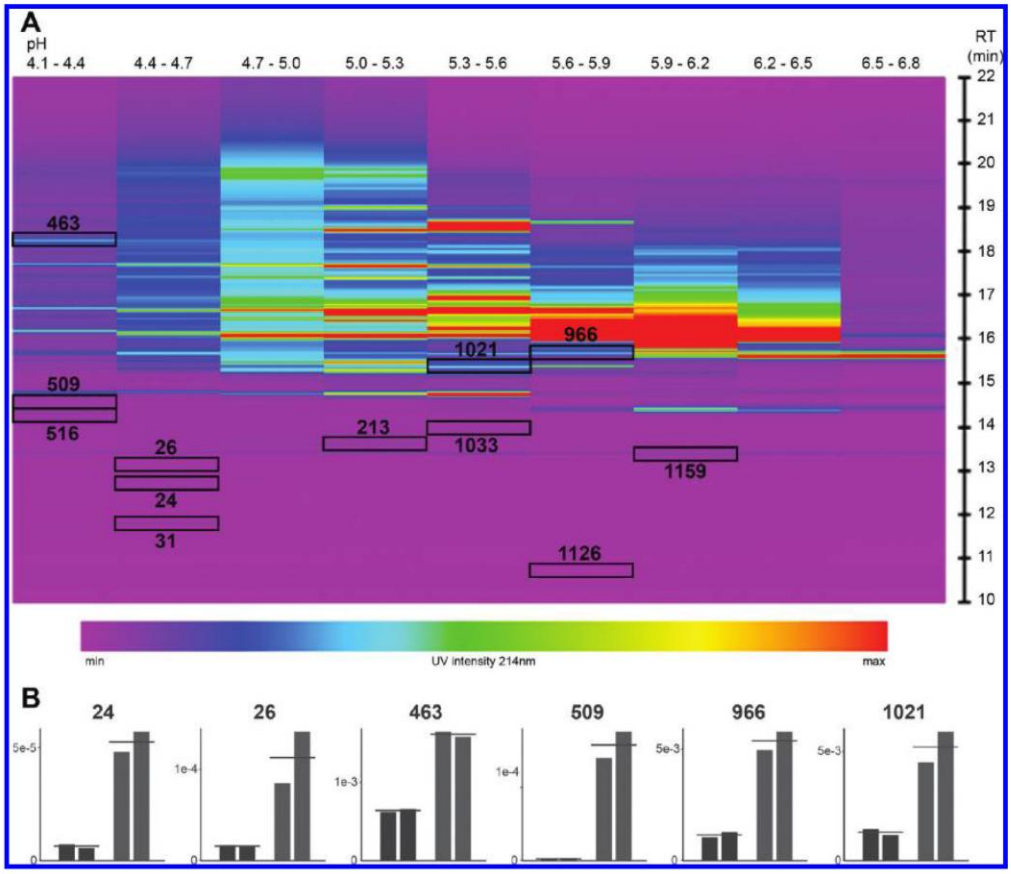

Figure 3. Two-dimensional liquid chromatography protein map of human follicular fluid depleted of the 12 most abundant plasma matched proteins and set of protein bands significantly different in follicular fluid compared to plasma. Protein lysates of paired samples of depleted human plasma and follicular fluid were subjected to 2-D liquid chromatography and protein fractionation/level was monitored using UV detection. 2-D protein expression maps were generated by ProteoVue software and their images were evaluated using Viper software. Panel (A) shows representative protein map from depleted follicular fluid and protein bands that were present in significantly different levels ($P < 0.05$) compared to plasma and were selected for follow-up identification using mass spectrometry. The colors of the protein bands correspond to UV intensity and provide information about protein quantification. Regulated proteins are indicated by their numbers assigned by Viper software. Panel (B) shows relative volume intensities of regulated protein bands calculated and graphically presented by Viper software. Two left columns correspond to two biological replicates of plasma and right columns to follicular fluid.

mation as reflected by level of C-reactive protein (CRP). This may help to prevent development of severe OHSS, the major complication of controlled ovarian hyperstimulation associated with presence of inflammatory cytokines, neutrophil activation and increased capillary permeability.[18,19] Treatment cycles are closely monitored and estradiol level and follicular growth are checked by gynecologic ultrasonography. Currently, there is a lack of assessment of oocyte quality or ability to predict success of the IVF treatment. Additionally, the diagnosis of OHSS is very limited and pathogenesis of this disease remains elusive; hence, its prevention is difficult, and currently, only symptomatic therapy can be applied. With current lack of diagnostic markers, the HFF represents a rich pool of proteins useful as a source of prognostic and/or diagnostic biomarker(s).

The oocyte matures in the milieu of FF rich in hormones, growth factors, cytokines, reactive oxygen and nitrogen species, antiapoptotic factors, polysaccharides and various proteins. Until now, study of single molecules such as FSH, LH, inhibins, insulin-like growth factor binding protein 3, pregnancy-associated plasma protein A and several cytokines has not revealed reliable markers of oocyte maturation, successful fertilization or pregnancy related complications or very early stage embryo development.[20] Implementation of *-omics* technologies, namely, metabolomics and proteomics may be extremely beneficial not only for monitoring complex regulatory networks involved in ovarian physiology and response to exogeneous stimulation, but additionally providing relevant group of candidate biomarkers.

Proteomic analyses of HFF mentioned above identified a variety of proteins present in HFF and most of them were matched to plasma proteins.[4−12] High proportion of acute phase proteins in human FF from women undergoing ovarian stimulation for IVF highlighted a possible involvement of the inflammatory process. Same could be true about the role of blood coagulation proteins in response to IVF treatment and impacting pregnancy or processes leading to miscarrage or abortion. To track down specific biomarkers in reproductive

Table 2. The List of Identified Differentially Expressed Proteins between HFF and Plasma Selected Using 2D-LC PF 2D[a]

peak no.	protein name	Swiss-Prot no.	upregulation/fold change	functionality
24	Apolipoprotein A-IV precursor[b]	APOA4_HUMAN	HFF	Cholesterol efflux
			8.46	Cholesterol homeostasis
				Cholesterol metabolic process
				Hydrogen peroxide catabolic process
				Innate immune response in mucosa
				Leukocyte adhesion
				Multicellular organismal lipid catabolic process
				Negative regulation of plasma lipoprotein oxidation
26	Apolipoprotein A-IV precursor[b]	APOA4_HUMAN	HFF	Phosphatidylcholine metabolic process
			7.32	Phopholipid efflux
				Protein−lipid complex assembly
				Regulation of cholesterol transport
				Removal of superoxide radicals
				Response to lipid hydroperoxide
				Reverse cholesterol transport
463	Alpha-1-antichymotrypsin precursor	AACT_HUMAN	HFF	Acute-phase response
			2.54	Regulation of lipid metabolic process
463	Antithrombin-III precursor	ANT3_HUMAN	HFF	Blood coagulation
			2.54	
509	Complement component C9 precursor	CO9_HUMAN	HFF	Complement alternate pathway
			99.74	Complement pathway
				Cytolysis Immune response
				Innate immunity
966	Hemopexin precursor	HEMO_HUMAN	HFF	Cellular iron ion homeostasis
			4.71	Heme transport
				Interspecies interaction between organisms
966	Transthyretin precursor	TTHY_HUMAN	HFF	Thyroid hormone generation
			4.71	Transport
1021	Histidine-rich glycoprotein precursor	HRG_HUMAN	HFF	unknown
			4.05	
1021	Complement factor H precursor	CFAH_HUMAN	HFF	Complement activation, alternative pathway
			4.05	
1021	Transthyretin precursor	TTHY_HUMAN	HFF	Thyroid hormone generation
			4.05	Transport

[a] The table shows peak number, protein name, Swiss-Prot no., regulation/fold of the change and functionality based on search in UniProt/Gene Ontology/Biological Process. [b] Fragments only.

medicine, depletion of highly abundant proteins enabled in-depth study of such proteins. This study was conducted after depletion of the 12 most abundant proteins from samples of HFF and plasma of women undergoing IVF followed by comparison of their 2-D protein patterns using two complementary techniques. The ultimate aim was to identify potential candidate proteins influencing follicle quality and development or impacting success of fertilization. Additionally, the understanding of any triggering of biochemical pathways affecting the final outcome of the reproductive process was of paramount interest in this study.

During folliculogenesis, follicles become more permeable to plasma proteins resulting in higher number of blood proteins crossing the blood−follicle barrier. Hence, there are notable similarities between protein composition of HFF and blood plasma/serum despite selective transport processes.[7,14] Comparison of fluids including plasma and serum can be facilitated by fractionation techniques such as immunoaffinity subtraction which provides an effective mean for simplifying the proteome while maintaining reasonable sample throughput.[21] Our study utilized an immunoaffinity system capable of removal of the 12 most abundant blood plasma proteins and human plasma and follicular fluid samples were processed using it. The removal of the 12 most abundant proteins was monitored using 2-DE fractionation of flow-through and bound fractions (Supplementary Figure 1) and determination of their protein content. The proteins of HFF and plasma depleted of major abundant proteins were fractionated using 2-DE and 2-D LC PF 2D and significant reproducible differences in protein composition of HFF versus plasma were then identified by mass spectrometry. A majority of these protein alterations, in contrast to the previous studies published by other authors,[5,6,9,12] were found to belong to the complement cascade (complement C4-A, complement C3, complement component C9) and its regulatory proteins (clusterin, complement factor H, ficolin-3) (Figure 6). Some other specific biological processes such as acute phase response (alpha1-antichymotrypsin, serum amyloid P-component), transport (hemopexin, transthyretin), blood coagulation (antithrombin-III), lipid metabolism (apolipoprotein A-IV) were affected to a lesser extent (Table 4).

The complement system, composed of over 30 proteins, responds by means of recognition and activating mechanisms to foreign proteins, tissue injury, apoptosis and necrosis. The three complement activation pathways, classical, lectin and alternative, converge on the C3 component which results in common effector pathway and functions. Complement activation initiates inflammation via recruitment and activation of inflammatory cells[22] (Figure 6). The low levels of complement components C3 and C4-A (or their fragments) together with high level of C9 in HFF observed in this study clearly indicated distinctive regulation of complement cascade in HFF. Additionally, low level of ficolin 3 in HFF can significantly limit complement activation via reduction of lectin-mediated pathway which is used for recognition of self (altered)/nonself.[23,24] Similar to blood serum, the level of complement factor H in HFF is supposed to regulate complement cascade by inactivat-

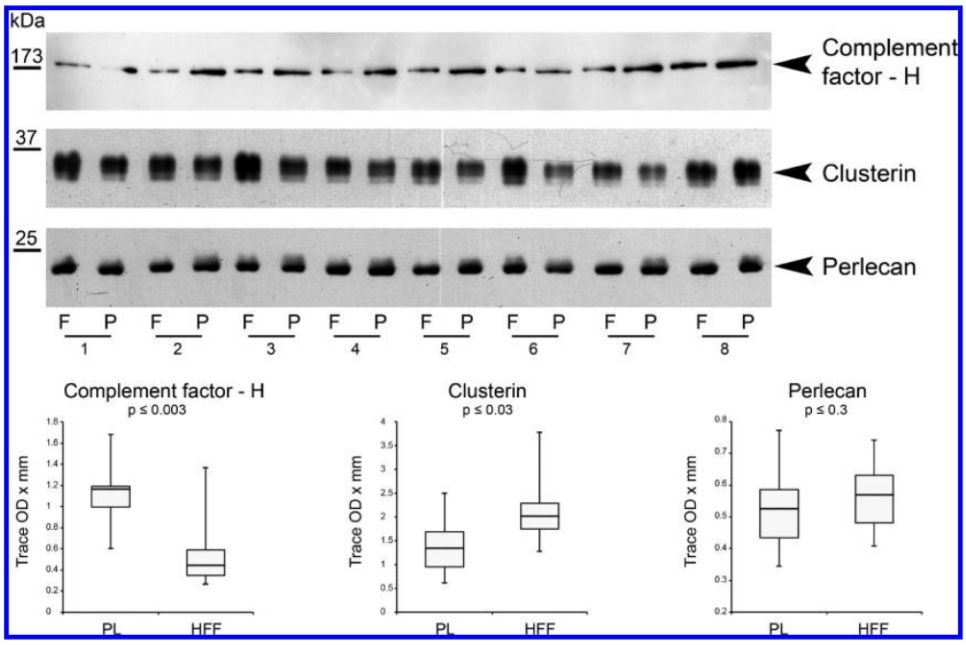

Figure 4. Immunoblot analysis of complement factor H, clusterin and perlecan (C-terminal fragment) in paired samples of nondepleted follicular fluid and plasma of women undergoing IVF. Protein lysates prepared from eight paired samples of follicular fluid (F) and plasma (P) were examined on immunoblots using specific antibodies recognizing complement factor H, clusterin and perlecan (C-terminal fragment). The protein bands were quantified using Quantity One software and distribution of the values was illustrated using boxplot. Significance of differences was calculated by Student *t* test (*p*-value).

ing C3 convertase and alternative pathway activation important for tissue homeostasis.[25,26] We observed low levels of complement factor H in HFF in this study which may be allowing the alternative pathway to remain active. The third complement regulatory protein highlighted in this study was clusterin. It plays an active role in inhibition of complement-mediated cell damage[27] and may also play protective role in reproduction. This study demonstrated high level of clusterin in HFF, which might contribute to the inhibition of cytolytic activity of complement-mediated membrane attack. Analysis of data obtained from our study and extrapolating its relationship to the schematic representation of complement cascade (Figure 6) provides an understanding of the complement cascade inhibiton in HFF of women undergoing ovarian stimulation for IVF. It appears that controlled complement activity in follicular fluid across several different levels of regulation may significantly contribute to optimized oocyte maturation and IVF success leading to higher pregnancy rates. Murine studies supporting the role of complement cascade in control of reproductive process in antiphospholipid syndrome characterized by pregnancy loss that occurs in the presence of antiphospholipid antibodies have also alluded to similar outcome. These studies identified a novel role for complement cascade linking abortion with inappropriate complement activation.[22,28] Additional data from such animal model studies have shown the important role played by complement regulatory proteins in prevention of harmful amplification of complement cascade and this too was evident in our study using human samples.[29] Interestingly, direct link between complement activation and angiogenesis was demonstrated in antibody independent mouse model of spontaneous miscarriage. Complement activation caused deficiency of free vascular endothelial growth factor (VEGF), the angiogenic factor required for normal placental development, that was captured by high levels of soluble VEGF receptor 1. Inhibition of complement activation prevented these angiogenesis failure and rescued pregnancies.[30] Our current ongoing studies using bead-based multiplex assays from the Endocrine and Cytokine Panels (Millipore, www.millipore.com/analytes) and Luminex 200 Instrumentation (data not shown) indicate that low level of complement activity in HFF described in this study is associated with increased level of VEGF compared to serum samples of women undergoing IVF which has important role in perifollicular angiogenesis and may significantly affect oocyte maturation and quality.

Besides the role of clusterin in complement inactivation, it is a multifunctional protein that is up-regulated during many different pathophysiological states and studies have focused on its role in reproductive complications. Clusterin expression in the placental tissues of the preeclampsia group was significantly higher than in the normal pregnancy group[31] and clusterin mRNA level in testicular biopsies was significantly lower in azoospermic patients with constitutive or idiopathic spermatogenic failure.[32] However, there are some discrepancies among studies showing either decreased level of clusterin in plasma of women carrying Down syndrome fetus[33] or increased level of clusterin.[34] The problem may be related to the necessity to target specific form or modification of clusterin to particular biological process and cellular or extracellular localization.

Among other proteins increased in HFF, we found perlecan, highly conserved multidomain heparan sulfate proteoglycan. This multifunctional molecule supports cell adhesion, growth factor binding, regulates apoptosis and it is responsible for charge selective ultrafiltration properties.[35] Perlecan expression and function is controlled at the level of transcription and

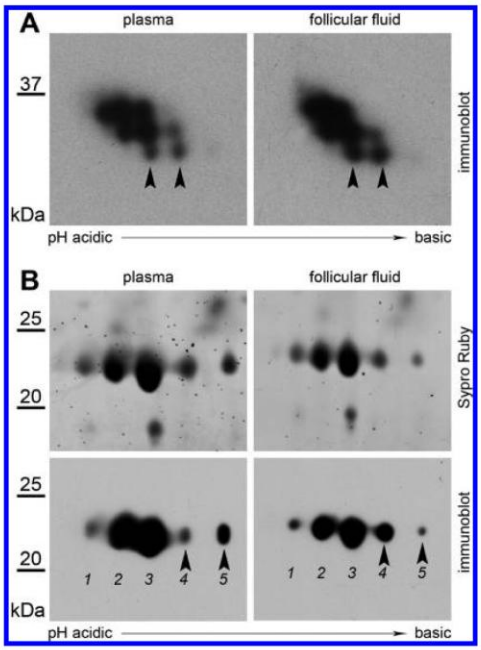

Figure 5. 2-D immunoblot analysis of clusterin and perlecan (C-terminal fragment) in samples of nondepleted follicular fluid and plasma of women undergoing controlled ovarian stimulation for IVF. Protein lysates prepared from paired samples of follicular fluid and plasma were examined on 2-D immunoblots using specific antibodies recognizing clusterin (A) and perlecan (C-terminal fragment) (B). The arrows indicate the positions of the differentially regulated proteins. The figure is representative of three different pairs of samples.

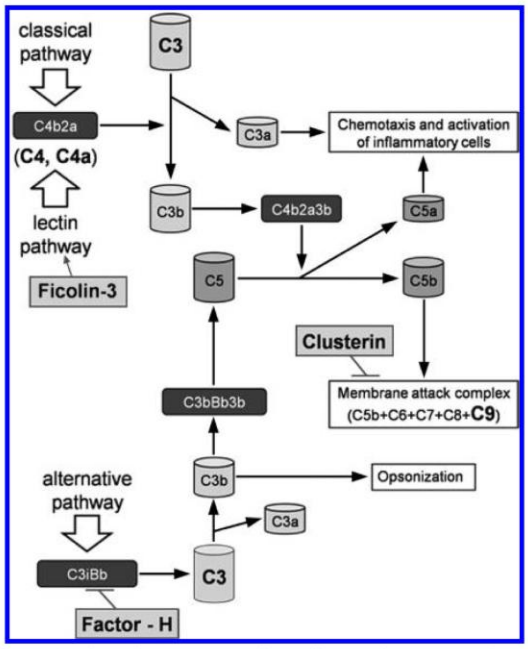

Figure 6. Complement cascade and complement regulatory proteins: proposed mechanism of complement inhibition in follicular fluid. The three complement activation pathways, the classical, lectin and alternative, converge on the C3 component which results in a common effector pathway and functions. Complement activation initiates inflammation via recruitment and activation of inflammatory cells. The changes in the levels of complement components C3, C4, C4a, and C9 (in bold) as well as complement regulatory proteins ficolin-3 complement factor H and clusterin (in box) were identified in this study. These changes may subsequently contribute to the inhibition of complement cascade activity in follicular fluid of women undergoing controlled ovarian stimulation for IVF. It appears that controlled complement activity in follicular fluid coming across several different levels of regulation is favorable for intrafollicular milieu and it may influence maturation of oocyte and its competence for successful fertilization. On the other hand, disregulation of this milieu may contribute to the pathologies associated with ovarian stimulation.

alternative splicing, but significant contribution comes also from extracellular proteolysis. It appears that perlecan fragments may have distinct activities than original intact molecule. In support of this, C-terminal fragment of perlecan has been shown to inhibit angiogenesis;[36] hence, it may be possible that its presence in HFF can contribute to regulation of vasculature in follicle.[37] It was demonstrated that selective degradation of perlecan occurred during ovulation in the focal intraepithelial matrix that develops between granulosa cells and the follicular basal lamina in ovarian follicles.[38] Using specific immunoblot, we confirmed the presence of at least five forms of C-terminal fragment of perlecan with two of them having distinct levels in HFF compared to plasma. Perlecan was for the first time identified in HFF by Hanrieder et al in 2007,[12] but distinctive perlecan forms were not defined in this study.

Histidine-rich glycoprotein was found in fraction collected in 2-D LC together with complement factor H and transthyretin. By UV quantification, protein content in this fraction was higher in HFF compared to plasma, but Western blot confirmed lower level of complement factor H in HFF, and with dissimilarities to other studies reporting transthyretin,[7,9,33] it is therefore likely that histidine-rich glycoprotein, described for the first time in this study to be present in HFF, is increased in HFF of women undergoing IVF. The physiological function of this protein is not yet known; however, on the basis of its homology with high molecular weight kininogen, the His-rich region of this protein may mediate the contact activation phase of intrinsic blood coagulation cascade.[39] Histidine-rich glycoprotein interacts with many ligands including Zn^{2+}, tropomyo-

Table 3. Total Hemolytic Activity of Complement Cascade in Hff and Serum and Concentration of Complement Components C3 and C4

	CA Serum (U/mL)	CA FF (U/mL)	CA FF/S ratio	C3 FF (g/L)	C3 serum (g/L)	C3 FF/S ratio	C4 FF (g/L)	C4 serum (g/L)	C4 FF/S ratio
Mean	803	465	0.574	0.594	1.000	0.595	0.115	0.207	0.565
SD	144	164	0.156	0.192	0.166	0.171	0.037	0.062	0.135
N	29	29	29	22	22	22	22	22	22
t test		$P < 10^{-13}$			$P < 10^{-9}$			$P < 10^{-7}$	

Table 4. Summary of the Differentially Expressed Proteins between HFF and Plasma Revealed by Complementary Proteomic Techniques and Their Classification According to the Biological Processes

protein name	Swiss-Prot no.	methodology	increase	functionality
Alpha-1-antichymotrypsin precursor	AACT_HUMAN	2D-LC	HFF	acute-phase response
Antithrombin-III precursor	ANT3_HUMAN	2D-LC	HFF	blood coagulation
Apolipoprotein A-IV precursor	APOA4_HUMAN	2D-LC	HFF	lipid transport
Perlecan (HSPG2)	PGBM_HUMAN	2D-E	HFF	cell adhesion
Clusterin precursor	CLUS_HUMAN	2D-E	HFF	complement pathway apoptosis
Complement C3 precursor	CO3_HUMAN	2D-E	PL	complement pathway innate immunity
Complement C4-A precursor	CO4A_HUMAN	2D-E	PL	complement pathway innate immunity
Complement component C9 precursor	CO9_HUMAN	2D-LC	HFF	complement pathway innate immunity
Complement factor H precursor	CFAH_HUMAN	2D-LC	HFF	complement pathway innate immunity
Fibrinogen beta chain precursor	FIBB_HUMAN	2D-E	PL	blood coagulation
Ficolin-3 precursor	FCN3_HUMAN	2D-E	PL	complement pathway innate immunity
Hemopexin precursor	HEMO_HUMAN	2D-LC	HFF	transport
Histidine-rich glycoprotein precursor	HRG_HUMAN	2D-LC	HFF	not yet known
Serum amyloid P-component precursor	SAMP_HUMAN	2D-E	PL	acute-phase response
Transthyretin precursor	TTHY_HUMAN	2D-LC	HFF	transport

sin, heparin and heparan sulfate, plasminogen, plasmin, fibrinogen, thrombospondin, imunoglobulins and strong bound to several complement proteins. Therefore, the maintenance of immune functions as well as coagulation may be extensively influenced in the presence of histidine-rich glycoprotein and such possible links deserve further investigation.

Conclusion

Paired comparison study examining HFF with plasma/serum from women undergoing successful IVF revealed important protein differences which may improve our knowledge of the follicular microenvironment and its biological role. This study showed involvement of innate immune function of complement cascade in HFF of women undergoing ovarian stimulation for IVF. Complement inhibition and the presence of C-terminal fragment of perlecan also suggested possible links to angiogenesis, a process paramount to follicle and embryo development. Additionally, differences in proteins associated with blood coagulation were observed and may influence follicular milieu. Depletion of abundant proteins combined with multidimensional protein fractionation was instrumental in allowing the study of middle- and lower-abundance proteins, many of which have not yet been associated with follicle/oocyte maturation. These proteins together with their regulatory pathways may play a vital role in reproductive process. We propose a set of key proteins as potential biomarker candidates to aid a successful IVF therapy in women desperate to have a child.

Abbreviations: ANOVA, analysis of variance; BCA, bicinchoninic acid; CCA, α-cyano-4-hydroxycinnamic acid; CRP, C-reactive protein; FF, follicular fluid; FSH, follicle-stimulating hormone; GnRH, gonadotropin-releasing hormone; hCG, human chorionic gonadotropin; HFF, human follicular fluid; HPCF, high performance chromatofocusing; HPLC, high performance liquid chromatography; HPRP, high performance reverse phase; IEF, isoelectric focusing; IVF, *in vitro* fertilization; LC, liquid chromatography; LH, luteinizing hormone; MALDI, matrix-assister laser desorption/ionization; MeCN, acetonitrile; MS, mass spectrometry; MW, molecular weight; OHSS, ovarian hyperstimulation syndrome; PF 2D, protein fractionation 2D; PMF, peptide mass fingerprinting; SELDI, surface-enhanced laser desorption/ionization; TOF, time-of-flight; VEGF, vascular endothelial growth factor.

Acknowledgment. This study was supported by GA AS CR (# 1QS500450568), Ministry of Health of the Czech Republic (NS9781-32009), and Institutional Research Concepts AV0Z50450515 (IAPG), AV0Z50200510 (IMIC). Special thanks to A. Ekefjärd and D. Enetoft from Ludesi for providing Viper software. The authors appreciate helpful discussion with Dr. Trebichavsky (Institute of Microbiology AS CR v.v.i., Novy Hradek) and prof. Ulcova-Gallova (Faculty Hospital, Plzen).

Supporting Information Available: Figure of 2-DE fractionation of flow-through and bound fractions. Tables of differentially expressed proteins identified from 2-DE experiment and 2D-HPLC experiment. This material is available free of charge via the Internet at http://pubs.acs.org.

References

(1) Gadher, S. J.; Jarkovska, K.; Kovarova, H. Reproductive therapies and a need for potential biomarkers for prognostic and diagnostic screening of women desperate to conceive. *Expert Rev. Proteomics* **2009**, *6* (6), 591–3.
(2) ehealthMD Home page. http://www.ehealthmd.com.
(3) Fortune, J. E. Ovarian follicular growth and development in mammals. *Biol. Reprod.* **1994**, *50* (2), 225–32.
(4) Spitzer, D.; Murach, K. F.; Lottspeich, F.; Staudach, A.; Illmensee, K. Different protein patterns derived from follicular fluid of mature and immature human follicles. *Hum. Reprod.* **1996**, *11* (4), 798–807.
(5) Anahory, T.; Dechaud, H.; Bennes, R.; Marin, P.; Lamb, N. J.; Laoudj, D. Identification of new proteins in follicular fluid of mature human follicles. *Electrophoresis* **2002**, *23* (7−8), 1197–202.
(6) Lee, H. C.; Lee, S. W.; Lee, K. W.; Cha, K. Y.; Kim, K. H.; Lee, S. Identification of new proteins in follicular fluid from mature human follicles by direct sample rehydration method of two-dimensional polyacrylamide gel electrophoresis. *J. Korean Med. Sci.* **2005**, *20* (3), 456–60.
(7) Schweigert, F. J.; Gericke, B.; Wolfram, W.; Kaisers, U.; Dudenhausen, J. W. Peptide and protein profiles in serum and follicular fluid of women undergoing IVF. *Hum. Reprod.* **2006**, *21* (11), 2960–2968.
(8) Liu, A. X.; Zhu, Y. M.; Luo, Q.; Wu, Y. T.; Gao, H. J.; Zhu, X. M.; Xu, C. M.; Huang, H. F. Specific peptide patterns of follicular fluids at different growth stages analyzed by matrix-assisted laser desorption/ionization time-of-flight mass spectrometry. *Biochim. Biophys. Acta* **2007**, *1770* (1), 29–38.
(9) Angelucci, S.; Ciavardelli, D.; Di Giuseppe, F.; Eleuterio, E.; Sulpizio, M.; Tiboni, G. M.; Giampietro, F.; Palumbo, P.; Di Ilio, C. Proteome analysis of human follicular fluid. *Biochim. Biophys Acta* **2006**, *1764* (11), 1775–85.

(10) Kim, Y. S.; Kim, M. S.; Lee, S. H.; Choi, B. C.; Lim, J. M.; Cha, K. Y.; Baek, K. H. Proteomic analysis of recurrent spontaneous abortion: Identification of an inadequately expressed set of proteins in human follicular fluid. *Proteomics* **2006**, *6* (11), 3445–54.
(11) Estes, S. J.; Ye, B.; Qiu, W.; Cramer, D.; Hornstein, M. D.; Missmer, S. A. A proteomic analysis of IVF follicular fluid in women ≤32 years old. *Fertil. Steril.* **2009**, *92* (5), 1569–78.
(12) Hanrieder, J.; Nyakas, A.; Naessen, T.; Bergquist, J. Proteomic analysis of human follicular fluid using an alternative bottom-up approach. *J. Proteome Res.* **2008**, *7* (1), 443–9.
(13) Navot, D.; Bergh, P. A.; Laufer, N. Ovarian hyperstimulation syndrome in novel reproductive technologies: prevention and treatment. *Fertil. Steril.* **1992**, *58* (2), 249–61.
(14) Moos, J.; Filova, V.; Pavelkova, J.; Moosova, M.; Peknicova, J.; Rezabek, K. Follicular fluid and serum levels of inhibin A and pregnancy-associated plasma protein A in patients undergoing IVF. *Fertil. Steril.* **2009**, *91* (5), 1739–44.
(15) Gobom, J.; Nordhoff, E.; Mirgorodskaya, E.; Ekman, R.; Roepstorff, P. Sample purification and preparation technique based on nano-scale reversed-phase columns for the sensitive analysis of complex peptide mixtures by matrix-assisted laser desorption/ionization mass spectrometry. *J. Mass Spectrom.* **1999**, *34* (2), 105–16.
(16) Skalnikova, H.; Halada, P.; Dzubak, P.; Hajduch, M.; Kovarova, H. Protein fingerprints of anti-cancer effects of cyclin-dependent kinase inhibition: identification of candidate biomarkers using 2-D liquid phase separation coupled to mass spectrometry. *Technol. Cancer Res. Treat.* **2005**, *4* (4), 447–54.
(17) Schepeler, T.; Mansilla, F.; Christensen, L. L.; Orntoft, T. F.; Andersen, C. L. Clusterin expression can be modulated by changes in TCF1-mediated Wnt signaling. *J. Mol. Signaling* **2007**, *2*, 6.
(18) Orvieto, R. Controlled ovarian hyperstimulation—an inflammatory state. *J. Soc. Gynecol. Invest.* **2004**, *11* (7), 424–6.
(19) Orvieto, R.; Zagatsky, I.; Yulzari-Roll, V.; La Marca, A.; Fisch, B. Substituting human chorionic gonadotropin by gonadotropin-releasing hormone agonist to trigger final follicular maturation, during controlled ovarian hyperstimulation, results in less systemic inflammation. *Gynecol. Endocrinol.* **2006**, *22* (8), 437–40.
(20) Revelli, A.; Delle Piane, L.; Casano, S.; Molinari, E.; Massobrio, M.; Rinaudo, P. Follicular fluid content and oocyte quality: from single biochemical markers to metabolomics. *Reprod. Biol. Endocrinol.* **2009**, *7*, 40.
(21) Whiteaker, J. R.; Zhang, H.; Eng, J. K.; Fang, R.; Piening, B. D.; Feng, L. C.; Lorentzen, T. D.; Schoenherr, R. M.; Keane, J. F.; Holzman, T.; Fitzgibbon, M.; Lin, C.; Cooke, K.; Liu, T.; Camp, D. G., II; Anderson, L.; Watts, J.; Smith, R. D.; McIntosh, M. W.; Paulovich, A. G. Head-to-head comparison of serum fractionation techniques. *J. Proteome Res.* **2007**, *6* (2), 828–36.
(22) Salmon, J. E.; Girardi, G. Antiphospholipid antibodies and pregnancy loss: a disorder of inflammation. *J. Reprod. Immunol.* **2008**, *77* (1), 51–6.
(23) Linton, N. F.; Wessels, J. M.; Cnossen, S. A.; Croy, B. A.; Tayade, C. Immunological mechanisms affecting angiogenesis and their relation to porcine pregnancy success. *Immunol. Invest.* **2008**, *37* (5), 611–29.
(24) Runza, V. L.; Schwaeble, W.; Mannel, D. N. Ficolins: novel pattern recognition molecules of the innate immune response. *Immunobiology* **2008**, *213* (3−4), 297–306.
(25) Jozsi, M.; Zipfel, P. F. Factor H family proteins and human diseases. *Trends Immunol.* **2008**, *29* (8), 380–7.
(26) Atkinson, J. P.; Goodship, T. H. Complement factor H and the hemolytic uremic syndrome. *J. Exp. Med.* **2007**, *204* (6), 1245–8.
(27) Jones, S. E.; Jomary, C. Clusterin. *Int. J. Biochem. Cell Biol.* **2002**, *34* (5), 427–31.
(28) Girardi, G.; Salmon, J. B. The role of complement in pregnancy and fetal loss. *Autoimmunity* **2003**, *36* (1), 19–26.
(29) Caucheteux, S. M.; Kanellopoulos-Langevin, C.; Ojcius, D. M. At the innate frontiers between mother and fetus: linking abortion with complement activation. *Immunity* **2003**, *18* (2), 169–72.
(30) Girardi, G. Complement inhibition keeps mothers calm and avoids fetal rejection. *Immunol. Invest.* **2008**, *37* (5), 645–59.
(31) Shin, J. K.; Han, K. A.; Kang, M. Y.; Kim, Y. S.; Park, J. K.; Choi, W. J.; Lee, S. A.; Lee, J. H.; Choi, W. S.; Paik, W. Y. Expression of clusterin in normal and preeclamptic placentas. *J. Obstet. Gynaecol. Res.* **2008**, *34* (4), 473–9.
(32) Plotton, I.; Sanchez, P.; Durand, P.; Lejeune, H. Decrease of both stem cell factor and clusterin mRNA levels in testicular biopsies of azoospermic patients with constitutive or idiopathic but not acquired spermatogenic failure. *Hum. Reprod.* **2006**, *21* (9), 2340–5.
(33) Kolialexi, A.; Tsangaris, G. T.; Papantoniou, N.; Anagnostopoulos, A. K.; Vougas, K.; Bagiokos, V.; Antsaklis, A.; Mavrou, A. Application of proteomics for the identification of differentially expressed protein markers for Down syndrome in maternal plasma. *Prenat. Diagn.* **2008**, *28* (8), 691–8.
(34) Nagalla, S. R.; Canick, J. A.; Jacob, T.; Schneider, K. A.; Reddy, A. P.; Thomas, A.; Dasari, S.; Lu, X.; Lapidus, J. A.; Lambert-Messerlian, G. M.; Gravett, M. G.; Roberts, C. T., Jr.; Luthy, D.; Malone, F. D.; D'Alton, M. E. Proteomic analysis of maternal serum in down syndrome: identification of novel protein biomarkers. *J. Proteome Res.* **2007**, *6* (4), 1245–57.
(35) Farach-Carson, M. C.; Carson, D. D. Perlecan—a multifunctional extracellular proteoglycan scaffold. *Glycobiology* **2007**, *17* (9), 897–905.
(36) Bix, G.; Iozzo, R. V. Novel interactions of perlecan: unraveling perlecan's role in angiogenesis. *Microsc. Res. Tech.* **2008**, *71* (5), 339–48.
(37) Zoeller, J. J.; Whitelock, J. M.; Iozzo, R. V. Perlecan regulates developmental angiogenesis by modulating the VEGF-VEGFR2 axis. *Matrix Biol.* **2009**, *28* (5), 284–91.
(38) Irving-Rodgers, H. F.; Catanzariti, K. D.; Aspden, W. J.; D'Occhio, M. J.; Rodgers, R. J. Remodeling of extracellular matrix at ovulation of the bovine ovarian follicle. *Mol. Reprod. Dev.* **2006**, *73* (10), 1292–302.
(39) Manderson, G. A.; Martin, M.; Onnerfjord, P.; Saxne, T.; Schmidtchen, A.; Mollnes, T. E.; Heinegard, D.; Blom, A. M. Interactions of histidine-rich glycoprotein with immunoglobulins and proteins of the complement system. *Mol. Immunol.* **2009**, *46* (16), 3388–98.

PR900802U

Prohlášení spoluautorů:

Prohlašuji, že Jiřina Tylečková (Martinková) se patřičně podílela na plánování proteomických experimentů, jejich provedení, interpretaci výsledků a sepisování následujících publikací:

70 % na „Cancer cells response to anthracycline effects: Mysteries of the hidden proteins associated with these drugs“

40 % na „Cancer drug-resistance and a look at specific proteins: Rho GDP-dissociation inhibitor 2, Y-box binding protein 1, and HSP70/90 organizing protein in proteomics clinical application“

30 % na „Cancer cell resistance to Aurora kinase inhibitors: identification of novel targets for cancer therapy“

40 % na „Challenges in cancer research and multifaceted approaches for cancer biomarker quest“

15 % na „Relative quantification of proteins fractionated by the ProteomeLab^{TM} PF 2D system using isobaric tags for relative and absolute quantification (iTRAQ)“

V Liběchově dne

RNDr. Hana Kovářová, CSc.